

Technical University of Crete, Greece  
School of Electrical & Computer Engineering  
Control Systems Division  
Automation Laboratory



# **Energy Efficient Control of Bipedal Robot Locomotion in Dynamic Environments**

by

Alexandros Tanzanakis

Thesis Committee:

Professor Michalis Zervakis (Thesis Supervisor)

Professor George Stavrakakis

Dr. Nikolaos Bekiaris - Liberis

A thesis submitted in part fulfilment of the requirements for the  
degree of  
Diploma in Electrical & Computer Engineering of the  
Technical University of Crete,  
Chania, September 2016



## Abstract

Bipedal Robot Locomotion is considered as one of the toughest problems in Control Engineering. In particular, one of the most challenging problems today is the design of extremely energy efficient trajectories, which reflect exactly the constraints of each individual walking step of a biped robot, combined with an effective trajectory tracking control scheme. More specifically, the problem of design and effective tracking control of trajectories that obey the rules of human walking and have the energy efficiency of human locomotion - which is considered the most energy efficient type of walking - is in the spotlight of the robotics and control community particularly for the last year. Unfortunately, no major efforts have been made.

For the abovementioned reasons, in the current thesis, we propose a novel control system, called Decrease & Conquer Feedback Control. The proposed system consists of the Gait Generation and Trajectory Tracking Control Modules.

The Gait Generation Module consists of two Phases. The First Phase calculates walking trajectories for a simplified biped robot (a robot model with fewer degrees of freedom), and the Second Phase (called Energy Efficient Trajectory Synthesis and Verification) based on the calculated trajectories of the First Phase proceeds with the calculation of energy optimal trajectories for the complete biped robot. We implement two variants of the Gait Generation Module, based on two discretization methods: Direct Collocation and Discrete Mechanics.

The Trajectory Tracking Control Module deals with the effective tracking control of the energy-optimal trajectories, under missing velocity signals and disturbances, leading to minimal energy consumption.

The walking capabilities of the biped robot are evaluated through numerous experiments in a variety of terrains, including flat ground, downward and upward slopes, as well as walking downstairs and upstairs. Furthermore, we proceed with the experimental study of the energetics of the resulted bipedal robot walking.

The proposed system, turns out to be extremely effective. It provides the ability to synthesize energy efficient trajectories for the biped-with energy requirements comparable to human walking-, while it applies effective trajectory tracking control under the situation of missing velocities and disturbances, leading to minimal energy consumption. In comparison with the

related One Phase methods and high performance commercial solutions, the proposed system is proved to be a reliable, energy efficient and effective way for human-like biped robot locomotion in a variety of terrains and situations.

## **Acknowledgements**

First of all, I would like to thank wholeheartedly my thesis supervisor, Professor Michalis Zervakis, for his neverending trust, support and encouragement that provided me with the confidence to pursue research directions to my heart's desire.

I would also like to thank Professor George Stavrakakis and Dr. Nikolaos Bekiaris-Liberis for all the fruitful discussions, their encouragement and for accepting to be members of the thesis committee.

Last but not least, I would like to thank my family, for their encouragement, support and love all these years.



## Dedication

Dedicated to my parents, for their unconditional love and support, and for teaching me that wonderful things can come from hard work and the pursuit of knowledge.

‘Prudent men take care that hard events do not occur, brave men restore those occurred.’

*Pittacus of Mytilene*

# Contents

<b>Abstract</b>	<b>i</b>
<b>Acknowledgements</b>	<b>iii</b>
<b>1 Introduction</b>	<b>1</b>
1.1 Motivation and Objectives . . . . .	1
1.2 Related Work . . . . .	5
1.3 Contributions . . . . .	6
1.4 Thesis Outline . . . . .	7
<b>2 First Phase of the Gait Generation Module</b>	<b>10</b>
2.1 Introduction and Key Points of the First Phase . . . . .	10
2.2 Swing Phase of the 2-DOF Biped Robot for the Direct Collocation Method (Leg1=Stance, Leg2=Swing) . . . . .	14
2.2.1 Derivation of the Euler-Lagrange Equations of Motion . . . . .	14
2.2.2 Formulation of the Impact Map . . . . .	23
2.2.3 Conservation of the angular momentum . . . . .	24
2.2.4 Definition of Impact Surface . . . . .	28

2.3	Swing Phase of the 2-DOF Biped Robot using Discrete Mechanics (Leg1=Stance, Leg2=Swing) . . . . .	30
2.4	General Configuration of the Walking Terrain . . . . .	33
2.5	Derivation of the Gait Generation Problem for the First Phase . . . . .	35
<b>3</b>	<b>Second Phase of the Gait Generation Module</b>	<b>40</b>
3.1	Introduction and Key Points of the Second Phase . . . . .	40
3.2	Swing Phase of the 4-DOF Biped Robot for the Direct Collocation Method (Leg1 = Stance, Leg2 = Swing) . . . . .	43
3.3	Swing Phase of the 4-DOF Biped Robot using Discrete Mechanics (Leg 1 = Stance, Leg 2 = Swing) . . . . .	53
3.4	Modeling of Constraint Forces at Stance Foot . . . . .	58
3.4.1	Constraint Forces at Stance Foot during the Swing Phase (Leg1 = Stance, Leg2 = Swing) . . . . .	58
3.4.2	Constraint Forces at Stance Foot during the Push-Off Phase (Leg1 = Stance, Leg2 = Swing) . . . . .	60
3.5	The Impact Phase Redefined: Derivation of the Heel Strike and Push-Off Phases of Walking . . . . .	62
3.5.1	The Heel Strike Phase of Walking (Leg1 = Stance, Leg2 = Swing) . . . . .	63
3.5.2	The Push-Off Phase of Walking (Leg 1 = Stance, Leg 2 = Swing) . . . . .	70
3.5.3	The Cost Function for the Gait Generation Problem of the Second Phase . . . . .	73
3.6	Derivation of the Gait Generation Problem for the Second Phase . . . . .	76
3.7	Energy Efficient Trajectory Synthesis and Verification . . . . .	80
<b>4</b>	<b>Trajectory Tracking Control Module</b>	<b>84</b>
4.1	Introduction . . . . .	84

---

4.1.1	Control of Fully Actuated and Underactuated Systems . . . . .	85
4.1.2	Introduction to Computed Torque Control . . . . .	87
4.2	Bipedal Robot Control with availability of velocity signals and absence of disturbances . . . . .	91
4.2.1	Partial Feedback Linearization Control of the Swing Phase . . . . .	91
4.2.2	Computed Torque Control of the Push-Off Phase . . . . .	95
4.2.3	Partial Feedback Linearization Control of the Heel Strike Phase . . . . .	96
4.3	Velocity and Disturbance Observers for Estimation of Velocity Signals and Disturbances . . . . .	100
<b>5</b>	<b>Simulation &amp; Results</b>	<b>103</b>
5.1	Introduction . . . . .	103
5.2	Forward Walking Experiment . . . . .	106
5.3	Downward Slope Walking Experiment . . . . .	115
5.4	Upward Slope Walking Experiment . . . . .	125
5.5	Down/Up Stairs Walking Experiment . . . . .	135
5.6	Energetics of Bipedal Robot Locomotion . . . . .	145
<b>6</b>	<b>Conclusion and Future Work</b>	<b>162</b>
<b>7</b>	<b>Bibliography</b>	<b>164</b>
<b>8</b>	<b>Appendix A: Modeling &amp; Control of Lagrangian Mechanical Systems</b>	<b>169</b>
8.1	Analytical Mechanics / Lagrangian mechanics . . . . .	169
8.1.1	Introduction . . . . .	169

8.1.2	Holonomic constraints and degrees of freedom . . . . .	170
8.1.3	D'Alembert's principle . . . . .	172
8.1.4	Hamilton's Principle . . . . .	175
8.1.5	Lagrangian Mechanical Systems with Forcing and Control . . . . .	176
8.1.6	Standard Form of the Euler-Lagrange Equations in a kinematic chain . .	179
8.2	Discrete Mechanics . . . . .	181
8.3	Geometric Optimal Control of Lagrangian Mechanical Systems . . . . .	185
8.3.1	The Continuous Case . . . . .	185
8.3.2	The discrete case . . . . .	187
8.3.3	Numerical Optimization Methods for Trajectory Generation . . . . .	189
8.3.4	Forward-Dynamics Based Optimization . . . . .	190
8.3.5	Inverse-Dynamics Based Approach - The Discrete Mechanics Approach .	194
<b>9</b>	<b>Appendix B: First Phase of the Gait Generation Module</b>	<b>197</b>
9.1	Analytical Expressions for the Swing Phase using Discrete Mechanics (Leg1=Stance, Leg2=Swing) . . . . .	197
9.2	Swing Phase for the Direct Collocation Method (Leg1 = Swing, Leg2=Stance) .	200
9.2.1	Derivation of the Euler-Lagrange Equations of Motion . . . . .	200
9.2.2	Formulation of the Impact Map . . . . .	207
9.2.3	Conservation of the angular momentum . . . . .	207
9.2.4	Definition of Impact Surface . . . . .	212
9.3	Swing Phase using Discrete Mechanics (Leg1=Swing, Leg2=Stance) . . . . .	214

<b>10 Appendix C: Second Phase of the Gait Generation Module</b>	<b>220</b>
10.1 Swing Phase for the Direct Collocation Method (Leg1 = Swing, Leg2 = Stance)	220
10.2 Analytical Expressions of Swing Phase using Discrete Mechanics(Leg 1= Stance, Leg 2 =Swing) . . . . .	225
10.3 Swing Phase using Discrete Mechanics (Leg 1= Swing, Leg 2 =Stance) . . . . .	233
10.4 Modeling of Constraint Forces at Stance Foot . . . . .	242
10.4.1 Constraint Forces at Stance Foot during the Swing Phase (Leg1 = Swing, Leg2 = Stance) . . . . .	242
10.4.2 Constraint Forces at Stance Foot during the Push-Off Phase (Leg1 = Swing, Leg2 = Stance) . . . . .	243
10.5 The Impact Phase Redefined: Derivation of the Heel Strike and Push-Off Phases of Walking . . . . .	244
10.5.1 The Heel Strike Phase of Walking (Leg1 = Swing, Leg2 = Stance) . . . .	244
10.5.2 The Push-Off Phase of Walking (Leg 1 = Swing, Leg 2 = Stance) . . . .	245
<b>11 Appendix D: Implemented Optimization Algorithms for the Gait Generation Problems</b>	<b>246</b>
11.1 Introduction . . . . .	246
11.2 A FSQP Algorithm for the Discrete Mechanics based Gait Generation Problems	247
11.3 A Nonlinear Interior-Point Algorithm for the Direct Collocation based Gait Gen- eration Problems . . . . .	254



# List of Tables



# List of Figures

1.1	<i>A 2-link, 4-DOF biped robot walking on a downward slope with angle <math>\theta</math></i> . . . . .	3
1.2	<i>General block diagram of the proposed system.</i> . . . . .	5
1.3	<i>Various types of walking terrains: flat ground (a), downward slopes (b), upward slopes (c), downstairs/upstairs (d).</i> . . . . .	6
2.1	<i>The simplified, 2-DOF biped robot walking on a downward slope with angle <math>\theta</math>.</i> . .	12
2.2	<i>Assignment of origins for the coordinate frames of the robot.</i> . . . . .	14
2.3	<i>Quantities used for the definition of the Impact Surface of the robot.</i> . . . . .	28
2.4	<i>Walking surfaces for the biped robot.</i> . . . . .	34
3.1	<i>Assignment of origins for the coordinate frames of the robot.</i> . . . . .	44
5.1	<i>Simulation Parameters.</i> . . . . .	104
5.2	<i>Average Cost of Transport (ACOT) for the Forward Walking Experiment.</i> . . . .	107
5.3	<i>Lower and Upper Bounds of Cost of Transport (COT) for the Forward Walking Experiment.</i> . . . . .	108
5.4	<i>Energy Savings of Decrease and Conquer Variants in comparison with One Phase Related Variants, for the Forward Walking Experiment (Percentage).</i> . . . . .	109
5.5	<i>Energy Savings of Decrease and Conquer Variants in comparison with SNOPT, for the Forward Walking Experiment (Percentage).</i> . . . . .	110

5.6	<i>Desired and actual angles during the Forward Walking Experiment - Decrease &amp; Conquer Feedback Control utilizing Direct Collocation. . . . .</i>	111
5.7	<i>Position error during the Forward Walking Experiment - Decrease &amp; Conquer Feedback Control utilizing Direct Collocation. . . . .</i>	111
5.8	<i>Position error during the Forward Walking Experiment - Decrease &amp; Conquer Feedback Control utilizing Direct Collocation. . . . .</i>	112
5.9	<i>Real and estimated angular velocities during the Forward Walking Experiment - Decrease &amp; Conquer Feedback Control utilizing Direct Collocation. . . . .</i>	112
5.10	<i>Angular velocity errors of the Leg 1 during the Forward Walking Experiment - Decrease &amp; Conquer Feedback Control utilizing Direct Collocation. . . . .</i>	113
5.11	<i>Angular velocity errors of the Leg 2 during the Forward Walking Experiment - Decrease &amp; Conquer Feedback Control utilizing Direct Collocation. . . . .</i>	113
5.12	<i>Control Signals <math>\tau_1</math>, <math>\tau_2</math> during the Forward Walking Experiment - Decrease &amp; Conquer Feedback Control utilizing Direct Collocation. . . . .</i>	114
5.13	<i>Ground Reaction Forces during the Forward Walking Experiment - Decrease &amp; Conquer Feedback Control utilizing Direct Collocation. . . . .</i>	115
5.14	<i>Push-Off Impulses during the Forward Walking Experiment - Decrease &amp; Conquer Feedback Control utilizing Direct Collocation. . . . .</i>	116
5.15	<i>Average Cost of Transport (ACOT) for the Downward Slope Walking Experiment.</i>	117
5.16	<i>Lower and Upper Bounds of Cost of Transport (COT) for the Downward Slope Walking Experiment. . . . .</i>	118
5.17	<i>Energy Savings of Decrease and Conquer Variants in comparison with One Phase Related Variants, for the Downward Slope Walking Experiment (Percentage). . .</i>	118
5.18	<i>Energy Savings of Decrease and Conquer Variants in comparison with SNOPT, for the Downward Slope Walking Experiment (Percentage). . . . .</i>	119
5.19	<i>Desired and actual angles during the Downward Slope Walking Experiment - Decrease &amp; Conquer Feedback Control utilizing Direct Collocation. . . . .</i>	120

5.20	<i>Position error during the Downward Slope Walking Experiment - Decrease &amp; Conquer Feedback Control utilizing Direct Collocation. . . . .</i>	120
5.21	<i>Position error during the Downward Slope Walking Experiment - Decrease &amp; Conquer Feedback Control utilizing Direct Collocation. . . . .</i>	121
5.22	<i>Real and estimated angular velocities during the Downward Slope Walking Experiment - Decrease &amp; Conquer Feedback Control utilizing Direct Collocation. . .</i>	122
5.23	<i>Angular velocity errors of the Leg 1 during the Downward Slope Walking Experiment - Decrease &amp; Conquer Feedback Control utilizing Direct Collocation. . . .</i>	122
5.24	<i>Angular velocity errors of the Leg 2 during the Downward Slope Walking Experiment - Decrease &amp; Conquer Feedback Control utilizing Direct Collocation. . . .</i>	123
5.25	<i>Control Signals <math>\tau_1</math>, <math>\tau_2</math> during the Downward Slope Walking Experiment - Decrease &amp; Conquer Feedback Control utilizing Direct Collocation. . . . .</i>	123
5.26	<i>Ground Reaction Forces during the Downward Slope Walking Experiment - Decrease &amp; Conquer Feedback Control utilizing Direct Collocation. . . . .</i>	124
5.27	<i>Push-Off Impulses during the Downward Slope Walking Experiment - Decrease &amp; Conquer Feedback Control utilizing Direct Collocation. . . . .</i>	125
5.28	<i>Average Cost of Transport (ACOT) for the Upward Slope Walking Experiment. .</i>	126
5.29	<i>Lower and Upper Bounds of Cost of Transport (COT) for the Upward Slope Walking Experiment. . . . .</i>	127
5.30	<i>Energy Savings of Decrease and Conquer Variants in comparison with One Phase Related Variants, for the Upward Slope Walking Experiment (Percentage). . . . .</i>	128
5.31	<i>Energy Savings of Decrease and Conquer Variants in comparison with SNOPT, for the Upward Slope Walking Experiment (Percentage). . . . .</i>	129
5.32	<i>Desired and actual angles during the Upward Slope Walking Experiment - Decrease &amp; Conquer Feedback Control utilizing Direct Collocation. . . . .</i>	130
5.33	<i>Position error during the Upward Slope Walking Experiment - Decrease &amp; Conquer Feedback Control utilizing Direct Collocation. . . . .</i>	130

5.34	<i>Position error during the Upward Slope Walking Experiment - Decrease &amp; Conquer Feedback Control utilizing Direct Collocation. . . . .</i>	131
5.35	<i>Real and estimated angular velocities during the Upward Slope Walking Experiment - Decrease &amp; Conquer Feedback Control utilizing Direct Collocation. . . . .</i>	131
5.36	<i>Angular velocity errors of the Leg 1 during the Upward Slope Walking Experiment - Decrease &amp; Conquer Feedback Control utilizing Direct Collocation. . . . .</i>	132
5.37	<i>Angular velocity errors of the Leg 2 during the Upward Slope Walking Experiment - Decrease &amp; Conquer Feedback Control utilizing Direct Collocation. . . . .</i>	132
5.38	<i>Control Signals <math>\tau_1</math>, <math>\tau_2</math> during the Downward Slope Walking Experiment - Decrease &amp; Conquer Feedback Control utilizing Direct Collocation. . . . .</i>	133
5.39	<i>Ground Reaction Forces during the Upward Slope Walking Experiment - Decrease &amp; Conquer Feedback Control utilizing Direct Collocation. . . . .</i>	134
5.40	<i>Push-Off Impulses during the Upward Slope Walking Experiment - Decrease &amp; Conquer Feedback Control utilizing Direct Collocation. . . . .</i>	134
5.41	<i>Average Cost of Transport (ACOT) for the Down/Up Stairs Walking Experiment.</i>	136
5.42	<i>Lower and Upper Bounds of Cost of Transport (COT) for the Down/Up Stairs Walking Experiment. . . . .</i>	137
5.43	<i>Energy Savings of Decrease and Conquer Variants in comparison with One Phase Related Variants, for the Down/Up Stairs Walking Experiment (Percentage). . .</i>	138
5.44	<i>Energy Savings of Decrease and Conquer Variants in comparison with SNOPT, for the Down/Up Stairs Walking Experiment (Percentage). . . . .</i>	139
5.45	<i>Desired and actual angles during the Down/Up Stairs Walking Experiment - Decrease &amp; Conquer Feedback Control utilizing Direct Collocation. . . . .</i>	140
5.46	<i>Position error during the Down/Up Stairs Walking Experiment - Decrease &amp; Conquer Feedback Control utilizing Direct Collocation. . . . .</i>	140
5.47	<i>Position error during the Down/Up Stairs Walking Experiment - Decrease &amp; Conquer Feedback Control utilizing Direct Collocation. . . . .</i>	141

5.48	<i>Real and estimated angular velocities during the Upward Slope Walking Experiment - Decrease &amp; Conquer Feedback Control utilizing Direct Collocation. . . . .</i>	141
5.49	<i>Angular velocity errors of the Leg 1 during the Upward Slope Walking Experiment - Decrease &amp; Conquer Feedback Control utilizing Direct Collocation. . . . .</i>	142
5.50	<i>Angular velocity errors of the Leg 2 during the Upward Slope Walking Experiment - Decrease &amp; Conquer Feedback Control utilizing Direct Collocation. . . . .</i>	142
5.51	<i>Control Signals <math>\tau_1</math>, <math>\tau_2</math> during the Down/Up Stairs Walking Experiment - Decrease &amp; Conquer Feedback Control utilizing Direct Collocation. . . . .</i>	143
5.52	<i>Ground Reaction Forces during the Down/Up Stairs Walking Experiment - Decrease &amp; Conquer Feedback Control utilizing Direct Collocation. . . . .</i>	144
5.53	<i>Push-Off Impulses during the Down/Up Stairs Walking Experiment - Decrease &amp; Conquer Feedback Control utilizing Direct Collocation. . . . .</i>	144
5.54	<i>Parameters for the current study and experiments. . . . .</i>	146
5.55	<i>The effects of <math>R_m</math> on COT with fixed <math>R_l=0.3</math> and <math>V=0.4</math>. . . . .</i>	147
5.56	<i>The effects of <math>R_m</math> on COT with fixed <math>R_l=0.3</math> and <math>V=0.4</math> (Sectional Plot). . . . .</i>	148
5.57	<i>Effect of slope angle <math>\theta</math> in the COT of Figures 5.55 and 5.56. . . . .</i>	149
5.58	<i>The effects of <math>R_m</math> on COT with fixed <math>R_l=0.3</math> and <math>V=0.6</math>. . . . .</i>	150
5.59	<i>The effects of <math>R_m</math> on COT with fixed <math>R_l=0.3</math> and <math>V=0.6</math> (Sectional Plot). . . . .</i>	151
5.60	<i>Effect of slope angle <math>\theta</math> in the COT of Figures 5.58 and 5.59. . . . .</i>	151
5.61	<i>The effects of <math>R_m</math> on COT with fixed <math>R_l=0.6</math> and <math>V=0.4</math>. . . . .</i>	152
5.62	<i>The effects of <math>R_m</math> on COT with fixed <math>R_l=0.6</math> and <math>V=0.4</math>(Sectional Plot). . . . .</i>	152
5.63	<i>Effect of slope angle <math>\theta</math> in the COT of Figures 5.61 and 5.62. . . . .</i>	153
5.64	<i>The effects of <math>R_m</math> on COT with fixed <math>R_l=0.6</math> and <math>V=0.6</math>. . . . .</i>	153
5.65	<i>The effects of <math>R_m</math> on COT with fixed <math>R_l=0.6</math> and <math>V=0.6</math> (Sectional Plot). . . . .</i>	154

5.66	<i>Effect of slope angle theta in the COT of Figures 5.64 and 5.65.</i>	154
5.67	<i>The effects of <math>R_l</math> on COT with fixed <math>R_m=0.3</math> and <math>V=0.4</math>.</i>	155
5.68	<i>The effects of <math>R_m</math> on COT with fixed <math>R_m=0.3</math> and <math>V=0.4</math> (Sectional Plot).</i>	155
5.69	<i>Effect of slope angle theta in the COT of Figures 5.67 and 5.68.</i>	156
5.70	<i>The effects of <math>R_l</math> on COT with fixed <math>R_m=0.3</math> and <math>V=0.6</math>.</i>	156
5.71	<i>The effects of <math>R_m</math> on COT with fixed <math>R_m=0.3</math> and <math>V=0.6</math> (Sectional Plot).</i>	157
5.72	<i>Effect of slope angle theta in the COT of Figures 5.70 and 5.71.</i>	157
5.73	<i>The effects of <math>R_l</math> on COT with fixed <math>R_m=0.5</math> and <math>V=0.4</math>.</i>	158
5.74	<i>The effects of <math>R_m</math> on COT with fixed <math>R_m=0.5</math> and <math>V=0.4</math> (Sectional Plot).</i>	158
5.75	<i>Effect of slope angle theta in the COT of Figures 5.73 and 5.74.</i>	159
5.76	<i>The effects of <math>R_l</math> on COT with fixed <math>R_m=0.5</math> and <math>V=0.6</math>.</i>	160
5.77	<i>The effects of <math>R_m</math> on COT with fixed <math>R_m=0.5</math> and <math>V=0.6</math> (Sectional Plot).</i>	160
5.78	<i>Effect of slope angle theta in the COT of Figures 5.76 and 5.77.</i>	161
9.1	<i>Assignment of origins for the coordinate frames of the biped.</i>	201
9.2	<i>Different quantities used for the definition of the impact surface of the robot.</i>	212

# Chapter 1

## Introduction

### 1.1 Motivation and Objectives

Bipedal Robot Locomotion is one of the toughest problems in Control Engineering. The control of biped walking remains a difficult problem due to high dimensionality, nonlinearity, the intermittent contact between the feet and the ground, and constraints on kinematics and dynamics, such as joint limitations, the foot clearance requirement, and foot-ground contact conditions [1].

A common approach to biped walking control is through tracking periodic reference trajectories. These trajectories can be computed based on the concept of ZMP (Zero Moment Point) [1], where emphasis is placed on enlarging the stability margin during gait planning [2, 3]. Trajectories can also be computed based on the LIPM (Linear Inverted Pendulum Model) [4]. By simplifying the dynamics to a linear system, modern control techniques can be used to plan gaits [5 - 7]. Feedback control methods, such as PID controllers, can be used to track the reference trajectories [2, 8 - 10]. However, the stability obtained with the use of periodic trajectories may be limited and even small perturbations may lead to a fall [11]. This is because a unified periodic reference trajectory for all the walking process of a robot is not the only requirement; various terrain variations and walking step characteristics, unknown or noisy measurements, possibly high energy requirements of the periodic trajectory (in most cases, the

energy consumption of the trajectory is not even considered as a constraint) and disturbances affect the suitability of the proposed trajectory under tracking, resulting of course in poor tracking performance. In addition, large joint torques are needed if a large deviation from the reference trajectories occurs [11].

One of the most challenging problems today is the design of extremely energy efficient trajectories, which reflect exactly the constraints of each individual walking step of a biped robot, combined with an effective tracking control scheme. More specifically, the problem of design and effective tracking control of trajectories that obey the rules of human walking and have the energy efficiency of human locomotion -which is considered the most energy efficient type of walking- is in the spotlight of the robotics and control community particularly for the last year. Unfortunately, no major efforts have been made. The problem of trajectory generation, considered mostly as an optimal control problem, due to the numerous and complex constraints involved, as well as the ineffective developed optimization algorithms, leads to poor or suboptimal solutions, which may produce an accepted walking trajectory, but it does not inherit biomechanical properties neither has its energy consumption minimized (when an energy consumption quantity is considered as a cost function).

For the abovementioned reasons, in the current thesis, we propose a novel control system, called Decrease & Conquer Feedback Control. Before proceeding with a brief description of the system, we will now refer to the model of the biped robot that will be used throughout the thesis.

The 2-link biped robot is one of the most important walking devices and is a standard benchmark for studying gaits. The robot consists of two links, or legs, connected by a revolute hip joint that allows for rotational motion in the two-dimensional plane. Figure 1.1 illustrates the planar biped along with some important parameters. The orientation of the legs are described, respectively, by the absolute angles  $q_1$  and  $q_2$  with positive direction defined counter-clockwise. The leg that is in contact with the ground is called stance leg, while the other one is called swing leg. The Cartesian Coordinates of the stance foot are described by  $q_3, q_4$ . Those generalized coordinates  $(q_1, q_2, q_3, q_4)$  characterize four degrees of freedom. The biped is walking

forwards, traveling up or down a slope with constant angle  $\theta$  measured from the horizontal, or is walking on a terrain that involves flat ground and down/up stairs walking. Each leg link is identical with total length  $l = a + b$  from hip joint to feet. The center of mass of each of the legs is located at the distances  $b$  and  $a$  from the hip and feet, respectively. The masses of the Legs are  $m_1$ ,  $m_2$  and  $M$  is the mass of the hip joint connecting each leg. The actuators that will be used are three: two rotational actuators (for applying torques to the two legs, thus affecting the generalized coordinates  $q_1$ ,  $q_2$ ) and one linear actuator (for applying impulsive forces to the Cartesian Coordinates of the stance foot, thus affecting  $q_3$ ,  $q_4$ ).

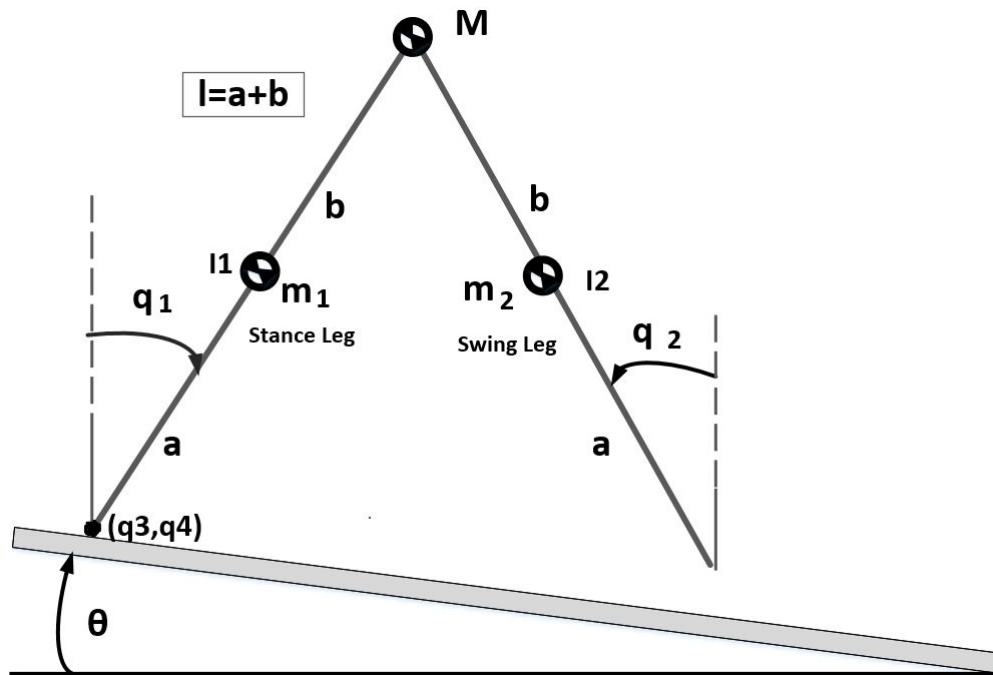


Figure 1.1: A 2-link, 4-DOF biped robot walking on a downward slope with angle  $\theta$

The proposed system consists of the Gait Generation and Trajectory Tracking Control modules. The Gait Generation Module consists of two Phases. The First Phase calculates walking trajectories for a simplified biped robot (a robot model with fewer degrees of freedom, in our case, with only two degrees of freedom), and the Second Phase (called Energy Efficient Trajectory Synthesis and Verification) based on the calculated trajectories of the First Phase proceeds with the calculation of energy optimal trajectories for the complete 4-DOF biped robot. As we can easily see, the Gait Generation Module is based on a Decrease and Conquer approach.

We will implement two variants of the Gait Generation Module, based on two discretization

methods: Direct Collocation and Discrete Mechanics. These methods have been tested only for the case of flat ground walking.

On the one hand, Discrete Mechanics proceeds with the discretization of the related principles of mechanical systems (e.g. Hamilton's Principle, Lagrange-D'Alembert principle, Euler-Lagrange Equations etc.), leading to discretized equations of motion, where the first and second derivative of the configuration of the system are approximated by finite differences. In addition, Boundary Conditions are inserted in order for the discretized system to continue obeying the laws of physics on the discrete domain, from start to finish.

On the other hand, Direct Collocation proceeds with the approximation of the states as continuously differentiable and piecewise defined as cubic polynomials between two consecutive grid points. In addition, the controls are chosen as piecewise linear interpolating functions between two consecutive grid points.

As we will see and on the simulation experiments on Chapter 5, the Decrease and Conquer approach utilizing Direct Collocation leads always to trajectories with lower energy consumption than the approach utilizing Discrete Mechanics.

Please refer to Appendix A (Subchapters 8.2, 8.3.3) for the complete description of these methods, as well as for the advantages and disadvantages of each one of them.

The Trajectory Tracking Control Module deals with the effective tracking of the calculated energy-optimal trajectories, under missing velocity signals and disturbances.

The walking of the biped robot will be evaluated in a variety of terrains, including flat ground, downward and upward slopes, as well as walking downstairs and upstairs.

The proposed system, as we will see throughout the thesis, proves to be extremely effective. It provides the ability to synthesize energy efficient trajectories for the biped-with energy consumption comparable to human walking-, while applying effective trajectory tracking control under missing velocities and disturbances. In comparison with conventional One Phase methods and high performance commercial solvers, the proposed system is proved to be a reliable, extremely energy efficient and effective way for human-like biped robot locomotion in a variety of terrains and situations.

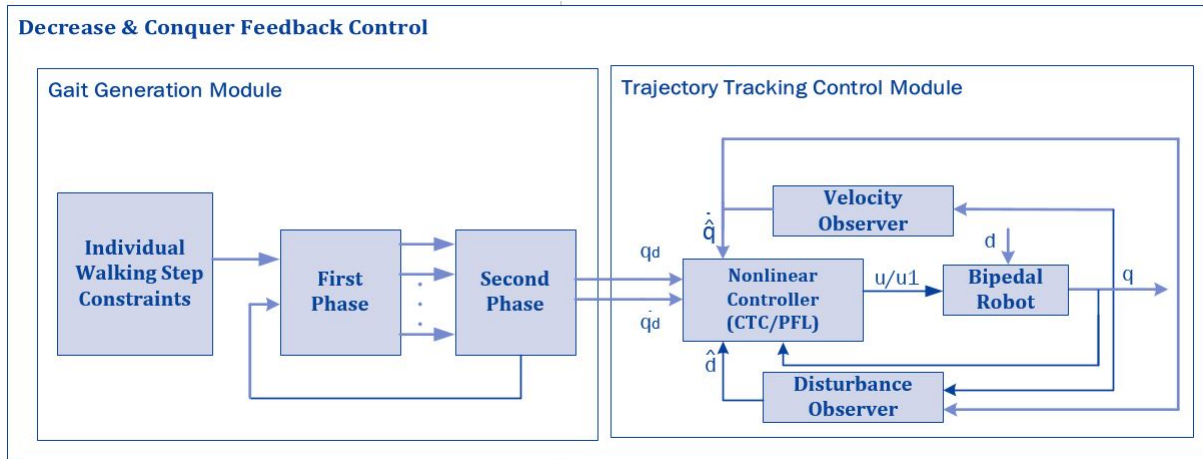


Figure 1.2: General block diagram of the proposed system.

## 1.2 Related Work

The research area of Bipedal Robot Locomotion has gained major attention and has been studied extensively in the past years, leading to various approaches (e.g. Zero Moment Point [1], Hybrid Zero Dynamics [21], etc.). However, all these methods utilize periodic reference trajectories, without taking into account the factor of energy efficiency and the specific requirements of a current walking step.

No one till the time of writing the thesis has proposed a Decrease and Conquer Approach for trajectory generation and optimization. Dembia[12] has worked on a preliminary trajectory generation method based on Direct Collocation, for the case of forward walking of point-mass biped, with not so satisfactory results (the gait generated was not looked like proper walking and it was unstable). Pekarek et al.[13] and Sun et al [25] have developed a gait generation method using Discrete Mechanics for a compass gait biped only for the case of forward walking and for a very limited number of walking steps, with satisfactory results in most cases of the experiments.

In the current thesis, we proceed with the implementation of the proposed system utilizing both Direct Collocation and Discrete Mechanics, proving experimentally that these methods can be used for stable and natural gait generation under various conditions and walking terrains.

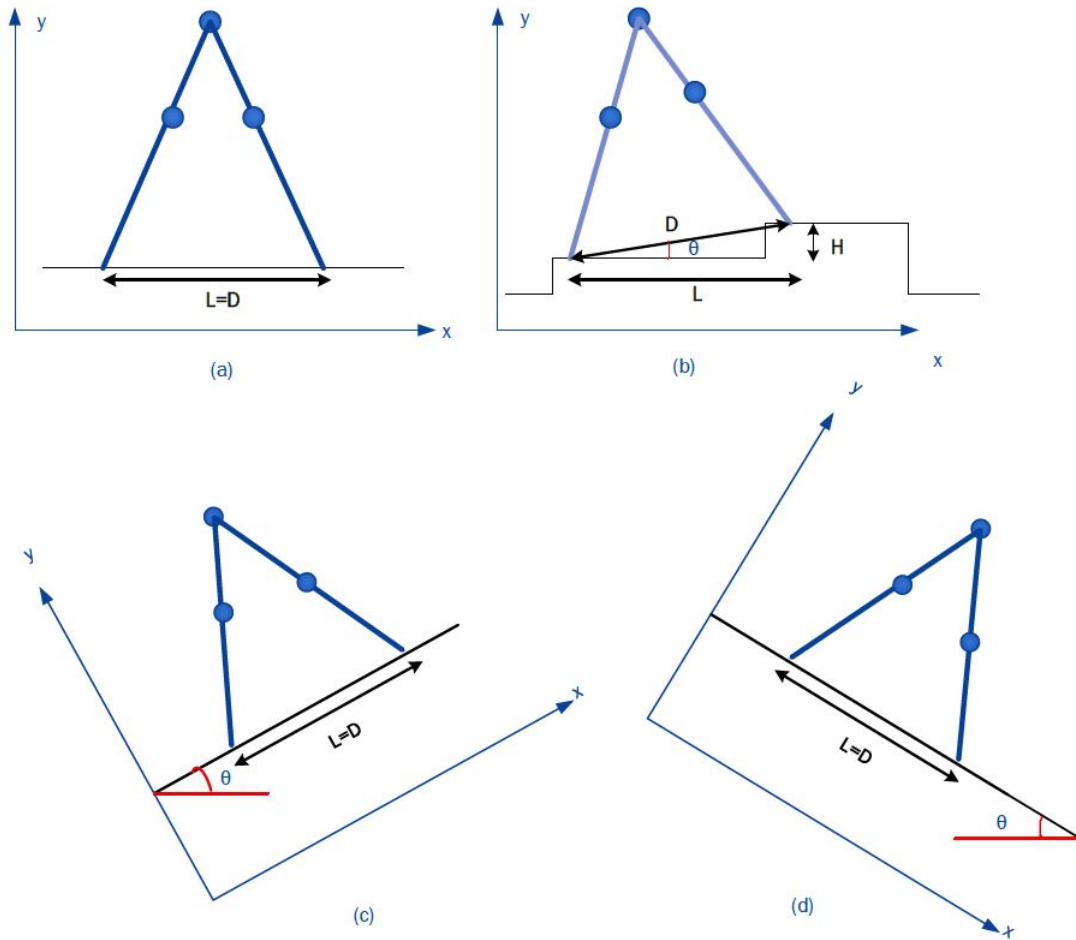


Figure 1.3: *Various types of walking terrains: flat ground (a), downward slopes (b), upward slopes (c), downstairs/upstairs (d).*

### 1.3 Contributions

In the current thesis, for the first time in the related bibliography, we propose and implement the idea of a Decrease and Conquer approach for Gait Generation. In particular, we propose a design in which, for the calculation of energy-optimal trajectories to be followed by a biped robot, we proceed with the solution of two Gait Generation problems. The first Gait Generation problem (First Phase of the Gait Generation Module) refers to the calculation of a trajectory for a simplified biped robot model, which has fewer degrees of freedom. The second Gait Generation Problem (Second Phase of the Gait Generation Module) refers to the calculation of energy-optimal trajectories for the complete biped robot model, using the calculated trajectories from the solution of the First Gait Generation Problem. The last is achieved with the implementation

of a novel method called Energy Efficient Trajectory Synthesis and Verification. This modeling approach proved to be crucial for the effectiveness of the proposed system.

In addition, we implement the related One Phase approaches using Discrete Mechanics and Direct Collocation as discretization methods and prove for the first time that they can be used for stable and natural gait generation in a variety of terrains, including flat ground, downward and upward slopes and walking downstairs and upstairs. Till the time of writing the thesis, these discretization methods have been tested only for the case of forward walking.

Furthermore, under the Decrease and Conquer framework we experimentally prove that, using the abovementioned discretization methods, we can synthesize energy-optimal trajectories for the biped robot, achieving the energy consumption of human locomotion.

Regarding the Trajectory Tracking Control, we develop an alternative approach. Based on whether a specific Gait Phase is considered as a fully-actuated or underactuated phase, we use either Computed Torque Control or Partial Feedback Linearization Control, respectively. Till the time of writing the thesis, in the related bibliography, only the Swing Phase of the biped was being controlled. This is due to the fact that in most cases the Push-Off and Heel Strike Phases were not modelled. In the thesis, modeling all walking phases gives the opportunity to effectively track the calculated energy optimal trajectories under missing velocity signals and disturbances (e.g. actuator friction). The last is done with the additional design of the related velocity and disturbance observers and their integration in the controllers.

Finally, we proceed with the testing and verification of the effectiveness of the proposed system under different conditions and walking terrains.

## 1.4 Thesis Outline

In Chapter 2, we develop the First Phase of the Gait Generation Module. Firstly, we derive the equations of motion for the Swing and Impact Phases of the simplified, 2-DOF Biped Robot, based on the two abovementioned discretization methods, extensively. In addition,

we derive the General Configuration of the walking terrain for the simplified biped, which will obviously be the same as for the complete, 4-DOF biped robot. Finally, we derive the Gait Generation Problem of the First Phase as a finite dimensional nonlinear optimal control problem. The solution of the Gait Generation Problem leads to the calculation of a trajectory for the simplified biped, which will be utilized by the Second Phase for the calculation of the energy optimal trajectory for the complete 4-DOF biped.

In Chapter 3, we develop the Second Phase of the Gait Generation Module. Firstly, we derive the equations of motion for the Swing, Push-Off and Heel Strike Phases of the complete, 4-DOF Biped robot, based on the abovementioned discretization methods, in great detail. Then, we derive the Gait Generation problem of the Second Phase also as a finite dimensional optimal control problem. Finally, we develop the core function of the Second Phase and the actual idea of the Decrease and Conquer approach, called Energy Efficient Trajectory Synthesis and Verification. Utilizing the calculated trajectory of the First Phase, Energy Efficient Trajectory Synthesis and Verification calculates the final, energy-optimal trajectory to be followed by the complete biped.

In Chapter 4, we develop the Trajectory Tracking Control Module. First of all, we develop the case where there is availability of all measurements and there are no disturbances to the system. Based on whether a walking phase is considered as fully actuated or underactuated ( a complete, detailed description is given in Chapter 4), we develop and apply control laws based on Computed Torque Control and Partial Feedback Linearization, respectively. Then, assuming that the velocity signals are not available and there are disturbances (e.g. actuator friction) to the system, we design velocity and disturbance observers, which are integrated in the abovementioned control laws.

In Chapter 5, we present four major experiments in great detail for all the four tested walking terrains (e.g. flat ground walking, downward slope walking, upward slope walking, and walking downstairs and upstairs). For each case of walking terrain, we compare the energy efficiency of the proposed Decrease and Conquer Gait Generation (utilizing Direct Collocation and Discrete Mechanics) with One Phase methods (utilizing also Direct Collocation and Discrete Mechan-

ics), and a high performance, commercial solver, called SNOPT. The Decrease and Conquer Approach turns out to be the most energy efficient method at all carried experiments, leading to trajectories with the minimal possible energy consumption. Then, for the Decrease and Conquer approach, graphs of the most important measurements are shown, emphasizing the features of the resulted gait which are also present on human locomotion, as well as the effectiveness of the proposed system. Finally, after numerous walking experiments, we carry out an experimental study on the energetics of the resulted biped walking.

For those readers who are not familiar with the theory of modeling and control of Lagrangian Mechanical Systems, it is better to have firstly a look on the Appendix A (Chapter 7), in which a revision on the most fundamental topics is being carried out.

# Chapter 2

## First Phase of the Gait Generation Module

### 2.1 Introduction and Key Points of the First Phase

- **Brief Analysis and Assumptions of the First Phase**

As we have mentioned on Chapter 1, the Gait Generation Module of the Decrease & Conquer-Based Feedback Control (D&C-BFC) consists of two Phases. The First Phase deals with the natural, stable, gait generation problem on general terrain of the simplified, 2-DOF biped robot.

The complete biped robot has four degrees of freedom (the two degrees of freedom refer to the generalized coordinates (angles)  $q_1^{(i)}$  and  $q_2^{(i)}$  of the legs during the  $i - th$  swing phase (during the  $i - th$  walking step,  $i = 1, \dots, H$ ) and the other two refer to the generalized Cartesian coordinates of the stance foot) and uses three actuators (two rotational joint torques  $\tau_1^{(i)}$ ,  $\tau_2^{(i)}$  at the hip, which are required for the rotational motion of the two legs at the  $i - th$  walking step, and one linear actuator for applying linear (impulsive) forces at each leg during the Push Off Phase, as we will see extensively at Chapter 3.

The simplified biped robot, which is being developed and used throughout the current Chapter, is a robot with just two degrees of freedom (the generalized coordinates (angles)  $q_1^{(i)}$  and  $q_2^{(i)}$  of

the legs during the  $i$  –  $th$  walking step) and the two rotational actuators (the rotational joint torques  $\tau_1^{(i)}$ ,  $\tau_2^{(i)}$  at the hip).

In the current chapter, we develop the First Phase of the Gait Generation Module. Firstly, the equations of motion that describe the walking phases of the 2-DOF Biped Robot (Swing Phase and Impact Phase) are derived. The derived equations of motion will refer to the case where the Leg 1 is the Stance Leg and the Leg 2 is the Swing Leg. For the case where the Leg 1 is the Swing Leg and the Leg 2 is the Stance Leg, please refer to Appendix B (Chapter 8). Then, we formulate the gait generation problem as a finite dimensional nonlinear optimal control problem. For the implemented optimization algorithms for the solution of the Gait Generation Problems, please refer to Appendix D (Chapter 11). In addition, we will derive the walking terrain of the robot that it will obviously be the same for the second phase of our control system.

We develop and evaluate two variants of the of the Gait Generation Module, based on two discretization methods: Direct Collocation and Discrete Mechanics. In order to numerically solve a continuous-time, infinite-dimensional optimal control problem, we have to transform it into a discretized, finite-dimensional optimal control problem.

For the First Phase of the Gait Generation Module, we make the following assumptions for the biped robot:

1. The stance leg is rigidly connected to the ground during a complete step of the walking gait, meaning that each point of the robot can be uniquely described by the two angles  $q_1^{(i)}$ ,  $q_2^{(i)}$ .
2. The robot has point feet that does not experience slipping or sliding on the ground.
3. The biped robot moves in two dimensions.
4. The swing leg hits the ground with completely inelastic collision.
5. The legs and the hip are not considered to be point masses and the moment of inertia  $I$  around their centers of mass does not equal zero.

#### • Robot Modeling Approach

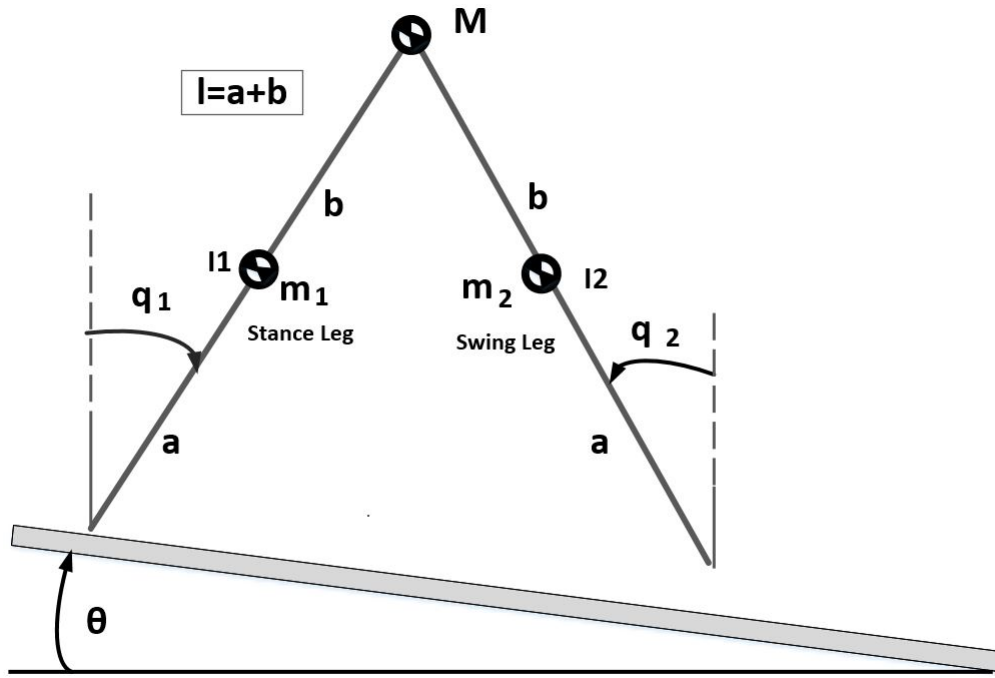


Figure 2.1: The simplified, 2-DOF biped robot walking on a downward slope with angle  $\theta$ .

In this thesis, we implement a step-to-step modeling approach for bipedal robot locomotion utilizing both variants, making the design more accurate by dividing the walking process of the robot to a total number of walking steps which has to make, rather than just letting the models describe the whole walking process.

This initial discretization procedure is not done at random. As we can see in Appendix A (Chapter 8), in order to numerically solve a continuous-time, infinite-dimensional optimal control problem, we have to transform it into a discretized finite-dimensional optimal control problem. Hence, instead of just waiting to reach the stage of the optimization to discretize the continuous-time gait generation problem with a discretization method, we will utilize the nature of the final finite dimensional optimal control problem from the very first moment of the continuous-time modeling.

More specifically, we define that each walking step consists of  $N$  time steps. Furthermore, we define that the first time step ( $t_1$ ) of each walking step starts the execution of the walking step (in other words, the execution of the swing phase), as well as that the collision of the swing leg on the ground (Impact Phase for the First Phase, Heel Strike Phase for the Second Phase) takes place in the last time step ( $t_N$ ) of each walking step.

Furthermore, in the Discrete Mechanics Based approach, due to the derivation of the Discrete Lagrangian through the direct discretization of the Continuous Lagrangian, the discretization process is done by default.

Regarding to the notation of all the parameters (e.g. states, angular coordinates/velocities/accelerations, control inputs, constrained forces) in the discretized setting, assuming that a walking step consists of  $N$  time steps, then when we see the mathematical representation  $x_{(1,k)}^{(i)}$  for instance, we refer to the value of the variable  $x_1$  for  $t = N(i-1)h + (k-1)h$  sec. Thus,  $x_{(1,k)}^{(i)} = x_1(t = N(i-1)h + (k-1)h$  sec),  $x_k^{(i)} = x(t = N(i-1)h + (k-1)h$  sec),  $q_{(1,k)}^{(i)} = q_1(t = N(i-1)h + (k-1)h$  sec),  $q_{(2,k)}^{(i)} = q_2(t = N(i-1)h + (k-1)h$  sec),  $u_k^{(i)} = u(t = N(i-1)h + (k-1)h$  sec) etc. The abovementioned notation is used throughout the current thesis.

### •Gait Generation Problem of the First Phase

On Subchapter 2.5 we derive the Gait Generation Problem for the First Phase of the Gait Generation Module. The aim of the First Phase is to minimize the control effort required to achieve a particular walking step, subject to constraints related to:

1. the derived equations of motion for each walking phase,
2. the configuration of the biped during the impact of the swing leg with the ground,
3. some features of the swing and stance legs that lead to a proper walking behavior,
4. the physical constraints of the used actuators, and
5. additional, optional constraints (e.g. average linear walking speed of the swing leg etc.).

## 2.2 Swing Phase of the 2-DOF Biped Robot for the Direct Collocation Method (Leg1=Stance, Leg2=Swing)

### 2.2.1 Derivation of the Euler-Lagrange Equations of Motion

The first step to deriving the Lagrangian of the biped is to define the homogeneous transfer matrices that describe the orientation and position of each link of the robot. One natural placement of local coordinate frames is indicated in Figure 2.2, where each frame is rigidly attached to the appropriate mass. The origins of each of these frames describe the following important points on the planar biped:

1.  $o_0$  - Global coordinate frame fixed to the ground.
2.  $o_1$  - Coordinate frame fixed to the center of mass for the stance leg(Leg 1).
3.  $o_M$  - Coordinate frame fixed to the center of mass of the hip joint.
4.  $o_2$  - Coordinate frame fixed to the center of mass for the swing leg(Leg 2).

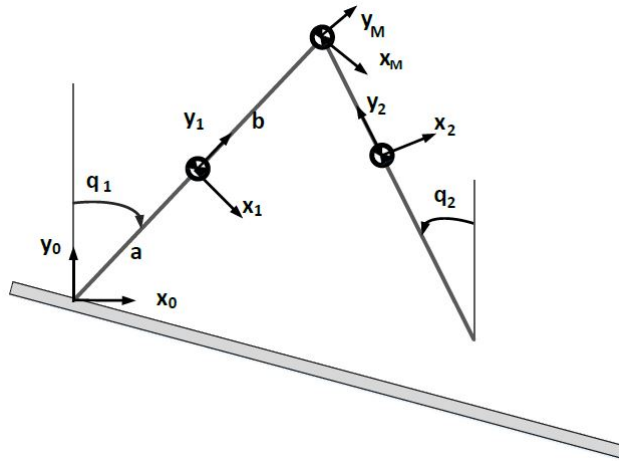


Figure 2.2: Assignment of origins for the coordinate frames of the robot.

These coordinate frames are used to form homogeneous transformation matrices on the form

$$H_j^i = \begin{bmatrix} R_j^i & p_j^i \\ 0_{1 \times 3} & 1 \end{bmatrix} \quad (2.1)$$

where  $R_j^i \in \mathbb{R}^{3 \times 3}$  is the rotation matrix from frame  $j$  to frame  $i$  and  $p_j^i \in \mathbb{R}^3$  is the distance between the origins of the respective frames expressed in frame  $i$ . Finding rotation matrices is complicated, requiring a parametrization of the total rotation of each frame in suitable coordinates. This process is greatly simplified by the fact that the planar biped only experiences motion in a 2-D plane. The transformation matrices can then be found by trigonometry and are stated for verification below:

$$\begin{aligned}
 H_1^0 &= \begin{bmatrix} \cos(q_1^{(i)}) & -\sin(q_1^{(i)}) & 0 & -a\sin(q_1^{(i)}) \\ -\sin(q_1^{(i)}) & \cos(q_1^{(i)}) & 0 & a\cos(q_1^{(i)}) \\ 0 & 0 & 1 & 0 \\ 0 & 0 & 0 & 1 \end{bmatrix} \\
 H_M^1 &= \begin{bmatrix} 1 & 0 & 0 & 0 \\ 0 & 1 & 0 & b \\ 0 & 0 & 1 & 0 \\ 0 & 0 & 0 & 1 \end{bmatrix} \\
 H_M^0 &= H_1^0 H_M^1 \\
 H_2^0 &= \begin{bmatrix} \cos(q_2^{(i)}) & -\sin(q_2^{(i)}) & 0 & l\sin(q_1^{(i)}) + b\sin(q_2^{(i)}) \\ \sin(q_2^{(i)}) & \cos(q_2^{(i)}) & 0 & l\cos(q_1^{(i)}) - b\cos(q_2^{(i)}) \\ 0 & 0 & 1 & 0 \\ 0 & 0 & 0 & 1 \end{bmatrix}
 \end{aligned} \tag{2.2}$$

The matrices (2.2) can now be employed to determine the position  $p^{(0)}$  and velocity  $v^{(0)}$  of the center of mass of each mass in  $xy$  coordinates in the global frame  $o_0$  as

$$\begin{aligned}
 p_1^{(0)} &= [I_{2 \times 2} \ 0_{2 \times 2}] \cdot H_1^0 \cdot \begin{bmatrix} 0_{3 \times 1} \\ 1 \end{bmatrix}, v_1^{(0)} = \frac{d}{dt} p_1^{(0)} \\
 p_M^{(0)} &= [I_{2 \times 2} \ 0_{2 \times 2}] \cdot H_M^0 \cdot \begin{bmatrix} 0_{3 \times 1} \\ 1 \end{bmatrix}, v_M^{(0)} = \frac{d}{dt} p_M^{(0)} \\
 p_2^{(0)} &= [I_{2 \times 2} \ 0_{2 \times 2}] \cdot H_2^0 \cdot \begin{bmatrix} 0_{3 \times 1} \\ 1 \end{bmatrix}, v_2^{(0)} = \frac{d}{dt} p_2^{(0)}
 \end{aligned} \tag{2.3}$$

where  $I_{2 \times 2}$  is the identity matrix and  $p^{(0)}, v^{(0)} \in \mathbb{R}^2$ .

In order to form the Lagrangian of the system and compute the Euler-Lagrange equations, the kinetic and potential energy of the system must be determined. The potential energy is the sum of the potential energy at the center of mass for each mass and can be expressed as

$$\mathcal{P} = (m_1 h_1^{(0)} + M h_M^{(0)} + m_2 h_2^{(0)})g \quad (2.4)$$

where  $g = (\sin(\theta_i) + \cos(\theta_i))g_{const}$ , with  $g_{const} = 9.81m/s^2$  and  $\theta_i$  defining the slope of the next walking step to be achieved, is the gravitational acceleration quantity in the horizontal and vertical axes and  $h^{(0)} = p^{(0)} \begin{bmatrix} 0 \\ 1 \end{bmatrix}$  is the height of the respective centers of mass expressed in the global frame  $o_0$ . The total kinetic energy is the sum of the body's centers-of-mass translational kinetic energy and the energy of rotation around the centers of mass (rotational energy), and can be expressed as

$$\mathcal{K} = \frac{1}{2}(m_1 v_1^T v_1 + M v_M^T v_M + m_2 v_2^T v_2) + \frac{1}{2}(I_1 (q_1^{(i)})^2 + I_2 (q_2^{(i)})^2) \quad (2.5)$$

Using the expressions (2.4) and (2.5) for the potential and kinetic energy, the Euler-Lagrange equations of motion can be calculated

$$\frac{d}{dt} \left( \frac{\partial \mathcal{L}}{\partial \dot{q}_{j^{(i)}}} \right) - \frac{\partial \mathcal{L}}{\partial q_{j^{(i)}}} = B_a(q^{(i)}) \begin{bmatrix} \tau_1^{(i)} \\ \tau_2^{(i)} \end{bmatrix}, \quad j \in [1, 2] \quad (2.6)$$

where  $\mathcal{L}$  is the Lagrangian of the system derived from (2.4) and (2.5) as

$$\mathcal{L} = \mathcal{K} - \mathcal{P}$$

that extends to:

$$\begin{aligned} L(q_1^{(i)}, q_2^{(i)}, \dot{q}_1^{(i)}, \dot{q}_2^{(i)}) &= \frac{1}{2}(I_1 + m_1 a^2 + m_2 l^2 + M l^2) \dot{q}_1^{(i)^2} + \frac{1}{2}(I_2 + m_2 b^2) \dot{q}_2^{(i)^2} \\ &\quad - m_2 b l \cos(q_1^{(i)} - q_2^{(i)}) \dot{q}_1^{(i)} \dot{q}_2^{(i)} - (m_1 a + m_2 g + M l) g \cos(q_2^{(i)}) + m_2 g b \cos(q_2^{(i)}), \quad (2.7) \end{aligned}$$

$B_a(q^{(i)})$  is the applied forces selection matrix (it maps the applied linear forces and/or torques to the related generalized coordinates). Here,  $B_a(q^{(i)}) = \begin{bmatrix} 1 & 0 \\ 0 & 1 \end{bmatrix}$  (thus,  $B_a(q^{(i)})$  here is a full row rank matrix) assuming that, due to the use of the two hip actuators, the torques  $\tau_1^{(i)}$ ,  $\tau_2^{(i)}$  to the hip can be controlled.

Using the expressions (8.39) – (8.41) for the elements of the respective matrices, the equations of motion for the biped can be formulated as

$$M(q^{(i)})\ddot{q}^{(i)} + C(q^{(i)}, \dot{q}^{(i)})\dot{q}^{(i)} + G(q^{(i)}, \theta_i) = B_a(q^{(i)}) \begin{bmatrix} \tau_1^{(i)} \\ \tau_2^{(i)} \end{bmatrix} \quad (2.8)$$

$\Leftrightarrow$

$$M(q^{(i)})\ddot{q}^{(i)} + C(q^{(i)}, \dot{q}^{(i)})\dot{q}^{(i)} + G(q^{(i)}, \theta_i) = \begin{bmatrix} \tau_1^{(i)} \\ \tau_2^{(i)} \end{bmatrix}$$

where

$$M(q) = \begin{bmatrix} p_1 + I_1 & -p_2 \cos(q_1^{(i)} - q_2^{(i)}) \\ -p_2 \cos(q_1^{(i)} - q_2^{(i)}) & p_3 + I_2 \end{bmatrix} \quad (2.9)$$

$$C(q^{(i)}, \dot{q}^{(i)}) = \begin{bmatrix} 0 & -p_2 \dot{q}_2^{(i)} \sin(q_1^{(i)} - q_2^{(i)}) \\ p_2 \dot{q}_1^{(i)} \sin(q_1^{(i)} - q_2^{(i)}) & 0 \end{bmatrix} \quad (2.10)$$

$$G(q^{(i)}, \theta_i) = \begin{bmatrix} -p_4 \sin(q_1^{(i)}) \\ p_5 \sin(q_2^{(i)}) \end{bmatrix} \quad (2.11)$$

where  $I_1$ ,  $I_2$  are the moments of inertia of the Legs 1 and 2 about their centers of mass, respectively, and the constant parameters are:  $I_1 = \frac{1}{12}m_1l^2$ ,  $I_2 = \frac{1}{12}m_2l^2$ ,  $p_1 = Ml^2 + m_1a^2 + m_2l^2$ ,  $p_2 = m_2lb$ ,  $p_3 = m_2b^2$ ,  $p_4 = (m_1a + m_2l + Ml)g$ ,  $p_5 = m_2bg$ . The equations of motion (2.8) describe the continuous dynamics of the biped during the gait and is independent of the walking surface. In order to describe what happens to the robot during the impact phase, an impact map must be formulated to prevent trespassing of the surface during motion.

### •Initial discretization of the Swing Phase for the Direct Collocation Method (Leg1

= Stance, Leg2 = Swing)

Now we will proceed with the initial discretization (without applying the Direct Collocation conditions yet) of the Swing Phase of the 2-DOF Biped Robot for the case where the Leg 1 is the stance leg and the Leg 2 is the swing leg. Let  $k = 1, \dots, N$  the time steps of a walking step. In addition, let  $i = 1, \dots, H$  the number and the order of the total walking steps. So, when we refer to a generalized angle  $q_{(x,k)}^{(i)}$ , where  $x = 1, 2$ ,  $k = 1, \dots, N$  and  $i = 1, \dots, H$  we will actually mean the angle  $q_x$  of the  $k$ -th time step of the  $i$ -th walking step. A discretization of the time interval for a walking step

$$t_0 = t_1 < t_2 < \dots < t_N = t_f$$

is chosen. Without implementing the complete discretization process (it will be later explained in the current chapter), the Swing Phase becomes:

$$M(q_k^{(i)})\ddot{q}_k^{(i)} + C(q_k^{(i)}, \dot{q}_k^{(i)})\dot{q}_k^{(i)} + G(q_k^{(i)}, \theta_i) = B_a \begin{bmatrix} \tau_{(1,k)}^{(i)} \\ \tau_{(2,k)}^{(i)} \end{bmatrix}, k = 1, \dots, N \quad (2.12)$$

$\Leftrightarrow$

$$M(q_k^{(i)})\ddot{q}_k^{(i)} + C(q_k^{(i)}, \dot{q}_k^{(i)})\dot{q}_k^{(i)} + G(q_k^{(i)}, \theta_i) = \begin{bmatrix} \tau_{(1,k)}^{(i)} \\ \tau_{(2,k)}^{(i)} \end{bmatrix}, k = 1, \dots, N$$

where

$$M(q_k) = \begin{bmatrix} p_1 + I_1 & -p_2 \cos(q_{(1,k)}^{(i)} - q_{(2,k)}^{(i)}) \\ -p_2 \cos(q_{(1,k)}^{(i)} - q_{(2,k)}^{(i)}) & p_3 + I_2 \end{bmatrix}, k = 1, \dots, N \quad (2.13)$$

$$C(q_k^{(i)}, \dot{q}_k^{(i)}) = \begin{bmatrix} 0 & -p_2 \dot{q}_{(2,k)}^{(i)} \sin(q_{(1,k)}^{(i)} - q_{(2,k)}^{(i)}) \\ p_2 \dot{q}_{(1,k)}^{(i)} \sin(q_{(1,k)}^{(i)} - q_{(2,k)}^{(i)}) & 0 \end{bmatrix}, k = 1, \dots, N \quad (2.14)$$

$$G(q_k^{(i)}, \theta_i) = \begin{bmatrix} -p_4 \sin(q_{(1,k)}^{(i)}) \\ p_5 \sin(q_{(2,k)}^{(i)}) \end{bmatrix}, k = 1, \dots, N \quad (2.15)$$

where  $I_1$ ,  $I_2$  are the moments of inertia of the Legs 1 and 2 about their centers of mass, respectively, and with the constant parameters  $p_1 = Ml^2 + m_1a^2 + m_2l^2$ ,  $p_2 = m_2lb$ ,  $p_3 = m_2b^2$ ,

$$p_4 = (m_1 a + m_2 l + Ml)g, \quad p_5 = m_2 b g.$$

**•State Space equations of the Swing Phase for the Direct Collocation Method (Leg 1 = Stance, Leg 2 = Swing)**

Now we will derive the state space equations of the Swing Phase of the 2-DOF Biped, and apply the Direct Collocation Conditions.

State equations can be obtained for state variables of systems described by input-output differential equations with the form of the equations depending on the nature of the system. For example, the equations are time-varying for time-varying systems and nonlinear for nonlinear systems. State equations for linear timeinvariant systems can also be obtained from their transfer functions.

The algebraic equation expressing the output in terms of the state variables is called the output equation. For multi-output systems, a separate output equation is needed to define each output. The state and output equations together provide a complete representation for the system described by the differential equation which is known as the state-space representation. For linear systems, it is often more convenient to write the state equations as a single matrix equation referred to as the state equation. Similarly, the output equations can be combined in a single output equation in matrix form.

The general form of state space equations for linear systems are:

$$\begin{aligned} \dot{x}(t) &= Ax(t) + Bu(t) \\ y &= Cx(t) + Du(t) \end{aligned}$$

where  $x(t)$  is a  $n \times 1$  real vector,  $u(t)$  is a  $m \times 1$  real vector, and  $y(t)$  is a  $l \times 1$  real vector. The matrices in the equations are:  $A = n \times n$  state matrix,  $B = n \times m$  input or control matrix,  $C = l \times n$  output matrix,  $D = l \times m$  direct transmission matrix.

Unfortunately, the abovementioned state space form is only valid for linear state equations. Nonlinear state equations involve nonlinear functions (as it is in our case) and cannot be written in terms of the matrix quadruple  $(A, B, C, D)$ . A state space representation for the

s-degree-of-freedom robot from the equations of motion:

$$M(q)\ddot{q} + C(q, \dot{q})\dot{q} + G(q) = B_a\tau$$

where  $q$  = vector of generalized coordinates,  $M(q) = s \times s$  positive definite inertia matrix,  $C(q, \dot{q}) = s \times s$  matrix of velocity related terms,  $G(q) = s \times 1$  vector of gravitational terms,  $B_a = s \times s$  applied forces selection matrix and  $\tau$  = vector of applied forces, are obtained as follows:

The system is of order  $2s$  since  $2s$  initial conditions are required to completely determine the solution. The most natural choice of state variables is the vector

$$x = \begin{bmatrix} x_1 \\ x_2 \end{bmatrix} = \begin{bmatrix} q \\ \dot{q} \end{bmatrix}$$

The associated state equations are:

$$\begin{bmatrix} \dot{x}_1 \\ \dot{x}_2 \end{bmatrix} = \begin{bmatrix} x_2 \\ -M^{-1}(x_1)(C(x_1, x_2)x_2 + G(x_1)) \end{bmatrix} + \begin{bmatrix} 0_{s \times s} \\ M^{-1}(x_1)B_a \end{bmatrix} u$$

with the applied forces vector  $\tau$  now denoted by  $u$ .

The output function is:

$$y = x_1$$

This equation is linear and can be written in the standard form

$$y = \begin{bmatrix} I_s & 0_{s \times s} \end{bmatrix} \begin{bmatrix} x_1 \\ x_2 \end{bmatrix}$$

The general form of nonlinear state-space equations is:

$$\dot{x} = f(x, u)$$

$$y = g(x, u)$$

where  $f(\cdot)$  ( $n \times 1$ ) and  $g(\cdot)$  ( $l \times 1$ ) are vectors of functions satisfying mathematical conditions that guarantee the existence and uniqueness of solution. But a form that is often encountered in practice and includes the equations of motion of robots is:

$$\dot{x} = f(x) + B(x)u$$

$$y = g(x) + D(x)u$$

The abovementioned state equation is said to be affine linear in the control because the right hand side is affine linear (in other words, includes a constant vector) for constant  $x$ .

For the 2-DOF biped robot, we will now derive the state space for the case where Leg 1 is the Stance Leg and Leg 2 is the Swing Leg. In addition, we will apply our step-to-step modeling approach and the initial discretization procedure to the derived state space equations. The system is of order 4 ( $2s$ ,  $s = 2$ ) since 4 initial conditions are required to completely determine the solution  $(q_{(1,1)}^{(i)}, q_{(2,1)}^{(i)}, \dot{q}_{(1,1)}^{(i)}, \dot{q}_{(2,1)}^{(i)})$ . The choice of state variables is the vector:

$$\begin{bmatrix} x_{(1,k)}^{(i)} \\ x_{(2,k)}^{(i)} \end{bmatrix} = \begin{bmatrix} q_k^{(i)} \\ \dot{q}_k^{(i)} \end{bmatrix}$$

$$\text{where } x_{(1,k)}^{(i)} = q_k^{(i)} = \begin{bmatrix} q_{(1,k)}^{(i)} \\ q_{(2,k)}^{(i)} \end{bmatrix} \text{ and } x_{(2,k)}^{(i)} = \dot{q}_k^{(i)} = \begin{bmatrix} \dot{q}_{(1,k)}^{(i)} \\ \dot{q}_{(2,k)}^{(i)} \end{bmatrix}$$

The state equations are:

$$\begin{bmatrix} \dot{x}_{(1,k)}^{(i)} \\ \dot{x}_{(2,k)}^{(i)} \end{bmatrix} = \begin{bmatrix} x_{(2,k)}^{(i)} \\ -M^{-1}(x_{(1,k)}^{(i)}) (C(x_{(1,k)}^{(i)}, x_{(2,k)}^{(i)}) x_{(2,k)}^{(i)} + G(x_{(1,k)}^{(i)}), \theta_i) \end{bmatrix} + \begin{bmatrix} 0_{2 \times 2} \\ M^{-1}(x_{(1,k)}^{(i)}) B_a \end{bmatrix} u_k^{(i)}$$

$\Leftrightarrow$

$$\begin{aligned}
\begin{bmatrix} x_{(1,k)}^{(i)} \\ x_{(2,k)}^{(i)} \end{bmatrix} &= \begin{bmatrix} x_{(2,k)}^{(i)} \\ \frac{(I_2+p_3)(p_2 \sin(q_{(1,k)}^{(i)} - q_{(2,k)}^{(i)})(q_{(2,k)}^{(i)})^2 + p_4 \sin(q_{(1,k)}^{(i)})) - p_2 \cos(q_{(1,k)}^{(i)} - q_{(2,k)}^{(i)})(p_2 \sin(q_{(1,k)}^{(i)} - q_{(2,k)}^{(i)})(q_{(1,k)}^{(i)})^2 - p_5 \sin(q_{(2,k)}^{(i)}))}{I_1 p_1 + I_2 p_3 + p_1 p_3 - p_2^2 \cos(q_{(1,k)}^{(i)} - q_{(2,k)}^{(i)})^2 + I_2^2} \\ \frac{p_2 \cos(q_{(1,k)}^{(i)} - q_{(2,k)}^{(i)})(p_2 \sin(q_{(1,k)}^{(i)} - q_{(2,k)}^{(i)})(q_{(2,k)}^{(i)})^2 + p_4 \sin(q_{(1,k)}^{(i)})) - (I_1 + p_1)(p_2 \sin(q_{(1,k)}^{(i)} - q_{(2,k)}^{(i)})(q_{(1,k)}^{(i)})^2 + p_5 \sin(q_{(2,k)}^{(i)}))}{I_1 p_1 + I_2 p_3 + p_1 p_3 - p_2^2 \cos(q_{(1,k)}^{(i)} - q_{(2,k)}^{(i)})^2 + I_2^2} \end{bmatrix} \\
&+ \begin{bmatrix} 0 & 0 \\ 0 & 0 \\ \frac{(I_2+p_3)}{I_1 p_1 + I_2 p_3 + p_1 p_3 - p_2^2 \cos(q_{(1,k)}^{(i)} - q_{(2,k)}^{(i)})^2 + I_2^2} & \frac{p_2 \cos(q_{(1,k)}^{(i)} - q_{(2,k)}^{(i)})}{I_1 p_1 + I_2 p_3 + p_1 p_3 - p_2^2 \cos(q_{(1,k)}^{(i)} - q_{(2,k)}^{(i)})^2 + I_2^2} \\ \frac{p_2 \cos(q_{(1,k)}^{(i)} - q_{(2,k)}^{(i)})}{I_1 p_1 + I_2 p_3 + p_1 p_3 - p_2^2 \cos(q_{(1,k)}^{(i)} - q_{(2,k)}^{(i)})^2 + I_2^2} & \frac{(I_1+p_1)}{I_1 p_1 + I_2 p_3 + p_1 p_3 - p_2^2 \cos(q_{(1,k)}^{(i)} - q_{(2,k)}^{(i)})^2 + I_2^2} \end{bmatrix} u_k^{(i)}
\end{aligned} \tag{2.16}$$

with the applied forces vector  $\tau_k^{(i)} = \begin{bmatrix} \tau_{(1,k)}^{(i)} \\ \tau_{(2,k)}^{(i)} \end{bmatrix}$  now denoted by  $u_k^{(i)} = \begin{bmatrix} u_{(1,k)}^{(i)} \\ u_{(2,k)}^{(i)} \end{bmatrix}$

The output function is:

$$y_k^{(i)} = x_{(1,k)}^{(i)}$$

For the Direct Collocation Method, based on subchapter 8.3.4, we proceed with the formulation

below. Let  $x_{approx}^{(i)}(t) = \begin{bmatrix} x_{(1,approx)}^{(i)}(t) \\ x_{(2,approx)}^{(i)}(t) \end{bmatrix}$ , where  $x_{(1,approx)}^{(i)}(t)$ ,  $x_{(2,approx)}^{(i)}(t)$  are the cubic approxi-

mations of the generalized coordinates  $q_1^{(i)}$ ,  $q_2^{(i)}$  as well as of their first and second derivatives, in the specified discretized time interval of the  $i$ -th walking step (relations 8.74-8.78). In ad-

dition, let  $\tau_{approx}^{(i)}(t) = \begin{bmatrix} \tau_{(1,approx)}^{(i)}(t) \\ \tau_{(2,approx)}^{(i)}(t) \end{bmatrix}$ , where  $\tau_{(1,approx)}^{(i)}(t)$ ,  $\tau_{(2,approx)}^{(i)}(t)$  are the approximations

of the control inputs (torques)  $\tau_1^{(i)}$ ,  $\tau_2^{(i)}$  in the specified discretized time interval of the  $i$ -th walking step (relation 8.73). Thus, the state space equations of the Swing Phase for the case Leg 1 is the Stance Leg and Leg 2 is the Swing Leg are (relations 8.79, 8.92):

$$\begin{bmatrix} x_{(1,approx)}^{(i)}(t_{ck}) \\ x_{(2,approx)}^{(i)}(t_{ck}) \end{bmatrix} =$$

$$\begin{bmatrix} x_{(2,approx)}^{(i)}(t_{ck}) \\ -M^{-1}(x_{(1,approx)}^{(i)}(t_{ck}))(C(x_{(1,approx)}^{(i)}(t_{ck}), x_{(2,approx)}^{(i)}(t_{ck}))x_{(2,approx)}^{(i)}(t_{ck}) + G(x_{(1,approx)}^{(i)}(t_{ck}), \theta_i)) \end{bmatrix} + \begin{bmatrix} 0_{2 \times 2} \\ M^{-1}(x_{(1,approx)}^{(i)}(t_{ck}))B_a \end{bmatrix} u_{(approx)}^{(i)}(t_{ck}) \quad (2.17)$$

which can be rewritten to the relation (2.16), having applied the collocation conditions. The output function is:

$$y_{approx}^{(i)}(t_{ck}) = x_{(1,approx)}^{(i)}(t_{ck})$$

### 2.2.2 Formulation of the Impact Map

When the swing foot impacts the surface of the ground, an update of the angular velocities  $\dot{q}_1^{(i)}, \dot{q}_2^{(i)}$  should occur to prevent the biped from falling through the floor. This update can be formulated as a mapping between the velocities just before and just after the collision with the ground on the form

$$\begin{bmatrix} \dot{q}_1^{(i,+)} \\ \dot{q}_2^{(i,+)} \end{bmatrix} = \Delta(q^{(i)}) \cdot \begin{bmatrix} \dot{q}_1^{(i,-)} \\ \dot{q}_2^{(i,-)} \end{bmatrix} \quad (2.18)$$

where  $-$ ,  $+$  denote the time instant right before and right after impact, respectively, so that specific time interval is considered extremely small. An important property of this impact mapping is the assumption that the configuration of the biped, the generalized coordinates  $q_1^{(i)}, q_2^{(i)}$ , remains unchanged during ground impact (which occurs in the abovementioned time interval). This is due to the fact that the impact forces  $F$  the biped experiences during impact are impulsive in nature. There are multiple ways of calculating the velocity updates of the biped. Presented below is a method that exploits properties of the impact to derive an impact map for the collision on the form (2.18).

### 2.2.3 Conservation of the angular momentum

Since the impact forces  $F$  are the only external forces affecting the biped, the angular momentum about the impacting foot is conserved before and after the collision for the system. The angular momentum  $L$  of a mass can be stated as

$$L = r \times mv + Iq_{COM}^{(i)} \quad (2.19)$$

where  $r$  is the position of the mass relative to a given reference point,  $m$  is the mass,  $v$  is the velocity of the mass,  $I$  is the moment of inertia around the particular center of mass and  $q_{COM}^{(i)}$  is the angular velocity of the particular leg where the center of mass is located. Given that the biped is a system of masses, the angular momentum of the robot about the impacting foot is given by:

$$L_{Biped}^{(0)} = \sum_i r_i^{(0)} \times m_i v_i^+ + I_1 q_1^{(i,+)} + I_2 q_2^{(i,+)} = \sum_i r_i^{(0)} \times m_i v_i^- + I_1 q_1^{(i,-)} + I_2 q_2^{(i,-)}, i \in \{1, 2, M\} \quad (2.20)$$

where the reference point is the origin  $o_0$  (see Figure 2.3), and the position vectors  $r_i^{(0)}$  relative to this point is given by

$$\begin{aligned} r_2^{(0)} &= \begin{bmatrix} -a \sin(q_2^{(i,-)}) \\ a \cos(q_2^{(i,-)}) \\ 0 \end{bmatrix} \\ r_M^{(0)} &= \begin{bmatrix} -l \sin(q_2^{(i,-)}) \\ l \cos(q_2^{(i,-)}) \\ 0 \end{bmatrix} \\ r_1^{(0)} &= r_M^{(0)} + \begin{bmatrix} -b \sin(q_1^{(i,-)}) \\ -b \cos(q_1^{(i,-)}) \\ 0 \end{bmatrix} \end{aligned} \quad (2.21)$$

The translational velocities  $v_i^\pm$  are independent of the reference point and can be expressed using the angular velocities  $\dot{q}^\pm$  as

$$\begin{aligned}
 v_M^- &= \begin{bmatrix} 0 \\ 0 \\ \dot{q}_1^{(i,-)} \end{bmatrix} \times \begin{bmatrix} l \sin(q_1^{(i,-)}) \\ l \cos(q_1^{(i,-)}) \\ 0 \end{bmatrix}, v_M^+ = \begin{bmatrix} 0 \\ 0 \\ \dot{q}_2^{(i,-)} \end{bmatrix} \times \begin{bmatrix} -l \sin(q_2^{(i,-)}) \\ l \cos(q_2^{(i,-)}) \\ 0 \end{bmatrix} \\
 v_1^- &= \begin{bmatrix} 0 \\ 0 \\ \dot{q}_1^{(i,-)} \end{bmatrix} \times \begin{bmatrix} a \sin(q_1^{(i,-)}) \\ a \cos(q_1^{(i,-)}) \\ 0 \end{bmatrix}, v_1^+ = v_M^+ + \begin{bmatrix} 0 \\ 0 \\ \dot{q}_1^{(i,+)} \end{bmatrix} \times \begin{bmatrix} -b \sin(q_1^{(i,-)}) \\ -b \cos(q_1^{(i,-)}) \\ 0 \end{bmatrix} \\
 v_2^- &= v_M^- + \begin{bmatrix} 0 \\ 0 \\ \dot{q}_2^{(i,-)} \end{bmatrix} \times \begin{bmatrix} b \sin(q_2^{(i,-)}) \\ -b \cos(q_2^{(i,-)}) \\ 0 \end{bmatrix}, v_2^+ = \begin{bmatrix} 0 \\ 0 \\ \dot{q}_2^{(i,+)} \end{bmatrix} \times \begin{bmatrix} -a \sin(q_2^{(i,-)}) \\ a \cos(q_2^{(i,-)}) \\ 0 \end{bmatrix}
 \end{aligned} \tag{2.22}$$

Substituting (2.21) and (2.22) into (2.20) and computing the crossproducts, yields one equation for the two unknown velocities  $\dot{q}_1^{(i,+)}$ ,  $\dot{q}_2^{(i,+)}$ . This means that another equation is needed to solve the system.

The only forces that the pre-impact swing leg experiences during the collision is the constraint force acting on it from the hip joint (we assume that the torques applied to the biped during the impact are zero). This means that the angular momentum of this leg about the hip is conserved through the impact, yielding another equation for the updated velocities on the form:

$$\begin{aligned}
 L_{Swing}^{(M)} &= r_2^{(M)} \times m_2 v_2^+ + I_2 \dot{q}_2^{(i,+)} = r_2^{(M)} \times m_2 v_2^- + I_2 \dot{q}_2^{(i,-)} \\
 r_2^{(M)} &= \begin{bmatrix} -b \sin(q_2^{(i,-)}) \\ -b \cos(q_2^{(i,-)}) \\ 0 \end{bmatrix}
 \end{aligned} \tag{2.23}$$

where the reference point is the origin  $o_M$  and the velocities  $v_2^\pm$  is given in (2.22). Equations

(2.20) and (2.23) combined results in the linear system:

$$\begin{aligned} \begin{bmatrix} L_{Biped}^{(0)} \\ L_{Swing}^{(M)} \end{bmatrix} &= \mathcal{Q}_+ \dot{q}^{(i,+)} = \mathcal{Q}_- \dot{q}^{(i,-)} \\ \begin{bmatrix} L_{Biped}^{(0)} \\ L_{Swing}^{(M)} \end{bmatrix} &= \begin{bmatrix} p_8 - p_7 c_{12} + I_1 & -p_7 c_{12} + p_6 + I_2 \\ p_8 + I_1 & -p_7 c_{12} \end{bmatrix} \begin{bmatrix} \dot{q}_1^{(i,+)} \\ \dot{q}_2^{(i,+)} \end{bmatrix} = \begin{bmatrix} p_{10} c_{12} + I_1 & -p_{11} + I_2 \\ -p_9 + I_1 & 0 \end{bmatrix} \begin{bmatrix} \dot{q}_1^{(i,-)} \\ \dot{q}_2^{(i,-)} \end{bmatrix} \end{aligned} \quad (2.24)$$

where  $c_{12} = \cos(q_1^{(i,-)} - q_2^{(i,-)})$  and the parameters  $p_6 = m_1 l^2 + M l^2 + m_2 b^2$ ,  $p_7 = m_1 b l$ ,  $p_8 = m_1 b^2$ ,  $p_9 = m_1 a b$ ,  $p_{10} = m_2 l a + M l^2 + m_1 l a$ ,  $p_{11} = m_2 a b$ .

### •Discretization of the Impact Phase for both Methods (Leg1 = Stance, Leg2 = Swing)

Based on the extensive analysis of the impact phase above, we will now proceed with the discretization of the impact phase for both methods, for the case where Leg1 is the stance leg and Leg2 is the swing leg. Let  $k = 1, \dots, N$  the time steps of a walking step. In addition, let  $i = 1, \dots, H$  the number and the order of the total walking steps. So, when we refer to a generalized angle  $q_{(x,k)}^{(i)}$ , where  $x = 1, 2$ ,  $k = 1, \dots, N$  and  $i = 1, \dots, H$  we will actually mean the angle  $q_x$  of the  $k$ -th time step of the  $i$ -th walking step. Each walking step has of course its own swing and impact phase.

We now define that the time instant before the impact of the swing leg at the ground (pre-impact phase) is the time step  $N$  of a walking step, and the time instant after the impact of the swing leg at the ground (post-impact phase) that also completes the current walking step is the time step 1 of the next walking step.

But at the end of a walking step the swing leg becomes the new stance leg and vice versa, for the next walking step to take place (in other words, both legs switch roles at the end of a walking step).

Hence:

- $\dot{q}_1^{(i,+)} = \dot{q}_{(1,1)}^{(i+1)}$ ,

- $\dot{q}_2^{(i,+)} = q_{(2,1)}^{(i+1)}$ ,
- $\dot{q}_1^{(i,-)} = q_{(1,N)}^{(i)}$ ,
- $\dot{q}_2^{(i,-)} = q_{(2,N)}^{(i)}$ .

Finally, (2.24) becomes:

$$\begin{aligned} & \begin{bmatrix} p_8 - p_7 c_{12} + I_1 & -p_7 c_{12} + p_6 + I_2 \\ p_8 + I_1 & -p_7 c_{12} \end{bmatrix} \begin{bmatrix} q_{(1,1)}^{(i+1)} \\ q_{(2,1)}^{(i+1)} \end{bmatrix} \\ &= \begin{bmatrix} p_{10} c_{12} + I_1 & -p_{11} + I_2 \\ -p_9 + I_1 & 0 \end{bmatrix} \begin{bmatrix} q_{(1,N)}^{(i)} \\ q_{(2,N)}^{(i)} \end{bmatrix} \end{aligned} \quad (2.25)$$

where  $c_{12} = \cos(q_{(1,N)}^{(i)} - q_{(2,N)}^{(i)})$  and the parameters  $p_6 = m_1 l^2 + M l^2 + m_2 b^2$ ,  $p_7 = m_1 b l$ ,  $p_8 = m_1 b^2$ ,  $p_9 = m_1 a b$ ,  $p_{10} = m_2 l a + M l^2 + m_1 l a$ ,  $p_{11} = m_2 a b$ .

Solving the system for  $\dot{q}^{(i,+)}$  by inverting the matrix  $\mathcal{Q}_+$  gives an impact map on the form (2.18)

$$\dot{q}^{(i+1)} = [\mathcal{Q}_+^{-1} \cdot \mathcal{Q}_-] \dot{q}^{(i)} \quad (2.26)$$

For the Direct Collocation Method, based on subchapter 8.3.4, we proceed with the formulation below. Let  $q_{approx}^{(i)}(t) = \begin{bmatrix} q_{(1,approx)}^{(i)}(t) \\ q_{(2,approx)}^{(i)}(t) \end{bmatrix}$ , where  $q_{(1,approx)}^{(i)}(t)$ ,  $q_{(2,approx)}^{(i)}(t)$  are the cubic approximations of the generalized coordinates  $q_1^{(i)}$ ,  $q_2^{(i)}$ , in the specified discretized time interval of the  $i$ -th walking step (relations 8.74-8.78). Thus, the Impact Phase for the case Leg 1 is the Stance Leg and Leg 2 is the Swing Leg are:

$$\begin{aligned} & \begin{bmatrix} p_8 - p_7 c_{12} + I_1 & -p_7 c_{12} + p_6 + I_2 \\ p_8 + I_1 & -p_7 c_{12} \end{bmatrix} \begin{bmatrix} \dot{q}_{(1,approx)}^{(i+1)}(t_1) \\ \dot{q}_{(2,approx)}^{(i+1)}(t_1) \end{bmatrix} \\ &= \begin{bmatrix} p_{10} c_{12} + I_1 & -p_{11} + I_2 \\ -p_9 + I_1 & 0 \end{bmatrix} \begin{bmatrix} \dot{q}_{(1,approx)}^{(i)}(t_N) \\ \dot{q}_{(2,approx)}^{(i)}(t_N) \end{bmatrix} \end{aligned} \quad (2.27)$$

where  $c_{12} = \cos(q_{(1,approx)}^{(i)}(t_N) - q_{(2,approx)}^{(i)}(t_N))$  and the parameters  $p_6 = m_1 l^2 + M l^2 + m_2 b^2$ ,

$$p_7 = m_1bl, p_8 = m_1b^2, p_9 = m_1ab, p_{10} = m_2la + Mt^2 + m_1la, p_{11} = m_2ab.$$

Solving the system for  $q_{approx}^{(i,+)}$  by inverting the matrix  $\mathcal{Q}_+$  gives an impact map on the form (2.18)

$$q_{approx}^{(i+1)} = [\mathcal{Q}_+^{-1} \cdot \mathcal{Q}_-]q_{approx}^{(i)} \quad (2.28)$$

## 2.2.4 Definition of Impact Surface

The abovementioned impact map calculated the change in angular velocities that occur when the biped robot impacts with the ground. In order for this update to be correctly applied when the swing foot strikes the ground (at the time step  $N$  during the  $i - th$  walking step), the configurations of the robot that result in an impact must be determined. These configurations correspond to the hypersurface  $S$  known as the impact surface or switching surface. A configuration of the biped that leads to impact (at the time step  $N$ ) with the ground during the  $i - th$  walking step (it may be a downward or upward slope, a general rough terrain or just simply a flat ground) must satisfy the relation:

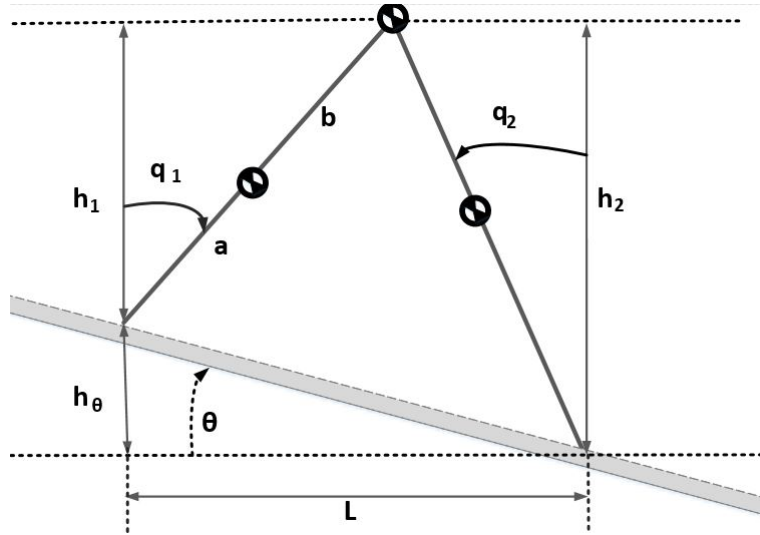


Figure 2.3: Quantities used for the definition of the Impact Surface of the robot.

$$H(q_{(1,N)}^{(i)}, q_{(2,N)}^{(i)}, \theta_i) = h_1(q_{(1,N)}^{(i)}) + h_\theta(\theta_i) - h_2(q_{(2,N)}^{(i)}) = 0 \quad (2.29)$$

where

$$\begin{aligned}
 h_1(q_{(1,N)}^{(i)}) &= l \cos(q_{(1,N)}^{(i)}) \\
 h_2(q_{(2,N)}^{(i)}) &= l \cos(q_{(2,N)}^{(i)}) \\
 h_\theta(\theta) &= L \tan(\theta_i) \\
 L &= l \sin(q_{(1,N)}^{(i)}) + l \sin(q_{(2,N)}^{(i)})
 \end{aligned} \tag{2.30}$$

are found by trigonometry. Substituting these expressions and simplifying using trigonometric identities leads to the following derivation

$$\begin{aligned}
 H(q_{(1,N)}^{(i)}, q_{(2,N)}^{(i)}, \theta_i) &= l \cos(q_{(1,N)}^{(i)}) + [l \sin(q_{(1,N)}^{(i)}) + l \sin(q_{(2,N)}^{(i)})] \frac{\sin(\theta_i)}{\cos(\theta_i)} - l \cos(q_{(2,N)}^{(i)}) = 0 \\
 H(q_{(1,N)}^{(i)}, q_{(2,N)}^{(i)}, \theta_i) &= \cos(q_{(1,N)}^{(i)}) \cos(\theta_i) + \sin(q_{(1,N)}^{(i)}) \sin(\theta_i) - \cos(q_{(2,N)}^{(i)}) \cos(\theta_i) + \\
 \sin(q_{(2,N)}^{(i)}) \sin(\theta_i) &= 0 \\
 H(q_{(1,N)}^{(i)}, q_{(2,N)}^{(i)}, \theta_i) &= \cos(-q_{(1,N)}^{(i)}) \cos(\theta_i) - \sin(-q_{(1,N)}^{(i)}) \sin(\theta_i) - \cos(q_{(2,N)}^{(i)}) \cos(\theta_i) + \\
 \sin(q_{(2,N)}^{(i)}) \sin(\theta_i) &= 0 \\
 H(q_{(1,N)}^{(i)}, q_{(2,N)}^{(i)}, \theta_i) &= [\cos(-q_{(1,N)}^{(i)}) \cos(\theta_i) - \sin(-q_{(1,N)}^{(i)}) \sin(\theta_i)] - [\cos(q_{(2,N)}^{(i)}) \cos(\theta_i) - \\
 \sin(q_{(2,N)}^{(i)}) \sin(\theta_i)] &= 0 \\
 H(q_{(1,N)}^{(i)}, q_{(2,N)}^{(i)}, \theta_i) &= \cos(-q_{(1,N)}^{(i)} + \theta_i) - \cos(q_{(2,N)}^{(i)} + \theta_i) = 0
 \end{aligned} \tag{2.31}$$

Furthermore, the configuration of the biped remains unchanged during ground impact, in the time interval between the  $N$ th time step of the  $i$ th walking step and the first time step of the  $i + 1$ th walking step,  $[t_N^{(i)}, t_1^{(i+1)}]$ . Thus, the switching surface  $S$  is defined as all configurations  $q$  of the biped that satisfies the above relations and conditions and can be stated in set notation as:

$$\begin{aligned}
 S = \{q_{(1,N)}^{(i)}, q_{(2,N)}^{(i)}, q_{(1,1)}^{(i+1)}, q_{(2,1)}^{(i+1)}, \theta_i \in \mathbb{R} : H(q_{(1,N)}^{(i)}, q_{(2,N)}^{(i)}, \theta_i) = \cos(-q_{(1,N)}^{(i)} + \theta_i) - \cos(q_{(2,N)}^{(i)} + \theta_i) = 0, \\
 H(q_{(1,1)}^{(i+1)}, q_{(2,1)}^{(i+1)}, \theta_i) = \cos(-q_{(1,1)}^{(i+1)} + \theta_i) - \cos(q_{(2,1)}^{(i+1)} + \theta_i) = 0\} \tag{2.32}
 \end{aligned}$$

For the Direct Collocation Method, based on subchapter 8.3.4, we proceed with the formulation

below. Let  $q_{approx}^{(i)}(t) = \begin{bmatrix} q_{(1,approx)}^{(i)}(t) \\ q_{(2,approx)}^{(i)}(t) \end{bmatrix}$ , where  $q_{(1,approx)}^{(i)}(t)$ ,  $q_{(2,approx)}^{(i)}(t)$  are the cubic approximations of the generalized coordinates  $q_1^{(i)}$ ,  $q_2^{(i)}$ , in the specified discretized time interval of the

$i$ -th walking step (relations 8.74-8.78). Thus, with a similar proof as above (having applied the Direct Collection Conditions), the switching surface  $S$  is defined as all configurations  $q_{approx}$  of the biped that satisfies the above relation and can be stated in set notation as:

$$S = \{q_{(1,approx)}^{(i)}(t_N), q_{(2,approx)}^{(i)}(t_N), q_{(1,approx)}^{(i+1)}(t_1), q_{(2,approx)}^{(i+1)}(t_1) \theta_i \in \mathbb{R} : H(q_{(1,approx)}^{(i)}(t_N), q_{(2,approx)}^{(i)}(t_N), \theta_i) = \cos(-q_{(1,approx)}^{(i)}(t_N) + \theta_i) - \cos(q_{(2,N)}^{(i)}(t_N) + \theta_i) = 0, H(q_{(1,approx)}^{(i+1)}(t_1), q_{(2,approx)}^{(i+1)}(t_1), \theta_i) = \cos(-q_{(1,approx)}^{(i+1)}(t_1) + \theta_i) - \cos(q_{(2,approx)}^{(i+1)}(t_1) + \theta_i) = 0\} \quad (2.33)$$

## 2.3 Swing Phase of the 2-DOF Biped Robot using Discrete Mechanics (Leg1=Stance, Leg2=Swing)

We now develop the discretized Swing Phase of our biped robot via the use of the Discrete Mechanics Theory. We define some important notations. Let  $h^{(i)}$  be the sampling time for the  $i$ th walking step,  $r$  a division ratio quantity in discrete mechanics,  $k = 1, \dots, N$  the number of time steps,  $H$  the total number of walking steps,  $i = 1, 2, \dots, H$  the walking step index,  $q_{(1,k)}^{(i)}, q_{(2,k)}^{(i)}$  the angles of Leg 1 and Leg 2 at the  $k$ -th time step during the  $i$ -th walking step respectively and  $\tau_{(1,k)}^{(i)}, \tau_{(2,k)}^{(i)}$  the discrete control inputs (torques) at the  $k$ -th time step during the  $i$ -th walking step for Leg 1 and Leg 2 respectively.

We now derive the discretized Swing Phase and Impact Phase for the 2-DOF biped robot where Leg 1 is the stance leg and Leg 2 is the swing leg. We firstly calculate the Discrete Lagrangian  $L_r^d(q_{(1,k)}^{(i)}, q_{(1,k+1)}^{(i)}, q_{(2,k)}^{(i)}, q_{(2,k+1)}^{(i)})$  from (8.44), (2.7) as:

$$L_r^d(q_{(1,k)}^{(i)}, q_{(1,k+1)}^{(i)}, q_{(2,k)}^{(i)}, q_{(2,k+1)}^{(i)}) = \frac{1}{2}(I_1 + m_1 a^2 + m_2 l^2 + Ml^2) \left( \frac{q_{(1,k+1)}^{(i)} - q_{(1,k)}^{(i)}}{h^{(i)}} \right)^2 + \frac{1}{2}(I_2 + m_2 b^2) \left( \frac{q_{(2,k+1)}^{(i)} - q_{(2,k)}^{(i)}}{h^{(i)}} \right)^2 - m_2 b l \cos((1-a)q_{(1,k)}^{(i)} + aq_{(1,k+1)}^{(i)} - (1-a)q_{(2,k)}^{(i)} - aq_{(2,k+1)}^{(i)}) \left( \frac{q_{(1,k+1)}^{(i)} - q_{(1,k)}^{(i)}}{h^{(i)}} \right) \left( \frac{q_{(2,k+1)}^{(i)} - q_{(2,k)}^{(i)}}{h^{(i)}} \right) - (m_1 a + m_2 g + Ml) g \cos((1-a)q_{(2,k)}^{(i)} + aq_{(2,k+1)}^{(i)}) + m_2 g b \cos((1-a)q_{(2,k)}^{(i)} + aq_{(2,k+1)}^{(i)}) \quad (2.34)$$

Due to the fact that the left and right discrete forces (8.46) satisfy  $f_d^+(q_k, q_{k+1}, \tau_k) = f_d^-(q_k, q_{k+1}, \tau_k)$  for  $r = \frac{1}{2}$ , we set a type of control input (the torques for Leg 1 and 2) that consists only of the left discrete external force  $f_d^-$  as:

$$\tau_k^{(i)} := f_d^-(q_k, q_{k+1}, \tau_k), k = 1, \dots, N \quad (2.35)$$

Substituting (2.34) into the discrete Euler-Lagrange Equations (8.49) while also deriving the boundary conditions (8.58, 8.60), and using the discrete control inputs (2.35), we develop the discretized Swing Phase of the 2-DOF biped:

$$D_2 L^d(q_{(1,k-1)}^{(i)}, q_{(1,k)}^{(i)}, q_{(2,k-1)}^{(i)}, q_{(2,k)}^{(i)}) + D_1 L^d(q_{(1,k)}^{(i)}, q_{(1,k+1)}^{(i)}, q_{(2,k)}^{(i)}, q_{(2,k+1)}^{(i)}) - \tau_{(1,k)}^{(i)} = 0, (k = 1, \dots, N) \quad (2.36)$$

$$D_4 L^d(q_{(1,k-1)}^{(i)}, q_{(1,k)}^{(i)}, q_{(2,k-1)}^{(i)}, q_{(2,k)}^{(i)}) + D_3 L^d(q_{(1,k)}^{(i)}, q_{(1,k+1)}^{(i)}, q_{(2,k)}^{(i)}, q_{(2,k+1)}^{(i)}) - \tau_{(2,k)}^{(i)} = 0, (k = 1, \dots, N) \quad (2.37)$$

The boundary conditions are given from the following equations:

$$D_2 L^c(q_{(1,1)}^{(i)}, q_{(1,1)}^{(i)}, q_{(2,1)}^{(i)}, q_{(2,1)}^{(i)}) + D_1 L^d(q_{(1,1)}^{(i)}, q_{(1,2)}^{(i)}, q_{(2,1)}^{(i)}, q_{(2,2)}^{(i)}) - \tau_{(1,1)}^{(i)} = 0 \quad (2.38)$$

$$D_4 L^c(q_{(1,1)}^{(i)}, q_{(1,1)}^{(i)}, q_{(2,1)}^{(i)}, q_{(2,1)}^{(i)}) + D_3 L^d(q_{(1,1)}^{(i)}, q_{(1,2)}^{(i)}, q_{(2,1)}^{(i)}, q_{(2,2)}^{(i)}) - \tau_{(2,1)}^{(i)} = 0 \quad (2.39)$$

$$-D_2 L^c(q_{(1,N)}^{(i)}, q_{(1,N)}^{(i)}, q_{(2,N)}^{(i)}, q_{(2,N)}^{(i)}) + D_1 L^d(q_{(1,N-1)}^{(i)}, q_{(1,N)}^{(i)}, q_{(2,N-1)}^{(i)}, q_{(2,N)}^{(i)}) - \tau_{(1,N)}^{(i)} = 0 \quad (2.40)$$

$$-D_4 L^c(q_{(1,N)}^{(i)}, q_{(1,N)}^{(i)}, q_{(2,N)}^{(i)}, q_{(2,N)}^{(i)}) + D_3 L^d(q_{(1,N-1)}^{(i)}, q_{(1,N)}^{(i)}, q_{(2,N-1)}^{(i)}, q_{(2,N)}^{(i)}) - \tau_{(2,N)}^{(i)} = 0 \quad (2.41)$$

Regarding some specific cases of values for the time step  $k$  for which the abovementioned equations are valid:

- For  $i = 1$  and  $k = 1$ ,  $q_{(1,k-1)}^{(i)} = q_{(1,0)}^{(1)} = 0$ ,  $q_{(2,k-1)}^{(i)} = q_{(2,0)}^{(1)} = 0$ ,  $\tau_{(1,k-1)}^{(i)} = \tau_{(1,0)}^{(1)} = 0$  and  $\tau_{(2,k-1)}^{(i)} = \tau_{(2,0)}^{(1)} = 0$  (due to the fact that  $k = [1, \dots, N]$ ),
- For  $i > 1$  and  $k = 1$ ,  $q_{(1,k-1)}^{(i)} = q_{(1,N)}^{(i-1)}$ ,  $q_{(2,k-1)}^{(i)} = q_{(2,N)}^{(i-1)}$ ,  $\tau_{(1,k-1)}^{(i)} = \tau_{(1,N)}^{(i-1)}$  and  $\tau_{(2,k-1)}^{(i)} = \tau_{(2,N)}^{(i-1)}$ ,
- For  $k = N$ ,  $q_{(1,k+1)}^{(i)} = q_{(1,1)}^{(i+1)}$  and  $q_{(2,k+1)}^{(i)} = q_{(2,1)}^{(i+1)}$ .

The set of equations (2.36, 2.37), can be rewritten to a similar form of the model (2.8):

$$M(q_k^{(i)}) \cdot \left( \frac{q_{k+1}^{(i)} - 2q_k^{(i)} + q_{k-1}^{(i)}}{(h^{(i)})^2} \right) + C(q_k^{(i)}, \frac{q_{k+1}^{(i)} - q_k^{(i)}}{h^{(i)}}) \cdot \left( \frac{q_{k+1}^{(i)} - q_k^{(i)}}{h^{(i)}} \right) + G(q_k^{(i)}, \theta_i) = B_a \begin{bmatrix} \tau_{(1,k)}^{(i)} \\ \tau_{(2,k)}^{(i)} \end{bmatrix} \quad (2.42)$$

$\Leftrightarrow$

$$M(q_k^{(i)}) \cdot \left( \frac{q_{k+1}^{(i)} - 2q_k^{(i)} + q_{k-1}^{(i)}}{(h^{(i)})^2} \right) + C(q_k^{(i)}, \frac{q_{k+1}^{(i)} - q_k^{(i)}}{h^{(i)}}) \cdot \left( \frac{q_{k+1}^{(i)} - q_k^{(i)}}{h^{(i)}} \right) + G(q_k^{(i)}, \theta_i) = \begin{bmatrix} \tau_{(1,k)}^{(i)} \\ \tau_{(2,k)}^{(i)} \end{bmatrix}$$

$\Leftrightarrow$

$$\begin{bmatrix} p_1 + I_1 & -p_2 \cos(q_{(1,k)}^{(i)} - q_{(2,k)}^{(i)}) \\ -p_2 \cos(q_{(1,k)}^{(i)} - q_{(2,k)}^{(i)}) & p_3 + I_2 \end{bmatrix} \begin{bmatrix} \frac{q_{(1,k+1)}^{(i)} - 2q_{(1,k)}^{(i)} + q_{(1,k-1)}^{(i)}}{(h^{(i)})^2} \\ \frac{q_{(2,k+1)}^{(i)} - 2q_{(2,k)}^{(i)} + q_{(2,k-1)}^{(i)}}{(h^{(i)})^2} \end{bmatrix} + \begin{bmatrix} 0 & -p_2 \left( \frac{q_{(2,k+1)}^{(i)} - q_{(2,k)}^{(i)}}{h^{(i)}} \right) \sin(q_{(1,k)}^{(i)} - q_{(2,k)}^{(i)}) \\ p_2 \left( \frac{q_{(1,k+1)}^{(i)} - q_{(1,k)}^{(i)}}{h^{(i)}} \right) \sin(q_{(1,k)}^{(i)} - q_{(2,k)}^{(i)}) & 0 \end{bmatrix} \begin{bmatrix} \frac{q_{(1,k+1)}^{(i)} - q_{(1,k)}^{(i)}}{h^{(i)}} \\ \frac{q_{(2,k+1)}^{(i)} - q_{(2,k)}^{(i)}}{h^{(i)}} \end{bmatrix} + \begin{bmatrix} -p_4 \sin(q_{(1,k)}^{(i)}) \\ p_5 \sin(q_{(2,k)}^{(i)}) \end{bmatrix} = \begin{bmatrix} \tau_{(1,k)}^{(i)} \\ \tau_{(2,k)}^{(i)} \end{bmatrix} \quad (2.43)$$

with  $k = 1, \dots, N$ ,  $I_1, I_2$  are the moments of inertia of the Legs 1 and 2 about their centers of mass, respectively, and with the constant parameters  $p_1 = Ml^2 + m_1a^2 + m_2l^2$ ,  $p_2 = m_2lb$ ,  $p_3 = m_2b^2$ ,  $p_4 = (m_1a + m_2l + Ml)g$ ,  $p_5 = m_2bg$ .

Hence, the discretized swing phase of the 2-DOF biped robot is described by the set of equations (2.36)-(2.41).

Now for the Impact Phase of the discretized biped robot, due to the fact that the impact phase is considered an instantaneous event, the Discrete Mechanics based model is the same as the model that was derived in previous subchapters. So the impact phase of the biped robot using

Discrete Mechanics is:

$$\begin{bmatrix} p_8 - p_7 c_{12} + I_1 & -p_7 c_{12} + p_6 + I_2 \\ p_8 + I_1 & -p_7 c_{12} \end{bmatrix} \begin{bmatrix} \frac{q_{(1,1)}^{(i+1)} - q_{(1,N)}^{(i)}}{h^{(i)}} \\ \frac{q_{(2,1)}^{(i+1)} - q_{(2,N)}^{(i)}}{h^{(i)}} \end{bmatrix} = \begin{bmatrix} p_{10} c_{12} + I_1 & -p_{11} + I_2 \\ -p_9 + I_1 & 0 \end{bmatrix} \begin{bmatrix} \frac{q_{(1,N)}^{(i)} - q_{(1,N-1)}^{(i)}}{h^{(i)}} \\ \frac{q_{(2,N)}^{(i)} - q_{(2,N-1)}^{(i)}}{h^{(i)}} \end{bmatrix} \quad (2.44)$$

where  $c_{12} = \cos(q_{(1,N)}^{(i)} - q_{(2,N)}^{(i)})$  and the parameters  $p_6 = m_1 l^2 + M l^2 + m_2 a^2$ ,  $p_7 = m_1 b l$ ,  $p_8 = m_1 b^2$ ,  $p_9 = m_1 a b$ ,  $p_{10} = m_2 l a + M l^2 + m_1 l a$ ,  $p_{11} = m_2 a b$ .

Solving the system for  $\dot{q}^{(i,+)}$  by inverting the matrix  $\mathcal{Q}_+$  gives an impact map on the form (2.18)

$$\dot{q}^{(i+1)} = [\mathcal{Q}_+^{-1} \cdot \mathcal{Q}_-] \dot{q}^{(i)} \quad (2.45)$$

## 2.4 General Configuration of the Walking Terrain

In this subsection we will define the configuration of the general walking terrain of our biped. Based on the figures below, the different types of walking terrains for our biped robot will be the following: flat ground, upward and downward slopes, and surfaces involving upward and downward stairs.

Let  $C_0$  be the initial grounding point from where the biped starts to walk. On each simulation, the biped shall perform  $H$  walking steps on the terrain. We define the grounding points  $C_i = (L_i, H_i, D_i, \theta_i)$ ,  $i = 1, \dots, H$  as coordinates with reference to the previous grounding point,  $C_{i-1}$ , where  $L_i$  is the tangential distance between consecutive reference grounding points ( $C_{i-1}, C_i$ ),  $H_i$  is the step height (in cases of down/up stairs walking),  $D_i$  is the step length, and  $\theta_i$  is the inclination angle (in cases of downward and upward slopes and stairs). The length  $D_i$  of the  $i$ -th walking step depends on the type of terrain that the walking step will take place (see Figure 2.4).

We assume that, of course,  $L_i, D_i > 0$  (the robot moves forward along the positive x-axis),  $H_i > 0$  in the case of upstairs walking,  $H_i < 0$  in the case of downstairs walking,  $H_i = 0$  in the case of flat ground and downward/upward slope walking, and  $-1.13 \text{ rad} \leq \theta_i \leq 1.13 \text{ rad}$ . If

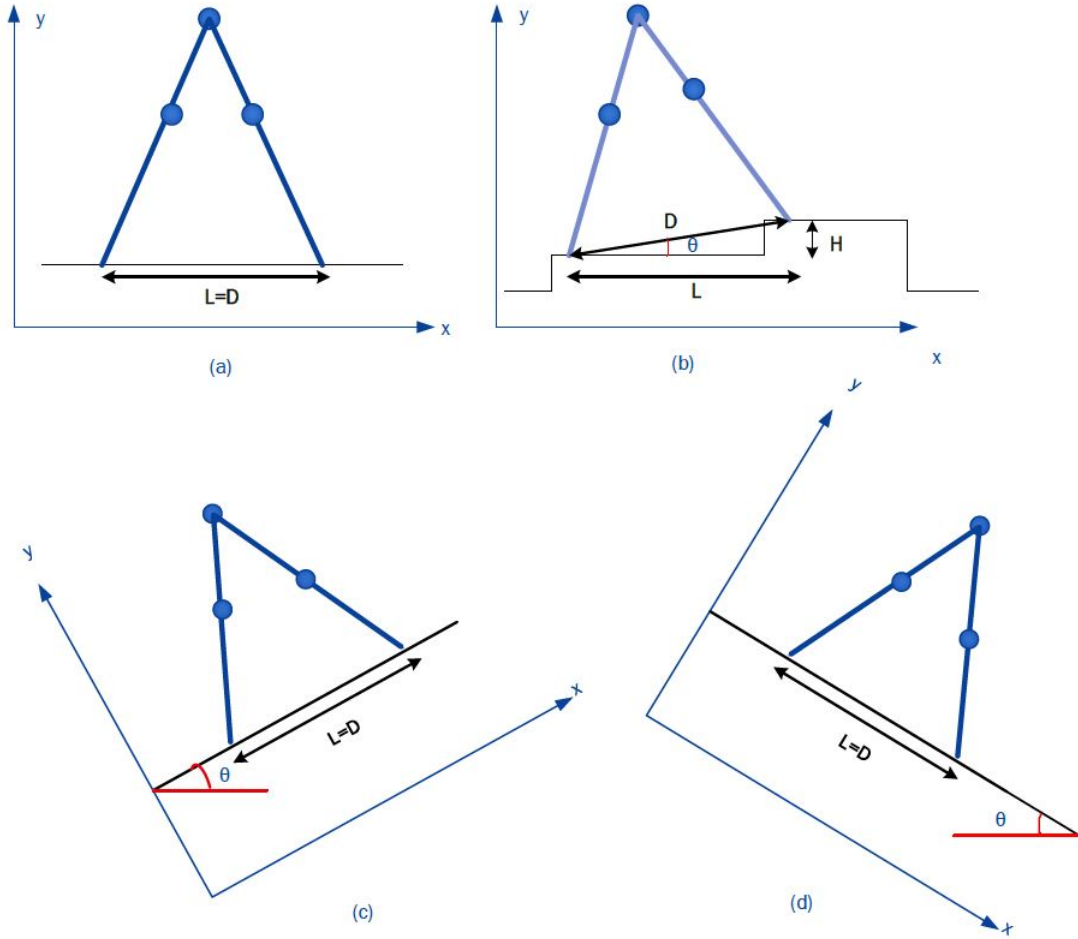


Figure 2.4: *Walking surfaces for the biped robot.*

$\theta_i = 0$ , then the  $i$ -th walking step will be done on a flat ground. If  $\theta_i > 0$ , then the  $i$ -th walking step will be done on an upward slope or stair. Finally if  $\theta_i < 0, i = 1, \dots, H$ , then the  $i$ -th walking step will be done on a downward slope or stair. For upstairs and downstairs walking, only parameters  $D_i = \sqrt{L_i^2 + H_i^2}$  and  $\theta_i = \sin^{-1}(\frac{H_i}{D_i})$ .

The set of points  $C_i, i = 1, \dots, H$  are, in other words, the reference points for the placement of the swing leg at the  $i$ -th walking step.

## 2.5 Derivation of the Gait Generation Problem for the First Phase

In the current subchapter, we will derive the Gait Generation Problem of the First Phase of D&CFC. The problem will be mathematically formulated as a finite-dimensional nonlinear constrained optimal control problem. The aim of the First Phase is the calculation of a trajectory for the 2-DOF Biped Robot for the  $i$ -th walking step,  $i = 1, \dots, H$ , ignoring any constraint forces (e.g. normal forces, friction forces).

We will now consider the following problem on the preliminary gait generation of the First Phase for the 2-DOF Biped Robot:

*For the 2-DOF Biped Robot that was developed throughout the Chapter 2, and ignoring any constraint forces on the stance foot, calculate a trajectory for the  $i$ -th walking step,  $i = 1, \dots, H$ , that includes the discretized control inputs and state variables, such that the corresponding swing leg of the 2-DOF Biped lands at the  $i$ -th reference grounding point of a general rough terrain with stable and natural gait.*

As we have mentioned on Chapter 1, we have implemented two variants of the proposed control system, thus we will derive the optimal gait generation problem for each one of them. In the following, we assume that the Leg 2 initially starts the walking process. In other words, during the odd walking steps, the Leg 1 is the stance leg and the Leg 2 is the swing leg, and during the even walking steps the Leg 1 is the swing leg and the Leg 2 is the stance leg.

### • Gait Generation Problem of the First Phase utilizing Direct Collocation

The mathematical formulation of the Gait Generation problem of the First Phase using Direct Collocation Method is stated as follows:

**For the odd walking steps:**

$$\text{minimize: } J = \sum_{k=1}^N [1, 2, 4] [(\tau_{(1,k)}^{(i)})^2 + (\tau_{(2,k)}^{(i)})^2] \frac{h^{(i)}}{3},$$

**subject to:**

- Swing Phase Model in State Space Form (2.17), (1)

- Impact Phase Model (2.27), (2)

- $q_{(1,approx)}^{(i)}(t_N) = q_{(1,approx)}^{(i+1)}(t_1) = \sin^{-1}\left(-\frac{D_i}{2l}\right) - \theta_i, (3)$

- $q_{(2,approx)}^{(i)}(t_N) = q_{(2,approx)}^{(i+1)}(t_1) = \sin^{-1}\left(\frac{D_i}{2l}\right) - \theta_i, (4)$

- $\cos(-q_{(1,approx)}^{(i)}(t_k) + \theta_i) - \cos(q_{(2,approx)}^{(i)}(t_k) + \theta_i) > 0, k = 2, \dots, N - 1, (5)$

- Impact Surface Conditions (2.33), (6)

- $\sin(-q_{(1,approx)}^{(i)}(t_{k+1}) + \theta_i) \frac{q_{(1,approx)}^{(i)}(t_{k+1}) - q_{(1,approx)}^{(i)}(t_k)}{h^{(i)}} - \sin(q_{(2,approx)}^{(i)}(t_k) + \theta_i) \frac{q_{(2,approx)}^{(i)}(t_{k+1}) - q_{(2,approx)}^{(i)}(t_k)}{h^{(i)}} > 0, k = 1, \dots, N - 1, (7)$

- $\tau_{min} \leq \tau_k^{(i)} \leq \tau_{max}, k = 1, \dots, N, (8)$

- $-\frac{\pi}{2} \leq q_{(1,k)}^{(i)}, q_{(2,k)}^{(i)} \leq \pi, k = 1, \dots, N, (9)$

- $-\dot{q}_{max} \leq \dot{q}_{(1,k)}^{(i)}, \dot{q}_{(2,k)}^{(i)} \leq \dot{q}_{max}, k = 1, \dots, N, (10)$

- Average linear walking speed  $V_i \Leftrightarrow V_i = \frac{D_i}{T_i} \Leftrightarrow T_i = \frac{D_i}{V_i} \Leftrightarrow (N - 1)h^{(i)} = \frac{D_i}{V_i} \Leftrightarrow h^{(i)} = \frac{D_i}{V_i(N - 1)}, (11)$

- **with initial conditions:**  $q_{(1,1)}^{(i)}, q_{(2,1)}^{(i)}, \dot{q}_{(1,1)}^{(i)}, \dot{q}_{(2,1)}^{(i)},$

- and **conservation of angular momentum necessary conditions.**

For the even walking steps, we formulate a similar Gait Generation Problem.

Based on the abovementioned (Direct Collocation-based/Forward Dynamics Based) optimization problem:

1. We want to minimize the control effort required to achieve the  $i - th$  walking step,  $i = 1, \dots, H$ . We have used the Simpson's rule for approximating the cost function. The coefficients [1, 2, 4] refer to the fact that, due to the use of the Simpson's Rule, all the function evaluations at points  $k$  with odd subscripts are multiplied by 4 and all the func-

tion evaluations at points  $k$  with even subscripts are multiplied by 2, except for the first and last ( in which the coefficient 1 refers to).

2. **Constraints (1) and (2)** define the Swing Phase (in State Space Form) and Impact Phase Models of the 2-DOF Biped that were extensively developed throughout Chapter 2.
3. **Constraints (3) and (4)** refer to the configuration of the two legs of the 2-DOF Biped during the Impact Phase (i.e. in the time interval  $[t_N^{(i)}, t_1^{(i+1)}]$ ).
4. **Constraint (5)** refers to the fact that the Swing Leg must be above the Stance Leg and not touch the ground surface for the duration of the Swing Phase. In other words, during the Swing Phase, the vertical length of the swing leg is smaller than the one of the stance leg.
5. **Constraint (6)** outline the configuration of the biped during the time steps of the Impact Phase; the configuration of each leg remains the same for the small duration of the impact of the swing leg with the ground.
6. **Constraint (7)** implies the height of the Swing Leg that is monotonously being decreased at each time step of the Swing Phase.
7. **Constraints (8) - (10)** refer to the physical constraints of the rotational actuators.
8. **Constraint (11)** refers to the average linear walking speed of the swing leg, if it is selected to be an active constraint. From the expression of the average linear walking speed, we can calculate the duration of a time interval for the  $i$ th walking step,  $h^{(i)}$ , otherwise a predefined value for the time interval is being used.
9. As **initial values** of the optimization problems are considered the generalized angles and velocities of the two legs at the first time step of a walking step.

#### • Gait Generation Problem of the First Phase utilizing Discrete Mechanics

The mathematical formulation of the Gait Generation problem of the First Phase using Discrete

Mechanics is stated as follows:

**For the odd walking steps:**

$$\text{minimize: } J = \sum_{k=1}^N [1, 2, 4] [(\tau_{(1,k)}^{(i)})^2 + (\tau_{(2,k)}^{(i)})^2] \frac{h^{(i)}}{3},$$

**subject to:**

- Swing Phase Model (2.43), (1)

- Boundary Conditions (2.38-2.41), (2)

- Impact Phase Model (2.44), (3)

- $q_{(1,N)}^{(i)} = q_{(1,1)}^{(i+1)} = \sin^{-1}\left(-\frac{D_i}{2l}\right) - \theta_i$ , (4)

- $q_{(2,N)}^{(i)} = q_{(2,1)}^{(i+1)} = \sin^{-1}\left(\frac{D_i}{2l}\right) - \theta_i$ , (5)

- $\cos(-q_{(1,k)}^{(i)} + \theta_i) - \cos(q_{(2,k)}^{(i)} + \theta_i) > 0, k = 2, \dots, N - 1$ , (6)

- Impact Surface Conditions (2.32), (7)

- $\sin(-q_{(1,k+1)}^{(i)} + \theta_i) \frac{q_{(1,k+1)}^{(i)} - q_{(1,k)}^{(i)}}{h^{(i)}} - \sin(q_{(2,k)}^{(i)} + \theta_i) \frac{q_{(2,k+1)}^{(i)} - q_{(2,k)}^{(i)}}{h^{(i)}} > 0, k = 1, \dots, N - 1$ , (8)

- $\tau_{min} \leq \tau_k^{(i)} \leq \tau_{max}, k = 1, \dots, N$ , (9)

- $-\frac{\pi}{2} \leq q_{(1,k)}^{(i)}, q_{(2,k)}^{(i)} \leq \pi, k = 1, \dots, N$ , (10)

- $-\dot{q}_{max} \leq \dot{q}_{(1,k)}^{(i)}, \dot{q}_{(2,k)}^{(i)} \leq \dot{q}_{max}, k = 1, \dots, N$  (11)

- Average linear walking speed  $V_i \Leftrightarrow V_i = \frac{D_i}{T_i} \Leftrightarrow T_i = \frac{D_i}{V_i} \Leftrightarrow (N - 1)h^{(i)} = \frac{D_i}{V_i}$   
 $\Leftrightarrow h^{(i)} = \frac{D_i}{V_i(N - 1)}$ , (12)

- **with initial conditions:**  $q_{(1,1)}^{(i)}, q_{(2,1)}^{(i)}, \dot{q}_{(1,1)}^{(i)}, \dot{q}_{(2,1)}^{(i)}$ ,

- and **conservation of angular momentum necessary conditions.**

For the even walking steps, we formulate a similar Gait Generation Problem.

In the abovementioned (Discrete Mechanics-Based/Inverse Dynamics-based) optimization problem, we have to use the Swing Phase Model (not the State Space Form) that was derived based

on Discrete Mechanics and to take into account the finite difference conditions related to the first and second derivative of the generalized angles of the swing and stance leg. In addition, we have to utilize the Boundary Conditions related to the initial and terminal values of the generalized angles and velocities of the two legs. The other constraints remain the same as in the direct collocation-based optimization problems.

# Chapter 3

## Second Phase of the Gait Generation Module

### 3.1 Introduction and Key Points of the Second Phase

In the current Chapter, we will implement the Second Phase of the Gait Generation Module for the proposed system. The Second Phase, based on the trajectory that was calculated at the First Phase, proceeds with the Gait Generation for the Complete, 4-DOF Biped Robot, using a novel method called Energy Efficient Trajectory Synthesis and Verification.

The walking motion of the complete 4-DOF biped includes three Phases: Swing Phase, Instantaneous Push-off Phase and Heel-Strike Phase. The Swing phase begins at the instant just after the stance foots hit the ground surface at heel-strike and the swing foot is away from the ground. Two instants before the swing foot makes contact with the ground, the swing phase ends. Then, the Push-Off Phase is applied instantaneously between the end of the swing phase and the heel-strike process which sets the stage for the Heel Strike Phase. In the walking process, the complete biped robot uses three actuators: two rotational joint torques at the hip for the rotational motion of the two legs and one instantaneous push-off impulse for the stance feet. As we will see in the equations of motion of the biped in the Second Phase, the control inputs vector will consist of four elements: the first two are the rotational torques applied to

the legs ( $\tau_1, \tau_2$ ) and the remaining two are the axial components of the instantaneous impulse applied at the Push-Of Phase ( $F_{(PO,x)}, F_{(PO,y)}$ ).

Here, we assume that the collision at heel-strike is a no-bounce process and there is no double support after heel-strike. The instantaneous push-off just before heel-strike is a strategy to reduce the collision loss as well as to stabilize the whole biped, which is a classical design for the energy-optimal walking motion. We assume that there is sufficient friction between the feet and the ground surface to prevent slippage during the whole walking process.

As we have seen in previous Chapters, the biped robot generally includes two legs that are hinged at the hip. The leg length is  $l$  and the mass on the leg is located at the point that the distance to the hip is  $l_t$ . The complete 4-DOF biped has four degrees of freedom,  $q_1, q_2, q_3, q_4$ .  $q_1, q_2$  represent the angles of the legs with respect to the ground surface normal, and  $(q_3, q_4)$  define the coordinates of the stance foot in the rectangular coordinate system that the forward and upward directions are positive and the initial position of the stance foot is  $(0, 0)$ . Therefore, the walking model can be described by the abovementioned generalized coordinates which characterize 4 degrees of freedom (DOF's) of the model.

Our walking model includes in the Second Phase not only the generalized coordinates  $q_1, q_2$  that describe the status of the two legs but also the generalized coordinates of the stance foot  $q_3, q_4$ . There are two advantages:

- During the swing phase, the stance foot is the only point that contact with the ground. The constrained forces of the stance foot that include the normal force and the friction force can be obtained by constraining the position of the stance foot. Therefore, the friction force, and whether the stance foot leaves the ground can be checked to meet the walking constraints.
- The instantaneous processes push-off and heel-strike can be described by the equivalent impulses that contact with the ground. The conventional angular momentum conservation theorem (used in the First Phase) is not needed for solving the heel-strike process.

Regarding to the notation of all the variables (e.g. states, angular coordinates/velocities/accelerations, control inputs, constrained forces) in the discretized setting, assuming that a walking step consists of  $N$  time steps, then when we see the mathematical representation  $x_{(1,k)}^{(i)}$  for instance, we

refer to the value of the variable  $x_1$  for  $t = N(i-1)h + (k-1)h$  sec. Thus,  $x_{(1,k)}^{(i)} = x_1(t = N(i-1)h + (k-1)h$  sec),  $x_k^{(i)} = x(t = N(i-1)h + (k-1)h$  sec),  $q_{(1,k)}^{(i)} = q_1(t = N(i-1)h + (k-1)h$  sec),  $q_{(2,k)}^{(i)} = q_2(t = N(i-1)h + (k-1)h$  sec),  $u_k^{(i)} = u(t = N(i-1)h + (k-1)h$  sec) etc. The abovementioned notation is used throughout the current thesis.

In the current Chapter, we firstly develop the equations of motion for all the walking phases of the biped, for both the Direct Collocation and Discrete Mechanics Methods. Furthermore, we derive extensively the Gait Generation Problems of the Second Phase for both methods. Then, we develop a novel method called "Energy Efficient Trajectory Synthesis and Verification", which calculates energy-optimal possible trajectory for each walking step, while respecting the technical and physical constraints of the biped, as well as the qualitative behavior of a proper walking step.

The key to our novel method is the calculated trajectory of the First Phase. Based on it, using all the sets of calculated variables from each time step of the calculated trajectory as initial values for the optimal control problems of the Second Phase, a set of new trajectories are being calculated for the complete robot. Then, the abovementioned method, for each time step of the walking step, finds and selects the related set of calculated variables from the newly created trajectories with the lowest possible Energy Consumption (or Cost of Transport, COT), and that obey all the constraints of the biped, following the qualitative behavior of a proper walking step. For the last requirement, the first trajectory that is calculated in the Second Phase (where we give as initial values for the optimal control problem the set of calculated variables from the first walking step, as calculated in the First Phase) is used as a "reference" trajectory.

The results of the proposed Decrease & Conquer architecture, as we will see in Chapter 4, are outstanding. The utilization of the proposed system, in contrast with conventional one Phase gait generation approaches and high performance commercial solvers, leads to the synthesis of the most energy efficient, stable and natural walking gaits for our biped, for virtually any ground surface: flat ground, downward and upward slopes/stairs, and general terrains involving downward and upward stairs.

### •Gait Generation Problem of the Second Phase

On Subchapter 3.6 we derive the Gait Generation Problem for the First Phase of the Gait Generation Module. The aim of the Second Phase is to minimize the so called Cost of Transport (COT) required to achieve a particular walking step, subject to constraints related to:

1. the derived equations of motion for each walking phase,
2. the configuration of the biped during the impact of the swing leg with the ground,
3. some features of the swing and stance legs that lead to a proper walking behavior,
4. the physical constraints of the used actuators, and
5. additional, optional constraints (e.g. average linear walking speed of the swing leg etc.).

## **3.2 Swing Phase of the 4-DOF Biped Robot for the Direct Collocation Method (Leg1 = Stance, Leg2 = Swing)**

As we have seen in Chapter 2, the first step to deriving the Lagrangian of the biped is to define the homogeneous transfer matrices that describe the orientation and position of each link of the robot. One natural placement of local coordinate frames is indicated in Figure 3.1, where each frame is rigidly attached to the appropriate mass. The origins of each of these frames describe the following important points on the planar biped:

1.  $o_0 = o_{3,4}$  - Global coordinate frame fixed to the ground, that is, the Cartesian Coordinates of the stance foot.
2.  $o_1$  - Coordinate frame fixed to the center of mass for the stance leg(Leg 1).
3.  $o_M$  - Coordinate frame fixed to the center of mass of the hip joint.
4.  $o_2$  - Coordinate frame fixed to the center of mass for the swing leg(Leg 2).

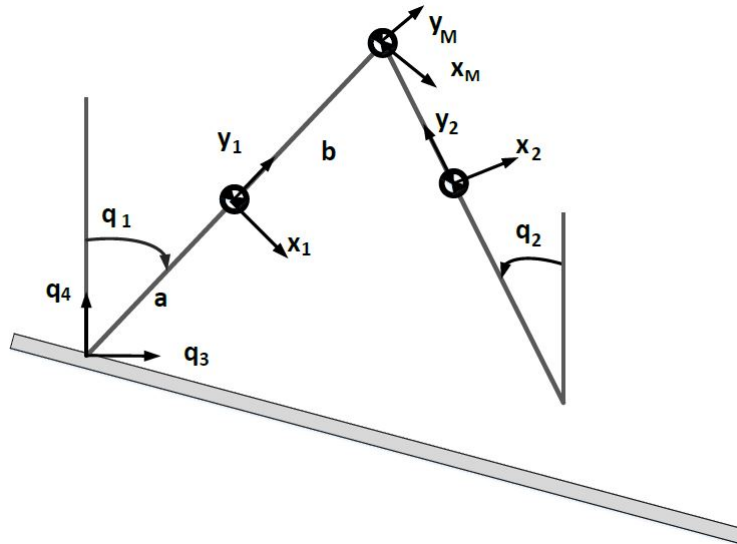


Figure 3.1: Assignment of origins for the coordinate frames of the robot.

These coordinate frames are used to form homogeneous transformation matrices on the form

$$H_j^i = \begin{bmatrix} R_j^i & p_j^i \\ 0_{1 \times 3} & 1 \end{bmatrix} \quad (3.1)$$

where  $R_j^i \in \mathbb{R}^{3 \times 3}$  is the rotation matrix from frame  $j$  to frame  $i$  and  $p_j^i \in \mathbb{R}^3$  is the distance between the origins of the respective frames expressed in frame  $i$ . Finding rotation matrices is complicated, requiring a parametrization of the total rotation of each frame in suitable coordinates. This process is greatly simplified by the fact that the planar biped only experiences motion in a 2-D plane. The transformation matrices can then be found by trigonometry and

are stated for verification below:

$$\begin{aligned}
 H_1^0 &= \begin{bmatrix} \cos(q_1^{(i)}) & -\sin(q_1^{(i)}) & 0 & q_3 - a\sin(q_1^{(i)}) \\ -\sin(q_1^{(i)}) & \cos(q_1^{(i)}) & 0 & q_4 + a\cos(q_1^{(i)}) \\ 0 & 0 & 1 & 0 \\ 0 & 0 & 0 & 1 \end{bmatrix} \\
 H_M^1 &= \begin{bmatrix} 1 & 0 & 0 & 0 \\ 0 & 1 & 0 & b \\ 0 & 0 & 1 & 0 \\ 0 & 0 & 0 & 1 \end{bmatrix} \\
 H_M^0 &= H_1^0 H_M^1 \\
 H_2^0 &= \begin{bmatrix} \cos(q_2^{(i)}) & -\sin(q_2^{(i)}) & 0 & q_3 + l\sin(q_1^{(i)}) + b\sin(q_2^{(i)}) \\ \sin(q_2^{(i)}) & \cos(q_2^{(i)}) & 0 & q_4 + l\cos(q_1^{(i)}) - b\cos(q_2^{(i)}) \\ 0 & 0 & 1 & 0 \\ 0 & 0 & 0 & 1 \end{bmatrix}
 \end{aligned} \tag{3.2}$$

The matrices (3.2) can now be employed to determine the position  $p^{(0)}$  and velocity  $v^{(0)}$  of the center of mass of each mass in  $xy$  coordinates in the global frame  $o_0$  as

$$\begin{aligned}
 p_1^{(0)} &= [I_{2 \times 2} \ 0_{2 \times 2}] \cdot H_1^0 \cdot \begin{bmatrix} 0_{3 \times 1} \\ 1 \end{bmatrix}, v_1^{(0)} = \frac{d}{dt} p_1^{(0)} \\
 p_M^{(0)} &= [I_{2 \times 2} \ 0_{2 \times 2}] \cdot H_M^0 \cdot \begin{bmatrix} 0_{3 \times 1} \\ 1 \end{bmatrix}, v_M^{(0)} = \frac{d}{dt} p_M^{(0)} \\
 p_2^{(0)} &= [I_{2 \times 2} \ 0_{2 \times 2}] \cdot H_2^0 \cdot \begin{bmatrix} 0_{3 \times 1} \\ 1 \end{bmatrix}, v_2^{(0)} = \frac{d}{dt} p_2^{(0)}
 \end{aligned} \tag{3.3}$$

where  $I_{2 \times 2}$  is the identity matrix and  $p^{(0)}, v^{(0)} \in \mathbb{R}^2$ .

In order to form the Lagrangian of the system and compute the Euler-Lagrange equations, the kinetic and potential energy of the system must be determined. The potential energy is the

sum of the potential energy at the center of mass for each mass and can be expressed as

$$\mathcal{P} = (m_1 h_1^{(0)} + M h_M^{(0)} + m_2 h_2^{(0)})g \quad (3.4)$$

where  $g = (\sin(\theta_i) + \cos(\theta_i))g_{const}$ , with  $g_{const} = 9.81m/s^2$  and  $\theta$  defining the slope of the next walking step to be achieved, is the gravitational acceleration quantity in the horizontal and vertical axes and  $h^{(0)} = p^{(0)} \begin{bmatrix} 0 \\ 1 \end{bmatrix}$  is the height of the respective centers of mass expressed in the global frame  $o_0$ . The total kinetic energy is the sum of the body's centers-of-mass translational kinetic energy and the energy of rotation around the centers of mass (rotational energy), and can be expressed as

$$\mathcal{K} = \frac{1}{2}(m_1 v_1^T v_1 + M v_M^T v_M + m_2 v_2^T v_2) + \frac{1}{2}(I_1 (\dot{q}_1^{(i)})^2 + I_2 (\dot{q}_2^{(i)})^2) \quad (3.5)$$

Using the expressions (3.4) and (3.5) for the potential and kinetic energy, the Euler-Lagrange equations of motion can be calculated

$$\frac{d}{dt} \left( \frac{\partial \mathcal{L}}{\partial \dot{q}_{j^{(i)}}} \right) - \frac{\partial \mathcal{L}}{\partial q_{j^{(i)}}} = B_a(q^{(i)}) \begin{bmatrix} \tau_1^{(i)} \\ \tau_2^{(i)} \\ F_{(PO,x)}^{(i)} \\ F_{(PO,y)}^{(i)} \end{bmatrix} + S_{con}^T f_{con}^{(i)}(q^{(i)}, \dot{q}^{(i)}) \quad j \in [1, 2, 3, 4] \quad (3.6)$$

where  $\mathcal{L}$  is the Lagrangian of the system derived from (3.4) and (3.5) as

$$\mathcal{L} = \mathcal{K} - \mathcal{P}$$

that extends to:

$$\begin{aligned} L(q_1^{(i)}, q_2^{(i)}, q_3^{(i)}, q_4^{(i)}, \dot{q}_1^{(i)}, \dot{q}_2^{(i)}, \dot{q}_3^{(i)}, \dot{q}_4^{(i)}) &= \frac{m_2 \left( \dot{q}_4^{(i)} + b \dot{q}_2^{(i)} \sin(q_2^{(i)}) - \dot{q}_1^{(i)} l \sin(q_1^{(i)}) \right)^2}{2} \\ &+ \frac{M \left( a \dot{q}_1^{(i)} \cos(q_1^{(i)}) - \dot{q}_3^{(i)} + b \dot{q}_1^{(i)} \cos(q_1^{(i)}) \right)^2}{2} + \frac{M \left( a \dot{q}_1^{(i)} \sin(q_1^{(i)}) - \dot{q}_4^{(i)} + b \dot{q}_1^{(i)} \sin(q_1^{(i)}) \right)^2}{2} \end{aligned}$$

$$\begin{aligned}
 & + \frac{m_1 \left( \dot{q}_3^{(i)} - a \dot{q}_1^{(i)} \cos(q_1^{(i)}) \right)^2}{2} + \frac{m_2 \left( \dot{q}_3^{(i)} + \dot{q}_2^{(i)} l \cos(q_2^{(i)}) + b \dot{q}_2^{(i)} \cos(q_2^{(i)}) \right)^2}{2} + \frac{m_1 \left( \dot{q}_4^{(i)} - a \dot{q}_1^{(i)} \sin(q_1^{(i)}) \right)^2}{2} \\
 & - g M \left( q_4^{(i)} + a \cos(q_1^{(i)}) + b \cos(q_1^{(i)}) \right) - g m_2 \left( q_4^{(i)} - b \cos(q_2^{(i)}) + l \cos(q_1^{(i)}) \right) \\
 & - g m_1 \left( q_4^{(i)} + a \cos(q_1^{(i)}) \right) + \frac{1}{2} (I_1 (\dot{q}_1^{(i)})^2 + I_2 (\dot{q}_2^{(i)})^2) \quad (3.7)
 \end{aligned}$$

$B_a(q^{(i)})$  is the applied forces selection matrix (it maps the applied linear forces and/or torques to

the related generalized coordinates). Here,  $B_a(q^{(i)}) = \begin{bmatrix} 1 & 0 & 0 & 0 \\ 0 & 1 & 0 & 0 \\ 0 & 0 & 0 & 0 \\ 0 & 0 & 0 & 0 \end{bmatrix}$  (thus,  $B_a(q^{(i)})$  here is not

a full row rank matrix) assuming that, due to the use of the two hip actuators (and not of the

linear actuator), only the torques  $\tau_1^{(i)}, \tau_2^{(i)}$  to the hip can be controlled.  $S_{con}^T f_{con}^{(i)}(q^{(i)}, \dot{q}^{(i)})$  is the

constrained force at stance foot at the  $i$ -th walking step, where  $S_{con} = \begin{bmatrix} 0 & 0 & 1 & 0 \\ 0 & 0 & 0 & 1 \end{bmatrix}$  is called

the constraint force selection matrix, and  $f_{con}^{(i)}(q^{(i)}, \dot{q}^{(i)}) = \begin{bmatrix} f_{fr}^{(i)}(q^{(i)}, \dot{q}^{(i)}) \\ f_N^{(i)}(q^{(i)}, \dot{q}^{(i)}) \end{bmatrix}$  is the constraint force

vector. The topology of the values of the constraint force selection matrix leads to the conclusion

that the constraint forces will be applied to the stance foot (in other words, they will affect the

generalized coordinates  $q_3^{(i)}, q_4^{(i)}$  of the stance foot). Note that the stance leg at each walking

step will be either Leg 1 or Leg 2. The constraint force vector consists of the constraint

forces that are applied to the stance foot at the  $i$ -th walking step and are the friction force

$f_{fr}^{(i)}(q^{(i)}, \dot{q}^{(i)})$  and the normal force  $f_N^{(i)}(q^{(i)}, \dot{q}^{(i)})$ , so  $S_{con}^T f_{con}^{(i)}(q^{(i)}, \dot{q}^{(i)})$  equals to  $\begin{bmatrix} 0 \\ 0 \\ f_{fr}^{(i)}(q^{(i)}, \dot{q}^{(i)}) \\ f_N^{(i)}(q^{(i)}, \dot{q}^{(i)}) \end{bmatrix}$

and each quantity will be derived later. Note that the linear actuators at the stance feet are

not used in the Swing Phase, but they will be extensively used in the Instantaneous Push Off

Phase.

Using the expressions (8.39) – (8.41) for the elements of the respective matrices, the equations

of motion for the biped can be formulated as

$$M(q^{(i)})\ddot{q}^{(i)} + C(q^{(i)}, \dot{q}^{(i)})\dot{q}^{(i)} + G(q^{(i)}, \theta_i) = B_a(q^{(i)}) \begin{bmatrix} \tau_1^{(i)} \\ \tau_2^{(i)} \\ F_{(PO,x)}^{(i)} \\ F_{(PO,y)}^{(i)} \end{bmatrix} + S_{con}^T \begin{bmatrix} f_{fr}^{(i)}(q^{(i)}, \dot{q}^{(i)}) \\ f_N^{(i)}(q^{(i)}, \dot{q}^{(i)}) \end{bmatrix} \quad (3.8)$$

$\Leftrightarrow$

$$M(q^{(i)})\ddot{q}^{(i)} + C(q^{(i)}, \dot{q}^{(i)})\dot{q}^{(i)} + G(q^{(i)}, \theta_i) = \begin{bmatrix} \tau_1^{(i)} \\ \tau_2^{(i)} \\ 0 \\ 0 \end{bmatrix} + \begin{bmatrix} 0 \\ 0 \\ f_{fr}^{(i)}(q^{(i)}, \dot{q}^{(i)}) \\ f_N^{(i)}(q^{(i)}, \dot{q}^{(i)}) \end{bmatrix}$$

where

$$M(q^{(i)}) = \begin{bmatrix} p_{12} + I_1 & -p_{13}\cos(q_1^{(i)}) & -p_{16}\cos(q_1^{(i)}) & -p_{16}\sin(q_1^{(i)}) \\ -p_{13}\cos(q_1^{(i)}) & p_{14} + I_2 & p_{15}\cos(q_2^{(i)}) & p_{15}\sin(q_2^{(i)}) \\ -p_{16}\cos(q_1^{(i)}) & p_{15}\cos(q_2^{(i)}) & p_{17} & 0 \\ -p_{16}\sin(q_1^{(i)}) & p_{15}\sin(q_2^{(i)}) & 0 & p_{17} \end{bmatrix} \quad (3.9)$$

$$C(q^{(i)}, \dot{q}^{(i)}) \Rightarrow C(:, 1) = \begin{bmatrix} p_{13}\sin(q_1^{(i)} - q_2^{(i)})\dot{q}_2^{(i)} + p_{16}(\sin(q_1^{(i)})\dot{q}_3^{(i)} - \cos(q_1^{(i)}))\dot{q}_4^{(i)} \\ p_{13}\sin(q_1^{(i)} - q_2^{(i)})(\dot{q}_1^{(i)} - \dot{q}_2^{(i)}) \\ p_{16}\sin(q_1^{(i)})\dot{q}_1^{(i)} \\ -p_{16}\cos(q_1^{(i)})\dot{q}_1^{(i)} \end{bmatrix}$$

$$C(:, 2) = \begin{bmatrix} p_{13}\sin(q_1^{(i)} - q_2^{(i)})(\dot{q}_1^{(i)} - \dot{q}_2^{(i)}) \\ p_{13}\sin(q_1^{(i)} - q_2^{(i)})\dot{q}_1^{(i)} - p_{15}\sin(q_2^{(i)})\dot{q}_3^{(i)} + p_{15}\cos(q_2^{(i)})\dot{q}_4^{(i)} \\ -p_{15}\sin(q_2^{(i)})\dot{q}_2^{(i)} \\ p_{15}\cos(q_2^{(i)})\dot{q}_2^{(i)} \end{bmatrix}$$

$$C(:, 3) = \begin{bmatrix} p_{16} \sin(q_1^{(i)}) \dot{q}_1^{(i)} \\ -p_{15} \sin(q_2^{(i)}) \dot{q}_2^{(i)} \\ 0 \\ 0 \end{bmatrix}$$

$$C(:, 4) = \begin{bmatrix} -p_{16} \cos(q_1^{(i)}) \dot{q}_1^{(i)} \\ p_{15} \cos(q_2^{(i)}) \dot{q}_2^{(i)} \\ 0 \\ 0 \end{bmatrix} \quad (3.10)$$

$$G(q^{(i)}, \theta_i) = \begin{bmatrix} -gM(a \sin(q_1^{(i)}) + b \sin(q_2^{(i)})) - agm_1 \sin(q_1^{(i)}) - glm_2 \sin(q_1^{(i)}) \\ bgm_2 \sin(q_2^{(i)}) \\ 0 \\ gm_1 + gm_2 + gM \end{bmatrix} \quad (3.11)$$

where  $I_1, I_2$  are the moments of inertia of the Legs 1 and 2 about their centers of mass, respectively,  $p_{12} = Ml^2 + m_1a^2 + m_2l^2, p_{13} = m_2bl, p_{14} = m_2b^2, p_{15} = m_2b, p_{16} = Ml + m_1a + m_2l, p_{17} = m_1 + m_2 + M$ .

**•Initial Discretization of the Swing Phase for the Direct Collocation Method (Leg1 = Stance, Leg2 = Swing)**

Now we will proceed with the initial discretization (without applying the Direct Collocation Conditions) of the Swing Phase of the 4-DOF Biped Robot for the case where the Leg 1 is the stance leg and the Leg 2 is the swing leg. Let  $k = 1, \dots, N$  the time steps of a walking step. In addition, let  $i = 1, \dots, H$  the number and the order of the total walking steps. So, when we refer to a generalized angle  $q_{(x,k)}^{(i)}$ , where  $x = 1, 2, k = 1, \dots, N$  and  $i = 1, \dots, H$  we will actually mean the angle  $q_x$  of the  $k$  -  $th$  time step of the  $i$  -  $th$  walking step. A discretization of the time

interval for a walking step

$$t_0 = t_1 < t_2 < \dots < t_N = t_f$$

is chosen. Without implementing the complete discretization process (it will be later explained in the current chapter), the Swing Phase becomes:

$$M(q_k^{(i)})\ddot{q}_k^{(i)} + C(q_k^{(i)}, \dot{q}_k^{(i)})\dot{q}_k^{(i)} + G(q_k^{(i)}, \theta_i) = B_a(q_k^{(i)}) \begin{bmatrix} \tau_{(1,k)}^{(i)} \\ \tau_{(2,k)}^{(i)} \\ F_{(PO,x)}^{(i)} \\ F_{(PO,y)}^{(i)} \end{bmatrix} + S_{con}^T f_{(con,k)}^{(i)}, \quad k = 1, \dots, N-2 \quad (3.12)$$

$\Leftrightarrow$

$$M(q_k^{(i)})\ddot{q}_k^{(i)} + C(q_k^{(i)}, \dot{q}_k^{(i)})\dot{q}_k^{(i)} + G(q_k^{(i)}, \theta_i) = \begin{bmatrix} \tau_{(1,k)}^{(i)} \\ \tau_{(2,k)}^{(i)} \\ 0 \\ 0 \end{bmatrix} + \begin{bmatrix} 0 \\ 0 \\ f_{(fr,k)}^{(i)} \\ f_{(N,k)}^{(i)} \end{bmatrix}, \quad k = 1, \dots, N-2$$

$$\text{where } f_{(con,k)}^{(i)} = \begin{bmatrix} f_{(fr,k)}^{(i)} \\ f_{(N,k)}^{(i)} \end{bmatrix} = \begin{bmatrix} f_{fr}^{(i)}(q_k^{(i)}, \dot{q}_k^{(i)}) \\ f_N^{(i)}(q_k^{(i)}, \dot{q}_k^{(i)}) \end{bmatrix}, \quad k = 1, \dots, N-2,$$

$$M(q_k^{(i)}) = \begin{bmatrix} p_{12} + I_1 & -p_{13}\cos(q_{(1,k)}^{(i)}) & -p_{16}\cos(q_{(1,k)}^{(i)}) & -p_{16}\sin(q_{(1,k)}^{(i)}) \\ -p_{13}\cos(q_{(1,k)}^{(i)}) & p_{14} + I_2 & p_{15}\cos(q_{(2,k)}^{(i)}) & p_{15}\sin(q_{(2,k)}^{(i)}) \\ -p_{16}\cos(q_{(1,k)}^{(i)}) & p_{15}\cos(q_{(2,k)}^{(i)}) & p_{17} & 0 \\ -p_{16}\sin(q_{(1,k)}^{(i)}) & p_{15}\sin(q_{(2,k)}^{(i)}) & 0 & p_{17} \end{bmatrix}, \quad k = 1, \dots, N-2 \quad (3.13)$$

$$C(q_k^{(i)}, \dot{q}_k^{(i)}) \Rightarrow C(:, 1) = \begin{bmatrix} p_{13}\sin(q_{(1,k)}^{(i)} - q_{(2,k)}^{(i)})\dot{q}_{(2,k)}^{(i)} + p_{16}(\sin(q_{(1,k)}^{(i)})\dot{q}_{(3,k)}^{(i)} - \cos(q_{(1,k)}^{(i)})\dot{q}_{(4,k)}^{(i)}) \\ p_{13}\sin(q_{(1,k)}^{(i)} - q_{(2,k)}^{(i)})(\dot{q}_{(1,k)}^{(i)} - \dot{q}_{(2,k)}^{(i)}) \\ p_{16}\sin(q_{(1,k)}^{(i)})\dot{q}_{(1,k)}^{(i)} \\ -p_{16}\cos(q_{(1,k)}^{(i)})\dot{q}_{(1,k)}^{(i)} \end{bmatrix}$$

$$C(:, 2) = \begin{bmatrix} p_{13} \sin(q_{(1,k)}^{(i)} - q_{(2,k)}^{(i)}) (\dot{q}_{(1,k)}^{(i)} - \dot{q}_{(2,k)}^{(i)}) \\ p_{13} \sin(q_{(1,k)}^{(i)} - q_{(2,k)}^{(i)}) \dot{q}_{(1,k)}^{(i)} - p_{15} \sin(q_{(2,k)}^{(i)}) \dot{q}_{(3,k)}^{(i)} + p_{15} \cos(q_{(2,k)}^{(i)}) \dot{q}_{(4,k)}^{(i)} \\ -p_{15} \sin(q_{(2,k)}^{(i)}) \dot{q}_{(2,k)}^{(i)} \\ p_{15} \cos(q_{(2,k)}^{(i)}) \dot{q}_{(2,k)}^{(i)} \end{bmatrix}$$

$$C(:, 3) = \begin{bmatrix} p_{16} \sin(q_{(1,k)}^{(i)}) \dot{q}_{(1,k)}^{(i)} \\ -p_{15} \sin(q_{(2,k)}^{(i)}) \dot{q}_{(2,k)}^{(i)} \\ 0 \\ 0 \end{bmatrix}, k = 1, \dots, N - 2$$

$$C(:, 4) = \begin{bmatrix} -p_{16} \cos(q_{(1,k)}^{(i)}) \dot{q}_{(1,k)}^{(i)} \\ p_{15} \cos(q_{(2,k)}^{(i)}) \dot{q}_{(2,k)}^{(i)} \\ 0 \\ 0 \end{bmatrix} \quad (3.14)$$

$$G(q^{(i)}, \theta_i) = \begin{bmatrix} -gM(a \sin(q_{(1,k)}^{(i)}) + b \sin(q_{(1,k)}^{(i)})) - agm_1 \sin(q_{(1,k)}^{(i)}) - glm_2 \sin(q_{(1,k)}^{(i)}) \\ bgm_2 \sin(q_{(2,k)}^{(i)}) \\ 0 \\ gm_1 + gm_2 + gM \end{bmatrix}, k = 1, \dots, N - 2 \quad (3.15)$$

where  $p_{12} = Ml^2 + m_1a^2 + m_2l^2$ ,  $p_{13} = m_2bl$ ,  $p_{14} = m_2b^2$ ,  $p_{15} = m_2b$ ,  $p_{16} = Ml + m_1a + m_2l$ ,  $p_{17} = m_1 + m_2 + M$ .

### •State Space Equations of the Swing Phase for the Direct Collocation Method (Leg1 = Stance, Leg2 = Swing)

We will now derive the state space equations of the Swing Phase and apply the Direct Collocation Conditions, for the case where Leg 1 is the Stance Leg and Leg 2 is the Swing Leg, for

the duration of the Swing Phase ( $k = 1, \dots, N - 2$ ). The choice of state variables is the vector:

$$\begin{bmatrix} x_{(1,k)}^{(i)} \\ x_{(2,k)}^{(i)} \end{bmatrix} = \begin{bmatrix} q_k^{(i)} \\ \dot{q}_k^{(i)} \end{bmatrix}$$

$$\text{where } x_{(1,k)}^{(i)} = q_k^{(i)} = \begin{bmatrix} q_{(1,k)}^{(i)} \\ q_{(2,k)}^{(i)} \\ q_{(3,k)}^{(i)} \\ q_{(4,k)}^{(i)} \end{bmatrix} \text{ and } x_{(2,k)}^{(i)} = \dot{q}_k^{(i)} = \begin{bmatrix} \dot{q}_{(1,k)}^{(i)} \\ \dot{q}_{(2,k)}^{(i)} \\ \dot{q}_{(3,k)}^{(i)} \\ \dot{q}_{(4,k)}^{(i)} \end{bmatrix}$$

The state equations are:

$$\begin{bmatrix} \dot{x}_{(1,k)}^{(i)} \\ \dot{x}_{(2,k)}^{(i)} \end{bmatrix} = \begin{bmatrix} x_{(2,k)}^{(i)} \\ -M^{-1}(x_{(1,k)}^{(i)})(C(x_{(1,k)}^{(i)}, x_{(2,k)}^{(i)})x_{(2,k)}^{(i)} + G(x_{(1,k)}^{(i)}, \theta_i) + S_{con}^T f_{(con,k)}^{(i)}) \end{bmatrix} + \begin{bmatrix} 0_{4 \times 4} \\ M^{-1}(x_{(1,k)}^{(i)})B_a(q_k^{(i)}) \end{bmatrix} u_k^{(i)}$$

where  $\begin{bmatrix} x_{(2,k)}^{(i)} \\ -M^{-1}(x_{(1,k)}^{(i)})(C(x_{(1,k)}^{(i)}, x_{(2,k)}^{(i)})x_{(2,k)}^{(i)} + G(x_{(1,k)}^{(i)}, \theta_i) + S_{con}^T f_{(con,k)}^{(i)}) \end{bmatrix}$  is a  $8 \times 1$  matrix and  $\begin{bmatrix} 0_{4 \times 4} \\ M^{-1}(x_{(1,k)}^{(i)})B_a(q_k^{(i)}) \end{bmatrix}$  is a  $8 \times 4$  matrix, the matrices  $M$ ,  $C$ ,  $G$  are given from the relations

$$(3.13-3.15), \text{ and with the applied forces vector } \begin{bmatrix} \tau_{(1,k)}^{(i)} \\ \tau_{(2,k)}^{(i)} \\ F_{(PO,x)}^{(i)} \\ F_{(PO,y)}^{(i)} \end{bmatrix} \text{ now denoted by } u_k^{(i)} = \begin{bmatrix} u_{(1,k)}^{(i)} \\ u_{(2,k)}^{(i)} \\ u_{(3,k)}^{(i)} \\ u_{(4,k)}^{(i)} \end{bmatrix}.$$

The output function is:

$$y_k^{(i)} = x_{(1,k)}^{(i)}$$

For the Direct Collocation Method, based on subchapter 8.3.4, we proceed with the formulation below. Let  $x_{appr}^{(i)}(t) = \begin{bmatrix} x_{(1,appr)}^{(i)}(t) \\ x_{(2,appr)}^{(i)}(t) \end{bmatrix}$ , where  $x_{(1,appr)}^{(i)}(t)$ ,  $x_{(2,appr)}^{(i)}(t)$  are the cubic approximations of the generalized coordinates  $q_1^{(i)}$ ,  $q_2^{(i)}$ ,  $q_3^{(i)}$ ,  $q_4^{(i)}$  as well as of their first and second derivatives, in the specified discretized time interval of the  $i$ -th walking step (relations 8.74-8.78). In addi-

tion, let  $u_{appr}^{(i)}(t) = \begin{bmatrix} \tau_{(1,appr)}^{(i)}(t) \\ \tau_{(2,appr)}^{(i)}(t) \\ F_{(PO,x,appr)}^{(i)}(t) \\ F_{(PO,y,appr)}^{(i)}(t) \end{bmatrix}$ , where  $\tau_{(1,appr)}^{(i)}(t)$ ,  $\tau_{(2,appr)}^{(i)}(t)$ ,  $F_{(PO,x,appr)}^{(i)}$ ,  $F_{(PO,y,appr)}^{(i)}$  are

the approximations of the control inputs (torques and linear forces)  $\tau_1^{(i)}$ ,  $\tau_2^{(i)}$ ,  $F_{(PO,x)}^{(i)}$ ,  $F_{(PO,y)}^{(i)}$  in the specified discretized time interval of the  $i - th$  walking step (relation 8.73). Thus, the state space equations of the Swing Phase for the case where Leg 1 is the Stance Leg and Leg 2 is the Swing Leg are (relations 8.79, 8.92):

$$\begin{bmatrix} \dot{x}_{(1,appr)}^{(i)}(t_{ck}) \\ \dot{x}_{(2,appr)}^{(i)}(t_{ck}) \end{bmatrix} = \begin{bmatrix} x_{(2,appr)}^{(i)}(t_{ck}) \\ -M^{-1}(x_{(1,appr)}^{(i)}(t_{ck}))(C(x_{(1,appr)}^{(i)}(t_{ck}), x_{(2,appr)}^{(i)}(t_{ck}))x_{(2,appr)}^{(i)}(t_{ck}) + G(x_{(1,appr)}^{(i)}(t_{ck}), \theta_i) + S_{con}^T f_{con,appr}^{(i)}(t_{ck})) \end{bmatrix} + \begin{bmatrix} 0_{4 \times 4} \\ M^{-1}(x_{(1,appr)}^{(i)}(t_{ck}))B_a(q_k^{(i)}) \end{bmatrix} u_{appr}^{(i)}(t_{ck}) \quad (3.16)$$

The output function is:

$$y_{appr}^{(i)}(t_{ck}) = x_{(1,appr)}^{(i)}(t_{ck})$$

We will derive the particular expressions of the constraint forces at stance foot,  $f_{(con,k)}^{(i)}$ , based on each case, at subchapter 3.4.

### 3.3 Swing Phase of the 4-DOF Biped Robot using Discrete Mechanics (Leg 1 = Stance, Leg 2 = Swing)

We now develop the discretized model of our biped robot via the use of the Discrete Mechanics Theory. We define some important notations. Let  $h^{(i)}$  be the sampling time for the  $i$ th walking step,  $r$  a division ratio quantity in discrete mechanics,  $k = 1, \dots, N$  the number of time steps,  $H$  the total number of walking steps,  $i = 1, 2, \dots, H$  the walking step index,  $q_{(1,k)}^{(i)}$ ,  $q_{(2,k)}^{(i)}$ ,  $q_{(3,k)}^{(i)}$  and

$q_{(4,k)}^{(i)}$  the generalized coordinates at the  $k$ -th time step during the  $i$ -th walking step respectively and  $\tau_{(1,k)}^{(i)}$ ,  $\tau_{(2,k)}^{(i)}$ ,  $F_{(POx,k)}^{(i)}$ ,  $F_{(POy,k)}^{(i)}$  the control inputs at the  $k$ -th time step during the  $i$ -th walking step for the Leg 1 and Leg 2.

We now derive the discretized Swing Phase for the 4-DOF biped robot where Leg 1 is the stance leg and Leg 2 is the swing leg. We firstly calculate the Discrete Lagrangian

$L_r^d(q_{(1,k)}^{(i)}, q_{(1,k+1)}^{(i)}, q_{(2,k)}^{(i)}, q_{(2,k+1)}^{(i)}, q_{(3,k)}^{(i)}, q_{(3,k+1)}^{(i)}, q_{(4,k)}^{(i)}, q_{(4,k+1)}^{(i)})$  from (8.44), (3.7). Due to the fact that the left and right discrete forces (7.46) satisfy  $f_d^+(q_k, q_{k+1}, \tau_k, f_k^{(i)}) = f_d^-(q_k, q_{k+1}, \tau_k, f_k^{(i)})$  for  $r = \frac{1}{2}$ , we set a discrete control input (the hip torque, that for now it is considered a unified, combined entity of  $\tau_{(1,k)}^{(i)}, \tau_{(2,k)}^{(i)}$ ) that consists of the left discrete external force  $f_d^-$  and we also set the instantaneous push-off impulse (that for now it is considered a unified, entity of  $f_{(fr,k)}^{(i)}, f_{(N,k)}^{(i)}$ ) that consists of the right discrete external force  $f_d^+$  as:

$$\tau_k^{(i)} := f_d^-(q_k, q_{k+1}, \tau_k, f_k^{(i)}), k = 1, \dots, N - 2 \quad (3.17)$$

$$F_{PO}^{(i)} := f_d^+(q_{k-1}, q_k, \tau_k^{(i)}, f_k) = 0, k = 1, \dots, N - 2 \quad (3.18)$$

Equation (3.26) is valid because the instantaneous push-off impulse is not applied during the Swing Phase of the biped. Substituting the discrete Lagrangian into the discrete Euler-Lagrange Equations (7.49) while also deriving the boundary conditions (8.58, 8.60), and using the discrete control input (3.17, 3.18), we develop the discretized Swing Phase of the biped:

$$\begin{aligned} & D_2 L^d(q_{(1,k-1)}^{(i)}, q_{(1,k)}^{(i)}, q_{(2,k-1)}^{(i)}, q_{(2,k)}^{(i)}, q_{(3,k-1)}^{(i)}, q_{(3,k)}^{(i)}, q_{(4,k-1)}^{(i)}, q_{(4,k)}^{(i)}) + \\ & D_1 L^d(q_{(1,k)}^{(i)}, q_{(1,k+1)}^{(i)}, q_{(2,k)}^{(i)}, q_{(2,k+1)}^{(i)}, q_{(3,k)}^{(i)}, q_{(3,k+1)}^{(i)}, q_{(4,k)}^{(i)}, q_{(4,k+1)}^{(i)}) - \tau_{(1,k)}^{(i)} = 0, (k = 1, \dots, N - 2) \end{aligned} \quad (3.19)$$

$$\begin{aligned} & D_4 L^d(q_{(1,k-1)}^{(i)}, q_{(1,k)}^{(i)}, q_{(2,k-1)}^{(i)}, q_{(2,k)}^{(i)}, q_{(3,k-1)}^{(i)}, q_{(3,k)}^{(i)}, q_{(4,k-1)}^{(i)}, q_{(4,k)}^{(i)}) + \\ & D_3 L^d(q_{(1,k)}^{(i)}, q_{(1,k+1)}^{(i)}, q_{(2,k)}^{(i)}, q_{(2,k+1)}^{(i)}, q_{(3,k)}^{(i)}, q_{(3,k+1)}^{(i)}, q_{(4,k)}^{(i)}, q_{(4,k+1)}^{(i)}) - \tau_{(2,k)}^{(i)} = 0, (k = 1, \dots, N - 2) \end{aligned} \quad (3.20)$$

$$\begin{aligned}
 & D_6 L^d(q_{(1,k-1)}^{(i)}, q_{(1,k)}^{(i)}, q_{(2,k-1)}^{(i)}, q_{(2,k)}^{(i)}, q_{(3,k-1)}^{(i)}, q_{(3,k)}^{(i)}, q_{(4,k-1)}^{(i)}, q_{(4,k)}^{(i)}) + \\
 & D_5 L^d(q_{(1,k)}^{(i)}, q_{(1,k+1)}^{(i)}, q_{(2,k)}^{(i)}, q_{(2,k+1)}^{(i)}, q_{(3,k)}^{(i)}, q_{(3,k+1)}^{(i)}, q_{(4,k)}^{(i)}, q_{(4,k+1)}^{(i)}) - f_{(fr,k)}^{(i)} = 0, (k = 1, \dots, N-2)
 \end{aligned} \tag{3.21}$$

$$\begin{aligned}
 & D_8 L^d(q_{(1,k-1)}^{(i)}, q_{(1,k)}^{(i)}, q_{(2,k-1)}^{(i)}, q_{(2,k)}^{(i)}, q_{(3,k-1)}^{(i)}, q_{(3,k)}^{(i)}, q_{(4,k-1)}^{(i)}, q_{(4,k)}^{(i)}) + \\
 & D_7 L^d(q_{(1,k)}^{(i)}, q_{(1,k+1)}^{(i)}, q_{(2,k)}^{(i)}, q_{(2,k+1)}^{(i)}, q_{(3,k)}^{(i)}, q_{(3,k+1)}^{(i)}, q_{(4,k)}^{(i)}, q_{(4,k+1)}^{(i)}) - f_{(N,k)}^{(i)} = 0, (k = 1, \dots, N-2)
 \end{aligned} \tag{3.22}$$

The boundary conditions are given by the following equations:

$$\begin{aligned}
 & D_2 L^c(q_{(1,1)}^{(i)}, q_{(1,1)}^{(i)}, q_{(2,1)}^{(i)}, q_{(2,1)}^{(i)}, q_{(3,1)}^{(i)}, q_{(3,1)}^{(i)}, q_{(4,1)}^{(i)}, q_{(4,1)}^{(i)}) + \\
 & D_1 L^d(q_{(1,1)}^{(i)}, q_{(1,2)}^{(i)}, q_{(2,1)}^{(i)}, q_{(2,2)}^{(i)}, q_{(3,1)}^{(i)}, q_{(3,2)}^{(i)}, q_{(4,1)}^{(i)}, q_{(4,2)}^{(i)}) - \tau_{(1,1)}^{(i)} = 0 \tag{3.23}
 \end{aligned}$$

$$\begin{aligned}
 & D_4 L^c(q_{(1,1)}^{(i)}, q_{(1,1)}^{(i)}, q_{(2,1)}^{(i)}, q_{(2,1)}^{(i)}, q_{(3,1)}^{(i)}, q_{(3,1)}^{(i)}, q_{(4,1)}^{(i)}, q_{(4,1)}^{(i)}) + \\
 & D_3 L^d(q_{(1,1)}^{(i)}, q_{(1,2)}^{(i)}, q_{(2,1)}^{(i)}, q_{(2,2)}^{(i)}, q_{(3,1)}^{(i)}, q_{(3,2)}^{(i)}, q_{(4,1)}^{(i)}, q_{(4,2)}^{(i)}) - \tau_{(2,1)}^{(i)} = 0 \tag{3.24}
 \end{aligned}$$

$$\begin{aligned}
 & D_6 L^c(q_{(1,1)}^{(i)}, q_{(1,1)}^{(i)}, q_{(2,1)}^{(i)}, q_{(2,1)}^{(i)}, q_{(3,1)}^{(i)}, q_{(3,1)}^{(i)}, q_{(4,1)}^{(i)}, q_{(4,1)}^{(i)}) + \\
 & D_5 L^d(q_{(1,1)}^{(i)}, q_{(1,2)}^{(i)}, q_{(2,1)}^{(i)}, q_{(2,2)}^{(i)}, q_{(3,1)}^{(i)}, q_{(3,2)}^{(i)}, q_{(4,1)}^{(i)}, q_{(4,2)}^{(i)}) - f_{(fr,1)}^{(i)} = 0 \tag{3.25}
 \end{aligned}$$

$$\begin{aligned}
 & D_8 L^c(q_{(1,1)}^{(i)}, q_{(1,1)}^{(i)}, q_{(2,1)}^{(i)}, q_{(2,1)}^{(i)}, q_{(3,1)}^{(i)}, q_{(3,1)}^{(i)}, q_{(4,1)}^{(i)}, q_{(4,1)}^{(i)}) + \\
 & D_7 L^d(q_{(1,1)}^{(i)}, q_{(1,2)}^{(i)}, q_{(2,1)}^{(i)}, q_{(2,2)}^{(i)}, q_{(3,1)}^{(i)}, q_{(3,2)}^{(i)}, q_{(4,1)}^{(i)}, q_{(4,2)}^{(i)}) - f_{(N,1)}^{(i)} = 0 \tag{3.26}
 \end{aligned}$$

The following terminal conditions, despite the fact that they are valid during the Heel Strike Phase, are given here for simplicity. Some undefined terms in the following equations (e.g.  $f_{HSx,N}^{(i)}$ ,  $f_{HSy,N}^{(i)}$ ) will be clarified later in the Chapter 3.5.

$$\begin{aligned}
& - D_2 L^c(q_{(1,N)}^{(i)}, q_{(1,N)}^{(i)}, q_{(2,N)}^{(i)}, q_{(2,N)}^{(i)}, q_{(3,N)}^{(i)}, q_{(3,N)}^{(i)}, q_{(4,N)}^{(i)}, q_{(4,N)}^{(i)}) + \\
& D_1 L^d(q_{(1,N-1)}^{(i)}, q_{(1,N)}^{(i)}, q_{(2,N-1)}^{(i)}, q_{(2,N)}^{(i)}, q_{(3,N-1)}^{(i)}, q_{(3,N)}^{(i)}, q_{(4,N-1)}^{(i)}, q_{(4,N)}^{(i)}) - \tau_{(1,N)}^{(i)} = 0 \quad (3.27)
\end{aligned}$$

$$\begin{aligned}
& - D_4 L^c(q_{(1,N)}^{(i)}, q_{(1,N)}^{(i)}, q_{(2,N)}^{(i)}, q_{(2,N)}^{(i)}, q_{(3,N)}^{(i)}, q_{(3,N)}^{(i)}, q_{(4,N)}^{(i)}, q_{(4,N)}^{(i)}) + \\
& D_3 L^d(q_{(1,N-1)}^{(i)}, q_{(1,N)}^{(i)}, q_{(2,N-1)}^{(i)}, q_{(2,N)}^{(i)}, q_{(3,N-1)}^{(i)}, q_{(3,N)}^{(i)}, q_{(4,N-1)}^{(i)}, q_{(4,N)}^{(i)}) - \tau_{(2,N)}^{(i)} = 0 \quad (3.28)
\end{aligned}$$

$$\begin{aligned}
& - D_6 L^c(q_{(1,N)}^{(i)}, q_{(1,N)}^{(i)}, q_{(2,N)}^{(i)}, q_{(2,N)}^{(i)}, q_{(3,N)}^{(i)}, q_{(3,N)}^{(i)}, q_{(4,N)}^{(i)}, q_{(4,N)}^{(i)}) + \\
& D_5 L^d(q_{(1,N-1)}^{(i)}, q_{(1,N)}^{(i)}, q_{(2,N-1)}^{(i)}, q_{(2,N)}^{(i)}, q_{(3,N-1)}^{(i)}, q_{(3,N)}^{(i)}, q_{(4,N-1)}^{(i)}, q_{(4,N)}^{(i)}) - f_{HSx,N}^{(i)} = 0 \quad (3.29)
\end{aligned}$$

$$\begin{aligned}
& - D_8 L^c(q_{(1,N)}^{(i)}, q_{(1,N)}^{(i)}, q_{(2,N)}^{(i)}, q_{(2,N)}^{(i)}, q_{(3,N)}^{(i)}, q_{(3,N)}^{(i)}, q_{(4,N)}^{(i)}, q_{(4,N)}^{(i)}) + \\
& D_7 L^d(q_{(1,N-1)}^{(i)}, q_{(1,N)}^{(i)}, q_{(2,N-1)}^{(i)}, q_{(2,N)}^{(i)}, q_{(3,N-1)}^{(i)}, q_{(3,N)}^{(i)}, q_{(4,N-1)}^{(i)}, q_{(4,N)}^{(i)}) - f_{HSy,N}^{(i)} = 0 \quad (3.30)
\end{aligned}$$

The set of equations (3.19-3.22), can be rewritten as:

$$M(q_k^{(i)}) \cdot \left( \frac{q_{k+1}^{(i)} - 2q_k^{(i)} + q_{k-1}^{(i)}}{(h^{(i)})^2} \right) + C(q_k^{(i)}, \frac{q_{k+1}^{(i)} - q_k^{(i)}}{h^{(i)}}) \cdot \left( \frac{q_{k+1}^{(i)} - q_k^{(i)}}{h^{(i)}} \right) + G(q_k^{(i)}, \theta_i) = B_a(q_k^{(i)}) \begin{bmatrix} \tau_{(1,k)}^{(i)} \\ \tau_{(2,k)}^{(i)} \\ F_{(PO,x)}^{(i)} \\ F_{(PO,y)}^{(i)} \end{bmatrix} + S_{con}^T f_{(con,k)}^{(i)}$$

$\Leftrightarrow$

$$M(q_k^{(i)}) \cdot \left( \frac{q_{k+1}^{(i)} - 2q_k^{(i)} + q_{k-1}^{(i)}}{(h^{(i)})^2} \right) + C(q_k^{(i)}, \frac{q_{k+1}^{(i)} - q_k^{(i)}}{h^{(i)}}) \cdot \left( \frac{q_{k+1}^{(i)} - q_k^{(i)}}{h^{(i)}} \right) + G(q_k^{(i)}, \theta_i) = \begin{bmatrix} \tau_{(1,k)}^{(i)} \\ \tau_{(2,k)}^{(i)} \\ 0 \\ 0 \end{bmatrix} + \begin{bmatrix} 0 \\ 0 \\ f_{(fr,k)}^{(i)} \\ f_{(N,k)}^{(i)} \end{bmatrix} \quad (3.31)$$

$$\text{where } f_{(con,k)}^{(i)} = \begin{bmatrix} f_{(fr,k)}^{(i)} \\ f_{(N,k)}^{(i)} \end{bmatrix} = \begin{bmatrix} f_{fr}^{(i)}(q_k^{(i)}, \dot{q}_k^{(i)}) \\ f_N^{(i)}(q_k^{(i)}, \dot{q}_k^{(i)}) \end{bmatrix}, k = 1, \dots, N - 2,$$

$$M(q_k^{(i)}) = \begin{bmatrix} p_{12} + I_1 & -p_{13}\cos(q_{(1,k)}^{(i)}) & -p_{16}\cos(q_{(1,k)}^{(i)}) & -p_{16}\sin(q_{(1,k)}^{(i)}) \\ -p_{13}\cos(q_{(1,k)}^{(i)}) & p_{14} + I_2 & p_{15}\cos(q_{(2,k)}^{(i)}) & p_{15}\sin(q_{(2,k)}^{(i)}) \\ -p_{16}\cos(q_{(1,k)}^{(i)}) & p_{15}\cos(q_{(2,k)}^{(i)}) & p_{17} & 0 \\ -p_{16}\sin(q_{(1,k)}^{(i)}) & p_{15}\sin(q_{(2,k)}^{(i)}) & 0 & p_{17} \end{bmatrix}, k = 1, \dots, N - 2 \quad (3.32)$$

$$C(:, 1) = \begin{bmatrix} p_{13}\sin(q_{(1,k)}^{(i)} - q_{(2,k)}^{(i)})\left(\frac{q_{(2,k+1)}^{(i)} - q_{(2,k)}^{(i)}}{h^{(i)}}\right) + p_{16}\left(\sin(q_{(1,k)}^{(i)})\left(\frac{q_{(3,k+1)}^{(i)} - q_{(3,k)}^{(i)}}{h^{(i)}}\right) - \cos(q_{(1,k)}^{(i)})\right)\left(\frac{q_{(4,k+1)}^{(i)} - q_{(4,k)}^{(i)}}{h^{(i)}}\right) \\ p_{13}\sin(q_{(1,k)}^{(i)} - q_{(2,k)}^{(i)})\left(\left(\frac{q_{(1,k+1)}^{(i)} - q_{(1,k)}^{(i)}}{h^{(i)}}\right) - \left(\frac{q_{(2,k+1)}^{(i)} - q_{(2,k)}^{(i)}}{h^{(i)}}\right)\right) \\ p_{16}\sin(q_{(1,k)}^{(i)})\left(\frac{q_{(1,k+1)}^{(i)} - q_{(1,k)}^{(i)}}{h^{(i)}}\right) \\ -p_{16}\cos(q_{(1,k)}^{(i)})\left(\frac{q_{(1,k+1)}^{(i)} - q_{(1,k)}^{(i)}}{h^{(i)}}\right) \end{bmatrix}$$

$$C(:, 2) = \begin{bmatrix} p_{13}\sin(q_{(1,k)}^{(i)} - q_{(2,k)}^{(i)})\left(\left(\frac{q_{(1,k+1)}^{(i)} - q_{(1,k)}^{(i)}}{h^{(i)}}\right) - \left(\frac{q_{(2,k+1)}^{(i)} - q_{(2,k)}^{(i)}}{h^{(i)}}\right)\right) \\ p_{13}\sin(q_{(1,k)}^{(i)} - q_{(2,k)}^{(i)})\left(\frac{q_{(1,k+1)}^{(i)} - q_{(1,k)}^{(i)}}{h^{(i)}}\right) - p_{15}\sin(q_{(2,k)}^{(i)})\left(\frac{q_{(3,k+1)}^{(i)} - q_{(3,k)}^{(i)}}{h^{(i)}}\right) + p_{15}\cos(q_{(2,k)}^{(i)})\left(\frac{q_{(4,k+1)}^{(i)} - q_{(4,k)}^{(i)}}{h^{(i)}}\right) \\ -p_{15}\sin(q_{(2,k)}^{(i)})\left(\frac{q_{(2,k+1)}^{(i)} - q_{(2,k)}^{(i)}}{h^{(i)}}\right) \\ p_{15}\cos(q_{(2,k)}^{(i)})\left(\frac{q_{(2,k+1)}^{(i)} - q_{(2,k)}^{(i)}}{h^{(i)}}\right) \end{bmatrix}$$

$$C(:, 3) = \begin{bmatrix} p_{16}\sin(q_{(1,k)}^{(i)})\left(\frac{q_{(1,k+1)}^{(i)} - q_{(1,k)}^{(i)}}{h^{(i)}}\right) \\ -p_{15}\sin(q_{(2,k)}^{(i)})\left(\frac{q_{(2,k+1)}^{(i)} - q_{(2,k)}^{(i)}}{h^{(i)}}\right) \\ 0 \\ 0 \end{bmatrix}, k = 1, \dots, N - 2$$

$$C(:, 4) = \begin{bmatrix} -p_{16} \cos(q_{(1,k)}^{(i)}) \left( \frac{q_{(1,k+1)}^{(i)} - q_{(1,k)}^{(i)}}{h^{(i)}} \right) \\ p_{15} \cos(q_{(2,k)}^{(i)}) \left( \frac{q_{(2,k+1)}^{(i)} - q_{(2,k)}^{(i)}}{h^{(i)}} \right) \\ 0 \\ 0 \end{bmatrix} \quad (3.33)$$

$$G(q^{(i)}, \theta_i) = \begin{bmatrix} -gM(a \sin(q_{(1,k)}^{(i)}) + b \sin(q_{(1,k)}^{(i)})) - agm_1 \sin(q_{(1,k)}^{(i)}) - glm_2 \sin(q_{(1,k)}^{(i)}) \\ bgm_2 \sin(q_{(2,k)}^{(i)}) \\ 0 \\ gm_1 + gm_2 + gM \end{bmatrix}, k = 1, \dots, N - 2 \quad (3.34)$$

where  $I_1, I_2$  are the moments of inertia of the Legs 1 and 2 about their centers of mass, respectively,  $p_{12} = Ml^2 + m_1a^2 + m_2l^2, p_{13} = m_2bl, p_{14} = m_2b^2, p_{15} = m_2b, p_{16} = Ml + m_1a + m_2l, p_{17} = m_1 + m_2 + M$ .

Hence, the discretized swing phase of the 4-DOF biped robot is described by the set of equations (3.19-3.26).

## 3.4 Modeling of Constraint Forces at Stance Foot

### 3.4.1 Constraint Forces at Stance Foot during the Swing Phase (Leg1 = Stance, Leg2 = Swing)

As we have mentioned in the current and previous chapters, the complete biped robot has four degrees of freedom. The two of them ( $q_3^{(i)}$  and  $q_4^{(i)}$ ), refer to the generalized Cartesian coordinates of the stance foot. The constraint force at the stance foot is developed to hold the position of the stance foot constant, for the physical constraints of walking to be met; no slippage between the stance foot and the ground which is constrained by the forward force that is parallel to the ground, and the stance foot is above the ground surface which is constrained

by the upward force that is vertical to the ground. The constrained condition at the stance foot is:

$$S_{con} \cdot (\dot{q}^{(i)}, \ddot{q}^{(i)}) = 0 \quad (3.35)$$

where  $S_{con} = \begin{bmatrix} 0 & 0 & 1 & 0 \\ 0 & 0 & 0 & 1 \end{bmatrix}$  is the constraint force selection matrix and the vectors  $\dot{q}^{(i)}, \ddot{q}^{(i)}$  are the 4x1 vectors of the generalized coordinates.

Using the general equations of motion for the swing phase of the complete biped robot:

$$M(q^{(i)})\ddot{q}^{(i)} + C(q^{(i)}, \dot{q}^{(i)})\dot{q}^{(i)} + G(q^{(i)}, \theta) = B_a(q^{(i)})u^{(i)} + S_{con}^T f_{con}^{(i)}(q^{(i)}, \dot{q}^{(i)}) \quad (3.36)$$

and Equation (3.35), we get the following relation:

$$S_{con}\ddot{q}^{(i)} = -S_{con}M(q^{(i)})^{-1}(C(q^{(i)}, \dot{q}^{(i)})\dot{q}^{(i)} + G(q^{(i)}, \theta) - S_{con}^T f_{con}^{(i)}(q^{(i)}, \dot{q}^{(i)}) - B_a(q^{(i)})u^{(i)}) = 0 \quad (3.37)$$

Hence, the constraint force at the stance foot at the  $i$ -th walking step (depending of course, which leg is the stance leg at each walking step)  $f_{con}^{(i)}(q^{(i)}, \dot{q}^{(i)}) = \begin{bmatrix} f_{fr}^{(i)}(q^{(i)}, \dot{q}^{(i)}) \\ f_N^{(i)}(q^{(i)}, \dot{q}^{(i)}) \end{bmatrix}$ , where  $f_{fr}^{(i)}(q^{(i)}, \dot{q}^{(i)})$  is the friction force and  $f_N^{(i)}(q^{(i)}, \dot{q}^{(i)})$  is the normal force, is obtained by the following relation:

$$f_{con}^{(i)}(q^{(i)}, \dot{q}^{(i)}) = (S_{con}M(q^{(i)})^{-1}S_{con}^T)^{-1}S_{con}M(q^{(i)})^{-1}(C(q^{(i)}, \dot{q}^{(i)})\dot{q}^{(i)} + G(q^{(i)}, \theta) - B_a(q^{(i)})u^{(i)}) \quad (3.38)$$

For the case where the Leg 1 is the Stance Leg and the Leg 2 is the Swing Leg, using the related equations of motion for the Swing Phase, the constraint force at stance foot becomes:

$$f_{con}^{(i)}(q^{(i)}, \dot{q}^{(i)}) = \begin{bmatrix} p_{16}\sin(q_1^{(i)})(\dot{q}_1^{(i)})^2 - p_{15}\sin(q_2^{(i)})(\dot{q}_2^{(i)})^2 \\ -p_{16}\cos(q_1^{(i)})(\dot{q}_1^{(i)})^2 + p_{15}\cos(q_2^{(i)})(\dot{q}_2^{(i)})^2 + p_{17}g \end{bmatrix} \quad (3.39)$$

By proceeding with the initial discretization and applying the Direct Collocation Conditions

(as we extensively analyzed in Chapter 2), the relation above becomes:

$$f_{(con,appr)}^{(i)}(t_{ck}) = \begin{bmatrix} p_{16} \sin(q_{(1,appr)}^{(i)}(t_{ck})) (\dot{q}_{(1,appr)}^{(i)}(t_{ck}))^2 - p_{15} \sin(q_{(2,appr)}^{(i)}(t_{ck})) (\dot{q}_{(2,appr)}^{(i)}(t_{ck}))^2 \\ -p_{16} \cos(q_{(1,appr)}^{(i)}(t_{ck})) (\dot{q}_{(1,appr)}^{(i)}(t_{ck}))^2 + p_{15} \cos(q_{(2,appr)}^{(i)}(t_{ck})) (\dot{q}_{(2,appr)}^{(i)}(t_{ck}))^2 + p_{17}g \end{bmatrix} \quad (3.40)$$

and using the Discrete Mechanics Approach, it becomes:

$$f_{(con,k)}^{(i)} = \begin{bmatrix} p_{16} \sin(q_{(1,k)}^{(i)}) \left(\frac{q_{(1,k+1)}^{(i)} - q_{(1,k)}^{(i)}}{h}\right)^2 - p_{15} \sin(q_{(2,k)}^{(i)}) \left(\frac{q_{(2,k+1)}^{(i)} - q_{(2,k)}^{(i)}}{h}\right)^2 \\ -p_{16} \cos(q_{(1,k)}^{(i)}) \left(\frac{q_{(1,k+1)}^{(i)} - q_{(1,k)}^{(i)}}{h}\right)^2 + p_{15} \cos(q_{(2,k)}^{(i)}) \left(\frac{q_{(2,k+1)}^{(i)} - q_{(2,k)}^{(i)}}{h}\right)^2 + p_{17}g \end{bmatrix} \quad (3.41)$$

### 3.4.2 Constraint Forces at Stance Foot during the Push-Off Phase (Leg1 = Stance, Leg2 = Swing)

Following the abovementioned method for the derivation of the Constraint Forces at the Stance Foot for the Swing Phase, using the general equations of motion for the Instantaneous Push-Off Phase of the complete biped (we will analyze the Push-Off Phase later in the current Chapter):

$$M(q^{(i,PO-)})q^{(i,\ddot{P}O-)} + C(q^{(i,PO-)}, \dot{q}^{(i,PO-)})\dot{q}^{(i,PO-)} + G(q^{(i,PO-)}, \theta) = B_{PO}(q^{(i,PO-)})u^{(i,PO-)} + S_{con}^T f_{con}^{(i,PO-)}(q^{(i,PO-)}, \dot{q}^{(i,PO-)}) \quad (3.42)$$

where  $PO-$  refers to the start of the time interval of the phase,  $B_{PO}(q^{(i,PO-)}) = \begin{bmatrix} 1 & 0 & 0 & 0 \\ 0 & 1 & 0 & 0 \\ 0 & 0 & 1 & 0 \\ 0 & 0 & 0 & 1 \end{bmatrix}$

is the applied forces selection matrix of the Push-Off Phase (the reasons for the values of the matrix will be explained later in the current chapter, when we will develop the Push-Off Phase) and equation (3.35), we get the following equations:

$$S_{con}\ddot{q}^{(i,PO-)} = -S_{con}M(q^{(i,PO-)})^{-1}(C(q^{(i,PO-)}, \dot{q}^{(i,PO-)})\dot{q}^{(i,PO-)} + G(q^{(i,PO-)}, \theta) - S_{con}^T f_{con}^{(i,PO-)}(q^{(i,PO-)}, \dot{q}^{(i,PO-)}) - B_{PO}(q^{(i,PO-)})u^{(i,PO-)}) = 0 \quad (3.43)$$

$\Leftrightarrow$

$$f_{con}^{(i,PO-)}(q^{(i,PO-)}, \dot{q}^{(i,PO-)}) = (S_{con}M(q^{(i,PO-)})^{-1}S_{con}^T)^{-1}S_{con}M(q^{(i,PO-)})^{-1}(C(q^{(i,PO-)}, \dot{q}^{(i,PO-)})\dot{q}^{(i,PO-)} + G(q^{(i,PO-)}, \theta) - B_{PO}(q^{(i,PO-)})u^{(i,PO-)}) \quad (3.44)$$

For the case where the Leg 1 is the Stance Leg and the Leg 2 is the Swing Leg, using the associated equations of motion for the Swing Phase, the constraint force at stance foot becomes:

$$f_{con}^{(i,PO-)}(q^{(i,PO-)}, \dot{q}^{(i,PO-)}) = \begin{bmatrix} p_{16}\sin(q_1^{(i,PO-)})\dot{(q_1^{(i,PO-)})}^2 - p_{15}\sin(q_2^{(i,PO-)})\dot{(q_2^{(i,PO-)})}^2 - F_{(PO,x)}^{(i,PO-)} \\ -p_{16}\cos(q_1^{(i,PO-)})\dot{(q_1^{(i,PO-)})}^2 + p_{15}\cos(q_2^{(i,PO-)})\dot{(q_2^{(i,PO-)})}^2 + p_{17}g - F_{(PO,y)}^{(i,PO-)} \end{bmatrix} \quad (3.45)$$

By proceeding with the initial discretization and applying the Direct Collocation Conditions (as we extensively analyzed in Chapter 2), the relation above becomes:

$$f_{(con,appr)}^{(i)}(t_{N-1}) = \begin{bmatrix} p_{16}\sin(q_{(1,appr)}^{(i)}(t_{N-1}))\dot{(q_{(1,appr)}^{(i)}(t_{N-1}))}^2 - p_{15}\sin(q_{(2,appr)}^{(i)}(t_{N-1}))\dot{(q_{(2,appr)}^{(i)}(t_{N-1}))}^2 - \\ F_{(PO,x,appr)}^{(i)}(t_{N-1}) \\ -p_{16}\cos(q_{(1,appr)}^{(i)}(t_{N-1}))\dot{(q_{(1,appr)}^{(i)}(t_{N-1}))}^2 + p_{15}\cos(q_{(2,appr)}^{(i)}(t_{N-1}))\dot{(q_{(2,appr)}^{(i)}(t_{N-1}))}^2 + p_{17}g - \\ F_{(PO,y,appr)}^{(i)}(t_{N-1}) \end{bmatrix} \quad (3.46)$$

and using the Discrete Mechanics Approach, it becomes:

$$f_{(con,k)}^{(i)} = \begin{bmatrix} p_{16}\sin(q_{(1,k)}^{(i)})\left(\frac{q_{(1,k+1)}^{(i)} - q_{(1,k)}^{(i)}}{h}\right)^2 - p_{15}\sin(q_{(2,k)}^{(i)})\left(\frac{q_{(2,k+1)}^{(i)} - q_{(2,k)}^{(i)}}{h}\right)^2 - F_{PO,x,N-1}^{(i)} \\ -p_{16}\cos(q_{(1,k)}^{(i)})\left(\frac{q_{(1,k+1)}^{(i)} - q_{(1,k)}^{(i)}}{h}\right)^2 + p_{15}\cos(q_{(2,k)}^{(i)})\left(\frac{q_{(2,k+1)}^{(i)} - q_{(2,k)}^{(i)}}{h}\right)^2 + p_{17}g - F_{PO,y,N-1}^{(i)} \end{bmatrix} \quad (3.47)$$

### 3.5 The Impact Phase Redefined: Derivation of the Heel Strike and Push-Off Phases of Walking

In the case of a stiff-legged robot on a surface, the notion of the impact point of the swing leg with the walking surface would appear to be physically ambiguous, since, without a knee, and with equal length legs, the swing leg must scuff along the ground if it remains in the sagittal plane. McGeer has shown with his ballistic walkers, both theoretically and experimentally, that one can basically ignore the leg clearance issue for stiff-legged models. He has done this in two ways: in one realization, he puts additional small motors on the legs that allow him to push the swing leg just slightly out of the sagittal plane during the swing phase and to pull the leg back into the sagittal plane whenever he wishes to initiate contact. The second way he has done this is to put small (essentially massless) flaps on the ends of the legs, and to fold up the flap of the swing leg during the swing phase, and to unfold it whenever he wants to initiate contact.

Based on the first abovementioned method of McGeer, we will deal with the scuffing of the swing leg with the use of a linear actuator, for the stance feet. We must not forget that at each walking step, either Leg 1 or Leg 2 is the swing leg, while the other one plays the role of the stance leg. In addition, we will extend the utility of the linear actuator by using them at the Push-Off Phase, which will be derived and analyzed later.

Regarding the configuration of the generalized coordinates  $q_1^{(i)}$ ,  $q_2^{(i)}$  of the legs at impact, the Impact Surface conditions that were derived in Chapter 2 must hold. The impact between the swing leg and the ground is modeled as a contact between two rigid bodies. As we have seen in Chapter 2, the Impact Phase is used to obtain an expression for the velocity of the generalized coordinates after the impact of the swing leg with the walking surface in terms of the velocity and position before the impact.

In this thesis, the motion of the biped robot is analyzed for the case that the impact of the swing leg with the ground results in no rebound and no slipping of the swing leg, and the stance leg naturally lifting from the ground without interaction. The contact model requires of course the full four degrees of freedom of the robot.

The Impact Phase of the complete biped robot consists of two Subphases: the Heel Strike and Push-Off Phases. The Heel Strike Phase describes the actual collision of the swing leg with the walking surface. The Push-Off Phase takes place just before the Heel Strike, in order to balance the new stance leg after the collision by providing the required energy to the system, while solving the swing leg scuffing with an impulsive axial force at the old stance foot just before the ground collision.

### 3.5.1 The Heel Strike Phase of Walking (Leg1 = Stance, Leg2 = Swing)

In Chapter 2, computing the impact map by conservation of angular momentum results in a compact mapping that only contains information about the updated velocities  $\dot{q}^+ (q_{(x,1)}^{(i+1)}, x = \{1, 2\}, i = 1, \dots, H)$  Another quantity of interest is the initial forces that occur at the end of the swing leg as a result of the impact, since the assumption that the biped does not slide or trespass the ground just after the collision is dependent on these forces. It might therefore be of interest to calculate the magnitude and direction of these initial forces to ensure that the assumption holds.

The Heel Strike Phase is described by the following equations of motion:

$$M(q^{(i,-)})\ddot{q}^{(i,-)} + C(q^{(i,-)}, \dot{q}^{(i,-)})\dot{q}^{(i,-)} + G(q^{(i,-)}, \theta) = B_{HS}(q^{(i)}) \begin{bmatrix} \tau_1^{(i,-)} \\ \tau_2^{(i,-)} \\ F_{(PO,x)}^{(i)} \\ F_{(PO,y)}^{(i)} \end{bmatrix} + S_{HS}^T f_{HS}^{(i)} \quad (3.48)$$

$\Leftrightarrow$

$$M(q^{(i,-)})\ddot{q}^{(i,-)} + C(q^{(i,-)}, \dot{q}^{(i,-)})\dot{q}^{(i,-)} + G(q^{(i,-)}, \theta) = \begin{bmatrix} \tau_1^{(i,-)} \\ \tau_2^{(i,-)} \\ 0 \\ 0 \end{bmatrix} + \begin{bmatrix} 0 \\ 0 \\ f_{HSx}^{(i)} \\ f_{HSy}^{(i)} \end{bmatrix}$$

where  $B_{HS}(q^{(i)}) = \begin{bmatrix} 1 & 0 & 0 & 0 \\ 0 & 1 & 0 & 0 \\ 0 & 0 & 0 & 0 \\ 0 & 0 & 0 & 0 \end{bmatrix}$  is the applied forces selection matrix for the Heel Strike Phase

(here, as in the Swing Phase, only the hip torques can be controlled),  $S_{HS} = \begin{bmatrix} 0 & 0 & 1 & 0 \\ 0 & 0 & 0 & 1 \end{bmatrix}$  is

the Heel Strike Forces Selection Matrix,  $f_{HS}^{(i)} = \begin{bmatrix} f_{(HSx)} \\ f_{(HSy)} \end{bmatrix}$  is the vector of the axial components of the Heel Strike (Impact) Forces affecting the swing foot during the collision with the ground, the matrices  $M$ ,  $C$ ,  $G$  are taken from the relations (3.9 - 3.11) and - denotes the pre-impact time instant.

The initial discretization of (3.48) leads to the following discretized equations of motion:

$$M(q_N^{(i)})\ddot{q}_N^{(i)} + C(q_N^{(i)}, \dot{q}_N^{(i)})\dot{q}_N^{(i)} + G(q_N^{(i)}, \theta) = B_{HS}(q_k^{(i)}) \begin{bmatrix} \tau_{(1,N)}^{(i)} \\ \tau_{(2,N)}^{(i)} \\ F_{(PO,x,N)}^{(i)} \\ F_{(PO,y,N)}^{(i)} \end{bmatrix} + S_{HS}^T f_{HS,N}^{(i)} \quad (3.49)$$

$\Leftrightarrow$

$$M(q_N^{(i)})\ddot{q}_N^{(i)} + C(q_N^{(i)}, \dot{q}_N^{(i)})\dot{q}_N^{(i)} + G(q_N^{(i)}, \theta) = \begin{bmatrix} \tau_{(1,N)}^{(i)} \\ \tau_{(2,N)}^{(i)} \\ 0 \\ 0 \end{bmatrix} + \begin{bmatrix} 0 \\ 0 \\ f_{(HSx,N)}^{(i)} \\ f_{(HSy,N)}^{(i)} \end{bmatrix},$$

where the  $N$ th time step of the  $i$ th walking step is the pre-impact time instant (and the 1st time step of the  $i+1$ th walking step is the post-impact time instant). The state space equations (derived from relation (3.49)), with the applied Direct Collocation Conditions are:

$$\begin{bmatrix} x_{(1,appr)}^{(i)}(t_N) \\ x_{(2,appr)}^{(i)}(t_N) \end{bmatrix} =$$

$$\left[ \begin{array}{c} x_{(2,appr)}^{(i)}(t_N) \\ -M^{-1}(x_{(1,appr)}^{(i)}(t_N))(C(x_{(1,appr)}^{(i)}(t_N), x_{(2,appr)}^{(i)}(t_N))x_{(2,appr)}^{(i)}(t_N) + G(x_{(1,appr)}^{(i)}(t_N)) + S_{HS}^T f_{(HS,appr)}^{(i)}(t_N)) \end{array} \right] + \left[ \begin{array}{c} 0_{4 \times 4} \\ M^{-1}(x_{(1,appr)}^{(i)}(t_N))B_{HS}(q_k^{(i)}) \end{array} \right] u_{appr}^{(i)}(t_N) \quad (3.50)$$

and the Equations of Motion for use with Discrete Mechanics Theory are:

$$M(q_N^{(i)}) \cdot \left( \frac{q_1^{(i+1)} - 2q_N^{(i)} + q_{N-1}^{(i)}}{h^2} \right) + C(q_N^{(i)}, \frac{q_1^{(i+1)} - q_N^{(i)}}{h}) \cdot \left( \frac{q_1^{(i+1)} - q_N^{(i)}}{h} \right) + G(q_N^{(i)}, \theta) = B_{HS}(q_k^{(i)}) \begin{bmatrix} \tau_{(1,N)}^{(i)} \\ \tau_{(2,N)}^{(i)} \\ F_{(PO,x,N)}^{(i)} \\ F_{(PO,y,N)}^{(i)} \end{bmatrix} + S_{HS}^T f_{HS,N}^{(i)} \quad (3.51)$$

$\Leftrightarrow$

$$M(q_N^{(i)}) \cdot \left( \frac{q_1^{(i+1)} - 2q_N^{(i)} + q_{N-1}^{(i)}}{h^2} \right) + C(q_N^{(i)}, \frac{q_1^{(i+1)} - q_N^{(i)}}{h}) \cdot \left( \frac{q_1^{(i+1)} - q_N^{(i)}}{h} \right) + G(q_N^{(i)}, \theta) = \begin{bmatrix} \tau_{(1,N)}^{(i)} \\ \tau_{(2,N)}^{(i)} \\ 0 \\ 0 \end{bmatrix} + \begin{bmatrix} 0 \\ 0 \\ f_{(HSx,N)}^{(i)} \\ f_{(HSy,N)}^{(i)} \end{bmatrix}$$

where the first and second derivatives of the generalized coordinates are approximated by the finite difference relations.

We remind that  $q^{(i)} = (q_1^{(i)}, q_2^{(i)}, q_3^{(i)}, q_4^{(i)})$  is the set of generalized coordinates and  $\begin{bmatrix} f_{(HSx)}^{(i)} \\ f_{(HSy)}^{(i)} \end{bmatrix} = f_{(HS)}^{(i)}$  represents the external forces acting on the robot at the impact point (at the generalized Cartesian Coordinates  $q_3^{(i)}, q_4^{(i)}$ ). The basic premises are that:

- The impact takes place over an infinitesimally small period of time,
- The external forces during the impact can be represented by impulses,
- Impulsive forces may result in an instantaneous change in the velocities of the generalized coordinates, but the positions remain continuous, and

- The torques supplied by the rotational actuators are not impulsive.

With these assumptions, the abovementioned equations of motion express an instantaneous impulse equal to the variation in the momentum of the model. In other words, we calculate the instantaneous angular velocity just after heel strike by an equivalent impulse method which is an easier and more accurate way for solving the discrete process in the robot dynamic systems than the angular momentum conservation method.

The intuition behind the impulse method is the following. The swing foot contacts with the ground with a certain linear velocity. After the since no bounce is assumed, the swing leg switches to be the stance leg, and the velocity of the new stance foot is zero. Before the heel strike, the two legs switch their roles. The new stance foot which is the old swing leg with linear velocity will contact with the ground. And the new swing leg will leave the ground. The collision between the new stance foot and the ground is equivalent to that an instantaneous impulse force pushes the leg along the leg axis. The velocity of the new stance foot will instantaneously decrease from a certain value to zero after the collision.

$$M(q^{(i,+)}\dot{q}^{(i,+)} - M(q^{(i,-)}\dot{q}^{(i,-)}) = F_{HS}^{(i)}$$

⇔

$$M(q^{(i,+)}\dot{q}^{(i,+)} - M(q^{(i,-)}\dot{q}^{(i,-)}) = \begin{bmatrix} 0 \\ 0 \\ F_{(HSx)}^{(i)} \\ F_{(HSy)}^{(i)} \end{bmatrix} \quad (3.52)$$

Proceeding with initial discretization and applying the Direct Collocation Conditions:

$$M(q_{(x,appr)}^{(i+1)}(t_1)\dot{q}_{(x,appr)}^{(i+1)}(t_1) - M(q_{(x,appr)}^{(i)}(t_N)\dot{q}_{(x,appr)}^{(i)}(t_N)) = \begin{bmatrix} 0 \\ 0 \\ F_{(HSx,appr)}^{(i)} \\ F_{(HSy,appr)}^{(i)} \end{bmatrix} \quad (3.53)$$

and with the Discrete Mechanics Approach:

$$M(q_{(x,1)}^{(i+1)}) \frac{q_{(x,1)}^{(i+1)} - q_{(x,N)}^{(i)}}{h^{(i)}} - M(q_{(x,N)}^{(i)}) \frac{q_{(x,N)}^{(i)} - q_{(x,N-1)}^{(i)}}{h^{(i)}} = \begin{bmatrix} 0 \\ 0 \\ F_{(HSx)}^{(i)} \\ F_{(HSy)}^{(i)} \end{bmatrix} \quad (3.54)$$

where  $F_{HS}^{(i)} = \int_{t_N^{(i)}}^{t_1^{(i+1)}} f_{HS}^{(i)} dt \approx \frac{h^{(i)}}{3} (f_{(HS,N)}^{(i)} + f_{(HS,1)}^{(i+1)})$  is the result of the integration of the contact impulse over the heel strike duration (where we have also approximated the definite integral with the Simpson's Rule), - is the pre-impact time instant, + the post-impact time instant, and in the relation (3.54) we applied the backward difference method for the first derivatives  $q_{(x,1)}^{(i+1)}$ ,  $q_{(x,N)}^{(i)}$ ,  $x \in (1, \dots, 4)$  respectively (relations 8.96-8.98). The forward difference method has the same truncation error with the backward difference method ( $O(h^{(i)})$ ). In addition, the sampling time of the  $i + 1$ th walking step  $h^{(i+1)}$  may not be known by default from the start of the walking process or from the previous walking step  $i$ . The use of the forward difference method leads to the addition of the generalized variables  $q_{(1,\dots,4)}$  at the time step 2 of the  $i + 1$ th walking step, which may make the gait generation problem too difficult to solve for all the variables of the biped. For all the abovementioned reasons, the backward difference method is used, which solves these issues.

Furthermore, the  $N$ th time step of the  $i$ th waking step is the pre-impact time instant, and the 1st time step of the  $i + 1$  walking step is the post-impact one. Thus,  $\dot{q}^{(i,-)} = \dot{q}_{(x,N)}^{(i)}$  refer to the angular velocities just before the impact and  $\dot{q}^{(i,+)} = \dot{q}_{(x,1)}^{(i+1)}$  refer to the angular velocities just after the impact. The duration of the impact is  $h^{(i)}$ . Since the positions of the legs do not change during the impact,  $q^{([1,2],+)} = q^{([1,2],-)} \Leftrightarrow q_{(1,1)}^{(i+1)} = q_{(1,N)}^{(i)}$  and  $q_{(2,1)}^{(i+1)} = q_{(2,N)}^{(i)}$ .

In order to be able to solve for all the unknowns, the linear system (3.52) must be augmented with additional equations that proscribe what happens at the two contact ends. It is assumed that the stance leg detaches from the ground without interaction after the collision, and thus  $F_{(HS)}$  need only to consider the external forces at the end of the swing leg. This point (in other words, the cartesian coordinates of the new stance foot) has the Cartesian Coordinates:

For the Discrete Mechanics Approach:

$$Y = \begin{bmatrix} q_{(3,N)}^{(i)} + l\sin(q_{(1,N)}^{(i)}) + l\sin(q_{(2,N)}^{(i)}) \\ q_{(4,N)}^{(i)} + l\cos(q_{(1,N)}^{(i)}) - l\cos(q_{(2,N)}^{(i)}) \end{bmatrix} = \begin{bmatrix} q_{(3,1)}^{(i+1)} \\ q_{(4,1)}^{(i+1)} \end{bmatrix} \quad (3.55)$$

and for the Direct Collocation Method:

$$Y = \begin{bmatrix} q_{(3,appr)}^{(i)}(t_N) + l\sin(q_{(1,appr)}^{(i)}(t_N)) + l\sin(q_{(2,appr)}^{(i)}(t_N)) \\ q_{(4,appr)}^{(i)}(t_N) + l\cos(q_{(1,appr)}^{(i)}(t_N)) - l\cos(q_{(2,appr)}^{(i)}(t_N)) \end{bmatrix} = \begin{bmatrix} q_{(3,appr)}^{(i+1)}(t_1) \\ q_{(4,appr)}^{(i+1)}(t_1) \end{bmatrix} \quad (3.56)$$

measured in a global frame with the same orientation as the  $q_3^{(i)}$ ,  $q_4^{(i)}$  frame. The external forces  $F_{(HS)}^{(i)}$  affecting the end of the swing leg can then be described in terms of the horizontal  $f_{fr}$  (friction force) and vertical  $f_N$  (normal force) components of the impact force  $f_{imp}$  which are the constraint forces at the swing leg (the new stance foot) for the first time step of the next walking step (if the current walking step has index  $i$ , then we notate the next walking step with index  $i + 1$ ) :

$$F_{(HS)}^{(i)} = \begin{bmatrix} F_{(HSx)}^{(i)} \\ F_{(HSy)}^{(i)} \end{bmatrix} = E^T f_{imp}^{(i+1)} = E^T \begin{bmatrix} f_{(fr,1)}^{(i+1)} \\ f_{(N,1)}^{(i+1)} \end{bmatrix} \quad (3.57)$$

where  $E = \frac{\partial Y}{\partial q_{(x,N)}^{(i)}} = \begin{bmatrix} l\cos(q_{(1,N)}^{(i)}) & l\cos(q_{(2,N)}^{(i)}) & 1 & 0 \\ -l\sin(q_{(1,N)}^{(i)}) & l\sin(q_{(2,N)}^{(i)}) & 0 & 1 \end{bmatrix}$  for the Discrete Mechanics Approach

and  $E = \frac{\partial Y}{\partial q_{(x,appr)}^{(i)}(t_N)} = \begin{bmatrix} l\cos(q_{(1,appr)}^{(i)}(t_N)) & l\cos(q_{(2,appr)}^{(i)}(t_N)) & 1 & 0 \\ -l\sin(q_{(1,appr)}^{(i)}(t_N)) & l\sin(q_{(2,appr)}^{(i)}(t_N)) & 0 & 1 \end{bmatrix}$  for the Direct Collocation Method.

The stance leg is assumed to act as a pivot before impact, and the generalized coordinates  $q_3^{(i)}$ ,  $q_4^{(i)}$  are being affected by the Push-off impulse (the Push-Off Phase will be analyzed extensively at the next subchapter) at the time step  $N - 1$  of the  $i$ th walking step, meaning that at the post-Push-Off time instant  $N$ ,  $q_{(3,N)}^{(i)}$ ,  $q_{(4,N)}^{(i)} \neq 0$ . Right after impact, the former swing leg becomes the new stance leg, and assuming no slipping or rebounding of this new pivot we have the relation:

For the Direct Collocation method:

$$\frac{dY}{dt} = \frac{\partial Y}{\partial q_{(x,appr)}^{(i)}(t_N)} q_{(x,appr)}^{(i+1)}(t_1) = E q_{(x,appr)}^{(i+1)}(t_1) = 0 \quad (3.58)$$

and for the Discrete Mechanics:

$$\frac{dY}{dt} = \frac{\partial Y}{\partial q_{(x,N)}^{(i)}} \frac{q_{(x,1)}^{(i+1)} - q_{(x,N)}^{(i)}}{h^{(i)}} = E \frac{q_{(x,1)}^{(i+1)} - q_{(x,N)}^{(i)}}{h^{(i)}} = 0 \quad (3.59)$$

where in the relation (3.59) we applied the backward difference method for the first derivative  $q_{(x,1)}^{(i+1)}$ ,  $x \in (1, \dots, 4)$  (relations 8.96-8.98), for the reasons mentioned above.

For the Direct Collocation Method, the combination of equations (3.53),(3.57),(3.58) results in a system linear in  $q_{(x,appr)}^{(i+1)}(t_1)$ , with six equations and six unknowns which can be stated as:

$$\begin{bmatrix} M & -E^T \\ E & 0_{2 \times 2} \end{bmatrix} \begin{bmatrix} q_{(x,appr)}^{(i+1)}(t_1) \\ f_{(imp,appr)}^{(i+1)} \end{bmatrix} = \begin{bmatrix} M q_{(x,appr)}^{(i)}(t_N) \\ 0_{2 \times 1} \end{bmatrix} \quad (3.60)$$

It is verified that an unique solution of the system always exist, and can be written:

$$\begin{bmatrix} q_{(x,appr)}^{(i+1)}(t_1) \\ f_{(imp,appr)}^{(i+1)} \end{bmatrix} = \begin{bmatrix} M & -E^T \\ E & 0_{2 \times 2} \end{bmatrix}^{-1} \begin{bmatrix} M q_{(x,appr)}^{(i)}(t_N) \\ 0_{2 \times 1} \end{bmatrix} \quad (3.61)$$

For the Discrete Mechanics Method, the combination of equations (3.54),(3.57),(3.59) results in the linear system below:

$$\begin{bmatrix} M & -E^T \\ E & 0_{2 \times 2} \end{bmatrix} \begin{bmatrix} \frac{q_{(x,1)}^{(i+1)} - q_{(x,N)}^{(i)}}{h^{(i)}} \\ f_{(imp)}^{(i+1)} \end{bmatrix} = \begin{bmatrix} M \frac{q_{(x,N)}^{(i)} - q_{(x,N-1)}^{(i)}}{h^{(i)}} \\ 0_{2 \times 1} \end{bmatrix} \quad (3.62)$$

It is verified that an unique solution of the system always exist, and can be written:

$$\begin{bmatrix} \frac{q_{(x,1)}^{(i+1)} - q_{(x,N)}^{(i)}}{h^{(i)}} \\ f_{(imp)}^{(i+1)} \end{bmatrix} = \begin{bmatrix} M & -E^T \\ E & 0_{2 \times 2} \end{bmatrix}^{-1} \begin{bmatrix} M \frac{q_{(x,N)}^{(i)} - q_{(x,N-1)}^{(i)}}{h^{(i)}} \\ 0_{2 \times 1} \end{bmatrix} \quad (3.63)$$

### 3.5.2 The Push-Off Phase of Walking (Leg 1 = Stance, Leg 2 = Swing)

The Push-Off Phase takes place just before the Heel Strike, in order to balance the new stance leg after the collision by providing the required energy to the system, while solving the swing leg scuffing with an impulsive axial force at the old stance foot just before the ground collision. Since we consider walking on a terrain, the impact losses during walking will monotonously reduce the energy of the walker until it falls over. So, additional energy input is required. We include this by allowing the stance leg to instantaneously push off just before the impact of the swing leg. This idea is an approximation of the push-off actions of humans, who can flex their stance foot just before impact of the swing foot, thus adding mechanical energy to the walking cycle.

The Push-Off Phase is described by the following equations of motion :

$$M(q^{(i,PO-)})q^{(i,\ddot{P}O-)} + C(q^{(i,PO-)}, q^{(i,\dot{P}O-)})q^{(i,\dot{P}O-)} + G(q^{(i,PO-)}, \theta) = B_{PO}(q^{(i)}) \begin{bmatrix} \tau_1^{(i,PO-)} \\ \tau_2^{(i,PO-)} \\ F_{(PO,x)}^{(i)} \\ F_{(PO,y)}^{(i)} \end{bmatrix} + S_{con}^T f_{(con)}^{(i,PO-)} \quad (3.64)$$

$\Leftrightarrow$

$$M(q^{(i,PO-)})q^{(i,\ddot{P}O-)} + C(q^{(i,PO-)}, q^{(i,\dot{P}O-)})q^{(i,\dot{P}O-)} + G(q^{(i,PO-)}, \theta) = \begin{bmatrix} \tau_1^{(i,PO-)} \\ \tau_2^{(i,PO-)} \\ F_{(PO,x)}^{(i)} \\ F_{(PO,y)}^{(i)} \end{bmatrix} + S_{con}^T f_{(con)}^{(i,PO-)}$$

where  $B_{PO}(q^{(i)}) = \begin{bmatrix} 1 & 0 & 0 & 0 \\ 0 & 1 & 0 & 0 \\ 0 & 0 & 1 & 0 \\ 0 & 0 & 0 & 1 \end{bmatrix}$  is the applied forces selection matrix for the Push-Off Phase (here,

the two rotational joint torques  $\tau_1^{(i)}$ ,  $\tau_2^{(i)}$  and the axial components of the instantaneous push-off impulse  $F_{(PO,x)}^{(i)}$ ,  $F_{(PO,y)}^{(i)}$  are being used), the axial components of the push-off impulse on x and y are  $F_{PO,x}^{(i)} = -\sin(q_1^{(i,PO+)})F_{PO}^{(i)}$  and  $F_{(PO,y)}^{(i)} = \cos(q_1^{(i,PO+)})F_{PO}^{(i)}$  respectively,  $F_{PO}^{(i)}$  is the push-off impulse, and the matrices  $M$ ,  $C$ ,  $G$  are taken from the relations (3.9 - 3.11) and PO- denotes the pre-push-off time instant. In addition,  $S_{con}^T f_{(con,PO)}^{(i)}$  is the constraint force at the stance foot at the Push-Off Phase.

Proceeding with the initial discretization of (3.94) gives the following equations of motion:

$$M(q_{N-1}^{(i)})\ddot{q}_{N-1}^{(i)} + C(q_{N-1}^{(i)}, \dot{q}_{N-1}^{(i)})\dot{q}_{N-1}^{(i)} + G(q_{N-1}^{(i)}, \theta) = B_{PO}^{(i)} \begin{bmatrix} \tau_{(1,N-1)}^{(i)} \\ \tau_{(2,N-1)}^{(i)} \\ F_{(PO,x)}^{(i)} \\ F_{(PO,y)}^{(i)} \end{bmatrix} + S_{con}^T f_{(con,N-1)}^{(i)} \quad (3.65)$$

$\Leftrightarrow$

$$M(q_{N-1}^{(i)})\ddot{q}_{N-1}^{(i)} + C(q_{N-1}^{(i)}, \dot{q}_{N-1}^{(i)})\dot{q}_{N-1}^{(i)} + G(q_{N-1}^{(i)}, \theta) = \begin{bmatrix} \tau_{(1,N-1)}^{(i)} \\ \tau_{(2,N-1)}^{(i)} \\ F_{(PO,x)}^{(i)} \\ F_{(PO,y)}^{(i)} \end{bmatrix} + S_{con}^T f_{(con,N-1)}^{(i)}$$

The state space equations (derived from relation (3.95)), with the applied Direct Collocation Conditions are:

$$\begin{bmatrix} x_{(1,ap)}^{(i)}(t_{N-1}) \\ x_{(2,ap)}^{(i)}(t_{N-1}) \end{bmatrix} = \begin{bmatrix} x_{(2,ap)}^{(i)}(t_{N-1}) \\ -M^{-1}(x_{(1,ap)}^{(i)}(t_{N-1}))(C(x_{(1,ap)}^{(i)}(t_{N-1}), x_{(2,ap)}^{(i)}(t_{N-1}))x_{(2,ap)}^{(i)}(t_{N-1}) + G(x_{(1,ap)}^{(i)}(t_{N-1})) + S_{con}^T f_{(con,ap)}^{(i)}(t_{N-1})) \end{bmatrix}$$

$$+ \begin{bmatrix} 0_{4 \times 4} \\ M^{-1}(x_{(1,ap)}^{(i)}(t_{N-1}))B_{PO}(q^{(i)}) \end{bmatrix} (u_{ap}^{(i)}(t_{N-1})) \quad (3.66)$$

where the  $N - 1$ th time step of the  $i$ th walking step is the pre-push-off time instant, the  $N$ th time step of the  $i$ th walking step is the post-push-off time instant, and the Equations of Motion for use with Discrete Mechanics Theory are:

$$M(q_{N-1}^{(i)}) \cdot \left( \frac{q_N^{(i)} - 2q_{N-1}^{(i)} + q_{N-2}^{(i)}}{h^2} \right) + C(q_{N-1}^{(i)}, \frac{q_N^{(i)} - q_{N-1}^{(i)}}{h}) \cdot \left( \frac{q_N^{(i)} - q_{N-1}^{(i)}}{h} \right) + G(q_{N-1}^{(i)}, \theta) = B_{PO}(q^{(i)}) \begin{bmatrix} \tau_{(1,N-1)}^{(i)} \\ \tau_{(2,N-1)}^{(i)} \\ F_{(PO,x)}^{(i)} \\ F_{(PO,y)}^{(i)} \end{bmatrix} + S_{con}^T f_{(con,N-1)}^{(i)} \quad (3.67)$$

$\Leftrightarrow$

$$M(q_{N-1}^{(i)}) \cdot \left( \frac{q_N^{(i)} - 2q_{N-1}^{(i)} + q_{N-2}^{(i)}}{h^2} \right) + C(q_{N-1}^{(i)}, \frac{q_N^{(i)} - q_{N-1}^{(i)}}{h}) \cdot \left( \frac{q_N^{(i)} - q_{N-1}^{(i)}}{h} \right) + G(q_{N-1}^{(i)}, \theta) = \begin{bmatrix} \tau_{(1,N-1)}^{(i)} \\ \tau_{(2,N-1)}^{(i)} \\ F_{(PO,x)}^{(i)} \\ F_{(PO,y)}^{(i)} \end{bmatrix} + S_{con}^T f_{(con,N-1)}^{(i)} \quad (3.68)$$

where the first and second derivatives of the generalized coordinates are approximated by the finite difference relations.

The push-off process is considered as that an instantaneous impulse at the stance foot push the model along the stance leg axis. This amount of the impulse equals to the variation in the momentum of the model:

For the Direct Collocation Method:

$$M(q_{(x,appr)}^{(i)}(t_N)) \dot{q}_{(x,appr)}^{(i)}(t_N) - M(q_{(x,appr)}^{(i)}(t_{N-1})) \dot{q}_{(x,appr)}^{(i)}(t_{N-1}) = (J_{(PO,appr)}^{(i)})^T F_{(PO,appr)}^{(i)} \quad (3.69)$$

and for Discrete Mechanics:

$$M(q_{(x,N)}^{(i)}) \frac{q_{(x,N)}^{(i)} - q_{(x,N-1)}^{(i)}}{h^{(i)}} - M(q_{(x,N-1)}^{(i)}) \frac{q_{(x,N-1)}^{(i)} - q_{(x,N-2)}^{(i)}}{h^{(i)}} = (J_{PO}^{(i)})^T F_{PO}^{(i)} \quad (3.70)$$

where  $J_{PO}^{(i)} = \begin{bmatrix} 0 \\ 0 \\ -\sin(q_1^{(i,PO+)}) \\ \cos(q_1^{(i,PO+)}) \end{bmatrix}$ . Therefore, the velocity just after the push-off is obtained by

the following relation: For the Direct Collocation Method:

$$q_{(x,appr)}^{(i)}(t_N) = (M(q_{(x,appr)}^{(i)}(t_N)))^{-1} (M(q_{(x,appr)}^{(i)}(t_{N-1})) q_{(x,appr)}^{(i)}(t_{N-1}) + (J_{(PO,appr)}^{(i)})^T F_{PO}^{(i)}) \quad (3.71)$$

and for Discrete Mechanics:

$$\frac{q_{(x,N)}^{(i)} - q_{(x,N-1)}^{(i)}}{h^{(i)}} = (M(q_{(x,N)}^{(i)}))^{-1} (M(q_{(x,N-1)}^{(i)}) \frac{q_{(x,N-1)}^{(i)} - q_{(x,N-2)}^{(i)}}{h^{(i)}} + (J_{PO}^{(i)})^T F_{PO}^{(i)}) \quad (3.72)$$

### 3.5.3 The Cost Function for the Gait Generation Problem of the Second Phase

The energy cost of transport (*COT*) quantifies the energy efficiency of transporting an animal or vehicle from one place to another. As a dimensionless quantity, it allows for the comparison of dissimilar animals or modes of transportation. It has a wide range of applications, from comparing human gaits to observing the change in efficiency of trains over time. It is calculated in one of two ways below:

$$COT = \frac{E}{mgd} = \frac{P}{mgv} \quad (3.73)$$

where  $E$  is the energy input to the system, which has mass  $m$ , that is used to move the system a distance  $d$ , and  $g$  is standard gravity ( $9.81m/s^2$ ). Alternatively, one can use the power input to the system  $P$  used to move the system at a constant velocity  $v$ . The cost of transport is non-dimensional.

It is also called specific tractive force or specific resistance, or the energy index. When the energy comes from metabolic processes (i.e., for animals, humans), it is often called the metabolic cost of transport. The metabolic cost of transport for human walking is about 0.1.

The Energy Cost of Transport is used as the objective function for finding the gait that minimizes the energy cost subject to several constraints. The energy cost of the  $i$ th walking step  $E_w^{(i)}$  is given by:

$$E_w^{(i)} = E_{rotational\ actuation}^{(i)} + E_{linear\ actuation}^{(i)} \quad (3.74)$$

$E_{rotational\ actuation}^{(i)}$  is the energy cost at all Gait Phases of the  $i$ th walking step (Swing Phase, Push-Off Phase, Heel Strike Phase) due to the applied torques (affecting the generalized coordinates  $q_1^{(i)}$ ,  $q_2^{(i)}$ ) from the two rotational actuators at the hip of the biped.

$E_{linear\ actuation}^{(i)}$  is the energy cost of the Push-Off Phase during the  $i$ th walking step, due to the applied linear force along the stance foot (affecting the generalized coordinates  $q_3^{(i)}$ ,  $q_4^{(i)}$ ).

These two energy cost components are described as follows:

$$E_{rotational\ actuation}^{(i)} = \int_{t_1^{(i)}}^{t_N^{(i)}} |P_{hip}^{(i)}| dt \quad (3.75)$$

$$E_{linear\ actuation}^{(i)} = E_{push-off,+}^{(i)} - E_{push-off,-}^{(i)} \quad (3.76)$$

where  $[t_1^{(i)}, t_N^{(i)}]$  is the time interval of the  $i$ th walking step, thus  $t_N^{(i)} - t_1^{(i)}$  is the time duration of the  $i$ th walking step, and  $P_{hip}^{(i)} = (\dot{q}_1^{(i)}\tau_1^{(i)} + \dot{q}_2^{(i)}\tau_2^{(i)})$  is the mechanical power of the hip joint torques.  $E_{push-off,+}^{(i)}$  and  $E_{push-off,-}^{(i)}$  are the mechanical energy due to the applied linear force of the stance foot just after and before the Push-off Phase, respectively. Since the potential energy is constant (because the linear force is applied to the stance foot which is in continuous contact with the ground during the Push-off Phase),  $E_{push-off}^{(i)}$  can be expressed by the kinetic energy difference between the moment just after and just before the Push-Off Phase. The following relations are valid:

For the Direct Collocation Method:

$$E_{rotational\ actuation}^{(i)} = \frac{h^{(i)}}{3} \sum_{k=1}^N [1, 2, 4] |P_{(hip, k)}^{(i)}| = \frac{h^{(i)}}{3} \sum_{k=1}^N [1, 2, 4] |(q_{(1,appr)}^{(i)}(t_k)\tau_{(1,appr)}^{(i)}(t_k) + q_{(2,appr)}^{(i)}(t_k)\tau_{(2,appr)}^{(i)}(t_k)| \quad (3.77)$$

$$E_{linear\ actuation}^{(i)} = \frac{1}{2}m_{stance} \sum_{n=3}^4 ((q_{(n,appr)}^{(i)}(t_N))^2 - (q_{(n,appr)}^{(i)}(t_{N-1}))^2)$$

and for Discrete Mechanics:

$$E_{rotational\ actuation}^{(i)} = \frac{h^{(i)}}{3} \sum_{k=1}^N [1, 2, 4] |P_{(hip, k)}^{(i)}| = \frac{h^{(i)}}{3} \sum_{k=1}^N [1, 2, 4] |(\frac{q_{(1,k)}^{(i)} - q_{(1,k-1)}^{(i)}}{h^{(i)}}\tau_{(1,k)}^{(i)} + \frac{q_{(2,k)}^{(i)} - q_{(2,k-1)}^{(i)}}{h^{(i)}}\tau_{(2,k)}^{(i)})| \quad (3.78)$$

$$E_{linear\ actuation}^{(i)} = \frac{1}{2}m_{stance} \sum_{i=3}^4 ((\frac{q_{(i,N)}^{(i)} - q_{(i,N-1)}^{(i)}}{h^{(i)}})^2 - (\frac{q_{(i,N-1)}^{(i)} - q_{(i,N-2)}^{(i)}}{h^{(i)}})^2)$$

where we have used the Simpson's rule for approximating the definite integral  $\int_{t_1^{(i)}}^{t_N^{(i)}} |P_{hip}^{(i)}| dt$ . The coefficients [1, 2, 4] refer to the fact that, due to the use of the Simpson's Rule, all the function evaluations at points  $k$  with odd subscripts are multiplied by 4 and all the function evaluations at points  $k$  with even subscripts are multiplied by 2, except for the first and last (in which the coefficient 1 refers to).

As we can see, there exist some discontinuities in the abovementioned equation of the Cost of Transport (the term  $|P_{(hip,k)}^{(i)}|$ ), which contains a non-smooth positive-value function. Discontinuities create difficulties for the numerical optimization procedure. To overcome this we use the square root smoothing technique, which is the approximation  $|x| \approx (\sqrt{x^2 + \epsilon^2})/2$  with a small  $\epsilon$ .

The *COT* for the  $i$ th walking step is defined as the total energy cost of the walking per distance

traveled and per unit body weight, leading to the following expression of  $COT^{(i)}$ :

$$\begin{aligned}
COT^{(i)} &= \frac{E_w^{(i)}}{M_{total}g_{const}D_i} \\
COT^{(i)} &= \frac{E_{rotational\ actuation}^{(i)} + E_{linear\ actuation}^{(i)}}{M_{total}g_{const}D_i} \\
COT^{(i)} &= COT_{rotational\ actuation}^{(i)} + COT_{linear\ actuation}^{(i)}
\end{aligned} \tag{3.79}$$

where  $M_{total} = M + m_1 + m_2$  is the total mass of the biped,  $D_i$  is the step length of the  $i$ th walking step, and  $g_{const}$  is the acceleration of gravity ( $9.81m/s^2$ ).

### 3.6 Derivation of the Gait Generation Problem for the Second Phase

In the current subchapter, we will derive the Gait Generation Problem of the Second Phase of D&CFC. The problem will be mathematically formulated as a finite-dimensional nonlinear constrained optimal control problem. The aim of the Second Phase is the calculation of the trajectory for the  $i$ -th walking step,  $i = 1, \dots, H$  of the Complete 4-DOF Biped Robot, as we have modeled extensively throughout Chapter 3.

We will now consider the following problem on the gait generation of the Second Phase for the Complete 4-DOF Biped Robot:

***For the Complete 4-DOF Biped Robot that was developed throughout the Chapter 3, and taking into account the constraint forces on the stance foot, calculate a trajectory for the  $i$ -th walking step,  $i = 1, \dots, H$ , that includes the control inputs and state variables, such that the corresponding swing leg of the 4-DOF Biped lands at the  $i$ -th reference grounding point of a general rough terrain with stable and natural gait.***

As we have mentioned on Chapter 1 & 2, we have implemented two variants of the proposed control system, thus we will derive the optimal gait generation problem for each one of them. In the following, (as we have done in the Gait Generation Problem of the First Phase), we assume that the Leg 2 initially starts the walking process. In other words, during the odd

walking steps, the Leg 1 is the stance leg and the Leg 2 is the swing leg, and during the even walking steps the Leg 1 is the swing leg and the Leg 2 is the stance leg.

### • Gait Generation Problem of the Second Phase utilizing Direct Collocation

The mathematical formulation of the Gait Generation problem of the Second Phase using Direct Collocation Method is stated as follows:

**For the odd walking steps:**

**minimize:**  $COT^{(i)}$  (3.79)

**subject to:**

• Swing Phase Model in State Space Form (3.16), (3.40), (1)

• Heel Strike Phase Model Equations (3.50), (3.61),(2)

• Push-Off Phase Model Equations (3.66), (3.71),(3.36)(3)

•  $q_{(1,approx)}^{(i)}(t_N) = q_{(1,approx)}^{(i+1)}(t_1) = \sin^{-1}\left(-\frac{D_i}{2l}\right) - \theta_i$ , (4)

•  $q_{(2,approx)}^{(i)}(t_N) = q_{(2,approx)}^{(i+1)}(t_1) = \sin^{-1}\left(\frac{D_i}{2l}\right) - \theta_i$ , (5)

•  $\cos(-q_{(1,approx)}^{(i)}(t_k) + \theta_i) - \cos(q_{(2,approx)}^{(i)}(t_k) + \theta_i) > 0, k = 2, \dots, N - 1$ , (6)

• Impact Surface Conditions (2.33), (7)

•  $\sin(-q_{(1,approx)}^{(i)}(t_{k+1}) + \theta_i) \frac{q_{(1,approx)}^{(i)}(t_{k+1}) - q_{(1,approx)}^{(i)}(t_k)}{h^{(i)}} - \sin(q_{(2,approx)}^{(i)}(t_k) + \theta_i) \frac{q_{(2,approx)}^{(i)}(t_{k+1}) - q_{(2,approx)}^{(i)}(t_k)}{h^{(i)}} > 0, k = 1, \dots, N - 1$ , (8)

•  $\tau_{min} \leq \tau_k^{(i)} \leq \tau_{max}, k = 1, \dots, N$ , (9)

•  $-\frac{\pi}{2} \leq q_{(1,k)}^{(i)}, q_{(2,k)}^{(i)} \leq \pi, k = 1, \dots, N$ , (10)

•  $-\dot{q}_{max} \leq \dot{q}_{(1,k)}^{(i)}, \dot{q}_{(2,k)}^{(i)} \leq \dot{q}_{max}, k = 1, \dots, N$ , (11)

•  $0 \leq F_{PO}^{(i)} \leq F_{(PO,max)}^{(i)}$ , (12)

• Average linear walking speed  $V_i \Leftrightarrow V_i = \frac{D_i}{T_i} \Leftrightarrow T_i = \frac{D_i}{V_i} \Leftrightarrow (N - 1)h^{(i)} = \frac{D_i}{V_i} \Leftrightarrow h^{(i)} = \frac{D_i}{V_i(N - 1)}$ , (13)

• **with initial conditions:**  $q_{(1,1)}^{(i)}, q_{(2,1)}^{(i)}, q_{(3,1)}^{(i)}, q_{(4,1)}^{(i)}, \dot{q}_{(1,1)}^{(i)}, \dot{q}_{(2,1)}^{(i)}, \dot{q}_{(3,1)}^{(i)}, \dot{q}_{(4,1)}^{(i)}$

Based on the abovementioned (Direct Collocation-based/Forward Dynamics Based) optimization problem:

1. We want to minimize the Cost of Transport of the  $i - th$  walking step,  $i = 1, \dots, H$ .
2. **Constraints (1),(2),(3)** define the Swing Phase (in State Space Form), Heel Strike and Push-off Phase equations of the 4-DOF Biped that were extensively developed throughout Chapter 3. For the odd walking steps we have to take into account the appropriate matrices and vectors for the Case 1: Leg 1 = Stance Leg, Leg 2 = Swing Leg. In addition, for the even walking steps we have to take into account the appropriate matrices and vectors for the Case 2: Leg 1 = Swing Leg, Leg 2 = Stance Leg.
3. **Constraints (4) and (5)** refer to the configuration of the two legs of the 4-DOF Biped during the Heel Strike Phase (i.e. in the time interval  $[t_N^{(i)}, t_1^{(i+1)}]$ ).
4. **Constraint (6)** refers to the fact that the Swing Leg must be above the Stance Leg and not touch the ground surface for the duration of the Swing Phase. In other words, during the Swing Phase, the vertical length of the swing leg is smaller than the one of the stance leg.
5. **Constraint (7)** outline the configuration of the biped during the time step of the Heel Strike Phase; the configuration of each leg remains the same for the small duration of the impact of the swing leg with the ground.
6. **Constraint (8)** implies the height of the Swing Leg that is monotonously being decreased at each time step of the Swing Phase.
7. **Constraints (9) - (12)** refer to the physical constraints of the rotational and linear actuators.
8. **Constraint (13)** refers to the average linear walking speed of the swing leg, if it is selected to be an active constraint. From the expression of the average linear walking speed, we can calculate the duration of a time interval for the  $ith$  walking step,  $h^{(i)}$ , otherwise a predefined value for the time interval is being used.

9. As **initial values** of the optimization problems are considered the four generalized coordinates and velocities of the two legs and the stance foot at the first time step of a walking step.

For the even walking steps, we formulate a similar Gait Generation Problem.

• **Gait Generation Problem of the Second Phase utilizing Discrete Mechanics**

The mathematical formulation of the Gait Generation problem of the Second Phase using Discrete Mechanics is stated as follows:

**For the odd walking steps:**

**minimize:**  $COT^{(i)}$  (3.79)

**subject to:**

• Swing Phase Model (3.31), (3.41), (1)

• Boundary Conditions (3.23-3.30), (2)

• Heel Strike Phase Model Equations (3.51), (3.63), (3)

• Push-Off Phase Model Equations (3.68), (3.72), (3.47) (4)

•  $q_{(1,N)}^{(i)} = q_{(1,1)}^{(i+1)} = \sin^{-1}\left(-\frac{D_i}{2l}\right) - \theta_i$ , (4)

•  $q_{(2,N)}^{(i)} = q_{(2,1)}^{(i+1)} = \sin^{-1}\left(\frac{D_i}{2l}\right) - \theta_i$ , (5)

•  $\cos(-q_{(1,k)}^{(i)} + \theta_i) - \cos(q_{(2,k)}^{(i)} + \theta_i) > 0, k = 2, \dots, N - 1$ , (6)

• Impact Surface Conditions (2.32), (7)

•  $\sin(-q_{(1,k+1)}^{(i)} + \theta_i) \frac{q_{(1,k+1)}^{(i)} - q_{(1,k)}^{(i)}}{h^{(i)}} - \sin(q_{(2,k)}^{(i)} + \theta_i) \frac{q_{(2,k+1)}^{(i)} - q_{(2,k)}^{(i)}}{h^{(i)}} > 0, k = 1, \dots, N - 1$ , (8)

•  $\tau_{min} \leq \tau_k^{(i)} \leq \tau_{max}, k = 1, \dots, N$ , (9)

•  $-\frac{\pi}{2} \leq q_{(1,k)}^{(i)}, q_{(2,k)}^{(i)} \leq \pi, k = 1, \dots, N$ , (10)

•  $-\dot{q}_{max} \leq \dot{q}_{(1,k)}^{(i)}, \dot{q}_{(2,k)}^{(i)} \leq \dot{q}_{max}, k = 1, \dots, N$  (11)

•  $0 \leq F_{PO}^{(i)} \leq F_{(PO,max)}^{(i)}$ , (12)

• Average linear walking speed  $V_i \Leftrightarrow V_i = \frac{D_i}{T_i} \Leftrightarrow T_i = \frac{D_i}{V_i} \Leftrightarrow (N - 1)h^{(i)} = \frac{D_i}{V_i}$

$\Leftrightarrow h^{(i)} = \frac{D_i}{V_i(N - 1)}$ , (13)

- **with initial conditions:**  $q_{(1,1)}^{(i)}, q_{(2,1)}^{(i)}, q_{(3,1)}^{(i)}, q_{(4,1)}^{(i)}, \dot{q}_{(1,1)}^{(i)}, \dot{q}_{(2,1)}^{(i)}, \dot{q}_{(3,1)}^{(i)}, \dot{q}_{(4,1)}^{(i)}$

In the abovementioned (Discrete Mechanics-Based/Inverse Dynamics-based) optimization problems, we have to use the equations of the Swing, Heel Strike and Push-Off Phases (not in the State Space Forms) that were derived based on Discrete Mechanics and to take into account the finite difference conditions related to the first and second derivative of the generalized coordinates. In addition, we have to utilize the Boundary Conditions related to the initial and terminal values of the generalized coordinates and velocities. The other constraints remain the same as in the direct collocation-based optimization problems.

For the even walking steps, we derive a similar Gait Generation Problem.

### 3.7 Energy Efficient Trajectory Synthesis and Verification

In the bibliography of bipedal robot locomotion, it is well known that a gait generation problem with numerous hard motion constraints is very challenging to be solved, despite the major advances in trajectory generation and optimization techniques. The calculated trajectories are in most cases suboptimal, meaning that, although the resulted trajectory satisfies all the required constraints, the value of the objective function is not the minimal possible. In addition, the number of the discretization points  $N$  plays a crucial role in the optimization process, leading to a lower value of the objective function as  $N$  increases, thus increasing the computational effort. In the case of bipedal robot locomotion, we would ideally seek for a method that achieves a trajectory with the lowest value of the cost function possible, while it satisfies all the optimization constraints and with the lowest achievable discretization points which will decrease the microcontroller's computational effort in the case of implementation in real time. Note that bipedal robots are autonomous systems with limited power resources, due to the use of onboard batteries for functioning.

In the current section we will develop one of the most important components of the proposed system. We call it Energy Efficient Trajectory Synthesizer and Verifier. The aim of it is to produce what is being called: a trajectory that satisfies all the physical and technical constraints of the walking gait with the lowest energy consumption possible, approaching in most cases the energy efficiency of human walking, which is considered the most energy efficient method of locomotion. In other words, the term "energy efficient" in our thesis implies that we seek for trajectories that achieve the smallest possible value of the Cost of Transport, COT for the  $i$ th walking step, while respecting the physical and technical constraints of a proper walking gait. Thus, we are developing an additional novel method to achieve trajectories with the least possible energy consumption, instead of just using the trajectories calculated by the optimization algorithms.

The key for our novel method is the calculated trajectory of the  $i$ th walking step of the First Phase. As we have mentioned and developed extensively in Chapter 3, the First Phase calculates a trajectory for the 2-DOF Biped Robot (the Biped with only two DOF's and without any constraint forces taken into account). In the Second Phase, the values  $(q^{(i)}, \dot{q}^{(i)})$  from the time steps  $k = 1, \dots, N - 1$  of the  $i$ th walking step (in other words, the values of the generalized coordinates  $q_k^{(i)}$  and generalized velocities  $\dot{q}_k^{(i)}$ ) that were derived from the solution of the Gait Generation Problem at the First Phase will be used as initial values for the solution (starting from the related  $k$ th time step) of the Gait Generation Problem at the Second Phase. As we have mentioned in previous chapters, a gait trajectory consists of  $N$  time steps, so this method will calculate one complete trajectory (where we give as initial conditions the values  $(q^{(i)}, \dot{q}^{(i)})$  that describe the first time step ( $k = 1$ )) and  $N-2$  sectional trajectories (where for the calculation of each sub-trajectory we give as initial conditions the values  $(q^{(i)}, \dot{q}^{(i)})$  that describe the related time step ( $1 < k \leq N - 1$ )), which form  $N-1$  trajectories.

After the calculation of these  $N-1$  trajectories, we are proceeding with the synthesis and verification of the final trajectory that will be followed by the complete 4-DOF biped robot. For each time step  $k$  of the  $i$ th walking step, we select the entire set of values from one of the resulted trajectories which has the lowest Point Cost of Transport ( $PCOT^{(i)}$ ). In Chapter 3.5 we have extensively derived the relation of the Cost of Transport for the  $i$ th walking step. The

Point Cost of Transport for time step  $k$  of the  $i$ th walking step is defined as:

For Direct Collocation:

$$PCOT_k^{(i)} = \begin{cases} |q_{(1,appr)}^{(i)}(t_k)\tau_{(1,appr)}^{(i)}(t_k) + q_{(2,appr)}^{(i)}(t_k)\tau_{(2,appr)}^{(i)}(t_k)|, & \text{for } k = 1, \dots, N-1, \\ |(q_{(1,appr)}^{(i)}(t_N)\tau_{(1,appr)}^{(i)}(t_N) + q_{(2,appr)}^{(i)}(t_N)\tau_{(2,appr)}^{(i)}(t_N))| + \\ \frac{1}{2}m_{stance} \sum_{n=3}^4 ((q_{(n,appr)}^{(i)}(t_N))^2 - (q_{(n,appr)}^{(i)}(t_{N-1}))^2), & \text{for } k = N \end{cases}$$

For Discrete Mechanics:

$$PCOT_k^{(i)} = \begin{cases} = |(\frac{q_{(1,k)}^{(i)} - q_{(1,k-1)}^{(i)}}{h^{(i)}}\tau_{(1,k)}^{(i)} + \frac{q_{(2,k)}^{(i)} - q_{(2,k-1)}^{(i)}}{h^{(i)}}\tau_{(2,k)}^{(i)})|, & \text{for } k = 1, \dots, N-1, \\ |(\frac{q_{(1,N)}^{(i)} - q_{(1,N-1)}^{(i)}}{h^{(i)}}\tau_{(1,N)}^{(i)} + \frac{q_{(2,N)}^{(i)} - q_{(2,N-1)}^{(i)}}{h^{(i)}}\tau_{(2,N)}^{(i)})| + \\ \frac{1}{2}m_{stance} \sum_{i=3}^4 ((\frac{q_{(i,N)}^{(i)} - q_{(i,N-1)}^{(i)}}{h^{(i)}})^2 - (\frac{q_{(i,N-1)}^{(i)} - q_{(i,N-2)}^{(i)}}{h^{(i)}})^2), & \text{for } k = N \end{cases}$$

Due to the fact that the generalized Coordinates  $q_3^{(i)}, q_4^{(i)}$ , are undefined at the First Phase (at the start of the whole walking process we initialize them as follows:  $(q_{(3,1)}^{(1)}, q_{(4,1)}^{(1)}) = (0, 0)$ ,  $(\dot{q}_{(3,1)}^{(1)}, \dot{q}_{(4,1)}^{(1)}) = (0, 0)$ ), the related values of  $q_3^{(i)}, q_4^{(i)}$  from the first complete trajectory, as calculated at the Second Phase of each walking step, will be used, where needed.

While the abovementioned trajectory synthesis method is being processed, a process called trajectory verification is being executed. Trajectory verification ensures that the final, energy optimal trajectory of the Second Phase has the qualitative behavior of a proper walking gait. Qualitative behavior refers to the typical value relation of the generalized coordinates  $(q_1^{(i)}, q_2^{(i)})$  and velocities  $(\dot{q}_1^{(i)}, \dot{q}_2^{(i)})$  during the  $N$  time steps, between the current and the previous time step of the  $i$ th walking step. As a "reference trajectory" in terms of that proper walking gait, the very first complete trajectory of the Second Phase is being used, where we give as initial conditions the set of values  $(q^{(i)}, \dot{q}^{(i)})$  of the first time step from the First Phase.

Trajectory Verification Method starts from the second time step of the abovementioned trajectory synthesis. After the selection of a set of values from a specific complete or sectional trajectory for the time step  $k$  of the  $i$ th walking step, trajectory verification method, based on

the qualitative properties of the reference trajectory, checks the typical value relation of the generalized coordinates  $q_1^{(i)}, q_2^{(i)}$  and angular velocities  $\dot{q}_1^{(i)}, \dot{q}_2^{(i)}$  between the current and the previous time step of the  $i$ th walking step. If the qualitative behavior is violated, then a set of values from another trajectory with the next highest Point Cost of Transport for the same time step is selected. If for a current time step all sets of values from all the available trajectories are violating the qualitative behavior of the reference trajectory (in other words, if they are violating the qualitative behavior of a proper walking gait), then trajectory synthesis method steps back to the previous time step and selects a set of values from a different trajectory with the next highest Point Cost of Transport than previously selected. Then we step ahead to the next time step where we had the violations, and we let trajectory synthesizer to select an appropriate set of values from a specific trajectory and the trajectory verifier to check the eligibility of the selected variables.

Once the abovementioned procedure has been completed and a candidate energy optimal trajectory has been formed, we calculate its  $COT$  as  $COT^{(i)} = \frac{\sum_{k=1}^N PCOT_k^{(i)}}{M_{total}gD_i}$ . Then, we turn all the sectional trajectories to complete ones. This is done by adding the set of values from the missing time steps from the previous trajectories. These newly created complete trajectories do not need to be verified for correctness, due to the fact that the majority of the newly added set of values for the missing time steps ( $q^{(i)}, \dot{q}^{(i)}$ ), are actually taken from the calculated trajectory of the First Phase, thus there are proper trajectories indeed. Then we calculate their Cost of Transport and compare our candidate energy optimal trajectory with all the N-1 complete trajectories in terms of their value of the Cost of Transport. The trajectory with the lowest possible Cost of Transport is selected as the final energy optimal trajectory.

Once the initial values for the first time step of the next walking step are specified, (they can be chosen randomly from any trajectory), the stage is set for the First And Second Phases of the Gait Generation Module for the next walking step, till all the predefined walking steps are done. Then we proceed to the Trajectory Tracking Control Module.

# Chapter 4

## Trajectory Tracking Control Module

### 4.1 Introduction

The main complexity in trajectory tracking for bipedal robot locomotion is the degree of actuation of the biped during the different gait phases. In the underactuated gait phases, the biped regroups fewer control signals than configuration variables (in contrast with the fully actuated phases), so different control strategies should be implemented based on the degree of actuation of a specific phase. Moreover, many of the existing controllers in literature require the complete state measurements, that is position and velocity, is available for feedback. Unfortunately, in practice this assumption can only partially be fulfilled, because the sensors for velocity measurements are often contaminated with a considerable amount of noise. In addition, when disturbances exist, this controller can only drive the system output to a neighborhood of the desired trajectory. A solution of this problem is the design of nonlinear observers to estimate the missing velocity signal and the disturbances for effective trajectory tracking control.

This chapter deals with the design of a control strategy to effectively track the desired trajectory that was obtained in the Second Phase and must be followed by the biped, under the assumption of missing velocity signals and disturbances (e.g. Coulomb and viscous actuator friction). This control strategy combines a nonlinear velocity observer for the estimation of the unmeasured velocity signals of the robot, a nonlinear disturbance observer for the estimation

of disturbances, and a computed torque controller or partial feedback linearization controller, based on the nature of actuation of the Gait Phase (e.g. the Gait Phase is either a fully actuated or underactuated phase). Thereafter, these observers are integrated with the controller.

Regarding to the notation of all the parameters (e.g. states, angular coordinates/velocities/accelerations, control inputs, constrained forces) in the discretized setting, assuming that a walking step consists of  $N$  time steps, then when we see the mathematical representation  $x_{(1,k)}^{(i)}$  for instance, we refer to the value of the variable  $x_1$  for  $t = N(i-1)h + (k-1)h$  sec. Thus,  $x_{(1,k)}^{(i)} = x_1(t = N(i-1)h + (k-1)h$  sec),  $x_k^{(i)} = x(t = N(i-1)h + (k-1)h$  sec),  $q_{(1,k)}^{(i)} = q_1(t = N(i-1)h + (k-1)h$  sec),  $q_{(2,k)}^{(i)} = q_2(t = N(i-1)h + (k-1)h$  sec),  $u_k^{(i)} = u(t = N(i-1)h + (k-1)h$  sec) etc. The abovementioned notation is used throughout the current thesis.

In the current chapter, we will follow a specific control design procedure for the biped robot:

- Design of a nonlinear controller for the biped robot to achieve stability and performance specification for tracking with availability of the velocity signals and with absence of disturbances.
- Integration of a velocity and disturbance observer, by replacing the velocity in the control law with its estimation from the velocity observer and the disturbance (which we add in the equations of motion for all gait phases) with its estimation yielded by the disturbance observer respectively.

### 4.1.1 Control of Fully Actuated and Underactuated Systems

According to Newton, the dynamics of mechanical systems are second order ( $F = m\alpha$ ). Their state is given by a vector of positions,  $q$ , and a vector of velocities,  $\dot{q}$ , and (possibly) time. The general form for a second-order controllable dynamical system is:

$$\ddot{q} = f(q, \dot{q}, u, t),$$

where  $u$  is the control vector. As we will see, the forward dynamics for many of the robots that we care about turn out to be affine in commanded torque, so let's consider a slightly constrained

form:

$$\ddot{q} = f_1(q, \dot{q}, t) + f_2(q, \dot{q}, t)u \quad (4.1)$$

**Definition (Fully-Actuated System).** A control system described by equation (4.1) is fully-actuated in configuration  $(q, \dot{q}, t)$  if it is able to command an instantaneous acceleration in an arbitrary direction in  $q$ :

$$\text{rank}[f_2(q, \dot{q}, t)] = \text{dim}[q] \quad (4.2)$$

**Definition (Underactuated System).** A control system described by equation (4.1) is fully-actuated in configuration  $(q, \dot{q}, t)$  if it is not able to command an instantaneous acceleration in an arbitrary direction in  $q$ :

$$\text{rank}[f_2(q, \dot{q}, t)] < \text{dim}[q] \quad (4.3)$$

Notice that whether or not a control system is underactuated may depend on the state of the system, although for most systems underactuation is a global property of the system.

In the case of our 4-DOF biped robot, based on the state space representations of the Gait Phases that were derived in previous Chapters, and the abovementioned definitions of fully-actuation and underactuation, the Swing and Heel Strike Phases are considered underactuated phases and the Push-Off Phase is considered fully actuated phase.

Fully actuated systems are easier to control than underactuated systems. The key observation is that, for fully-actuated systems with known dynamics (e.g. if  $f_1$  and  $f_2$  are known), it is possible to use feedback to change a nonlinear control problem into a linear control problem. The field of linear control theory is incredibly advanced, and there are many well-known solutions for controlling linear systems.

For fully actuated systems, we are going to use feedback linearization. When  $f_2$  is full row rank, it is invertible. Consider the nonlinear feedback law:

$$u = \pi(q, \dot{q}, t) = f_2^{-1}(q, \dot{q}, t)[v - f_1(q, \dot{q}, t)],$$

where  $v$  is an additional control input. Applying this feedback controller to equation (4.1)

results in the linear, decoupled, second-order system:

$$\ddot{q} = v.$$

In other words, if  $f_1$  and  $f_2$  are known and  $f_2$  is invertible, then the system is feedback equivalent to  $\ddot{q} = v$ . In the next subchapter we will develop a special case of feedback linearization, called computed torque control, which will be applied for the fully actuated phases (Push-Off Phase).

Underactuated systems are not feedback linearizable. An interesting property that holds for the entire class of underactuated mechanical systems is the so-called collocated partial feedback linearization. Partial feedback linearization can lead to one of the two possible control approaches for an underactuated system. Collocated linearization refers to a control that linearizes the equations associated with the actuated degrees of freedom and it will be extensively developed and used in the current thesis. Noncollocated linearization refers to linearizing the passive (non-actuated) degrees of freedom and is possible under a special assumption on the inertia matrix of the robot. It will not be used in the current thesis.

### 4.1.2 Introduction to Computed Torque Control

In this section, we consider the trajectory tracking control problem for biped robots: given a desired trajectory, how should the joint torques be chosen so that the biped follows that trajectory. We would like to choose a control strategy which is robust with respect to initial condition errors, sensor noise, and modeling errors. We ignore the problems of actuator dynamics, and assume that we can command arbitrary torques which are exerted at the joints (legs).

We are given a description of the dynamics of a general biped robot in the form of the equation

$$M(q)\ddot{q} + C(q, \dot{q})\dot{q} + G(q) = \tau, \quad (4.4)$$

where  $q \in \mathbb{R}^n$  is the set of configuration variables for the robot and  $\tau \in \mathbb{R}^n$  denotes the torques applied at the joints. We are also given a joint trajectory  $q_d$  which we wish to track. For

simplicity, we assume that  $q_d$  is specified for all time and that it is at least twice differentiable. If we have a perfect model of the robot and  $q(0) = q_d(0), \dot{q}(0) = \dot{q}_d(0)$ , then we may solve our problem by choosing

$$\tau = M(q_d)\ddot{q}_d + C(q_d, \dot{q}_d)\dot{q}_d + G(q_d).$$

Since both  $q$  and  $q_d$  satisfy the same differential equation and have the same initial conditions, it follows from the uniqueness of the solutions of differential equations that  $q(t) = q_d(t)$  for all  $t \geq 0$ . This is an example of an open-loop control law: the current state of the robot is not used in choosing the control inputs.

Unfortunately, this strategy is not very robust. If  $q(0) \neq q_d(0)$ , then the open-loop control law will never correct for this error. This is clearly undesirable, since we almost never know the current position of a robot *exactly*. Furthermore, we have no guarantee that if our starting configuration is near the desired initial configuration that the trajectory of the robot will stay near the desired trajectory for all time. For this reason, we introduce feedback into our control law. This feedback must be chosen such that the actual robot trajectory converges to the desired trajectory. In particular, if our trajectory is a single setpoint, the closed-loop system should be asymptotically stable about the desired setpoint. There are several approaches for designing stable robot control laws. Using the structural properties of robot dynamics, we will be able to prove stability of these control laws for *all* robots having those properties.

Consider the following refinement of the open-loop control law presented above: given the current position and velocity of the biped, cancel all nonlinearities and apply exactly the torque needed to overcome the inertia of the actuator,

$$\tau = M(q)\ddot{q}_d + C(q, \dot{q})\dot{q} + G(q)$$

Substituting this control law into the dynamic equations of the biped (4.4), we see that

$$M(q)\ddot{q} = M(q)\ddot{q}_d,$$

and since  $M(q)$  is uniformly positive definite in  $q$ , we have

$$\ddot{q} = \ddot{q}_d \quad (4.5)$$

Hence, if the initial position and velocity of the robot matches the desired position and velocity, the biped will follow the desired trajectory. As before, this control law will not correct for any initial condition errors which are present.

The tracking properties of the control law can be improved by adding state feedback. The linearity of equation (4.5) suggests the following control law:

$$\tau = M(q)(\ddot{q}_d - K_v\dot{e} - K_p e) + C(q, \dot{q})\dot{q} + G(q) \quad (4.6)$$

where  $e = q - q_d$ , and  $K_v$  and  $K_p$  are constant gain matrices. When substituted into equation (4.4), the error dynamics can be written as:

$$M(q)(\ddot{e} + K_v\dot{e} + K_p e) = 0.$$

Since  $M(q)$  is always positive definite, we have

$$\ddot{e} + K_v\dot{e} + K_p e = 0. \quad (4.7)$$

This is a linear differential equation which governs the error between the actual and desired trajectories. Equation (4.6) is called the *computed torque* control law.

The computed torque control law consists of two components. We can write equation (5.6) as

$$\tau = M(q)\ddot{q}_d + C\dot{q} + G + M(q)(-K_v\dot{e} - K_p e)$$

where  $M(q)\ddot{q}_d + C\dot{q} + G$  is the feedforward component and  $M(q)(-K_v\dot{e} - K_p e)$  is the feedback component. The feedforward component provides the amount of torque necessary to drive the system along its nominal path. The feedback component provides correction torques to reduce any errors in the trajectory of the robot.

Since the error equation (4.7) is linear, it is easy to choose  $K_v$  and  $K_p$  so that the overall system is stable and  $e \rightarrow 0$  exponentially as  $t \rightarrow \infty$ . Moreover, we can choose  $K_v$  and  $K_p$  such that we get independent exponentially stable systems (by choosing  $K_p$  and  $K_v$  diagonal). The following proposition gives one set of conditions under which the computed torque control law (5.6) results in exponential tracking.

**Theorem (Stability of the Computed Torque Control).** If  $K_p, K_v \in \mathbb{R}^{n \times n}$  are positive definite, symmetric matrices, then the control law (4.6) applied to the system (4.4) results in exponential trajectory tracking.

**Proof.** The error dynamics can be written as a first-order linear system:

$$\frac{d}{dt} \begin{bmatrix} e \\ \dot{e} \end{bmatrix} = \begin{bmatrix} 0 & I \\ -K_p & -K_v \end{bmatrix} \begin{bmatrix} e \\ \dot{e} \end{bmatrix}$$

where  $\begin{bmatrix} 0 & I \\ -K_p & -K_v \end{bmatrix} = A$ .

It suffices to show that each of the eigenvalues of  $A$  has negative real part. Let  $\lambda \in \mathbb{C}$  be an eigenvalue of  $A$  with corresponding eigenvector  $v = (v_1, v_2) \in \mathbb{C}^{2n}$ ,  $v \neq 0$ . Then,

$$\lambda \begin{bmatrix} v_1 \\ v_2 \end{bmatrix} = \begin{bmatrix} 0 & I \\ -K_p & -K_v \end{bmatrix} \begin{bmatrix} v_1 \\ v_2 \end{bmatrix} = \begin{bmatrix} v_2 \\ -K_p v_1 - K_v v_2 \end{bmatrix}$$

It follows that if  $\lambda = 0$  then  $v = 0$ , and hence  $\lambda = 0$  is not an eigenvalue of  $A$ . Further, if  $\lambda \neq 0$ , then  $v_2 = 0$  implies that  $v_1 = 0$ . Thus,  $v_1, v_2 \neq 0$  and we may assume without loss of generality that  $\|v_1\| = 1$ . Using this, we write

$$\begin{aligned} \lambda^2 &= v_1^* \lambda^2 v_1 = v_1^* \lambda v_2 \\ &= v_1^* (-K_p v_1 - K_v v_2) = -v_1^* K_p v_1 - \lambda v_1^* K_v v_1, \end{aligned}$$

where  $*$  denotes complex conjugate transpose. Since  $\alpha = v_1^* K_p v_1 > 0$  and  $\beta = v_1^* K_v v_1 > 0$ , we have

$$\lambda^2 + \alpha \lambda + \beta = 0 \quad \alpha, \beta > 0$$

and hence the real part of  $\lambda$  is negative.

The power of the computed torque control law is that it converts a nonlinear dynamical system into a linear one, allowing the use of any of a number of linear control synthesis tools. This is an example of a more general technique known as *feedback linearization*, where a nonlinear system is rendered linear via full-state nonlinear feedback. One disadvantage of using feedback linearization is that it can be demanding (in terms of computation time and input magnitudes) to use feedback to globally convert a nonlinear system into a single linear system. For biped robots, unboundedness of the inputs is rarely a problem since the inertia matrix of the system is bounded and hence the control torques which must be exerted always remain bounded. In addition, experimental results show that the computed torque controller has very good performance characteristics and it is becoming increasingly popular.

## 4.2 Bipedal Robot Control with availability of velocity signals and absence of disturbances

### 4.2.1 Partial Feedback Linearization Control of the Swing Phase

Consider the general state space representation of the Swing Phase equations of motion for the complete 4-DOF biped robot and assume that the vector of configuration (the angular positions of the legs  $q_{(1,k)}^{(i)}, q_{(2,k)}^{(i)}$  and the Cartesian Coordinates of the stance foot  $q_{(3,k)}^{(i)}, q_{(4,k)}^{(i)}$ ) can be partitioned into the actuated configurations  $q_{(a,k)}^{(i)} = [q_{(1,k)}^{(i)}, q_{(2,k)}^{(i)}]^T$  and the non-actuated configurations  $q_{(na,k)}^{(i)} = [q_{(3,k)}^{(i)}, q_{(4,k)}^{(i)}]^T$ . As we have mentioned before, since the robot in the Swing Phase is underactuated (the biped has 4 degrees of freedom but only two control inputs during the Swing Phase), we assume that the vector of the control inputs (applied torques) can be partitioned as  $u_k^{(i)} = [u_{(a,k)}^{(i)}, 0, 0]^T$  where  $u_{(a,k)}^{(i)} \in R^{2 \times 1}$ . Finally, we assume that the matrices

$M$ ,  $C$ ,  $G$  defining the dynamic model of the biped can be partitioned as follows:

$$\begin{aligned} M(q_k^{(i)}) &= \begin{bmatrix} M_{11} & M_{12} \\ M_{21} & M_{22} \end{bmatrix}, \\ C(q_k^{(i)}, \dot{q}_k^{(i)}) &= \begin{bmatrix} C_{11} & C_{12} \\ C_{21} & C_{22} \end{bmatrix}, \\ G(q_k^{(i)}, \theta) &= \begin{bmatrix} G_1 & G_2 \end{bmatrix}^T, \\ S_{con}^T f_{con}(q_k^{(i)}, \dot{q}_k^{(i)}) &= \begin{bmatrix} 0 & 0 & F_{(con,k)}^{(i)} \end{bmatrix}^T \end{aligned}$$

where:

$$\begin{aligned} M_{11} &= \begin{bmatrix} M[1,1] & M[1,2] \\ M[2,1] & M[2,2] \end{bmatrix}, \quad M_{12} = \begin{bmatrix} M[1,3] & M[1,4] \\ M[2,3] & M[2,4] \end{bmatrix}, \quad M_{21} = \begin{bmatrix} M[3,1] & M[3,2] \\ M[4,1] & M[4,2] \end{bmatrix}, \quad M_{22} = \\ &\begin{bmatrix} M[3,3] & M[3,4] \\ M[4,3] & M[4,4] \end{bmatrix}, \\ C_{11} &= \begin{bmatrix} C[1,1] & C[1,2] \\ C[2,1] & C[2,2] \end{bmatrix}, \quad C_{12} = \begin{bmatrix} C[1,3] & C[1,4] \\ C[2,3] & C[2,4] \end{bmatrix}, \quad C_{21} = \begin{bmatrix} C[3,1] & C[3,2] \\ C[4,1] & C[4,2] \end{bmatrix}, \quad C_{22} = \begin{bmatrix} C[3,3] & C[3,4] \\ C[4,3] & C[4,4] \end{bmatrix}, \\ G_1 &= \begin{bmatrix} G[1,1] \\ G[2,1] \end{bmatrix}, \quad G_2 = \begin{bmatrix} G[3,1] \\ G[4,1] \end{bmatrix}, \\ F_{(con,k)}^{(i)} &= \begin{bmatrix} f_{(fr,k)}^{(i)} \\ f_{(N,k)}^{(i)} \end{bmatrix}. \end{aligned}$$

After partitioning all matrices, the model of the underactuated biped in the Swing Phase takes the form of:

$$\begin{aligned} M_{11}q_{(a,k)}^{(i)} + M_{12}q_{(na,k)}^{(i)} + C_{11}q_{(a,k)}^{(i)} + C_{12}q_{(na,k)}^{(i)} + G_1 &= u_{(a,k)}^{(i)} \\ M_{21}q_{(a,k)}^{(i)} + M_{22}q_{(na,k)}^{(i)} + C_{21}q_{(a,k)}^{(i)} + C_{22}q_{(na,k)}^{(i)} + G_2 - F_{(con,k)}^{(i)} &= 0 \end{aligned} \quad (4.8)$$

Now we consider the output function

$$y_k^{(i)} = q_{(a,k)}^{(i)}, \quad (4.9)$$

where  $y_k^{(i)}$  is called the collocated output with the input  $u_{(a,k)}^{(i)}$ . Furthermore, due to the fact that  $\det(M_{22}) \neq 0$ ,  $M_{22}$  is invertible, thus we may solve for  $q_{(na,k)}^{(i)}$  in equation (4.8) as:

$$q_{(na,k)}^{(i)} = -M_{22}^{-1}(M_{21}q_{(a,k)}^{(i)} + C_{21}q_{(a,k)}^{(i)} + C_{22}q_{(na,k)}^{(i)} + G_2 - F_{(con,k)}^{(i)}) \quad (4.10)$$

When substituting (4.10) into (4.8), we get:

$$M_a q_{(a,k)}^{(i)} + C_a q_{(a,k)}^{(i)} + C_{na} q_{(na,k)}^{(i)} + C_a q_{(a,k)}^{(i)} + \tilde{G} + F_{(con,k)}^{(i)} = u_{(a,k)}^{(i)} \quad (4.11)$$

where:

$$M_a = M_{11} - \frac{M_{21}M_{12}}{M_{22}}, \quad C_a = C_{11} - \frac{M_{12}C_{21}}{M_{22}}, \quad C_{na} = C_{12} - \frac{M_{12}C_{22}}{M_{22}}, \quad \tilde{G} = G_1 - \frac{M_{12}G_2}{M_{22}}, \quad \text{and } F_{(con,k)}^{(i)} = \frac{M_{12}F_{(con,k)}^{(i)}}{M_{22}}$$

Since the matrix  $M_a$  is positive definite, we can linearize the actuated configuration of the system dynamics. Thus, the feedback linearization controller is defined for (4.11) and is given by the following relation:

$$M_a v_{(a,k)}^{(i)} + C_a q_{(a,k)}^{(i)} + C_{na} q_{(na,k)}^{(i)} + C_a q_{(a,k)}^{(i)} + \tilde{G} + F_{(con,k)}^{(i)} = u_{(a,k)}^{(i)} \quad (4.12)$$

where  $v_{(a,k)}^{(i)} \in R^2$  is an additional control input to be defined later. The closed loop system is then given by:

$$\begin{aligned} q_{(na,k)}^{(i)} &= -M_{22}^{-1}(M_{21}q_{(a,k)}^{(i)} + C_{21}q_{(a,k)}^{(i)} + C_{22}q_{(na,k)}^{(i)} + G_2 - F_{(con,k)}^{(i)}) \\ q_{(a,k)}^{(i)} &= v_{(a,k)}^{(i)} \\ y_k^{(i)} &= q_{(a,k)}^{(i)} \end{aligned} \quad (4.13)$$

Furthermore, it can be seen from (4.13) that the vector of actuated configurations is completely decoupled from the vector of unactuated configurations and linearized second order. We define  $y_{(k,d)}^{(i)} = [y_{(1,k,d)}^{(i)} \ y_{(2,k,d)}^{(i)}]^T = [q_{(1,k,d)}^{(i)} \ q_{(2,k,d)}^{(i)}]^T$  be the vector of reference trajectories and  $e_k^{(i)} = [e_{(1,k)}^{(i)} \ e_{(2,k)}^{(i)}]^T$  the tracking error vector where each component is given by:

$$e_{(j,k)}^{(i)} = q_{(j,k)}^{(i)} - q_{(j,k,d)}^{(i)}, \quad j = 1, 2 \quad (4.14)$$

Now, the additional control input  $v_{(a,k)}^{(i)} \in R^2$  may be chosen by the following relation:

$$v_{(a,j,k)}^{(i)} = y_{(j,k,d)}^{(i)} - K_{pj}e_{(j,k)}^{(i)} - K_{vj}e_{(j,k)}^{(i)}, \quad j = 1, 2 \quad (4.15)$$

where coefficients  $K_{pj}$ ,  $K_{vj}$ ,  $j = 1, 2$  are chosen so that the two polynomials  $\ddot{s} - K_{pj}s - K_{vj}\dot{s}$ ,  $j = 1, 2$  are Hurwitz. Then the error system dynamics can be given by:

$$\ddot{e}_k^{(i)} = v_{(a,k)}^{(i)} - y_{(k,d)}^{(i)} \quad (4.16)$$

where each component of (5.16) is given by:

$$e_{(j,k)}^{(i)} = -K_{pj}e_{(j,k)}^{(i)} - K_{vj}e_{(j,k)}^{(i)} \quad (4.17)$$

From (4.17), we can clearly see that for a suitable choice of the abovementioned coefficients, the error tracking vector converges globally exponentially to zero. Let  $Z_1 = e_k^{(i)}$ ,  $Z_2 = \dot{e}_k^{(i)}$ ,  $\eta_1 = q_{(na,k)}^{(i)} = [q_{(3,k)}^{(i)} \quad q_{(4,k)}^{(i)}]$ ,  $\eta_2 = q_{(na,k)}^{(i)} = [q_{(3,k)}^{(i)} \quad q_{(4,k)}^{(i)}]$ . Thus, the complete closed loop system can be written as :

$$\begin{aligned} \dot{Z}_1 &= Z_2 \\ \dot{Z}_2 &= -K_p Z_1 - K_d Z_2 \\ \dot{\eta}_1 &= \eta_2 \\ \dot{\eta}_2 &= \Omega(Z, \eta, t^{(i)}) \\ e_k^{(i)} &= y_k^{(i)} - y_{(k,d)}^{(i)} = Z_t \end{aligned} \quad (4.18)$$

where:

$$\Omega(Z, \eta, t^{(i)}) = -M_{22}^{-1}(C_{21}q_{(a,k)}^{(i)} + G_2 - F_{(con,k)}^{(i)}) - M_{22}^{-1}C_{22}\eta_2 - M_{22}^{-1}M_{21}(y_{(k,d)}^{(i)} - K_p Z_1 - K_v Z_2) \quad (4.19)$$

$$\text{where } K_p = \begin{bmatrix} K_{p1} & 0 \\ 0 & K_{p2} \end{bmatrix} \text{ and } K_v = \begin{bmatrix} K_{v1} & 0 \\ 0 & K_{v2} \end{bmatrix}.$$

In matrix form, the system (4.18) can be rewritten as:

$$\begin{aligned}\dot{Z} &= AZ \\ \dot{\eta} &= w(Z, \eta, t^{(i)}) \\ e_k^{(i)} &= CZ\end{aligned}\quad (4.20)$$

where  $Z = \begin{bmatrix} Z_1 \\ Z_2 \end{bmatrix}$ ,  $\eta = \begin{bmatrix} \eta_1 \\ \eta_2 \end{bmatrix}$ ,  $A = \begin{bmatrix} 0 & I_{2 \times 2} \\ -K_p & -K_v \end{bmatrix}$ ,  $C = \begin{bmatrix} I_{2 \times 2} & 0 \end{bmatrix}$  and  $w(Z, \eta, t^{(i)}) = \begin{bmatrix} \eta_2 \\ \Omega(Z, \eta, t^{(i)}) \end{bmatrix}$ .

### 4.2.2 Computed Torque Control of the Push-Off Phase

Consider the general equations of motion for the Instantaneous Push-Off Phase:

$$M(q_k^{(i)})\ddot{q}_k^{(i)} + C(q_k^{(i)}, \dot{q}_k^{(i)})\dot{q}_k^{(i)} + G(q_k^{(i)}, \theta^{(i)}) = B_{PO}(q_k^{(i)})u_k^{(i)} + S_{con}^T f_{(con,k)}^{(i)}$$

$\Leftrightarrow$

$$M(q_{N-1}^{(i)})\ddot{q}_{N-1}^{(i)} + C(q_{N-1}^{(i)}, \dot{q}_{N-1}^{(i)})\dot{q}_{N-1}^{(i)} + G(q_{N-1}^{(i)}, \theta^{(i)}) = u_{N-1}^{(i)} + S_{con}^T f_{(con,N-1)}^{(i)} \quad (4.21)$$

where  $B_{PO}(q_{N-1}^{(i)}) = \begin{bmatrix} 1 & 0 & 0 & 0 \\ 0 & 1 & 0 & 0 \\ 0 & 0 & 1 & 0 \\ 0 & 0 & 0 & 1 \end{bmatrix}$ ,  $u_{N-1}^{(i)} = \begin{bmatrix} \tau_{(1,N-1)}^{(i)} \\ \tau_{(2,N-1)}^{(i)} \\ F_{(PO,x,N-1)}^{(i)} \\ F_{(PO,y,N-1)}^{(i)} \end{bmatrix}$  The suggested control law, as we

have analyzed extensively in the previous subchapter, for the Instantaneous Push-Off Phase is the following:

$$u_{N-1}^{(i)} = M(q_{N-1}^{(i)})(q_{N-1,d}^{(i)} - K_v e_{N-1}^{(i)} - K_p e_{N-1}^{(i)}) + C(q_{N-1}^{(i)}, \dot{q}_{N-1}^{(i)})\dot{q}_{N-1}^{(i)} + G(q_{N-1}^{(i)}, \theta^{(i)}) - S_{con}^T f_{(con,N-1)}^{(i)} \quad (4.22)$$

where  $e_{N-1}^{(i)} = q_{N-1}^{(i)} - q_{(N-1,d)}^{(i)}$ , and  $K_v$  and  $K_p$  are constant gain matrices. When substituted into equation (4.21), the error dynamics can be written as:

$$M(q_{N-1}^{(i)})(e_{N-1}^{(i)} + K_v \dot{e}_{N-1}^{(i)} + K_p e_{N-1}^{(i)}) = 0.$$

Since  $M(q_{N-1}^{(i)})$  is always positive definite, we have

$$e_{N-1}^{(i)} + K_v \dot{e}_{N-1}^{(i)} + K_p e_{N-1}^{(i)} = 0. \quad (4.23)$$

### 4.2.3 Partial Feedback Linearization Control of the Heel Strike Phase

Consider the general state space representation of the Heel Strike Phase equations of motion for the complete 4-DOF biped robot and assume that the vector of configuration (the angular positions of the legs  $q_{(1,N)}^{(i)}, q_{(2,N)}^{(i)}$  and the Cartesian Coordinates of the stance foot  $q_{(3,N)}^{(i)}, q_{(4,N)}^{(i)}$ ) can be partitioned into the actuated configurations  $q_{(a,N)}^{(i)} = [q_{(1,N)}^{(i)}, q_{(2,N)}^{(i)}]^T$  and the non-actuated configurations  $q_{(na,N)}^{(i)} = [q_{(3,N)}^{(i)}, q_{(4,N)}^{(i)}]^T$ . As we have mentioned before, since the robot in the Heel Strike Phase is underactuated (the biped has 4 degrees of freedom but only two control inputs during the Heel Strike Phase), we assume that the vector of the control inputs (applied torques) can be partitioned as  $u_N^{(i)} = [u_{(a,N)}^{(i)}, 0, 0]^T$  where  $u_{(a,N)}^{(i)} \in R^{2 \times 1}$ . Finally, we assume that the matrices  $M$ ,  $C$ ,  $G$  defining the dynamic model of the biped can be partitioned as follows:

$$\begin{aligned} M(q_N^{(i)}) &= \begin{bmatrix} M_{11} & M_{12} \\ M_{21} & M_{22} \end{bmatrix}, \\ C(q_N^{(i)}, \dot{q}_N^{(i)}) &= \begin{bmatrix} C_{11} & C_{12} \\ C_{21} & C_{22} \end{bmatrix}, \\ G(q_N^{(i)}) &= \begin{bmatrix} G_1 & G_2 \end{bmatrix}^T, \\ S_{HS}^T f_{HS}^{(i)} &= \begin{bmatrix} 0 & 0 & F_{(HS,N)}^{(i)} \end{bmatrix}^T \end{aligned}$$

where:

$$\begin{aligned}
 M_{11} &= \begin{bmatrix} M[1,1] & M[1,2] \\ M[2,1] & M[2,2] \end{bmatrix}, \quad M_{12} = \begin{bmatrix} M[1,3] & M[1,4] \\ M[2,3] & M[2,4] \end{bmatrix}, \quad M_{21} = \begin{bmatrix} M[3,1] & M[3,2] \\ M[4,1] & M[4,2] \end{bmatrix}, \quad M_{22} = \\
 &\begin{bmatrix} M[3,3] & M[3,4] \\ M[4,3] & M[4,4] \end{bmatrix}, \\
 C_{11} &= \begin{bmatrix} C[1,1] & C[1,2] \\ C[2,1] & C[2,2] \end{bmatrix}, \quad C_{12} = \begin{bmatrix} C[1,3] & C[1,4] \\ C[2,3] & C[2,4] \end{bmatrix}, \quad C_{21} = \begin{bmatrix} C[3,1] & C[3,2] \\ C[4,1] & C[4,2] \end{bmatrix}, \quad C_{22} = \begin{bmatrix} C[3,3] & C[3,4] \\ C[4,3] & C[4,4] \end{bmatrix}, \\
 G_1 &= \begin{bmatrix} G[1,1] \\ G[2,1] \end{bmatrix}, \quad G_2 = \begin{bmatrix} G[3,1] \\ G[4,1] \end{bmatrix}, \\
 F_{(HS,N)}^{(i)} &= \begin{bmatrix} f_{(HSx,N)}^{(i)} \\ f_{(HSy,N)}^{(i)} \end{bmatrix}.
 \end{aligned}$$

After partitioning all matrices, the model of the underactuated biped in the Swing Phase takes the form of:

$$\begin{aligned}
 M_{11}q_{(a,N)}^{(i)} + M_{12}q_{(na,N)}^{(i)} + C_{11}q_{(a,N)}^{(i)} + C_{12}q_{(na,N)}^{(i)} + G_1 &= u_{(a,N)}^{(i)} \\
 M_{21}q_{(a,N)}^{(i)} + M_{22}q_{(na,N)}^{(i)} + C_{21}q_{(a,N)}^{(i)} + C_{22}q_{(na,N)}^{(i)} + G_2 - F_{(HS,N)}^{(i)} &= 0
 \end{aligned} \tag{4.24}$$

Now we consider the output function

$$y_N^{(i)} = q_{(a,N)}^{(i)}, \tag{4.25}$$

where  $y_N^{(i)}$  is called the collocated output with the input  $u_{(a,N)}^{(i)}$ . Furthermore, due to the fact that  $\det(M_{22}) \neq 0$ ,  $M_{22}$  is invertible, thus we may solve for  $q_{(na,N)}^{(i)}$  in equation (4.24) as:

$$q_{(na,N)}^{(i)} = -M_{22}^{-1}(M_{21}q_{(a,N)}^{(i)} + C_{21}q_{(a,N)}^{(i)} + C_{22}q_{(na,N)}^{(i)} + G_2 - F_{(HS,N)}^{(i)}) \tag{4.26}$$

When substituting (5.26) into (4.24), we get:

$$M_a q_{(a,N)}^{(i)} + C_a q_{(a,N)}^{(i)} + C_{na} q_{(na,N)}^{(i)} + C_a q_{(a,N)}^{(i)} + \tilde{G} + F_{(HS,N)}^{(i)} = u_{(a,N)}^{(i)} \tag{4.27}$$

where:

$$M_a = M_{11} - \frac{M_{21}M_{12}}{M_{22}}, \quad C_a = C_{11} - \frac{M_{12}C_{21}}{M_{22}}, \quad C_{na} = C_{12} - \frac{M_{12}C_{22}}{M_{22}}, \quad \tilde{G} = G_1 - \frac{M_{12}G_2}{M_{22}}, \quad \text{and } F_{(HS,N)}^{(i)} = \frac{M_{12}F_{(HS,N)}^{(i)}}{M_{22}}$$

Since the matrix  $M_a$  is positive definite, we can linearize the actuated configuration of the system dynamics. Thus, the feedback linearization controller is defined for (4.27) and is given by the following relation:

$$M_a v_{(a,N)}^{(i)} + C_a q_{(a,N)}^{(i)} + C_{na} q_{(na,N)}^{(i)} + C_a q_{(a,N)}^{(i)} + \tilde{G} + F_{(HS,N)}^{(i)} = u_{(a,N)}^{(i)} \quad (4.28)$$

where  $v_{(a,N)}^{(i)} \in R^2$  is an additional control input to be defined later. The closed loop system is then given by:

$$\begin{aligned} q_{(na,N)}^{(i)} &= -M_{22}^{-1} (M_{21} q_{(a,N)}^{(i)} + C_{21} q_{(a,N)}^{(i)} + C_{22} q_{(na,N)}^{(i)} + G_2 - F_{(HS,N)}^{(i)}) \\ q_{(a,N)}^{(i)} &= v_{(a,N)}^{(i)} \\ y_N^{(i)} &= q_{(a,N)}^{(i)} \end{aligned} \quad (4.29)$$

Furthermore, it can be seen from (4.29) that the vector of actuated configurations is completely decoupled from the vector of unactuated configurations and linearized second order. We define  $y_{(N,d)}^{(i)} = [y_{(1,N,d)}^{(i)} \ y_{(2,N,d)}^{(i)}]^T = [q_{(1,N,d)}^{(i)} \ q_{(2,N,d)}^{(i)}]^T$  be the vector of reference trajectories and  $e_N^{(i)} = [e_{(1,N)}^{(i)} \ e_{(2,N)}^{(i)}]^T$  the tracking error vector where each component is given by:

$$e_{(j,N)}^{(i)} = q_{(j,N)}^{(i)} - q_{(j,N,d)}^{(i)}, \quad j = 1, 2 \quad (4.30)$$

Now, the additional control input  $v_{(a,N)}^{(i)} \in R^2$  may be chosen by the following relation:

$$v_{(a,j,N)}^{(i)} = y_{(j,N,d)}^{(i)} - K_{pj} e_{(j,N)}^{(i)} - K_{vj} \dot{e}_{(j,N)}^{(i)}, \quad j = 1, 2 \quad (4.31)$$

where coefficients  $K_{pj}$ ,  $K_{vj}$ ,  $j = 1, 2$  are chosen so that the two polynomials  $\ddot{s} - K_{pj}s - K_{vj}\dot{s}$ ,  $j = 1, 2$  are Hurwitz. Then the error system dynamics can be given by:

$$\ddot{e}_N^{(i)} = v_{(a,N)}^{(i)} - y_{(N,d)}^{(i)} \quad (4.32)$$

where each component of (4.32) is given by:

$$e_{(j,N)}^{\ddot{}} = -K_{pj}e_{(j,N)}^{(i)} - K_{vj}e_{(j,N)}^{\dot{}} \quad (4.33)$$

From (4.33), we can clearly see that for a suitable choice of the abovementioned coefficients, the error tracking vector converges globally exponentially to zero. Let  $Z_1 = e_N^{(i)}$ ,  $Z_2 = e_N^{\dot{}}$ ,  $\eta_1 = q_{(na,N)}^{(i)} = [q_{(3,N)}^{(i)} \ q_{(4,N)}^{(i)}]$ ,  $\eta_2 = q_{(na,N)}^{\dot{}} = [q_{(3,N)}^{\dot{}} \ q_{(4,N)}^{\dot{}}]$ . Thus, the complete closed loop system can be written as :

$$\begin{aligned} \dot{Z}_1 &= Z_2 \\ \dot{Z}_2 &= -K_p Z_1 - K_d Z_2 \\ \dot{\eta}_1 &= \eta_2 \\ \dot{\eta}_2 &= \Omega(Z, \eta, t^{(i)}) \\ e_N^{(i)} &= y_N^{(i)} - y_{(N,d)}^{(i)} = Z_t \end{aligned} \quad (4.34)$$

where:

$$\Omega(Z, \eta, t^{(i)}) = -M_{22}^{-1}(C_{21}q_{(a,N)}^{\dot{}} + G_2 - F_{(HS,N)}^{(i)}) - M_{22}^{-1}C_{22}\eta_2 - M_{22}^{-1}M_{21}(y_{(N,d)}^{\ddot{}} - K_p Z_1 - K_v Z_2) \quad (4.35)$$

$$\text{where } K_p = \begin{bmatrix} K_{p1} & 0 \\ 0 & K_{p2} \end{bmatrix} \text{ and } K_v = \begin{bmatrix} K_{v1} & 0 \\ 0 & K_{v2} \end{bmatrix}.$$

In matrix form, the system (4.34) can be rewritten as:

$$\begin{aligned} \dot{Z} &= AZ \\ \dot{\eta} &= w(Z, \eta, t^{(i)}) \\ e_N^{(i)} &= CZ \end{aligned} \quad (4.36)$$

$$\text{where } Z = \begin{bmatrix} Z_1 \\ Z_2 \end{bmatrix}, \eta = \begin{bmatrix} \eta_1 \\ \eta_2 \end{bmatrix}, A = \begin{bmatrix} 0 & I_{2 \times 2} \\ -K_p & -K_v \end{bmatrix}, C = \begin{bmatrix} I_{2 \times 2} & 0 \end{bmatrix} \text{ and } w(Z, \eta, t^{(i)}) = \begin{bmatrix} \eta_2 \\ \Omega(Z, \eta, t^{(i)}) \end{bmatrix}.$$

### 4.3 Velocity and Disturbance Observers for Estimation of Velocity Signals and Disturbances

Up to this point we have assumed that there are no disturbances to the biped and that the velocity signals are available. The above controllers (Computed Torque Control, Partial Feedback Linearization Control) cannot be practically implemented since the velocity is required. In addition, when uncertainties exist, these controllers can only drive the system output to a neighborhood of the desired trajectory. However, as we have mentioned earlier, real systems experience disturbances (e.g. actuator friction, uncertainty in the parameters of the system model) and the sensors for velocity measurements are often contaminated with a considerable amount of noise. Now, we will implement velocity and disturbance observers which estimate the disturbances and reconstruct the missing velocity signals. Thus, in the equations of motion of the Swing, Instantaneous Push-Off and Heel Strike Phases we add a disturbance quantity  $d(q, \dot{q}, t)$ . In addition, in the abovementioned relations of the Computed Torque and Partial Feedback Linearization controllers, we replace the velocity  $\dot{q}$  with its estimation,  $\tilde{\dot{q}}$  and we also add a component for the estimation of the disturbance,  $\tilde{d}(q, \tilde{\dot{q}}, t)$ :

The Complete Control Law for the Swing Phase (based on Partial Feedback Linearization Control and the velocity and disturbance observers):

$$M_a v_{(a,k)}^{(i)} + C_a \tilde{\dot{q}}_{(a,k)}^{(i)} + C_{na} \tilde{\dot{q}}_{(na,k)}^{(i)} + C_a \tilde{\dot{q}}_{(a,k)}^{(i)} + \tilde{G} + F_{(con,k)}^{(i)} + \tilde{d}(q_{(a,k)}^{(i)}, \tilde{\dot{q}}_{(a,k)}^{(i)}, t_k^{(i)}) = u_{(a,k)}^{(i)}, \quad k = 1, \dots, N-2. \quad (4.37)$$

The Complete Control Law for the Push-Off Phase (based on Computed Torque Control and the velocity and disturbance observers):

$$u_{N-1}^{(i)} = M(q_{(N-1)}^{(i)})(q_{(N-1,d)}^{(i)} - K_v \tilde{e}_{N-1}^{(i)} - K_p e_{N-1}^{(i)}) + C(q_{N-1}^{(i)}, \tilde{\dot{q}}_{N-1}^{(i)}) \tilde{\dot{q}}_{N-1}^{(i)} + G(q_{N-1}^{(i)}, \theta^{(i)}) - S_{con}^T f_{(con,N-1)}^{(i)} + \tilde{d}(q_{N-1}^{(i)}, \tilde{\dot{q}}_{N-1}^{(i)}, t_{N-1}^{(i)}), \text{ where } \tilde{e}_{N-1}^{(i)} = \tilde{\dot{q}}_{N-1}^{(i)} - \dot{q}_{N-1,d}^{(i)}, \quad (4.38)$$

The Complete Control Law for the Heel Strike Phase (based on Partial Feedback Linearization

Control and the velocity and disturbance observers):

$$M_a v_{(a,N)}^{(i)} + C_a \dot{\tilde{q}}_{(a,N)}^{(i)} + C_{na} \dot{\tilde{q}}_{(na,N)}^{(i)} + C_a \dot{\tilde{q}}_{(a,N)}^{(i)} + \tilde{G} + F_{(HS,N)}^{(i)} + \tilde{d}(q_{(a,N)}^{(i)}, \dot{\tilde{q}}_{(a,N)}^{(i)}, t_N^{(i)}) = u_{(a,N)}^{(i)} \quad (4.39)$$

The velocity estimation  $\dot{\tilde{q}}$  is obtained by the following velocity observer:

$$\begin{aligned} \dot{\tilde{q}} &= z + Lq \\ \dot{z} &= \ddot{q}_d - L\dot{\tilde{q}} + M^{-1}K_p E \end{aligned} \quad (4.40)$$

and the disturbance estimation  $\tilde{d}$  is obtained from the following disturbance observer

$$\begin{aligned} \dot{\tilde{d}} &= p - \Phi \dot{\tilde{q}} \\ \dot{p} &= \Phi(\ddot{q}_d + K_p E) \end{aligned} \quad (4.41)$$

where  $\dot{\tilde{q}}$  represents the estimated velocity,  $z, p$  are the velocity and disturbance observer states respectively,  $\Phi = \phi I_n$  and  $L = lI_n$  are the disturbance and velocity observer gain matrices respectively (diagonal positive definite matrices), where  $l, \phi > 0$  and  $I_n \in R^{n \times n}$  is an identity matrix.

To proceed with the development, the following assumptions are required:

1. The disturbance varies slowly relative to the observer dynamics. Thus, it is reasonable to suppose that  $\dot{d} = 0$ . Since, in general there is no prior information about the derivative of the disturbance  $d$ . Moreover, this assumption is recurrent in the literature on control of robots.
2. The robot velocity is bounded by a known constant  $V_m$  such that  $\|\dot{q}\| \leq V_m, \forall t \in R$ . This assumption is definitely realistic. In fact, it is reasonable to expect that the joint velocities of a robot will not exceed certain apriori bounds that come from the mechanic limitations of the robot and/or from the way the robot operates.

The following theorem can be proved:

**Theorem** Consider the robot dynamics, and let Assumptions 1 and 2 be satisfied. Applying the control laws (4.37-4.39), where the velocity estimation  $\dot{\tilde{q}}$  is obtained from (4.40), and the disturbance estimation  $\tilde{d}$  is obtained from (4.41). The closed - loop system under the

nonlinear controllers (CTC,PFL) and the velocity and disturbance observers, is semi-globally asymptotically stable, in the sense that for an initial state within the region of attraction given by:

$$B = \{y \in R^{3n} \|y\| < \sqrt{\frac{q_m}{q_M} \left( \frac{\sqrt{2K_{vm}(M_m L_m - K_{vM})}}{c_m} - 2V_m \right)}\} \quad (4.42)$$

we have

$$\lim_{t \rightarrow \infty} E(t) = \lim_{t \rightarrow \infty} \dot{E}(t) = 0 \quad (4.43)$$

and

$$\lim_{t \rightarrow \infty} \tilde{q}(t) = 0 \quad (4.44)$$

and

$$\lim_{t \rightarrow \infty} E_d(t) = 0 \quad (4.45)$$

if the following conditions are satisfied:

$$L_m > \left( \frac{9}{2} \frac{(C_m V_m)^2}{K_{vm}} + K_{vM} \right) M_m^{-1},$$

$$L_m > \left( K_{vM} + \frac{(\phi_M)^2}{\phi_{\min}} \right) M_m^{-1}$$

where  $y^T = [\dot{E}^T \ \tilde{q}^T \ E^T \ (F - E_d)^T]$ ,  $\tilde{q} = \dot{q} - q\mu$  is diagonal positive definite matrix, with  $K_p > \mu$ ,  $K_{vM} = \|K_v\|$ ,  $K_{pM} = \|K_p\|$  and  $\phi_M = \|\phi\|$ .  $L_m, \mu_m, K_{vm}, K_{pm}$  and  $\phi_{\min}$  denote the minimum eigenvalue of  $L, \mu, K_v, K_p$  and  $\phi$ , respectively.  $q_M = \lambda_{\max}(Q) = \max\{M_M, K_{pM}, \mu_M\}$  and  $q_m = \lambda_{\min}(Q) = \min\{M_m, K_{pm}, \mu_m\}$ .  $F$  is a vector to be determined.

# Chapter 5

## Simulation & Results

### 5.1 Introduction

In the current section we will proceed with the simulation experiments of the two variants (Direct Collocation & Discrete Mechanics) of the proposed system. We will test our 4-DOF Biped Robot on different terrains, including flat ground, upward and downward slopes, and a combination of flat ground with upward and downward stairs, in order to check the energy efficiency, robustness, and smoothness of gait along various terrain variations. In addition, we will compare the results of the proposed system with two alternative problem solving methods:

1. Solving the Gait Generation Problem for the complete, 4-DOF Biped Robot directly (One Phase approach using the two variants). In other words, we will solve the Gait Generation Problem of the Second Phase directly, without involving a preliminary First Phase. The initial conditions of the First Phase are also initial conditions of the Second Phase.
2. Using a commercial high-performance solver, called SNOPT. SNOPT, (for Sparse Non-linear OPTimizer), is a software package for solving large-scale nonlinear optimization problems written by Philip Gill, Walter Murray and Michael Saunders. SNOPT is mainly written in Fortran, but interfaces to C, C++, Python and MATLAB are available. It employs a sparse sequential quadratic programming (SQP) algorithm with limited-memory

quasi-Newton approximations to the Hessian of Lagrangian. It is especially effective for nonlinear problems with functions and gradients that are expensive to evaluate. The functions should be smooth but need not be convex. SNOPT is used in several trajectory optimization software packages, including AeroSpace Trajectory Optimization and Software (ASTOS), General Mission Analysis Tool, and Optimal Trajectories by Implicit Simulation (OTIS). It also uses parallel cores for high performance computing.

The list of parameters used throughout the experiments are given below:

Parameters	Values
<b>M (kg)</b>	[10, 120]
<b>m1 = m2 (kg)</b>	[0.2*M, 0.5*M]
<b>l (m)</b>	[0.5, 2]
<b>a (m)</b>	[0.4*l, 0.8*l]
<b>b (m)</b>	[0.2*l, 0.6*l]
<b>Dstep (m)</b>	[0.3*l, 2*l]
<b>Hstep (m)</b>	[0.3*l, 1.5*l]
<b>Lstep (m)</b>	[0.3*l, 2*l]
<b><math>\tau</math> (Nm)</b>	[-500,500]
<b>f_con (N)</b>	[0, 3*Mg]
<b>F_PO (Ns)</b>	[0, 200]
<b>q (rad)</b>	$[-\pi/2, \pi]$
<b><math>\theta</math> (rad)</b>	[-1.13, 1.13]
<b><math>\dot{q}</math> (rad/s)</b>	[-6, 6]
<b>g (m/s<sup>2</sup>)</b>	9.81
<b>Kp</b>	diag {7000,7000}
<b>Kv</b>	diag {50,50}
<b><math>\Phi</math></b>	diag {50,50}
<b>L</b>	diag {3000,3000}
<b>Square Root Smoothing Error Parameter <math>\epsilon</math></b>	0.1

Figure 5.1: *Simulation Parameters.*

Regarding the square root smoothing error parameter  $\epsilon$ , two different  $\epsilon = 1, 0.1$  are used for smoothing (see Chapter 3.6). In fact, decreasing  $\epsilon$  by 10 reduces the COT by only about 2.8%

with small changes in the value, but we have the same qualitative behavior, of gait parameters. Due to the negligible differences, only those results produced by  $\epsilon = 0.1$  are presented.

Furthermore, as a disturbance we will use the steady state actuator friction model, which is the sum of Coulomb, static, viscous and Stribeck friction:

$$D(\dot{q}_j^{(i)}) = F_{cj} + (F_{sj} - F_{cj})e^{-\left(\frac{\dot{q}_j^{(i)}}{v_{sj}}\right)^n} + f_{vj}\dot{q}_j^{(i)}, \quad j = 1, \dots, 4$$

where:

1.  $D(\dot{q}_j^{(i)})$  is the disturbance applied at the  $j - th$  generalized coordinate,
2.  $F_{cj}$  is the Coulomb friction at the  $j - th$  generalized coordinate. Coulomb friction is a constant friction force (does not vary with the magnitude of the velocity) and represents friction associated with mechanical surfaces rubbing together and includes bearing friction, and so on,
3.  $F_{sj}$  is the static friction at the  $j - th$  generalized coordinate. Static friction is observed immediately before there is a slide of the contacting surfaces,
4.  $f_{vj}$  is the viscous friction coefficient at the  $j - th$  generalized coordinate. Viscous friction represents the force required to push hydraulic (viscous) fluid through restrictive passages. This would include the force required (or used) for leakage or to push fluid through any small passages that may exist in the actuator. Viscous friction is small at low velocity and increases linearly with piston velocity,
5.  $v_{sj}$  is the Stribeck velocity at the  $j - th$  generalized coordinate, and it is related to the velocity range of the negative resistance regime,
6.  $n$  is the exponent that affects the slope of the Stribeck curve, and
7.  $\dot{q}_j^{(i)}$  is the angular or linear velocity.

## 5.2 Forward Walking Experiment

In the current simulation we let the 4-DOF Biped walk forwards. The related parameters of the particular experiment are given below:

1.  $H = 11$  walking steps,
2.  $M = 40kg$ ,
3.  $m_1 = m_2 = 20kg$ ,
4. The duration of a walking step : 0.7343 seconds,
5.  $a = b = 0.5m, l = 1m$ ,
6.  $D_1 = 0.6m, D_2 = 0.8m, D_3 = 1m, D_4 = 1.4m, D_5 = 1.7m, D_6 = 1.9m, D_7 = 1.6m, D_8 = 1.3m, D_9 = 1.1m, D_{10} = 0.8m, D_{11} = 0.6m$ ,
7. Initial conditions:  $q_1 = 0.2187rad, q_2 = -0.2187rad, \dot{q}_1 = -1.0924rad/s, \dot{q}_2 = -0.3774rad/s, q_3 = 0m, q_4 = 0m, \dot{q}_3 = 0m/s, \dot{q}_4 = 0m/s$ ,
8. For the disturbances, we use the following parameter values:  $F_{c1} = F_{c2} = 6 Nm, F_{c3} = F_{c4} = 5h^{(i)} Ns, f_{v1} = f_{v2} = 8 Nm/(rad/s), F_{v3} = F_{v4} = 6h^{(i)} Ns/(m/s), F_{s1} = F_{s2} = 10 Nm, F_{s3} = F_{s4} = 5h^{(i)} Ns, v_{s1} = v_{s2} = 0.19 rad/s, v_{s3} = v_{s4} = 0.03 m/s$ .

In Figure 5.2, we show the overall results of the Forward Walking experiment. More specifically, we show the Average Cost Of Transport ( $\frac{1}{H} \sum_{i=1}^H COT^{(i)}$ ) of the H=11 desired trajectories of the biped, subject to the number of points/time steps (N) that approximate the desired trajectory of each walking step, for all the abovementioned Gait Generation Problem solving approaches. The red coloured results indicate the minimum Average Cost Of Transport (lower is better) achieved by a particular method. We have verified the results by reconducting the experiment numerous times, proving the convergence of the results to the values of the Figure.

As we can see, the Decrease & Conquer Approach is extremely effective:

<i>Average Cost of Transport (ACOT) for the Forward Walking Experiment</i>					
	One Phase		SNOPT	Decrease and Conquer - 2 Phases	
N (points)	Discrete Mechanics	Direct Collocation	commercial package	Discrete Mechanics	Direct Collocation
10	1.21	1.18	1.13	0.9246	0.9135
20	0.95	0.908	0.87	0.8005	0.7969
30	0.84	0.8215	0.813	0.6935	0.6635
40	0.77	0.7543	0.7168	0.5315	0.5267
50	0.693	0.6745	0.6531	0.4763	0.445
60	0.6458	0.6299	0.6003	0.3485	0.3185
70	0.5935	0.5635	0.5415	0.2565	0.2214
80	0.5321	0.5035	0.4731	0.1541	0.1235
90	0.4935	0.4765	0.4415	0.0935	0.0695
100	0.4467	0.4219	0.4135	0.0814	0.0695
110	0.4135	0.3941	0.3615	0.0814	0.0695
120	0.3905	0.3743	0.3315	0.0814	0.0695
130	0.3749	0.3653	0.3158	0.0814	0.0695
140	0.3698	0.3615	0.3041	0.0814	0.0695
150	0.3698	0.3615	0.2958	0.0814	0.0695
160	0.3698	0.3615	0.2217	0.0814	0.0695
170	0.3698	0.3615	0.1935	0.0814	0.0695
180	0.3698	0.3615	0.1875	0.0814	0.0695

Figure 5.2: *Average Cost of Transport (ACOT) for the Forward Walking Experiment.*

1. Regarding the One Phase based Methods, Discrete Mechanics needs at least 140 points to achieve an ACOT of 0.3698, while Direct Collocation needs at least the same number of points (140) to achieve an ACOT of 0.3615.
2. Regarding the commercial package SNOPT, it needs at least 180 points to achieve an ACOT of 0.1875.
3. Regarding the Decrease & Conquer based Methods, Discrete Mechanics need only 100 points to achieve an ACOT of 0.0814, while Direct Collocation needs only 90 points to achieve an ACOT of 0.0695. Thus, the Decrease & Conquer approach achieves the lowest possible values of energy consumption (subject to each variant) for the Forward Walking experiment.

In Figure 5.3, we show the lower and upper bounds of the Cost of Transport that observed throughout the abovementioned Forward Walking Experiment, subject to the various tested solving methods. This is to prove that, during the experiment and particularly for the proposed approach, there were not any extremely high values of COT that were averaged with smaller ones, but the resulted values were in the domain of the minimal possible ACOT for each tested approach.

<i>Lower and Upper Bounds of Cost of Transport (COT) for the Forward Walking Experiment</i>				
<b>One Phase</b>		<b>SNOPT</b>	<b>Decrease and Conquer - 2 Phases</b>	
<b>Discrete Mechanics</b>	<b>Direct Collocation</b>	<b>commercial package</b>	<b>Discrete Mechanics</b>	<b>Direct Collocation</b>
<b>[0.95 - 1.22]</b>	<b>[0.96-1.33]</b>	<b>[0.97 - 1.18]</b>	<b>[0.90 - 1.05]</b>	<b>[0.91-1.04]</b>
<b>*ACOT</b>	<b>*ACOT</b>	<b>*ACOT</b>	<b>*ACOT</b>	<b>*ACOT</b>

Figure 5.3: *Lower and Upper Bounds of Cost of Transport (COT) for the Forward Walking Experiment.*

In Figure 5.4, the energy savings of the Decrease & Conquer based Methods, in comparison with the One-Phase based ones, are shown.

As we can see, the Decrease & Conquer based Discrete Mechanics Method achieves energy savings between 15.74% (for  $N = 20$ ) - 81.78% (for  $N = 100$ ), in comparison with the One Phase based related Method, while the Decrease & Conquer based Direct Collocation Method achieves energy savings between 12.24% (for  $N = 20$ ) - 85.41% (for  $N = 90$ ), in comparison with the One Phase based related Method.

In Figure 5.5, the energy savings of the Decrease & Conquer based Methods, in comparison with SNOPT, are shown.

As we can see, the Decrease & Conquer based Discrete Mechanics Method achieves energy savings between 7.99% (for  $N = 20$ ) - 80.31% (for  $N = 100$ ), in comparison with SNOPT, while the Decrease & Conquer based Direct Collocation Method achieves energy savings between 8.4% (for  $N = 20$ ) - 84.26% (for  $N = 90$ ), in comparison with it.

<i>Energy Savings of Decrease and Conquer Variants Vs One Phase Related Variants, for the Forward Walking Experiment (Percentage)</i>		
<b>N (points)</b>	<b>Discrete Mechanics</b>	<b>Direct Collocation</b>
10	23,59	22,58
20	15,74	12,24
30	17,44	19,23
40	30,97	30,17
50	31,27	34,03
60	46,04	49,44
70	56,78	60,71
80	71,04	75,47
90	81,05	85,41
100	81,78	83,53
110	80,31	82,36
120	79,15	81,43
130	78,29	80,97
140	77,99	80,77
150	77,99	80,77
160	77,99	80,77
170	77,99	80,77
180	77,99	80,77

Figure 5.4: *Energy Savings of Decrease and Conquer Variants in comparison with One Phase Related Variants, for the Forward Walking Experiment (Percentage).*

Now we will show the plots of the 4-DOF biped robot, for  $N=100$ , which is the number of points where the Decrease & Conquer Feedback Control utilizing Direct Collocation Method achieves the lowest possible ACOT in the Forward Walking Experiment. Due to the fact that the Decrease & Conquer Feedback Control utilizing Discrete Mechanics Method results in similar results, only the results of the First Approach will be presented.

Next, the actual plots of the 4-DOF Biped Robot, will be shown, under missing velocity signals and disturbances. In addition, we assume that Leg 2 initially starts the walking process, thus it is the swing leg for the first walking step. In Figure 5.6, the plots of desired and actual angles of the two Legs over time are shown. In addition, in Figures 5.7 and 5.8, the plots of the position errors over time are depicted.

From Figure 5.6, at each walking step, it can be seen that the angular displacement of the swing leg gradually increases over time. Some moments before the completion of each walking step (Heel Strike Moment), the angular displacement of the swing leg reaches the maximum, and then the swing leg swings back. When human stride reaches the maximum during walking,

<b>Energy Savings of Decrease and Conquer Variants Vs SNOPT, for the Forward Walking Experiment (Percentage)</b>		
<b>N (points)</b>	<b>Discrete Mechanics</b>	<b>Direct Collocation</b>
10	18,18	19,16
20	7,99	8,4
30	14,7	18,39
40	25,85	26,52
50	27,07	31,86
60	41,95	46,94
70	52,63	59,11
80	67,43	73,9
90	78,82	84,26
100	80,31	83,19
110	77,48	80,77
120	75,44	79,03
130	74,22	77,99
140	73,23	77,15
150	72,48	76,5
160	63,28	68,65
170	57,93	64,08
180	56,59	62,93

Figure 5.5: *Energy Savings of Decrease and Conquer Variants in comparison with SNOPT, for the Forward Walking Experiment (Percentage).*

a swinging back process also occurs, which is consistent with the mechanism of the human movement. The angular displacement of the stance leg monotonically decreases, and when  $t=0.7343$  sec (Heel Strike Moment), the swing leg is in collision with the ground and the two legs switch roles. As the step length increases, the values of the angular displacements increase and vice versa.

Furthermore, the desired and actual angular displacements of the two legs are nearly the same. From Figure 5.7 and 5.8, we can see that the position errors are extremely low ( $\approx 10^{-4}$ ), showing the effectiveness of the implemented trajectory tracking control.

In Figure 5.9, the plot of real and estimated angular velocities of the two legs over time is shown. In addition, in Figures 5.10 and 5.11, the plots of the velocity errors over time are depicted.

Based on Figures 5.9, 5.10 and 5.11, the real and estimated angular velocities of the two legs are nearly the same. From Figure 5.10 and 5.11, we can see that the velocity errors are extremely low ( $\approx 10^{-4}$ ), showing again the effectiveness of the trajectory tracking control. As the step

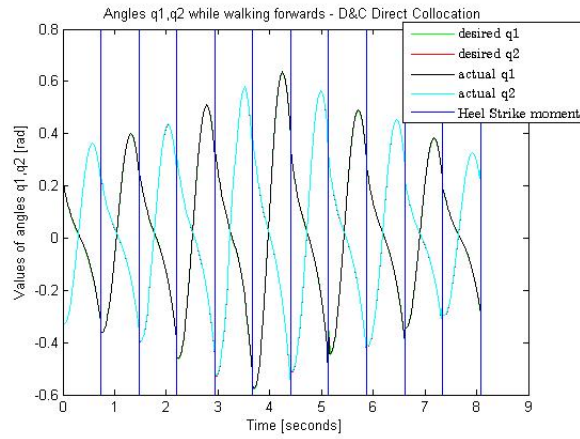


Figure 5.6: *Desired and actual angles during the Forward Walking Experiment - Decrease & Conquer Feedback Control utilizing Direct Collocation.*

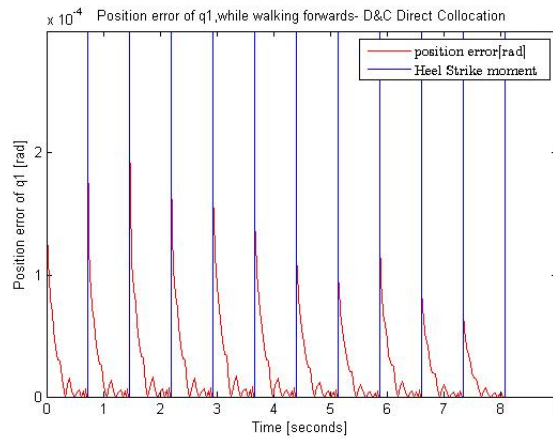


Figure 5.7: *Position error during the Forward Walking Experiment - Decrease & Conquer Feedback Control utilizing Direct Collocation.*

length increases, the values of the angular velocities increase and vice versa.

In Figure 5.12, the control signals of the swing and stance leg over time during the Forward Walking Experiment are shown. We can see that at the beginning of each walking step, a larger torque should be input to the robot to realize dynamic walking, and with the input of the torque, the kinetic and potential energy are reasonably converted into driving energy; thereafter, only a small energy input can complete a walking step. The impact of the small inaccuracies on the estimation of the velocity signals and disturbances is an increase of ACOT by just 0.5%.

In Figure 5.13, the plot of Ground Reaction Forces (Vertical component: Normal Force, and horizontal component: Friction force) experienced during the Forward Walking Experiment,

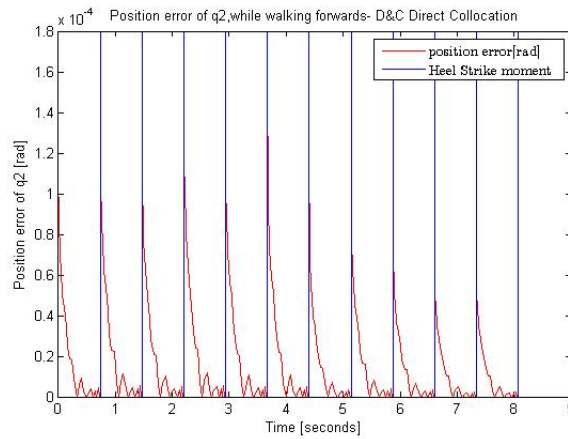


Figure 5.8: *Position error during the Forward Walking Experiment - Decrease & Conquer Feedback Control utilizing Direct Collocation.*

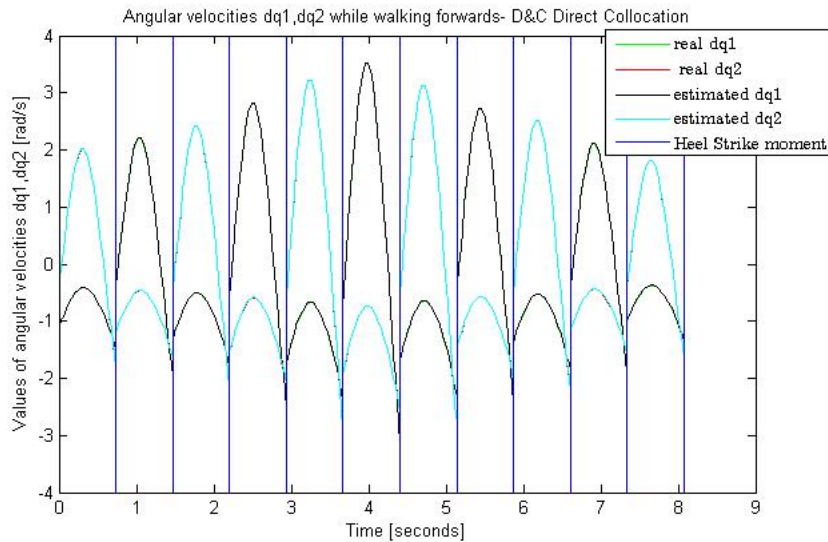


Figure 5.9: *Real and estimated angular velocities during the Forward Walking Experiment - Decrease & Conquer Feedback Control utilizing Direct Collocation.*

are shown. In biomechanics, that plot is called butterfly diagram, due to the fact that the two peaks of the Normal Force look like the wings of a butterfly. As the step length increases, the values of the Ground Reaction Forces increase and vice versa.

More specifically, in the first moment (time step) of each walking step, the new stance leg, due to the experienced Heel Strike Forces a moment before, tries to adjust posture to support dynamic walking, resulting in higher torque and thus leading to the first peak of the Normal Force. From the next time step till the 25 % of the walking step, the Normal Force is decreasing, due to the adjusted posture of the stance leg, leading to a smaller required torque to keep balancing.

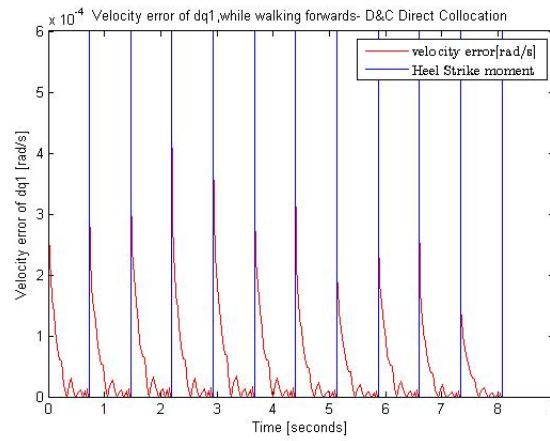


Figure 5.10: *Angular velocity errors of the Leg 1 during the Forward Walking Experiment - Decrease & Conquer Feedback Control utilizing Direct Collocation.*

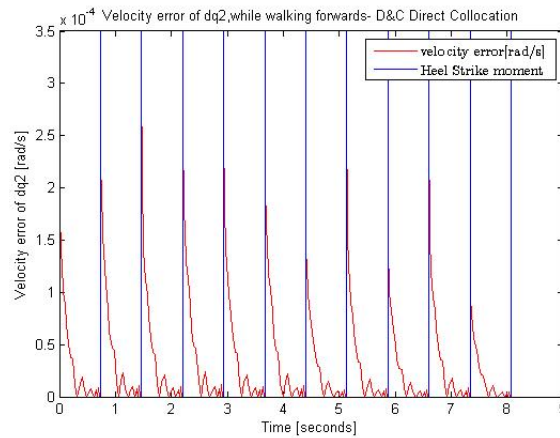


Figure 5.11: *Angular velocity errors of the Leg 2 during the Forward Walking Experiment - Decrease & Conquer Feedback Control utilizing Direct Collocation.*

From that moment till the 50% of the walking step, we have an increase in the Normal Force, due to the fact that the stance leg becomes more vertical with the ground and at the half of the walking step the stance leg is completely vertical with it, supporting the whole weight of the robot, and resulting in the second peak of the Normal Force (this intermediate phase of the walking step is called midstance phase). From that moment till the end of the walking step, the Normal Force is decreasing (and it approaches zero), as the stance leg tends to be less vertical with the ground and the swing leg tends to approach the ground, taking an actual role for the support of the robot weight, both preparing to switch roles after the effects of the Push-Off and Heel Strike Phases. The Normal Force, throughout the entire walking step, is positive.

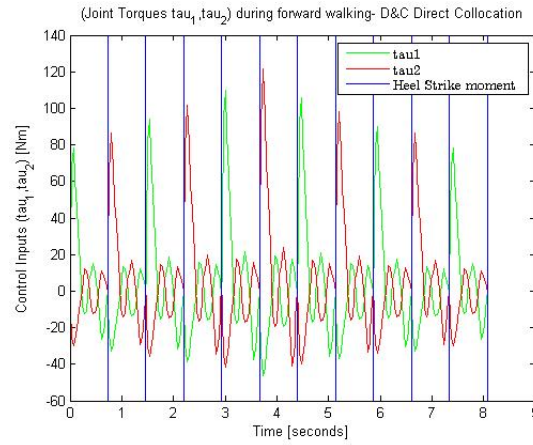


Figure 5.12: Control Signals  $\tau_1$ ,  $\tau_2$  during the Forward Walking Experiment - Decrease & Conquer Feedback Control utilizing Direct Collocation.

Regarding the values of the Friction Force, from the first time step of a walking step till the 10% of it, the friction force is decreasing and negative (at the 10% of the walking step we have a negative peak of the Friction force), due to the braking direction of the stance leg, resulting the Friction Force to act a backward (negative) force. From that moment till the 50% of the walking step, as we approach the midstance phase, the Friction Force is increasing (at the 50% of the walking step we have a positive peak of the Friction Force) as the stance leg becomes more vertical with the ground and tends to move in a more propulsive direction. From the 50% of the walking step, till the completion of it, the stance leg keeps its propulsive direction, and waits for the Push-Off and Heel Strike Phases to take effect and switch roles with the swing leg, thus the friction force tends to zero.

In Figure 5.14, the Instantaneous Push-Off Impulses applied during the Forward Walking experiment, are shown. A Push-Off Impulse, as we have mentioned in previous Chapters, is required for the stance leg to be detached from the ground, while adding the required energy for the biped robot to be stabilized after the energy losses of the Heel Strike Phase. As the step length increases, the values of the Push-Off Impulse increase and vice versa.

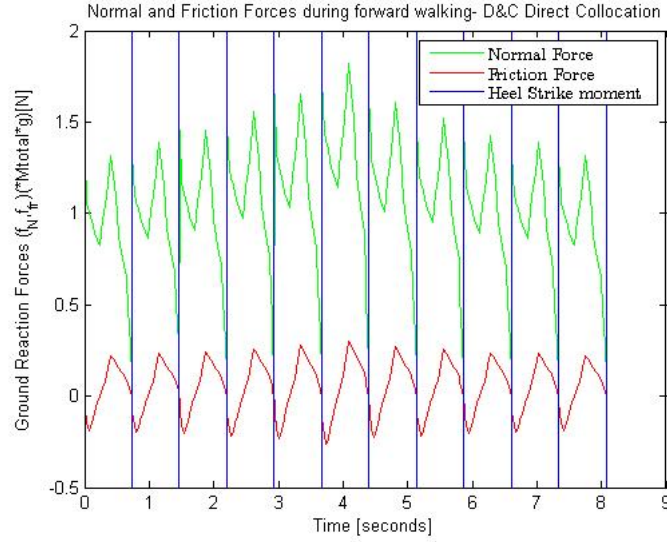


Figure 5.13: *Ground Reaction Forces during the Forward Walking Experiment - Decrease & Conquer Feedback Control utilizing Direct Collocation.*

### 5.3 Downward Slope Walking Experiment

In the current simulation we let the 4-DOF Biped walk on a downward slope. The related parameters of the particular experiment are given below:

1.  $H = 11$  walking steps,
2.  $M = 60kg$ ,
3.  $m_1 = m_2 = 30kg$ ,
4. The duration of a walking step : 0.7343 seconds,
5.  $a = b = 0.75m, l = 1.5m$ ,
6.  $\theta = -0.677$  rad (-38.8 deg)
7.  $D_1 = 2.8m, D_2 = 2.6m, D_3 = 2.3m, D_4 = 2.15m, D_5 = 1.95m, D_6 = 1.8m, D_7 = 1.75m, D_8 = 1.35m, D_9 = 1.15m, D_{10} = 1.05m, D_{11} = 0.6m$ ,
8. Initial conditions:  $q_1 = 0.4330rad, q_2 = -0.4330rad, \dot{q}_1 = -2.162rad/s, \dot{q}_2 = -0.7472rad/s, q_3 = 0m, q_4 = 0m, \dot{q}_3 = 0m/s, \dot{q}_4 = 0m/s$ ,

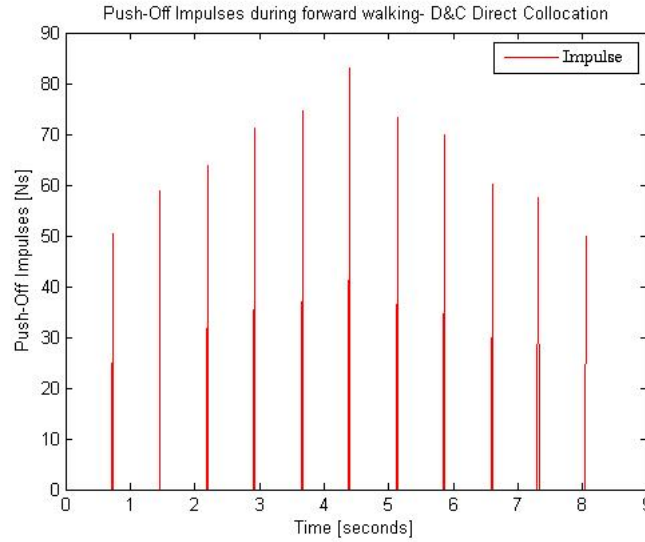


Figure 5.14: *Push-Off Impulses during the Forward Walking Experiment - Decrease & Conquer Feedback Control utilizing Direct Collocation.*

9. For the disturbances, we use the following parameter values:  $F_{c1} = F_{c2} = 7 \text{ Nm}$ ,  $F_{c3} = F_{c4} = 6h^{(i)} \text{ Ns}$ ,  $f_{v1} = f_{v2} = 9 \text{ Nm}/(\text{rad}/\text{s})$ ,  $F_{v3} = F_{v4} = 7h^{(i)} \text{ Ns}/(\text{m}/\text{s})$ ,  $F_{s1} = F_{s2} = 11 \text{ Nm}$ ,  $F_{s3} = F_{s4} = 6h^{(i)} \text{ Ns}$ ,  $v_{s1} = v_{s2} = 0.21 \text{ rad}/\text{s}$ ,  $v_{s3} = v_{s4} = 0.07 \text{ m}/\text{s}$ .

In Figure 5.15, we show the overall results of the Downward Slope Walking experiment. More specifically, we show the Average Cost Of Transport ( $\frac{1}{H} \sum_{i=1}^H \text{COT}^{(i)}$ ) of the  $H=11$  desired trajectories of the biped, subject to the number of points/time steps ( $N$ ) that approximate the desired trajectory of each walking step, for all the abovementioned Gait Generation Problem solving approaches. The red coloured results indicate the minimum Average Cost Of Transport (lower is better) achieved by a particular method. We have verified the results by reconducting the experiment numerous times, proving the convergence of the results to the values of the Figure.

As we can see, the Decrease & Conquer Approach is extremely effective:

1. Regarding the One Phase based Methods, Discrete Mechanics needs at least 160 points to achieve an ACOT of 0.1922, while Direct Collocation needs at least the same number of points (140) to achieve an ACOT of 0.1734.
2. Regarding the commercial package SNOPT, it needs at least 170 points to achieve an

Average Cost of Transport for the Downwards Walking Experiment					
N (points)	One Phase		SNOPT	Decrease and Conquer - 2 Phases	
	Discrete Mechanics	Direct Collocation	commercial package	Discrete Mechanics	Direct Collocation
10	1.023	0.987	0.9142	0.8432	0.8166
20	0.9758	0.9415	0.8835	0.7944	0.7432
30	0.9315	0.9184	0.8399	0.6871	0.6532
40	0.8765	0.8435	0.7635	0.5732	0.5144
50	0.8132	0.7941	0.7131	0.4432	0.4005
60	0.7432	0.7288	0.6922	0.3167	0.3011
70	0.6915	0.67342	0.6432	0.2458	0.2117
80	0.6284	0.5977	0.5977	0.1667	0.1235
90	0.5974	0.5632	0.5132	0.0762	0.0532
100	0.5103	0.4858	0.4341	0.0762	0.0532
110	0.4703	0.4492	0.3988	0.0762	0.0532
120	0.4432	0.4198	0.3321	0.0762	0.0532
130	0.3784	0.3462	0.2814	0.0762	0.0532
140	0.2829	0.2732	0.2191	0.0762	0.0532
150	0.2144	0.1932	0.1432	0.0762	0.0532
160	0.1922	0.1734	0.1298	0.0762	0.0532
170	0.1922	0.1734	0.1024	0.0762	0.0532
180	0.1922	0.1734	0.1024	0.0762	0.0532

Figure 5.15: Average Cost of Transport (ACOT) for the Downward Slope Walking Experiment.

ACOT of 0.1024.

- Regarding the Decrease & Conquer based Methods, Discrete Mechanics need only 90 points to achieve an ACOT of 0.0762, while Direct Collocation needs only 90 points also to achieve an ACOT of 0.0532. Thus, the Decrease & Conquer approach achieves the lowest possible values of energy consumption (subject to each variant) for the Downward Slope Walking experiment.

In Figure 5.16, we show the lower and upper bounds of the Cost of Transport that observed throughout the abovementioned Downward Slope Walking Experiment, subject to the various tested solving methods. This is to prove that, during the experiment and particularly for the proposed approach, there were not any extremely high values of COT that were averaged with smaller ones, but the resulted values were in the domain of the minimal possible ACOT for

each tested approach.

<i>Lower and Upper Bounds of Cost of Transport (COT) for the Downwards Walking Experiment</i>				
<b>One Phase</b>		<b>SNOPT</b>	<b>Decrease and Conquer - 2 Phases</b>	
<b>Discrete Mechanics</b>	<b>Direct Collocation</b>	<b>commercial package</b>	<b>Discrete Mechanics</b>	<b>Direct Collocation</b>
<b>[0.93 - 1.28]</b>	<b>[0.98-1.36]</b>	<b>[0.95 – 1.2]</b>	<b>[0.92 – 1.05]</b>	<b>[0.93-1.04]</b>
<b>*ACOT</b>	<b>*ACOT</b>	<b>*ACOT</b>	<b>*ACOT</b>	<b>*ACOT</b>

Figure 5.16: *Lower and Upper Bounds of Cost of Transport (COT) for the Downward Slope Walking Experiment.*

In Figure 5.17, the energy savings of the Decrease & Conquer based Methods, in comparison with the One-Phase based ones, are shown.

<i>Energy Savings of Decrease and Conquer Variants Vs One Phase Related Variants, for the Downwards Walking Experiment (Percentage)</i>		
<b>N (points)</b>	<b>Discrete Mechanics</b>	<b>Direct Collocation</b>
<b>10</b>	<b>17,58</b>	<b>17,26</b>
<b>20</b>	<b>18,59</b>	<b>21,06</b>
<b>30</b>	<b>26,24</b>	<b>28,88</b>
<b>40</b>	<b>34,6</b>	<b>39,02</b>
<b>50</b>	<b>45,5</b>	<b>49,57</b>
<b>60</b>	<b>57,39</b>	<b>58,69</b>
<b>70</b>	<b>64,45</b>	<b>68,56</b>
<b>80</b>	<b>73,47</b>	<b>79,34</b>
<b>90</b>	<b>87,24</b>	<b>90,55</b>
<b>100</b>	<b>85,07</b>	<b>89,05</b>
<b>110</b>	<b>83,8</b>	<b>88,16</b>
<b>120</b>	<b>82,81</b>	<b>87,33</b>
<b>130</b>	<b>79,86</b>	<b>84,63</b>
<b>140</b>	<b>73,06</b>	<b>80,53</b>
<b>150</b>	<b>64,46</b>	<b>72,46</b>
<b>160</b>	<b>60,35</b>	<b>69,32</b>
<b>170</b>	<b>60,35</b>	<b>69,32</b>
<b>180</b>	<b>60,35</b>	<b>69,32</b>

Figure 5.17: *Energy Savings of Decrease and Conquer Variants in comparison with One Phase Related Variants, for the Downward Slope Walking Experiment (Percentage).*

As we can see, the Decrease & Conquer based Discrete Mechanics Method achieves energy savings between 17.58% (for  $N = 10$ ) - 87.24% (for  $N = 90$ ), in comparison with the One Phase based related Method, while the Decrease & Conquer based Direct Collocation Method

achieves energy savings between 17.26% (for  $N = 10$ ) - 90.55% (for  $N = 90$ ), in comparison with the One Phase based related Method.

In Figure 5.18, the energy savings of the Decrease & Conquer based Methods, in comparison with SNOPT, are shown.

<i>Energy Savings of Decrease and Conquer Variants Vs SNOPT, for the Downwards Walking Experiment (Percentage)</i>		
<b>N (points)</b>	<b>Discrete Mechanics</b>	<b>Direct Collocation</b>
<b>10</b>	<b>7,77</b>	<b>10,68</b>
<b>20</b>	<b>10,08</b>	<b>15,88</b>
<b>30</b>	<b>18,19</b>	<b>22,23</b>
<b>40</b>	<b>24,92</b>	<b>32,63</b>
<b>50</b>	<b>37,85</b>	<b>43,84</b>
<b>60</b>	<b>54,25</b>	<b>56,5</b>
<b>70</b>	<b>61,78</b>	<b>67,09</b>
<b>80</b>	<b>72,11</b>	<b>79,34</b>
<b>90</b>	<b>85,15</b>	<b>89,63</b>
<b>100</b>	<b>82,45</b>	<b>87,74</b>
<b>110</b>	<b>80,89</b>	<b>86,66</b>
<b>120</b>	<b>77,06</b>	<b>83,98</b>
<b>130</b>	<b>72,92</b>	<b>81,09</b>
<b>140</b>	<b>65,22</b>	<b>75,72</b>
<b>150</b>	<b>46,79</b>	<b>62,85</b>
<b>160</b>	<b>41,29</b>	<b>59,01</b>
<b>170</b>	<b>25,59</b>	<b>48,05</b>
<b>180</b>	<b>25,59</b>	<b>48,05</b>

Figure 5.18: *Energy Savings of Decrease and Conquer Variants in comparison with SNOPT, for the Downward Slope Walking Experiment (Percentage).*

As we can see, the Decrease & Conquer based Discrete Mechanics Method achieves energy savings between 7.77% (for  $N = 10$ ) - 85.15% (for  $N = 90$ ), in comparison with SNOPT, while the Decrease & Conquer based Direct Collocation Method achieves energy savings between 10.68% (for  $N = 10$ ) - 89.63% (for  $N = 90$ ), in comparison with it.

Now we will show the plots of the 4-DOF biped robot, for  $N=90$ , which is the number of points where the Decrease & Conquer Feedback Control utilizing Direct Collocation Method achieves the lowest possible ACOT in the Downward Slope Walking Experiment. Due to the fact that the Decrease & Conquer Feedback Control utilizing Discrete Mechanics Method results in similar results, only the results of the First Approach will be presented. Next, the actual plots of the 4-DOF Biped Robot, will be shown, under missing velocity signals and disturbances. In

addition, we assume that Leg 2 initially starts the walking process, thus it is the swing leg for the first walking step.

In Figure 5.19, the plots of desired and actual angles of the two Legs over time are shown. In addition, in Figures 5.20 and 5.21, the plots of the position errors over time are depicted.

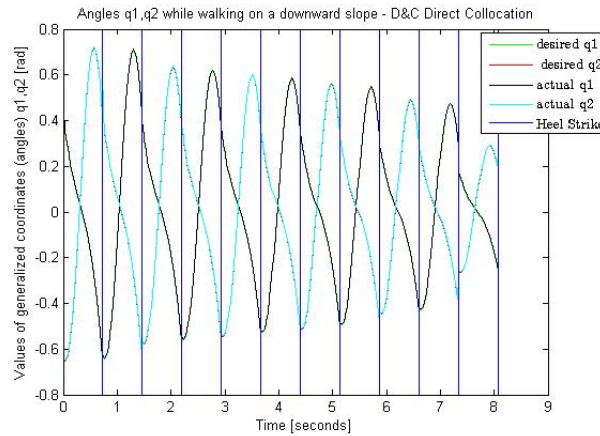


Figure 5.19: *Desired and actual angles during the Downward Slope Walking Experiment - Decrease & Conquer Feedback Control utilizing Direct Collocation.*

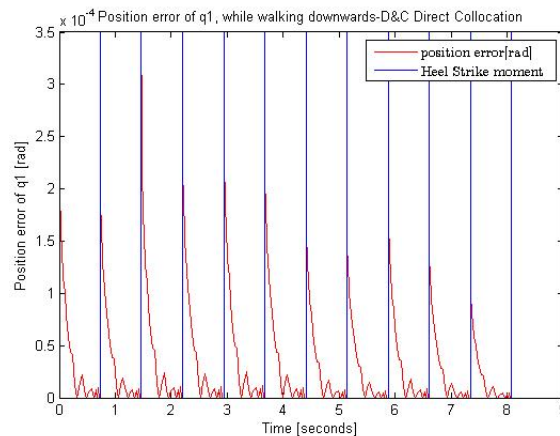


Figure 5.20: *Position error during the Downward Slope Walking Experiment - Decrease & Conquer Feedback Control utilizing Direct Collocation.*

From Figure 5.19, at each walking step, it can be seen that the angular displacement of the swing leg gradually increases over time. Some moments before the completion of each walking step (Heel Strike Moment), the angular displacement of the swing leg reaches the maximum, and then the swing leg swings back. When human stride reaches the maximum during walking, a swinging back process also occurs, which is consistent with the mechanism of the human movement. The angular displacement of the stance leg monotonically decreases, and when

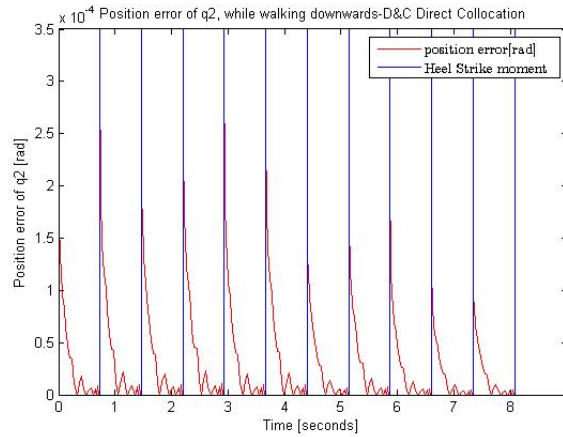


Figure 5.21: *Position error during the Downward Slope Walking Experiment - Decrease & Conquer Feedback Control utilizing Direct Collocation.*

$t=0.7343$  sec (Heel Strike Moment), the swing leg is in collision with the ground and the two legs switch roles. As the step length increases, the values of the angular displacements increase and vice versa.

Furthermore, the desired and actual angular displacements of the two legs are nearly the same. From Figure 5.20 and 5.21, we can see that the position errors are extremely low ( $\approx 10^{-4}$ ), showing the effectiveness of the implemented trajectory tracking control.

In Figure 5.22, the plot of real and estimated angular velocities of the two legs over time is shown. In addition, in Figures 5.23 and 5.24, the plots of the velocity errors over time are depicted.

Based on Figures 5.22, 5.23 and 5.24, the real and estimated angular velocities of the two legs are nearly the same. From Figure 5.23 and 5.24, we can see that the velocity errors are extremely low ( $\approx 10^{-4}$ ), showing again the effectiveness of the trajectory tracking control. As the step length increases, the values of the angular velocities increase and vice versa.

In Figure 5.25, the control signals of the swing and stance leg over time during the Downward Slope Walking Experiment are shown. We can see that at the beginning of each walking step, a larger torque should be input to the robot to realize dynamic walking, and with the input of the torque, the kinetic and potential energy are reasonably converted into driving energy; thereafter, only a small energy input can complete a walking step. The impact of the small inaccuracies on the estimation of the velocity signals and the disturbances is an increase of the

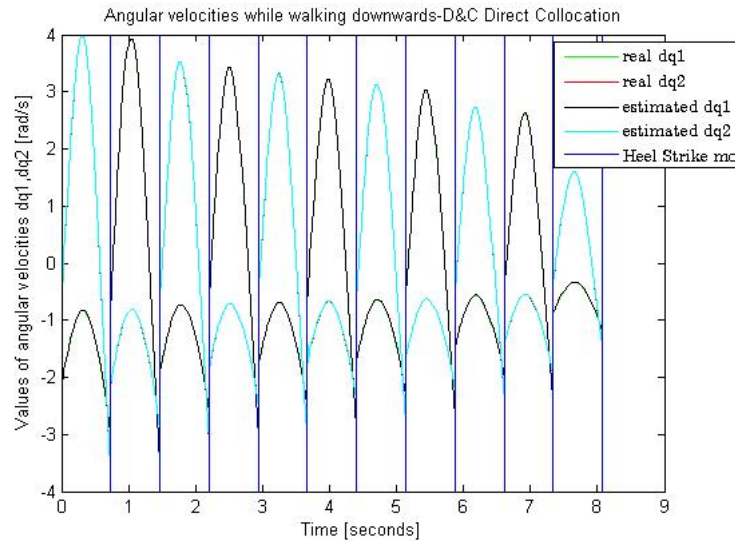


Figure 5.22: *Real and estimated angular velocities during the Downward Slope Walking Experiment - Decrease & Conquer Feedback Control utilizing Direct Collocation.*

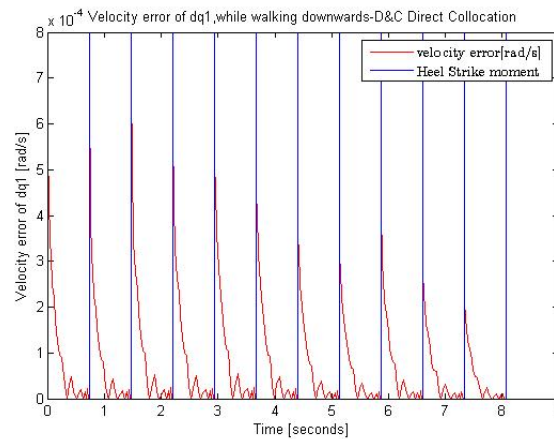


Figure 5.23: *Angular velocity errors of the Leg 1 during the Downward Slope Walking Experiment - Decrease & Conquer Feedback Control utilizing Direct Collocation.*

ACOT by just 0.6%.

In Figure 5.26, the plot of Ground Reaction Forces (Vertical component: Normal Force, and horizontal component: Friction force) experienced during the Downward Slope Walking Experiment, are shown. In biomechanics, that plot is called butterfly diagram, due to the fact that the two peaks of the Normal Force look like the wings of a butterfly. As the step length increases, the values of the Ground Reaction Forces increase and vice versa.

More specifically, in the first moment (time step) of each walking step, the new stance leg, due to the experienced Heel Strike Forces a moment before, tries to adjust posture to support dynamic

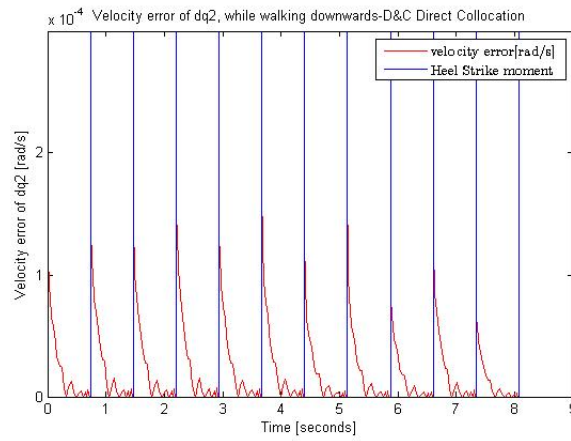


Figure 5.24: *Angular velocity errors of the Leg 2 during the Downward Slope Walking Experiment - Decrease & Conquer Feedback Control utilizing Direct Collocation.*

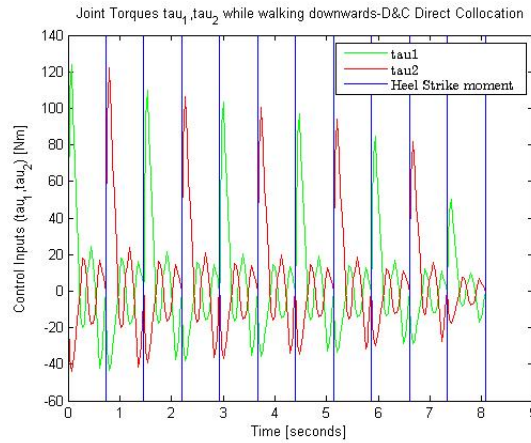


Figure 5.25: *Control Signals  $\tau_1$ ,  $\tau_2$  during the Downward Slope Walking Experiment - Decrease & Conquer Feedback Control utilizing Direct Collocation.*

walking, resulting in higher torque and thus leading to the first peak of the Normal Force. From the next time step till the 25 % of the walking step, the Normal Force is decreasing, due to the adjusted posture of the stance leg, leading to a smaller required torque to keep balancing. From that moment till the 50% of the walking step, we have an increase in the Normal Force, due to the fact that the stance leg becomes more vertical with the ground and at the half of the walking step the stance leg is completely vertical with it, supporting the whole weight of the robot, and resulting in the second peak of the Normal Force (this intermediate phase of the walking step is called midstance phase). From that moment till the end of the walking step, the Normal Force is decreasing (and it approaches zero), as the stance leg tends to be less vertical with the ground and the swing leg tends to approach the ground, taking an actual role for the

support of the robot weight, both preparing to switch roles after the effects of the Push-Off and Heel Strike Phases. The Normal Force, throughout the entire walking step, is positive.

Regarding the values of the Friction Force, from the first time step of a walking step till the 10% of it, the friction force is decreasing and negative (at the 10% of the walking step we have a negative peak of the Friction force), due to the braking direction of the stance leg, resulting the Friction Force to act a backward (negative) force. From that moment till the 50% of the walking step, as we approach the midstance phase, the Friction Force is increasing (at the 50% of the walking step we have a positive peak of the Friction Force) as the stance leg becomes more vertical with the ground and tends to move in a more propulsive direction. From the 50% of the walking step, till the completion of it, the stance leg keeps its propulsive direction, and waits for the Push-Off and Heel Strike Phases to take effect and switch roles with the swing leg, thus the friction force tends to zero.

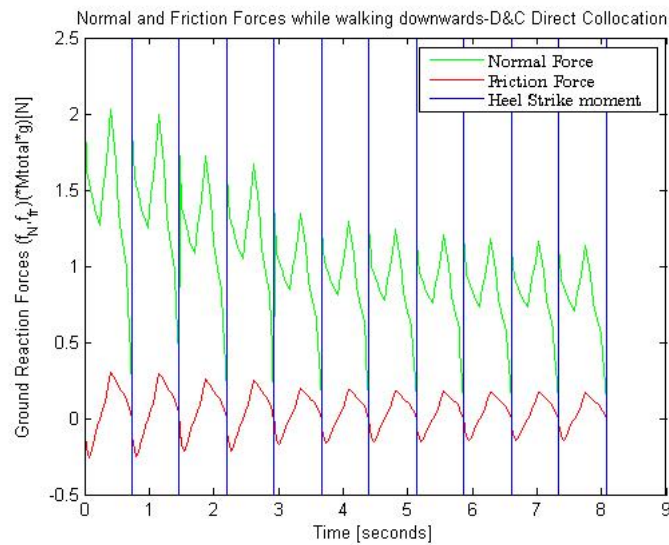


Figure 5.26: *Ground Reaction Forces during the Downward Slope Walking Experiment - Decrease & Conquer Feedback Control utilizing Direct Collocation.*

In Figure 5.27, the Instantaneous Push-Off Impulses applied during the Downward Slope Walking experiment, are shown. A Push-Off Impulse, as we have mentioned in previous Chapters, is required for the stance leg to be detached from the ground, while adding the required energy for the biped robot to be stabilized after the energy losses of the Heel Strike Phase. As the step length increases, the values of the Push-Off Impulse increase and vice versa.

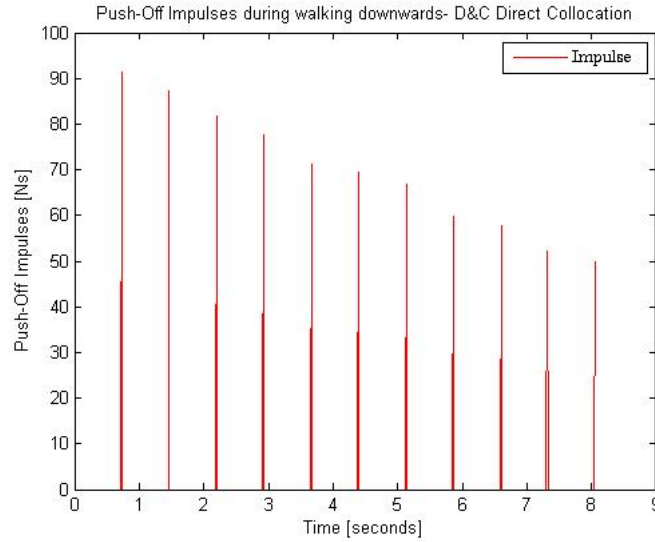


Figure 5.27: *Push-Off Impulses during the Downward Slope Walking Experiment - Decrease  $\mathcal{E}$  Conquer Feedback Control utilizing Direct Collocation.*

## 5.4 Upward Slope Walking Experiment

In the current simulation we let the 4-DOF Biped walk on an upward slope. The related parameters of the particular experiment are given below:

1.  $H = 11$  walking steps,
2.  $M = 55kg$ ,
3.  $m_1 = m_2 = 27.5kg$ ,
4. The duration of a walking step : 0.7343 seconds,
5.  $a = b = 0.6m, l = 1.2m$ ,
6.  $\theta = 0.698$  rad (40 deg)
7.  $D_1 = 0.7m, D_2 = 0.8m, D_3 = 1m, D_4 = 1.2m, D_5 = 1.35m, D_6 = 1.45m, D_7 = 1.55m, D_8 = 1.6m, D_9 = 1.85m, D_{10} = 2.1m, D_{11} = 2.25m$ ,
8. Initial conditions:  $q_1 = 0.2296rad, q_2 = -0.2296rad, \dot{q}_1 = -1.1470rad/s, \dot{q}_2 = -0.3962rad/s, q_3 = 0m, q_4 = 0m, \dot{q}_3 = 0m/s, \dot{q}_4 = 0m/s$ ,

9. For the disturbances, we use the following parameter values:  $F_{c1} = F_{c2} = 6 \text{ Nm}$ ,  $F_{c3} = F_{c4} = 6h^{(i)} \text{ Ns}$ ,  $f_{v1} = f_{v2} = 8.5 \text{ Nm/(rad/s)}$ ,  $F_{v3} = F_{v4} = 7.5h^{(i)} \text{ Ns/(m/s)}$ ,  $F_{s1} = F_{s2} = 12 \text{ Nm}$ ,  $F_{s3} = F_{s4} = 7h^{(i)} \text{ Ns}$ ,  $v_{s1} = v_{s2} = 0.25 \text{ rad/s}$ ,  $v_{s3} = v_{s4} = 0.08 \text{ m/s}$ .

In Figure 5.28, we show the overall results of the Upward Slope Walking experiment. More specifically, we show the Average Cost Of Transport ( $\frac{1}{H} \sum_{i=1}^H COT^{(i)}$ ) of the H=11 desired trajectories of the biped, subject to the number of points/time steps (N) that approximate the desired trajectory of each walking step, for all the abovementioned Gait Generation Problem solving approaches. The red coloured results indicate the minimum Average Cost Of Transport (lower is better) achieved by a particular method. We have verified the results by reconducting the experiment numerous times, proving the convergence of the results to the values of the Figure.

Average Cost of Transport for the Upwards Walking Experiment					
N (points)	One Phase		SNOPT	Decrease and Conquer - 2 Phases	
	Discrete Mechanics	Direct Collocation	commercial package	Discrete Mechanics	Direct Collocation
10	1.273	1.198	1.177	1.1358	1.0459
20	1.156	1.093	1.045	0.9858	0.9135
30	1.073	1.016	0.929	0.8447	0.7932
40	1.021	0.983	0.8763	0.6958	0.6131
50	0.913	0.873	0.8138	0.5541	0.4998
60	0.848	0.786	0.771	0.4773	0.3997
70	0.801	0.7236	0.68	0.3165	0.2878
80	0.763	0.6683	0.613	0.2456	0.1978
90	0.714	0.5971	0.555	0.156	0.1112
100	0.6324	0.5463	0.4765	0.081	0.0561
110	0.593	0.497	0.442	0.081	0.0561
120	0.511	0.434	0.3958	0.081	0.0561
130	0.4498	0.4132	0.3167	0.081	0.0561
140	0.3798	0.325	0.2886	0.081	0.0561
150	0.314	0.284	0.224	0.081	0.0561
160	0.274	0.223	0.1958	0.081	0.0561
170	0.1755	0.1564	0.1331	0.081	0.0561
180	0.142	0.1258	0.1158	0.081	0.0561
190	0.142	0.1258	0.1141	0.081	0.0561

Figure 5.28: Average Cost of Transport (ACOT) for the Upward Slope Walking Experiment.

As we can see, the Decrease & Conquer Approach is extremely effective:

1. Regarding the One Phase based Methods, Discrete Mechanics needs at least 180 points to achieve an ACOT of 0.142, while Direct Collocation needs at least the same number of points (140) to achieve an ACOT of 0.1258.
2. Regarding the commercial package SNOPT, it needs at least 190 points to achieve an ACOT of 0.1141.
3. Regarding the Decrease & Conquer based Methods, Discrete Mechanics need only 100 points to achieve an ACOT of 0.081, while Direct Collocation needs only 90 points also to achieve an ACOT of 0.0561. Thus, the Decrease & Conquer approach achieves the lowest possible values of energy consumption (subject to each variant) for the Upward Slope Walking experiment.

In Figure 5.29, we show the lower and upper bounds of the Cost of Transport that observed throughout the abovementioned Upward Slope Walking Experiment, subject to the various tested solving methods. This is to prove that, during the experiment and particularly for the proposed approach, there were not any extremely high values of COT that were averaged with smaller ones, but the resulted values were in the domain of the minimal possible ACOT for each tested approach.

<i>Lower and Upper Bounds of Cost of Transport (COT) for the Upwards Walking Experiment</i>				
<b>One Phase</b>		<b>SNOPT</b>	<b>Decrease and Conquer - 2 Phases</b>	
<b>Discrete Mechanics</b>	<b>Direct Collocation</b>	<b>commercial package</b>	<b>Discrete Mechanics</b>	<b>Direct Collocation</b>
<b>[0.91 - 1.25]</b>	<b>[0.94-1.31]</b>	<b>[0.96 – 1.24]</b>	<b>[0.9 – 1.06]</b>	<b>[0.95-1.07]</b>
<b>*ACOT</b>	<b>*ACOT</b>	<b>*ACOT</b>	<b>*ACOT</b>	<b>*ACOT</b>

Figure 5.29: *Lower and Upper Bounds of Cost of Transport (COT) for the Upward Slope Walking Experiment.*

In Figure 5.30, the energy savings of the Decrease & Conquer based Methods, in comparison with the One-Phase based ones, are shown.

<i>Energy Savings of Decrease and Conquer Variants Vs One Phase Related Variants, for the Upwards Walking Experiment (Percentage)</i>		
<b>N (points)</b>	<b>Discrete Mechanics</b>	<b>Direct Collocation</b>
10	10,78	12,7
20	14,72	16,42
30	21,28	21,93
40	31,85	37,63
50	39,31	42,75
60	43,71	49,15
70	60,49	60,23
80	67,81	70,4
90	78,15	81,38
100	87,19	89,73
110	86,34	88,71
120	84,15	87,07
130	81,99	86,42
140	78,67	82,74
150	74,2	80,25
160	70,44	74,84
170	53,85	64,13
180	42,96	55,41
190	42,96	55,41

Figure 5.30: *Energy Savings of Decrease and Conquer Variants in comparison with One Phase Related Variants, for the Upward Slope Walking Experiment (Percentage).*

As we can see, the Decrease & Conquer based Discrete Mechanics Method achieves energy savings between 10.72% (for  $N = 10$ ) - 87.19% (for  $N = 100$ ), in comparison with the One Phase based related Method, while the Decrease & Conquer based Direct Collocation Method achieves energy savings between 12.7% (for  $N = 10$ ) - 89.73% (for  $N = 100$ ), in comparison with the One Phase based related Method.

In Figure 5.31, the energy savings of the Decrease & Conquer based Methods, in comparison with SNOPT, are shown.

As we can see, the Decrease & Conquer based Discrete Mechanics Method achieves energy savings between 3.5% (for  $N = 10$ ) - 83% (for  $N = 100$ ), in comparison with SNOPT, while the Decrease & Conquer based Direct Collocation Method achieves energy savings between 11.14% (for  $N = 10$ ) - 88.23% (for  $N = 100$ ), in comparison with it.

Now we will show the plots of the 4-DOF biped robot, for  $N=100$ , which is the number of points where the Decrease & Conquer Feedback Control utilizing Direct Collocation Method

<i>Energy Savings of Decrease and Conquer Variants Vs SNOPT, for the Upwards Walking Experiment (Percentage)</i>		
<b>N (points)</b>	<b>Discrete Mechanics</b>	<b>Direct Collocation</b>
<b>10</b>	<b>3,5</b>	<b>11,14</b>
<b>20</b>	<b>5,67</b>	<b>12,58</b>
<b>30</b>	<b>9,07</b>	<b>14,62</b>
<b>40</b>	<b>20,6</b>	<b>30,04</b>
<b>50</b>	<b>31,91</b>	<b>38,58</b>
<b>60</b>	<b>38,09</b>	<b>48,16</b>
<b>70</b>	<b>53,46</b>	<b>57,68</b>
<b>80</b>	<b>59,93</b>	<b>67,73</b>
<b>90</b>	<b>71,89</b>	<b>79,96</b>
<b>100</b>	<b>83</b>	<b>88,23</b>
<b>110</b>	<b>81,67</b>	<b>87,31</b>
<b>120</b>	<b>79,54</b>	<b>85,83</b>
<b>130</b>	<b>74,42</b>	<b>82,29</b>
<b>140</b>	<b>71,93</b>	<b>80,56</b>
<b>150</b>	<b>63,84</b>	<b>74,96</b>
<b>160</b>	<b>58,63</b>	<b>71,35</b>
<b>170</b>	<b>39,14</b>	<b>57,85</b>
<b>180</b>	<b>30,05</b>	<b>51,55</b>
<b>190</b>	<b>29,01</b>	<b>50,83</b>

Figure 5.31: *Energy Savings of Decrease and Conquer Variants in comparison with SNOPT, for the Upward Slope Walking Experiment (Percentage).*

achieves the lowest possible ACOT in the Upward Slope Walking Experiment. Due to the fact that the Decrease & Conquer Feedback Control utilizing Discrete Mechanics Method results in similar results, only the results of the First Approach will be presented. Next, the actual plots of the 4-DOF Biped Robot, will be shown, under missing velocity signals and disturbances. In addition, we assume that Leg 2 initially starts the walking process, thus it is the swing leg for the first walking step.

In Figure 5.32, the plots of desired and actual angles of the two Legs over time are shown. In addition, in Figures 5.33 and 5.34, the plots of the position errors over time are depicted.

From Figure 5.32, at each walking step, it can be seen that the angular displacement of the swing leg gradually increases over time. Some moments before the completion of each walking step (Heel Strike Moment), the angular displacement of the swing leg reaches the maximum, and then the swing leg swings back. When human stride reaches the maximum during walking, a swinging back process also occurs, which is consistent with the mechanism of the human

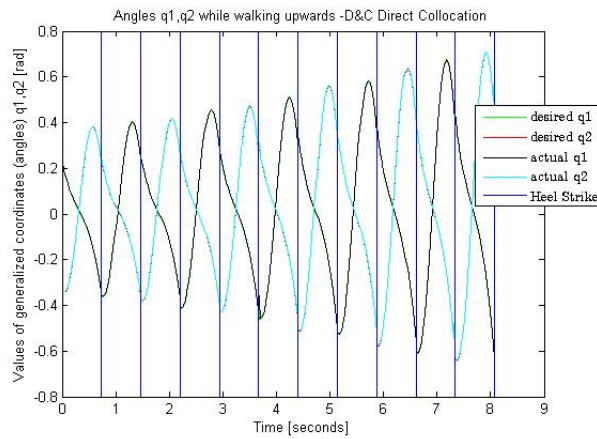


Figure 5.32: *Desired and actual angles during the Upward Slope Walking Experiment - Decrease & Conquer Feedback Control utilizing Direct Collocation.*

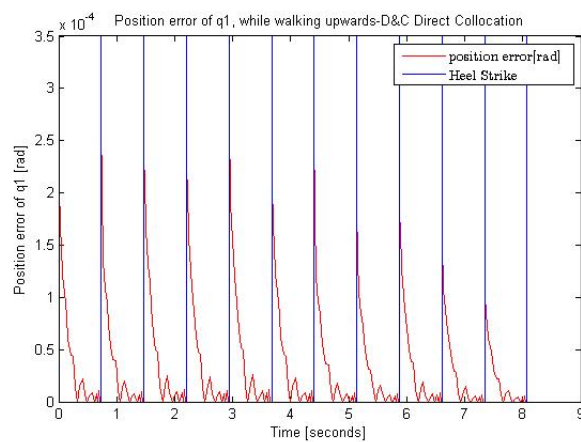


Figure 5.33: *Position error during the Upward Slope Walking Experiment - Decrease & Conquer Feedback Control utilizing Direct Collocation.*

movement. The angular displacement of the stance leg monotonically decreases, and when  $t=0.7343$  sec (Heel Strike Moment), the swing leg is in collision with the ground and the two legs switch roles. As the step length increases, the values of the angular displacements increase and vice versa.

Furthermore, the desired and actual angular displacements of the two legs are nearly the same. From Figure 5.33 and 5.34, we can see that the position errors are extremely low ( $\approx 10^{-4}$ ), showing the effectiveness of the implemented trajectory tracking control.

In Figure 5.35, the plot of real and estimated angular velocities of the two legs over time is shown. In addition, in Figures 5.36 and 5.37, the plots of the velocity errors over time are depicted.

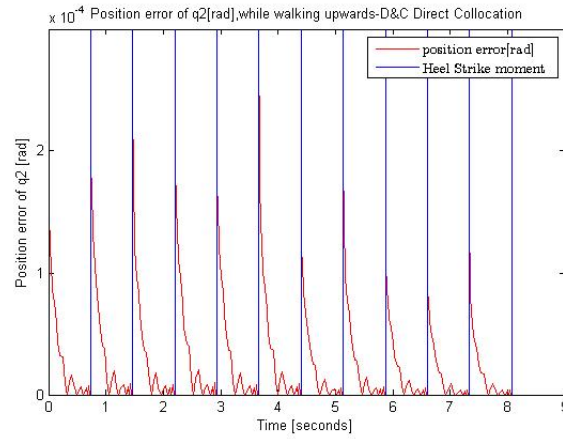


Figure 5.34: *Position error during the Upward Slope Walking Experiment - Decrease & Conquer Feedback Control utilizing Direct Collocation.*

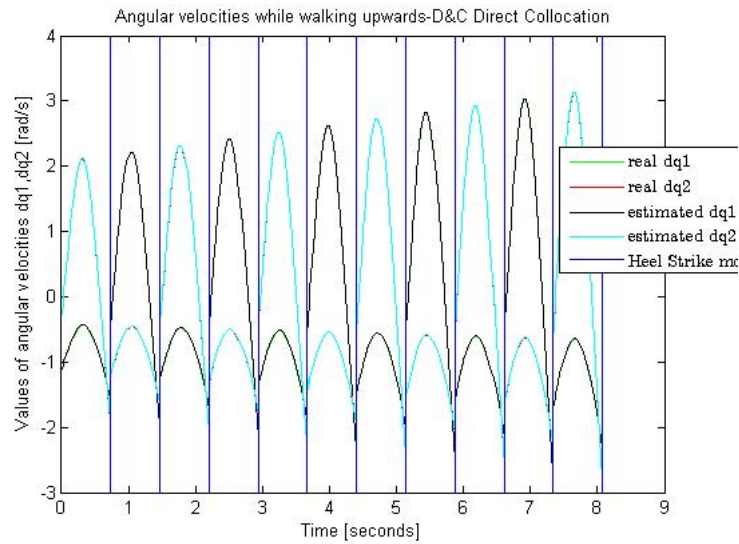


Figure 5.35: *Real and estimated angular velocities during the Upward Slope Walking Experiment - Decrease & Conquer Feedback Control utilizing Direct Collocation.*

Based on Figures 5.35, 5.36 and 5.37, the real and estimated angular velocities of the two legs are nearly the same. From Figure 5.36 and 5.37, we can see that the velocity errors are extremely low ( $\approx 10^{-4}$ ), showing again the effectiveness of the trajectory tracking control. As the step length increases, the values of the angular velocities increase and vice versa.

In Figure 5.38, the control signals of the swing and stance leg over time during the Upward Slope Walking Experiment are shown. We can see that at the beginning of each walking step, a larger torque should be input to the robot to realize dynamic walking, and with the input of the torque, the kinetic and potential energy are reasonably converted into driving energy; thereafter, only a small energy input can complete a walking step. The impact of the small

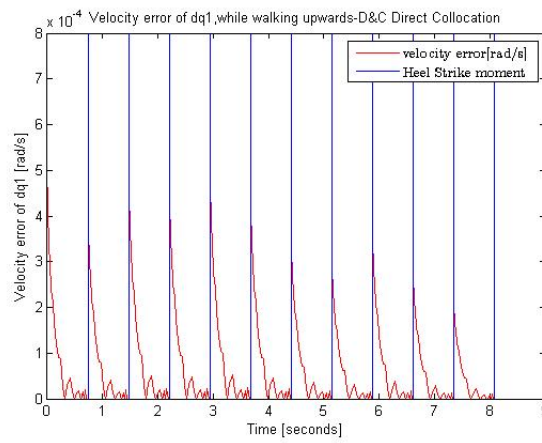


Figure 5.36: *Angular velocity errors of the Leg 1 during the Upward Slope Walking Experiment - Decrease & Conquer Feedback Control utilizing Direct Collocation.*

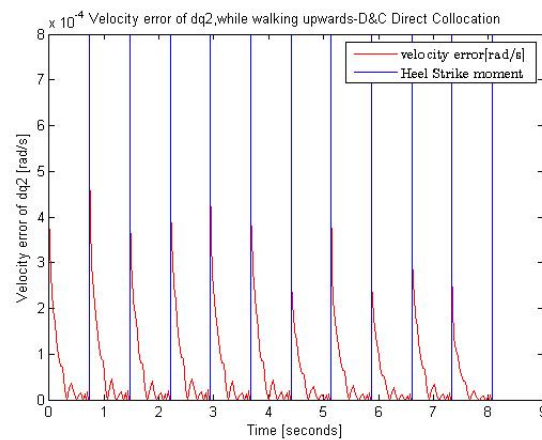


Figure 5.37: *Angular velocity errors of the Leg 2 during the Upward Slope Walking Experiment - Decrease & Conquer Feedback Control utilizing Direct Collocation.*

inaccuracies on the estimation of the velocity signals and the disturbances is an increase of the ACOT by just 0.7%.

In Figure 5.39, the plot of Ground Reaction Forces (Vertical component: Normal Force, and horizontal component: Friction force) experienced during the Upward Slope Walking Experiment, are shown. In biomechanics, that plot is called butterfly diagram, due to the fact that the two peaks of the Normal Force look like the wings of a butterfly. As the step length increases, the values of the Ground Reaction Forces increase and vice versa.

More specifically, in the first moment (time step) of each walking step, the new stance leg, due to the experienced Heel Strike Forces a moment before, tries to adjust posture to support dynamic walking, resulting in higher torque and thus leading to the first peak of the Normal Force. From

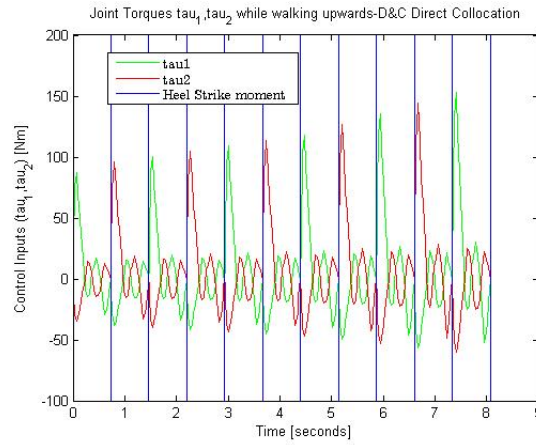


Figure 5.38: *Control Signals  $\tau_1$ ,  $\tau_2$  during the Downward Slope Walking Experiment - Decrease & Conquer Feedback Control utilizing Direct Collocation.*

the next time step till the 25 % of the walking step, the Normal Force is decreasing, due to the adjusted posture of the stance leg, leading to a smaller required torque to keep balancing. From that moment till the 50% of the walking step, we have an increase in the Normal Force, due to the fact that the stance leg becomes more vertical with the ground and at the half of the walking step the stance leg is completely vertical with it, supporting the whole weight of the robot, and resulting in the second peak of the Normal Force (this intermediate phase of the walking step is called midstance phase). From that moment till the end of the walking step, the Normal Force is decreasing (and it approaches zero), as the stance leg tends to be less vertical with the ground and the swing leg tends to approach the ground, taking an actual role for the support of the robot weight, both preparing to switch roles after the effects of the Push-Off and Heel Strike Phases. The Normal Force, throughout the entire walking step, is positive.

Regarding the values of the Friction Force, from the first time step of a walking step till the 10% of it, the friction force is decreasing and negative (at the 10% of the walking step we have a negative peak of the Friction force), due to the braking direction of the stance leg, resulting the Friction Force to act a backward (negative) force. From that moment till the 50% of the walking step, as we approach the midstance phase, the Friction Force is increasing (at the 50% of the walking step we have a positive peak of the Friction Force) as the stance leg becomes more vertical with the ground and tends to move in a more propulsive direction. From the 50% of the walking step, till the completion of it, the stance leg keeps its propulsive direction, and

waits for the Push-Off and Heel Strike Phases to take effect and switch roles with the swing leg, thus the friction force tends to zero.

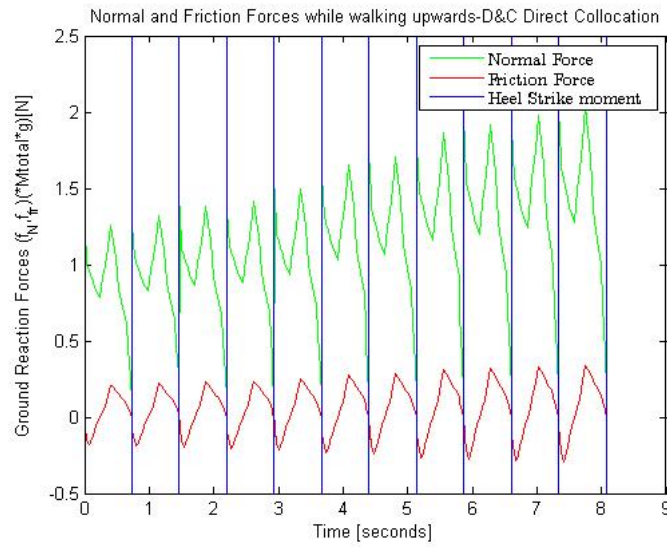


Figure 5.39: *Ground Reaction Forces during the Upward Slope Walking Experiment - Decrease & Conquer Feedback Control utilizing Direct Collocation.*

In Figure 5.40, the Instantaneous Push-Off Impulses applied during the Upward Slope Walking experiment, are shown. A Push-Off Impulse, as we have mentioned in previous Chapters, is required for the stance leg to be detached from the ground, while adding the required energy for the biped robot to be stabilized after the energy losses of the Heel Strike Phase. As the step length increases, the values of the Push-Off Impulse increase and vice versa.

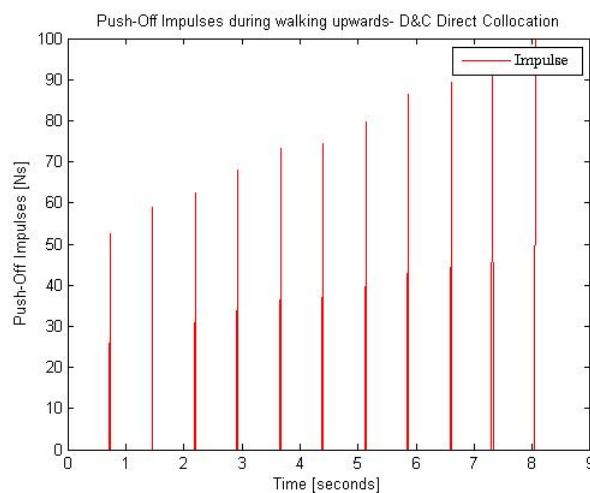


Figure 5.40: *Push-Off Impulses during the Upward Slope Walking Experiment - Decrease & Conquer Feedback Control utilizing Direct Collocation.*

## 5.5 Down/Up Stairs Walking Experiment

In the current simulation we let the 4-DOF Biped walk down/up stairs. The related parameters of the particular experiment are given below:

1.  $H = 11$  walking steps,
2.  $M = 70kg$ ,
3.  $m_1 = m_2 = 35kg$ ,
4. The duration of a walking step : 0.7343 seconds,
5.  $a = b = 0.5m, l = 1m$ ,
6.  $(L_1 = 1m, H_1 = 0.6m \Leftrightarrow D_1 = 1.166m, \theta_1 = 52.96 \text{ deg}), (L_2 = 1.4m, H_2 = 0.6m \Leftrightarrow D_2 = 1.56m, \theta_2 = 26.18 \text{ deg}), (L_3 = 1.5m, H_3 = 0.8m \Leftrightarrow D_3 = 1.7m, \theta_3 = 28.07 \text{ deg}), (L_4 = 1.2m, H_4 = 0.4m \Leftrightarrow D_4 = 1.2649m, \theta_4 = 18.43 \text{ deg}), (L_5 = 1.1m, H_5 = 0.5m \Leftrightarrow D_5 = 1.208m, \theta_5 = 24.41 \text{ deg}), (L_6 = 0.9m, H_6 = -0.8m \Leftrightarrow D_6 = 1.204m, \theta_6 = -41.63 \text{ deg}), (L_7 = 0.8m, H_7 = -1m \Leftrightarrow D_7 = 1.28m, \theta_7 = -51.32 \text{ deg}), (L_8 = 0.75m, H_8 = -0.7m \Leftrightarrow D_8 = 1.029m, \theta_8 = -43.21 \text{ deg}), (L_9 = 0.6m, H_9 = -0.6m \Leftrightarrow D_9 = 0.84m, \theta_9 = -44.42 \text{ deg}), (L_{10} = 0.5m, H_{10} = -0.6m \Leftrightarrow D_{10} = 0.781m, \theta_{10} = -50.19 \text{ deg}), (L_{11} = 0.2m, H_{11} = -0.4m \Leftrightarrow D_{11} = 0.44m, \theta_{11} = -62.96 \text{ deg})$
7. Initial conditions:  $q_1 = 0.2843rad, q_2 = -0.2893rad, \dot{q}_1 = -1.4201rad/s, \dot{q}_2 = -0.4906rad/s, q_3 = 0m, q_4 = 0m, \dot{q}_3 = 0m/s, \dot{q}_4 = 0m/s$ ,
8. For the disturbances, we use the following parameter values:  $F_{c1} = F_{c2} = 7 Nm, F_{c3} = F_{c4} = 6.5h^{(i)} Ns, f_{v1} = f_{v2} = 8.5 Nm/(rad/s), F_{v3} = F_{v4} = 7h^{(i)} Ns/(m/s), F_{s1} = F_{s2} = 10.5 Nm, F_{s3} = F_{s4} = 6h^{(i)} Ns, v_{s1} = v_{s2} = 0.21 rad/s, v_{s3} = v_{s4} = 0.06 m/s$ .

In Figure 5.41, we show the overall results of the Down/Up Stairs Walking experiment. More specifically, we show the Average Cost Of Transport ( $\frac{1}{H} \sum_{i=1}^H COT^{(i)}$ ) of the H=11 desired trajectories of the biped, subject to the number of points/time steps (N) that approximate the

desired trajectory of each walking step, for all the abovementioned Gait Generation Problem solving approaches. The red coloured results indicate the minimum Average Cost Of Transport (lower is better) achieved by a particular method. We have verified the results by reconducting the experiment numerous times, proving the convergence of the results to the values of the Figure.

Average Cost of Transport for the (Down/Up) Stairs Walking Experiment					
N (points)	One Phase		SNOPT	Decrease and Conquer - 2 Phases	
	Discrete Mechanics	Direct Collocation	commercial package	Discrete Mechanics	Direct Collocation
10	0.976	0.9431	0.9132	0.8714	0.8132
20	0.918	0.8971	0.8765	0.8235	0.7438
30	0.843	0.8164	0.776	0.7165	0.6984
40	0.796	0.7415	0.7315	0.6635	0.6158
50	0.7135	0.6944	0.6758	0.5484	0.5008
60	0.6519	0.6324	0.6124	0.4835	0.4158
70	0.6135	0.5935	0.5523	0.4084	0.3564
80	0.5635	0.5414	0.4849	0.256	0.2165
90	0.5005	0.4886	0.4432	0.1432	0.1184
100	0.4435	0.4224	0.4041	0.0854	0.065
110	0.4003	0.3884	0.3563	0.0632	0.039
120	0.3665	0.3551	0.3184	0.0632	0.039
130	0.3215	0.3005	0.2884	0.0632	0.039
140	0.2814	0.2614	0.2453	0.0632	0.039
150	0.2413	0.2158	0.2058	0.0632	0.039
160	0.1984	0.1784	0.1432	0.0632	0.039
170	0.1543	0.1321	0.1184	0.0632	0.039
180	0.1484	0.1285	0.1115	0.0632	0.039
190	0.1484	0.1285	0.108	0.0632	0.039
200	0.1484	0.1285	0.099	0.0632	0.039

Figure 5.41: Average Cost of Transport (ACOT) for the Down/Up Stairs Walking Experiment.

As we can see, the Decrease & Conquer Approach is extremely effective:

1. Regarding the One Phase based Methods, Discrete Mechanics needs at least 180 points to achieve an ACOT of 0.1484, while Direct Collocation needs at least the same number of points (140) to achieve an ACOT of 0.1285.
2. Regarding the commercial package SNOPT, it needs at least 200 points to achieve an

ACOT of 0.099.

- Regarding the Decrease & Conquer based Methods, Discrete Mechanics need only 110 points to achieve an ACOT of 0.0632, while Direct Collocation needs only 110 points also to achieve an ACOT of 0.039. Thus, the Decrease & Conquer approach achieves the lowest possible values of energy consumption (subject to each variant) for the Down/Up Stairs Walking experiment.

In Figure 5.42, we show the lower and upper bounds of the Cost of Transport that observed throughout the abovementioned Down/Up Stairs Walking Experiment, subject to the various tested solving methods. This is to prove that, during the experiment and particularly for the proposed approach, there were not any extremely high values of COT that were averaged with smaller ones, but the resulted values were in the domain of the minimal possible ACOT for each tested approach.

<i>Lower and Upper Bounds of Cost of Transport (COT) for the (Down/Up) Stairs Walking Experiment</i>				
<b>One Phase</b>		<b>SNOPT</b>	<b>Decrease and Conquer - 2 Phases</b>	
<b>Discrete Mechanics</b>	<b>Direct Collocation</b>	<b>commercial package</b>	<b>Discrete Mechanics</b>	<b>Direct Collocation</b>
<b>[0.89 - 1.26]</b>	<b>[0.9-1.33]</b>	<b>[0.94 - 1.28]</b>	<b>[0.95 - 1.07]</b>	<b>[0.96-1.08]</b>
<b>*ACOT</b>	<b>*ACOT</b>	<b>*ACOT</b>	<b>*ACOT</b>	<b>*ACOT</b>

Figure 5.42: *Lower and Upper Bounds of Cost of Transport (COT) for the Down/Up Stairs Walking Experiment.*

In Figure 5.43, the energy savings of the Decrease & Conquer based Methods, in comparison with the One-Phase based ones, are shown.

As we can see, the Decrease & Conquer based Discrete Mechanics Method achieves energy savings between 10.29% (for  $N = 20$ ) - 84.21% (for  $N = 110$ ), in comparison with the One Phase based related Method, while the Decrease & Conquer based Direct Collocation Method achieves energy savings between 13.77% (for  $N = 10$ ) - 89.96% (for  $N = 110$ ), in comparison with the One Phase based related Method.

<i>Energy Savings of Decrease and Conquer Variants Vs One Phase Related Variants, for the (Down/Up) Stairs Walking Experiment (Percentage)</i>		
<b>N (points)</b>	<b>Discrete Mechanics</b>	<b>Direct Collocation</b>
10	10,72	13,77
20	10,29	17,09
30	15,01	14,45
40	16,65	16,95
50	23,14	27,88
60	25,83	34,25
70	33,43	39,95
80	54,57	60,01
90	71,39	75,77
100	80,74	84,61
110	84,21	89,96
120	82,76	89,02
130	80,34	87,02
140	77,54	85,08
150	73,81	81,93
160	68,15	78,14
170	59,04	70,48
180	57,41	69,65
190	57,41	69,65
200	57,41	69,65

Figure 5.43: *Energy Savings of Decrease and Conquer Variants in comparison with One Phase Related Variants, for the Down/Up Stairs Walking Experiment (Percentage).*

In Figure 5.44, the energy savings of the Decrease & Conquer based Methods, in comparison with SNOPT, are shown.

As we can see, the Decrease & Conquer based Discrete Mechanics Method achieves energy savings between 4.58% (for  $N = 10$ ) - 82.26% (for  $N = 110$ ), in comparison with SNOPT, while the Decrease & Conquer based Direct Collocation Method achieves energy savings between 10% (for  $N = 30$ ) - 89.05% (for  $N = 110$ ), in comparison with it.

Now we will show the plots of the 4-DOF biped robot, for  $N=110$ , which is the number of points where the Decrease & Conquer Feedback Control utilizing Direct Collocation Method achieves the lowest possible ACOT in the Down/Up Stairs Walking Experiment. Due to the fact that the Decrease & Conquer Feedback Control utilizing Discrete Mechanics Method results in similar results, only the results of the First Approach will be presented. Next, the actual plots of the 4-DOF Biped Robot, will be shown, under missing velocity signals and disturbances. In

<i>Energy Savings of Decrease and Conquer Variants Vs SNOPT, for the (Down/Up) Stairs Walking Experiment (Percentage)</i>		
<b>N (points)</b>	<b>Discrete Mechanics</b>	<b>Direct Collocation</b>
10	4,58	10,95
20	6,05	15,14
30	7,67	10
40	9,3	15,82
50	18,85	25,9
60	21,05	32,1
70	26,05	35,47
80	47,21	55,35
90	67,69	73,29
100	78,87	83,91
110	82,26	89,05
120	80,15	87,75
130	78,09	86,48
140	74,24	84,1
150	69,29	81,05
160	55,87	72,77
170	46,62	67,06
180	43,32	65,02
190	41,48	63,89
200	36,16	60,61

Figure 5.44: *Energy Savings of Decrease and Conquer Variants in comparison with SNOPT, for the Down/Up Stairs Walking Experiment (Percentage).*

addition, we assume that Leg 2 initially starts the walking process, thus it is the swing leg for the first walking step.

In Figure 5.45, the plots of desired and actual angles of the two Legs over time are shown. In addition, in Figures 5.46 and 5.47, the plots of the position errors over time are depicted.

From Figure 5.45, at each walking step, it can be seen that the angular displacement of the swing leg gradually increases over time. Some moments before the completion of each walking step (Heel Strike Moment), the angular displacement of the swing leg reaches the maximum, and then the swing leg swings back. When human stride reaches the maximum during walking, a swinging back process also occurs, which is consistent with the mechanism of the human movement. The angular displacement of the stance leg monotonically decreases, and when  $t=0.7343$  sec (Heel Strike Moment), the swing leg is in collision with the ground and the two legs switch roles. As the step length increases, the values of the angular displacements increase and vice versa.

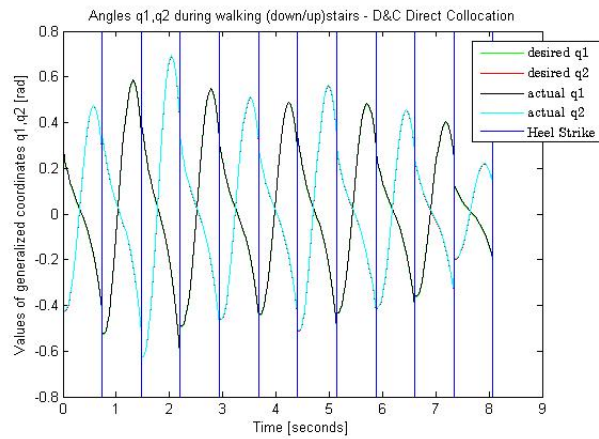


Figure 5.45: *Desired and actual angles during the Down/Up Stairs Walking Experiment - Decrease & Conquer Feedback Control utilizing Direct Collocation.*

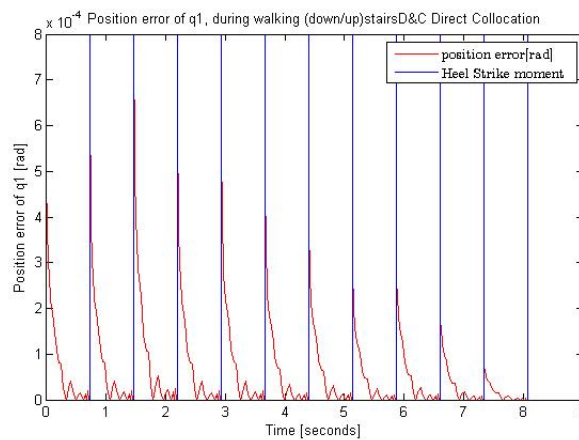


Figure 5.46: *Position error during the Down/Up Stairs Walking Experiment - Decrease & Conquer Feedback Control utilizing Direct Collocation.*

Furthermore, the desired and actual angular displacements of the two legs are nearly the same. From Figure 5.46 and 5.47, we can see that the position errors are extremely low ( $\approx 10^{-4}$ ), showing the effectiveness of the implemented trajectory tracking control.

In Figure 5.48, the plot of real and estimated angular velocities of the two legs over time is shown. In addition, in Figures 5.49 and 5.50, the plots of the velocity errors over time are depicted.

Based on Figures 5.48, 5.49 and 5.50, the real and estimated angular velocities of the two legs are nearly the same. From Figure 5.49 and 5.50, we can see that the velocity errors are extremely low ( $\approx 10^{-3} - 10^{-4}$ ), showing again the effectiveness of the trajectory tracking control. As the step length increases, the values of the angular velocities increase and vice versa.

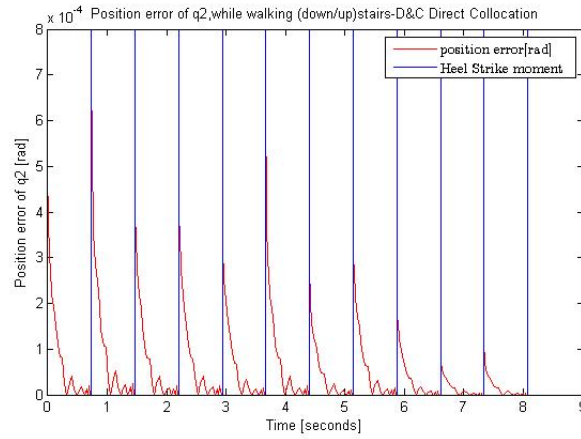


Figure 5.47: *Position error during the Down/Up Stairs Walking Experiment - Decrease & Conquer Feedback Control utilizing Direct Collocation.*

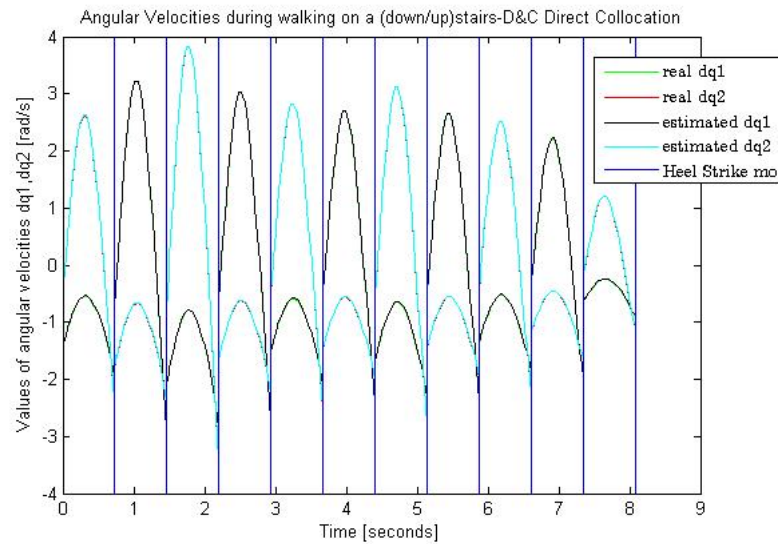


Figure 5.48: *Real and estimated angular velocities during the Upward Slope Walking Experiment - Decrease & Conquer Feedback Control utilizing Direct Collocation.*

In Figure 5.51, the control signals of the swing and stance leg over time during the Down/Up Stairs Walking Experiment are shown. We can see that at the beginning of each walking step, a larger torque should be input to the robot to realize dynamic walking, and with the input of the torque, the kinetic and potential energy are reasonably converted into driving energy; thereafter, only a small energy input can complete a walking step. The impact of the small inaccuracies on the estimation of the velocity signals and disturbances is an increase of the ACOT by just 1.2%.

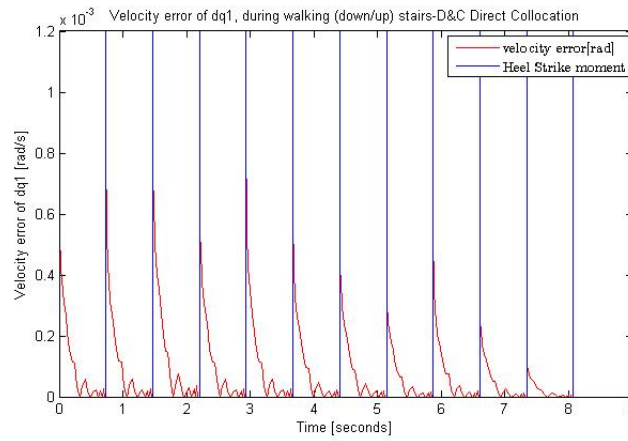


Figure 5.49: *Angular velocity errors of the Leg 1 during the Upward Slope Walking Experiment - Decrease & Conquer Feedback Control utilizing Direct Collocation.*

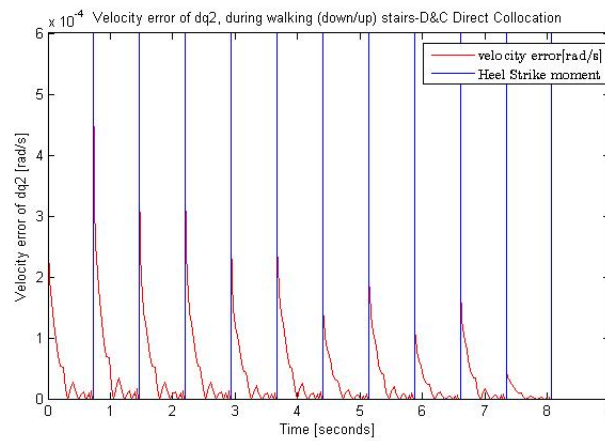


Figure 5.50: *Angular velocity errors of the Leg 2 during the Upward Slope Walking Experiment - Decrease & Conquer Feedback Control utilizing Direct Collocation.*

In Figure 5.52, the plot of Ground Reaction Forces (Vertical component: Normal Force, and horizontal component: Friction force) experienced during the Down/Up Stairs Walking Experiment, are shown. In biomechanics, that plot is called butterfly diagram, due to the fact that the two peaks of the Normal Force look like the wings of a butterfly. As the step length increases, the values of the Ground Reaction Forces increase and vice versa.

More specifically, in the first moment (time step) of each walking step, the new stance leg, due to the experienced Heel Strike Forces a moment before, tries to adjust posture to support dynamic walking, resulting in higher torque and thus leading to the first peak of the Normal Force. From the next time step till the 25 % of the walking step, the Normal Force is decreasing, due to the adjusted posture of the stance leg, leading to a smaller required torque to keep balancing.

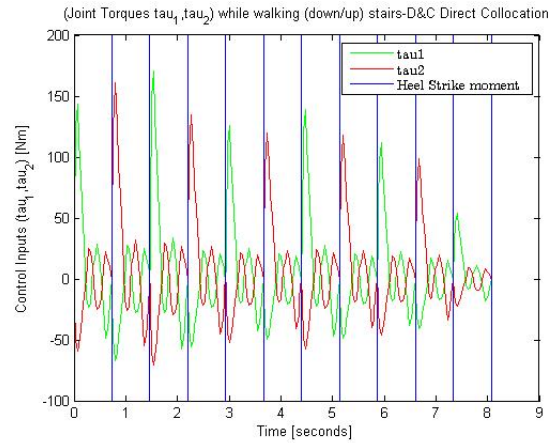


Figure 5.51: *Control Signals  $\tau_1$ ,  $\tau_2$  during the Down/Up Stairs Walking Experiment - Decrease & Conquer Feedback Control utilizing Direct Collocation.*

From that moment till the 50% of the walking step, we have an increase in the Normal Force, due to the fact that the stance leg becomes more vertical with the ground and at the half of the walking step the stance leg is completely vertical with it, supporting the whole weight of the robot, and resulting in the second peak of the Normal Force (this intermediate phase of the walking step is called midstance phase). From that moment till the end of the walking step, the Normal Force is decreasing (and it approaches zero), as the stance leg tends to be less vertical with the ground and the swing leg tends to approach the ground, taking an actual role for the support of the robot weight, both preparing to switch roles after the effects of the Push-Off and Heel Strike Phases. The Normal Force, throughout the entire walking step, is positive.

Regarding the values of the Friction Force, from the first time step of a walking step till the 10% of it, the friction force is decreasing and negative (at the 10% of the walking step we have a negative peak of the Friction force), due to the braking direction of the stance leg, resulting the Friction Force to act a backward (negative) force. From that moment till the 50% of the walking step, as we approach the midstance phase, the Friction Force is increasing (at the 50% of the walking step we have a positive peak of the Friction Force) as the stance leg becomes more vertical with the ground and tends to move in a more propulsive direction. From the 50% of the walking step, till the completion of it, the stance leg keeps its propulsive direction, and waits for the Push-Off and Heel Strike Phases to take effect and switch roles with the swing leg, thus the friction force tends to zero.

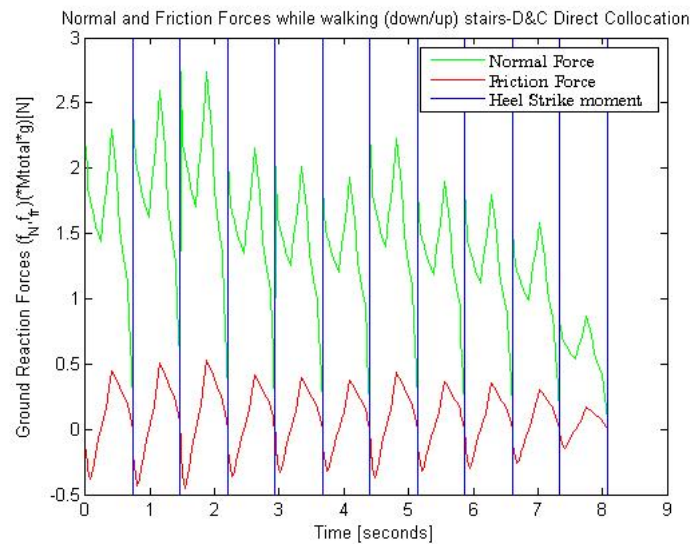


Figure 5.52: *Ground Reaction Forces during the Down/Up Stairs Walking Experiment - Decrease & Conquer Feedback Control utilizing Direct Collocation.*

In Figure 5.53, the Instantaneous Push-Off Impulses applied during the Down/Up Stairs Walking experiment, are shown. A Push-Off Impulse, as we have mentioned in previous Chapters, is required for the stance leg to be detached from the ground, while adding the required energy for the biped robot to be stabilized after the energy losses of the Heel Strike Phase. As the step length increases, the values of the Push-Off Impulse increase and vice versa.

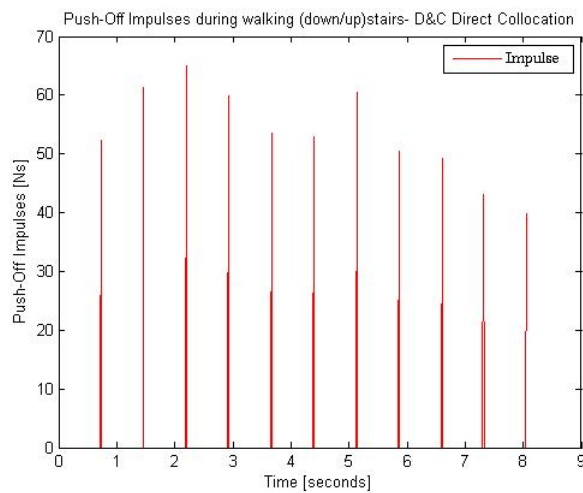


Figure 5.53: *Push-Off Impulses during the Down/Up Stairs Walking Experiment - Decrease & Conquer Feedback Control utilizing Direct Collocation.*

## 5.6 Energetics of Bipedal Robot Locomotion

Walking robots with different mechanical parameters, such as mass and length distribution, have different walking performance. This leads us to believe that for designing energy-optimal bipedal robot locomotion, the study and optimization of mechanical parameters is also an important issue as the study of walking gait features.

Thus, in the current subchapter we will investigate the effect of the mechanical parameters (mass and length distribution) on the energy efficiency of walking. In addition, we will study the energetic walking gait features with the combinations of walking speed ( $V_i$ ) and step length ( $D_i$ ). Such an interesting simulation study can lead to very important insights regarding the dynamics of walking and its related energetic gait features.

The non-dimensional parameters of the mass and length distribution are defined as:

$$\begin{cases} R_m = m_{(leg)}/M, \\ R_l = b/l \end{cases} \quad (5.1)$$

where the mass distribution parameter  $R_m$  is the ratio of the mass of a leg and the mass of the hip, and the length distribution parameter  $R_l$  is the ratio of the distance between the center of mass of a leg and the hip, and the leg length. The Cost of Transport, which is subjected to the constraints  $D_i$  and  $V_i$ , is calculated by varying one of the two distribution parameters, while another is fixed. In the following figure, the range of parameters used in the current study (in addition with the parameters for the experiments of the previous subchapters) are shown, taking into account biological parameter features.

All the current simulations are done for  $N=110$ , which is the largest value of  $N$  for which the Decrease & Conquer Feedback Control utilizing Direct Collocation achieves the least possible value of Cost of Transport for each carried experiment. Due to the fact that the Decrease & Conquer Feedback Control utilizing Discrete Mechanics Method results in similar results, only the results of the First Approach will be presented. Based on Figure 5.54, the parameters for the following simulations are non-dimensionalized.

Parameters	Values
Mass Distribution Parameter $R_m$	[0.2, 0.5]
Length Distribution Parameter $R_l$	[0.2, 0.6]
Non-Dimensional Step Length $D_i$ (*l) (m)	[0.2, 2]
Non-Dimensional Average Walking Speed $V_i$ (* $\sqrt{lg}$ ) (m/s)	[0.3, 0.8]
Grid Points	110
Square Root Smoothing Error Parameter $\epsilon$	0.1

Figure 5.54: Parameters for the current study and experiments.

In particular, we have initialized over 8000 biped robots with a variety of parameters. Then we let each one walk in the four types of terrain similar to the experiments in the previous subchapters. For Forward Walking, each biped runs 15 simulations of 80 walking steps of different step lengths and average walking speeds. For Walking on a Upward/Downward Slope and Stairs, each biped runs 15 simulations in a variety of step lengths, average walking speeds, step heights and slope/stair angles. The effect of a particular step height,  $H_i$ , for the Down/Up Stairs Experiments, is similar with the effects of the slope angle, while the effect of  $H_i$  is only 0.1 – 0.45% greater in comparison with the effect of the related slope angles and step lengths. Thus, it is not considered a biomechanical parameter in the current study.

For studying the effects of the mass distribution parameter  $R_m$  on the Cost of Transport (COT), we choose two representative fixed values in the range of length distribution parameter  $R_l$ . These values are  $R_l = 0.3$  and 0.6.

Figure 5.55 shows the COT as a function of  $R_m$  with various step lengths and a fixed walking speed of  $V=0.4$  and  $R_l = 0.3$ , while Figure 5.56 shows a sectional plot of the COT subject to  $R_m$  with fixed step length  $D$ , and Figure 5.57 shows the effect of the slope angle  $\theta$  in the COT of Figure 5.55 and 5.56.

Furthermore, Figure 5.58 shows the COT as a function of  $R_m$  with various step lengths and a fixed walking speed of  $V=0.6$  and  $R_l = 0.3$ , while Figure 5.59 shows a sectional plot of the COT subject to  $R_m$  with fixed step length  $D$ , and Figure 6.60 shows the effect of the slope

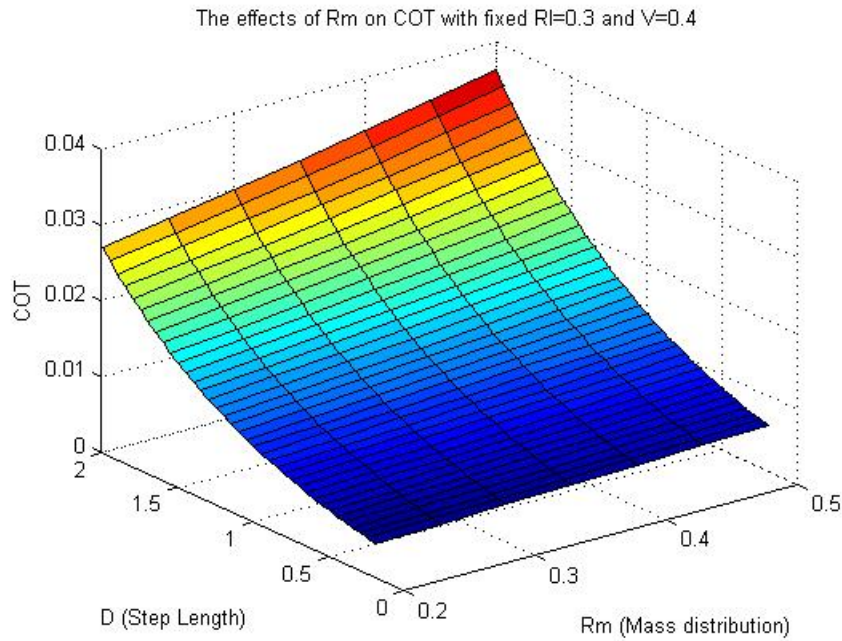


Figure 5.55: *The effects of  $R_m$  on COT with fixed  $R_l=0.3$  and  $V=0.4$ .*

angle  $\theta$  in the COT of Figure 5.58 and 5.59.

Based on Figures 5.55, 5.56, 5.58 and 5.59, we can see that the COT increases with the increase of  $R_m$  when  $R_l$ ,  $V$  and  $D$  are fixed. For a certain set of  $R_l$  and  $V$ , there will be a corresponding range of  $D$ , in which the COT is nearly minimal and  $R_m$  has little effect on the value of COT. As the step length  $D$  increases, the effect of  $R_m$  on COT becomes larger and more obvious.

Figures 5.57 and 5.60 show that for a negative slope angle ( $\theta < 0$ ) we have a decrease on the values of COT in the abovementioned Figures, from 0.9 to 26.8% for the first case and from 0.3 to 28.7% for the second case. In addition, for a positive slope angle ( $\theta > 0$ ), we have an increase on the values of COT in the abovementioned Figures, from 1.2 to 27.8% for the first case and from 1.9 to 30.3% for the second case.

Figure 5.61 shows the COT as a function of  $R_m$  with various step lengths and a fixed walking speed of  $V=0.4$  and  $R_l = 0.6$ , while Figure 5.62 shows a sectional plot of the COT subject to  $R_m$  with fixed step length  $D$ , and Figure 5.63 shows the effect of the slope angle  $\theta$  in the COT of Figure 5.61 and 5.62.

Figure 6.64 shows the COT as a function of  $R_m$  with various step lengths and a fixed walking

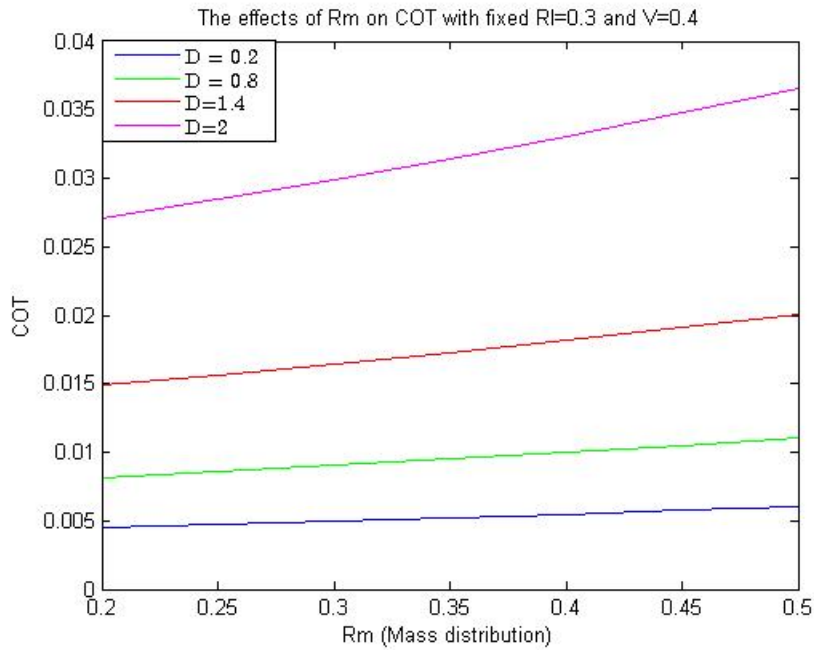


Figure 5.56: *The effects of  $R_m$  on COT with fixed  $R_l=0.3$  and  $V=0.4$  (Sectional Plot).*

speed of  $V=0.6$  and  $R_l = 0.6$ , while Figure 5.65 shows a sectional plot of the COT subject to  $R_m$  with fixed step length  $D$ , and Figure 5.66 shows the effect of the slope angle  $\theta$  in the COT of Figure 5.64 and 5.65.

The values of COT in Figures 5.61, 5.62 and 5.63 follow a similar behaviour as in the Figures 5.55-5.60, with a small difference on the fact that, for very small values of  $D$  (e.g.  $D=0.2$  in Figure 6.62), we have a larger value of COT in comparison with middle-sized step lengths (e.g.  $D=0.8$  in Figure 6.62). Figure 5.63 shows that for a negative slope angle ( $\theta < 0$ ) we have a decrease on the values of COT, from 0.73 to 14.7%. In addition, for a positive slope angle ( $\theta > 0$ ), we have an increase on the values of COT, from 4.9 to 20.6%.

Based on Figures 5.64 and 5.65 show clearly that the COT is bigger with short step length than long step length, which is different at all scales from the abovementioned analyzed figures. This is because the rotational actuator in the swing leg consumes more energy for the provided torque, under the situation of fast walking speed and short step length. Figure 5.66 shows that for a negative slope angle ( $\theta < 0$ ) we have a decrease on the values of COT in the abovementioned Figures, from 0.9 to 9.13%. In addition, for a positive slope angle ( $\theta > 0$ ), we have an increase on the values of COT, from 0.1 to 10.9%.

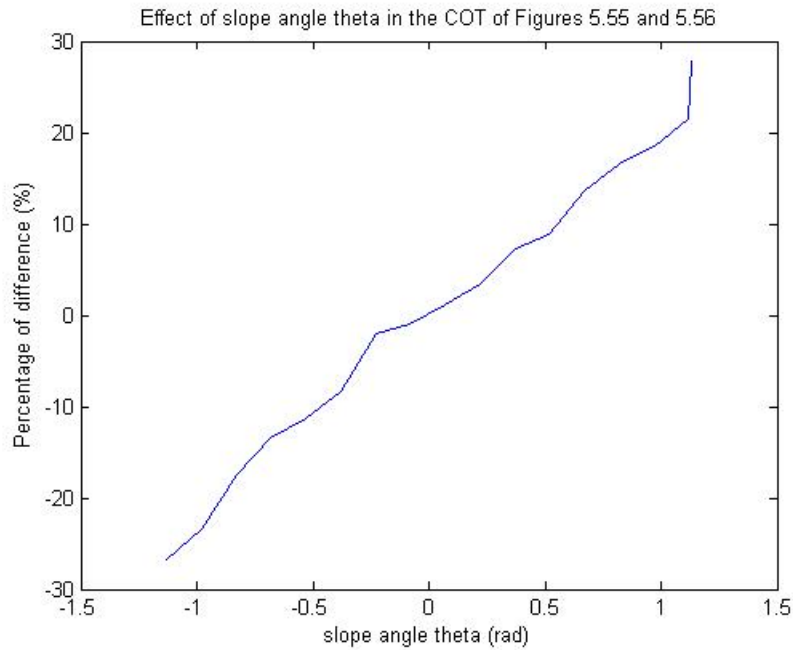


Figure 5.57: *Effect of slope angle  $\theta$  in the COT of Figures 5.55 and 5.56.*

Figure 5.67 shows the COT as a function of  $R_l$  with various step lengths and a fixed walking speed of  $V=0.4$  and  $R_m = 0.3$ , while Figure 5.68 shows a sectional plot of the COT subject to  $R_m$  with fixed step length  $D$ , and Figure 5.69 shows the effect of the slope angle  $\theta$  in the COT of Figures 5.67 and 5.68.

Figure 5.70 shows the COT as a function of  $R_l$  with various step lengths and a fixed walking speed of  $V=0.6$  and  $R_m = 0.3$ , while Figure 6.71 shows a sectional plot of the COT subject to  $R_m$  with fixed step length  $D$ , and Figure 5.72 shows the effect of the slope angle  $\theta$  in the COT of Figure 5.70 and 5.71.

In these figures (5.68-5.72) we can see that when the step length  $D$  is short, the COT increases with the increase in  $R_l$ . In addition, as  $R_l$  increases, the COT in cases of small step length may become greater than of the COT in cases of middle-valued step lengths (as it can be seen clearly on Figured 5.70, 5.72). With the increase in  $D$ , the curve of the COT versus  $R_l$  gets flat, which indicates that for a certain set of  $R_m$  and  $V$ , the effect of  $R_l$  on COT is also not so obvious within a range of step length  $D$  (as we can see on Figures 5.70, 5.72). In addition, we can see that, for long step length, the COT gradually increases and then decreases with the increase in  $R_l$ .

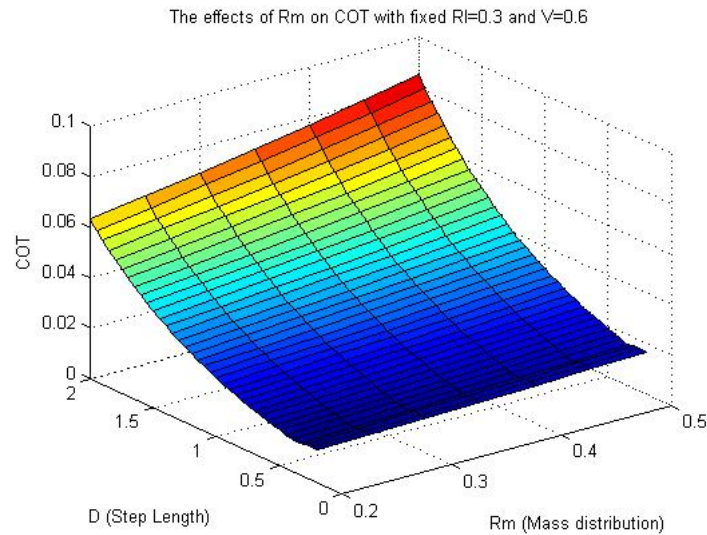


Figure 5.58: *The effects of  $R_m$  on COT with fixed  $R_l=0.3$  and  $V=0.6$ .*

In Figure 5.70, we can see that for a negative slope angle ( $\theta < 0$ ) we have a decrease on the values of COT in the related Figures, from 0.1 to 18.4%. In addition, for a positive slope angle ( $\theta > 0$ ), we have an increase on the values of COT, from 2.4 to 19.8%.

In Figure 5.72, we can see that for a negative slope angle ( $\theta < 0$ ) we have a decrease on the values of COT in the related Figures, from 1.1 to 21.4%. In addition, for a positive slope angle ( $\theta > 0$ ), we have an increase on the values of COT, from 3.4 to 24.55%.

Finally, Figure 5.73 shows the COT as a function of  $R_l$  with various step lengths and a fixed walking speed of  $V=0.4$  and  $R_m = 0.5$ , while Figure 5.74 shows a sectional plot of the COT subject to  $R_m$  with fixed step length  $D$ , and Figure 5.75 shows the effect of the slope angle  $\theta$  in the COT of Figure 5.73 and 5.74. In addition, Figure 5.76 shows the COT as a function of  $R_l$  with various step lengths and a fixed walking speed of  $V=0.6$  and  $R_m = 0.5$ , while Figure 5.77 shows a sectional plot of the COT subject to  $R_m$  with fixed step length  $D$ , and Figure 5.78 shows the effect of the slope angle  $\theta$  in the COT of Figure 5.76 and 5.77.

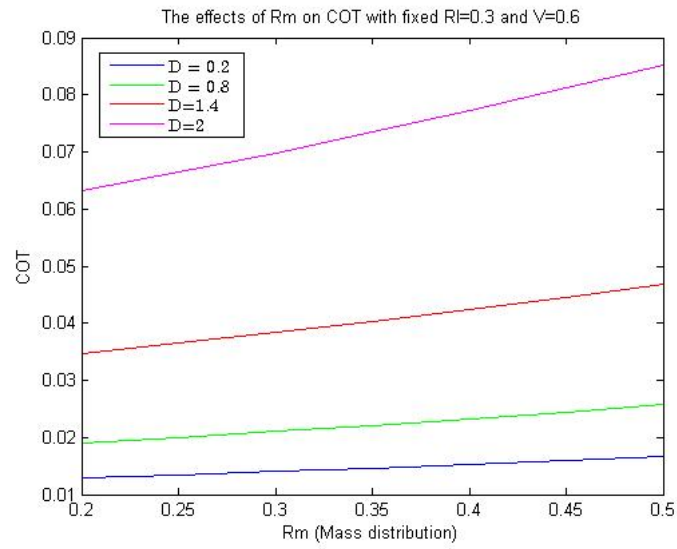


Figure 5.59: *The effects of Rm on COT with fixed  $Rl=0.3$  and  $V=0.6$  (Sectional Plot).*

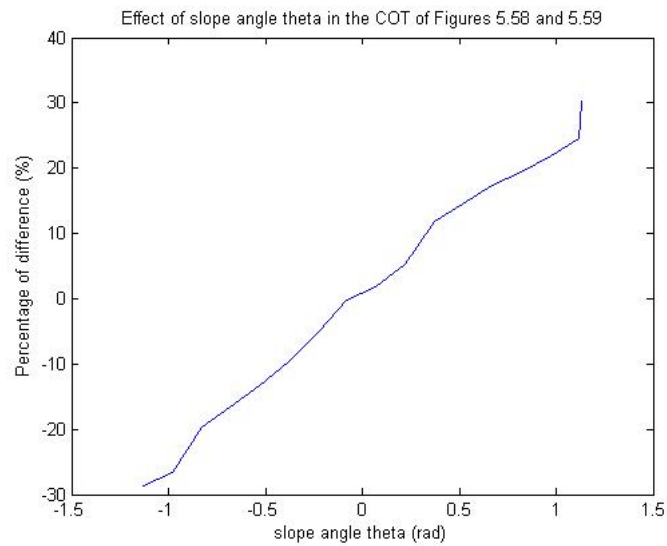


Figure 5.60: *Effect of slope angle theta in the COT of Figures 5.58 and 5.59.*

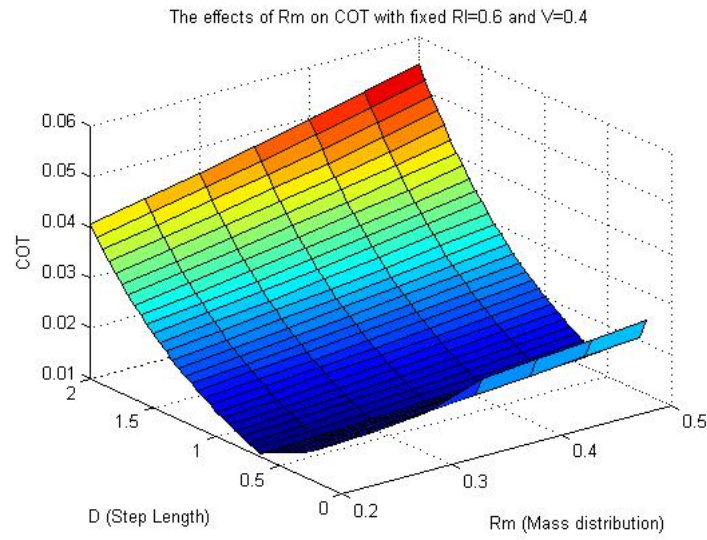


Figure 5.61: *The effects of Rm on COT with fixed Rl=0.6 and V=0.4.*

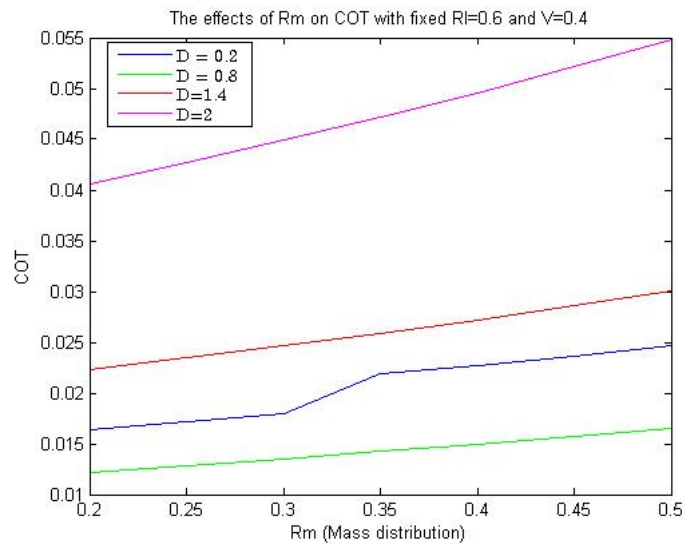


Figure 5.62: *The effects of Rm on COT with fixed Rl=0.6 and V=0.4 (Sectional Plot).*

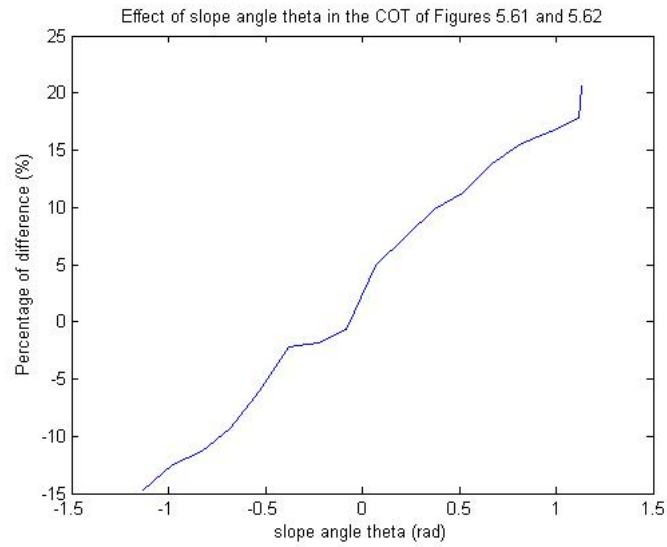


Figure 5.63: *Effect of slope angle theta in the COT of Figures 5.61 and 5.62.*

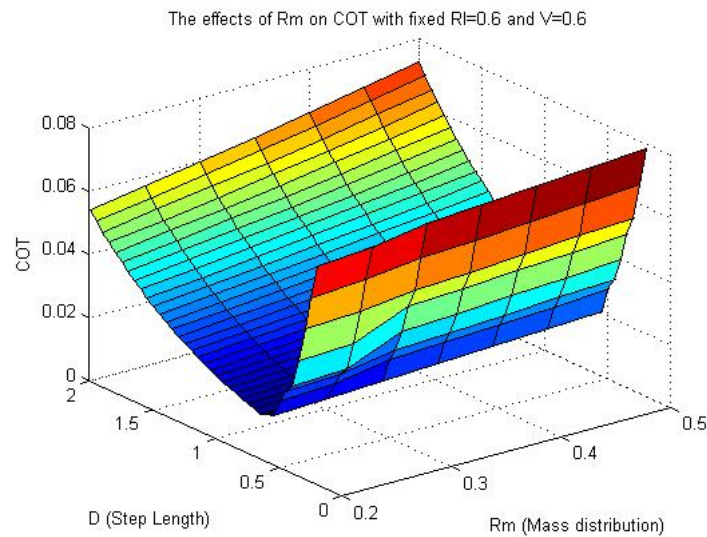


Figure 5.64: *The effects of Rm on COT with fixed Rl=0.6 and V=0.6.*

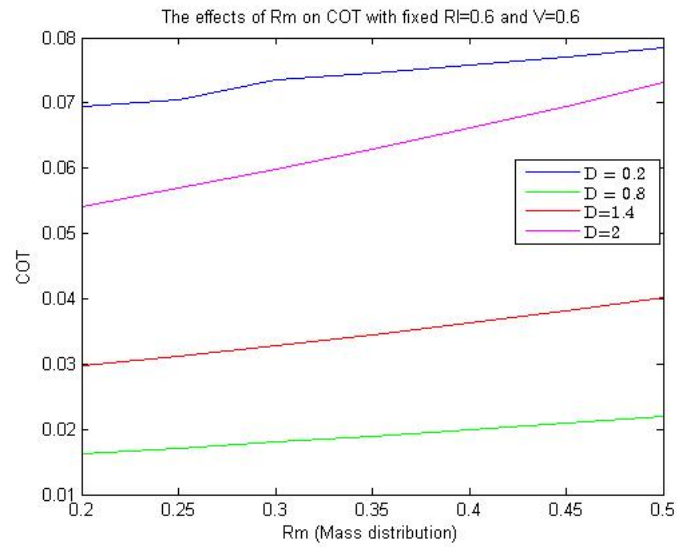


Figure 5.65: *The effects of  $R_m$  on COT with fixed  $R_l=0.6$  and  $V=0.6$  (Sectional Plot).*

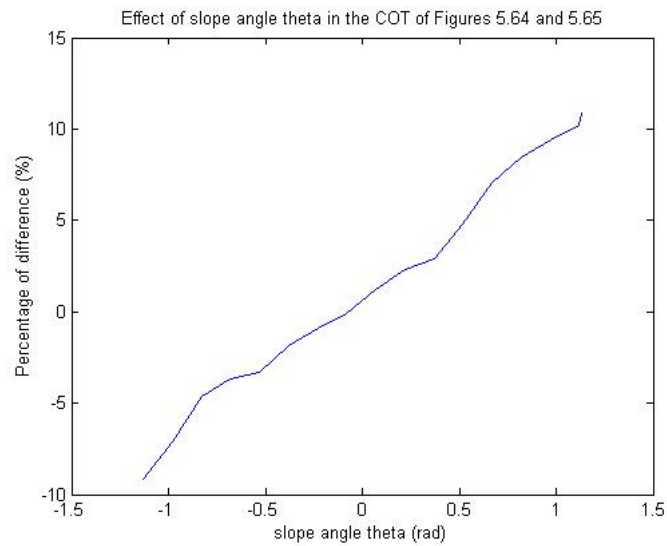


Figure 5.66: *Effect of slope angle  $\theta$  in the COT of Figures 5.64 and 5.65.*

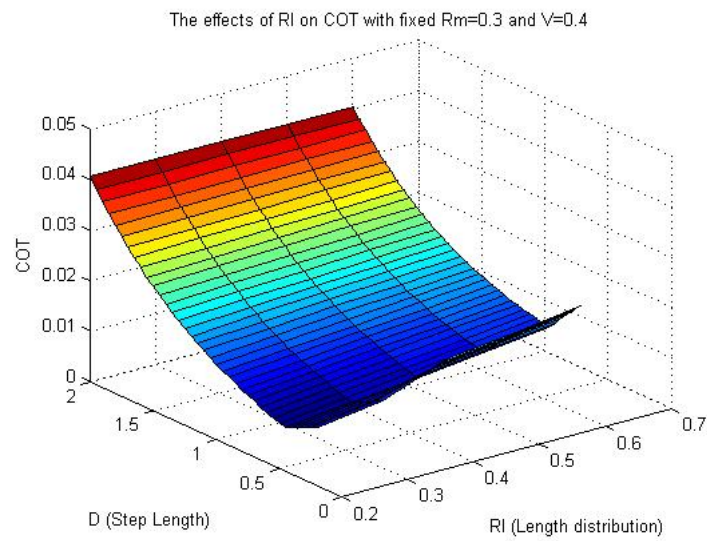


Figure 5.67: *The effects of RI on COT with fixed  $R_m=0.3$  and  $V=0.4$ .*

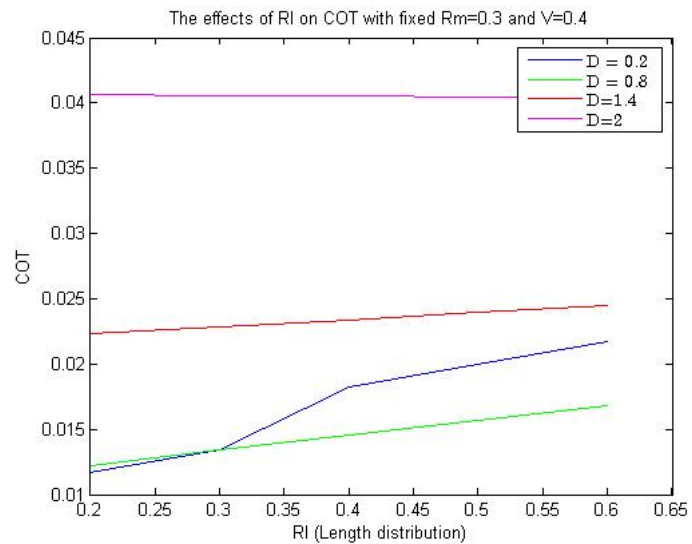


Figure 5.68: *The effects of  $R_m$  on COT with fixed  $R_m=0.3$  and  $V=0.4$  (Sectional Plot).*

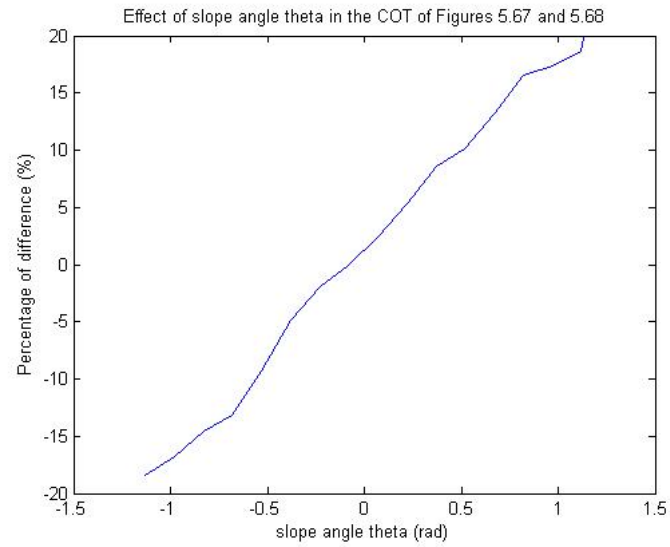


Figure 5.69: *Effect of slope angle theta in the COT of Figures 5.67 and 5.68.*

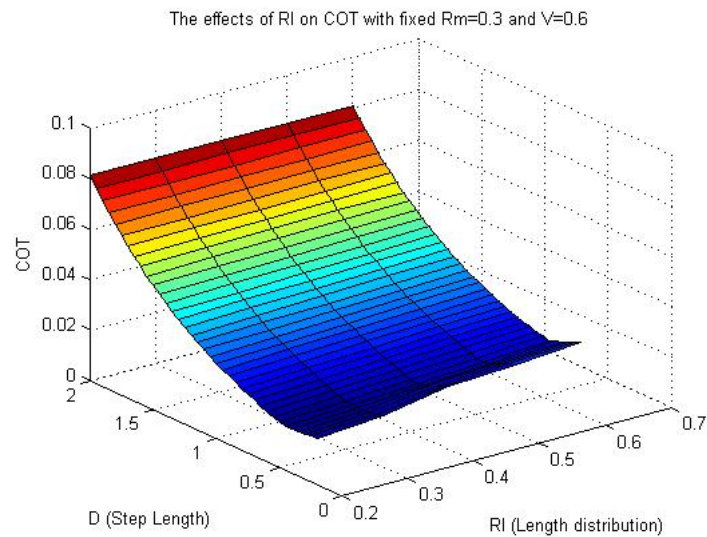


Figure 5.70: *The effects of RI on COT with fixed  $R_m=0.3$  and  $V=0.6$ .*

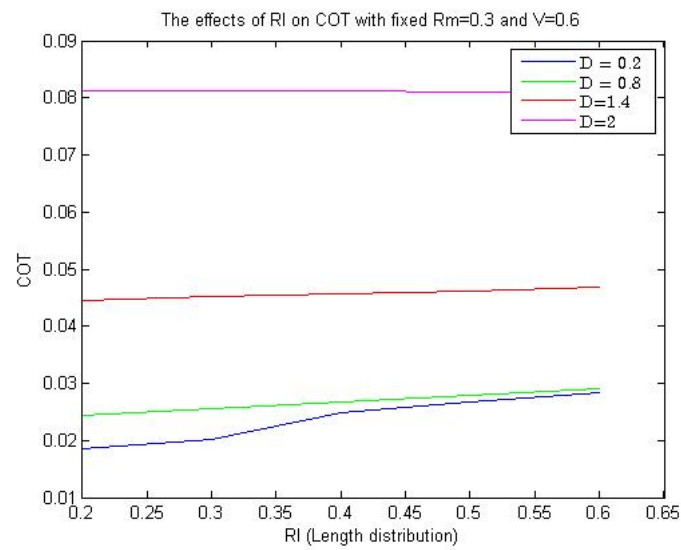


Figure 5.71: *The effects of  $R_m$  on COT with fixed  $R_m=0.3$  and  $V=0.6$  (Sectional Plot).*

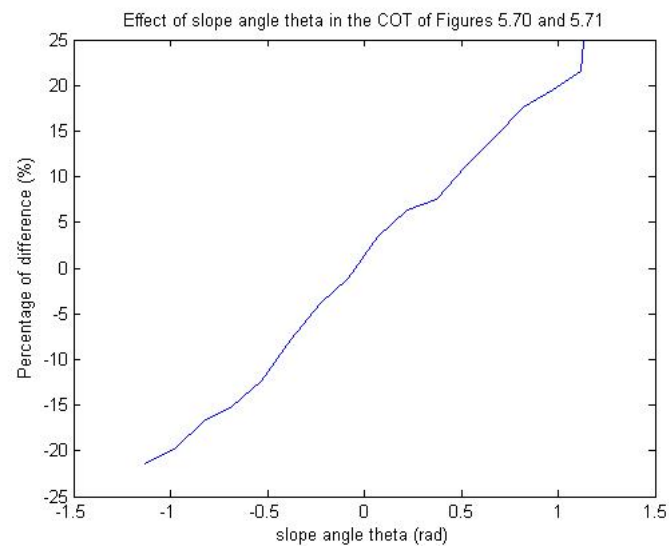


Figure 5.72: *Effect of slope angle  $\theta$  in the COT of Figures 5.70 and 5.71.*

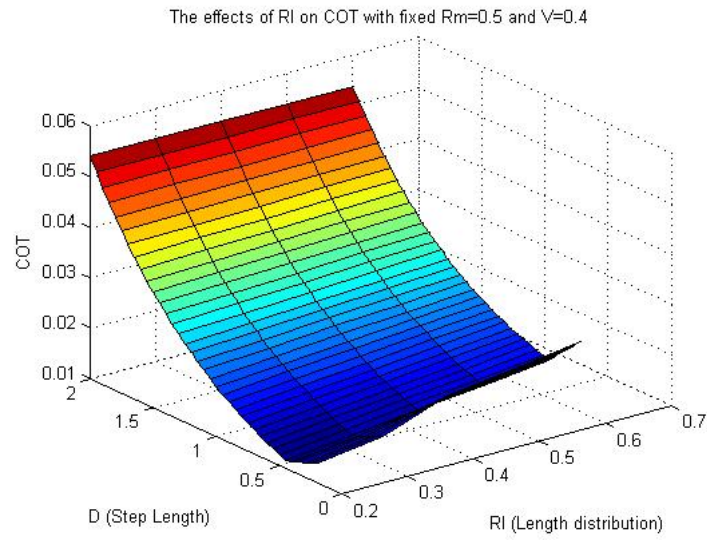


Figure 5.73: *The effects of RI on COT with fixed  $Rm=0.5$  and  $V=0.4$ .*

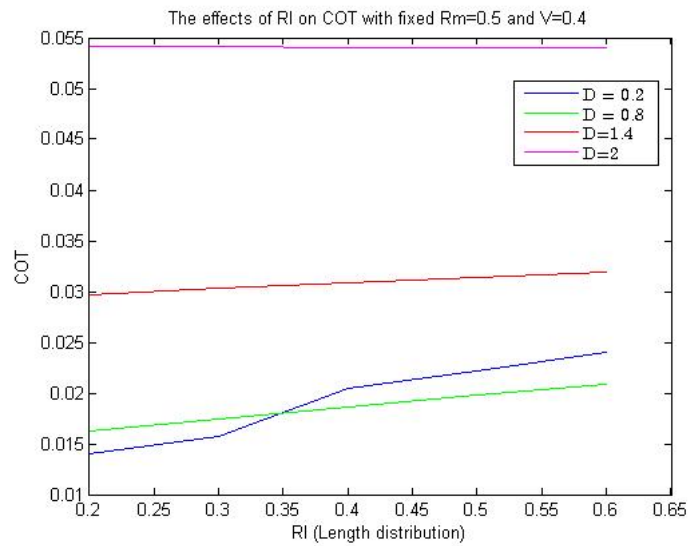


Figure 5.74: *The effects of  $Rm$  on COT with fixed  $Rm=0.5$  and  $V=0.4$  (Sectional Plot).*

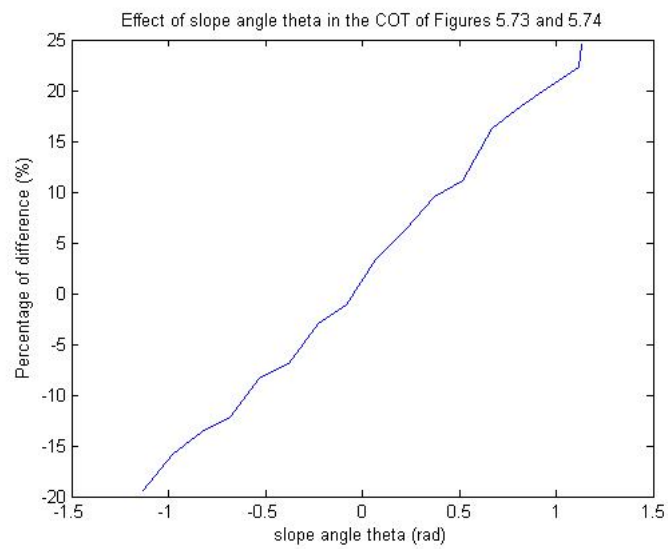


Figure 5.75: *Effect of slope angle theta in the COT of Figures 5.73 and 5.74.*

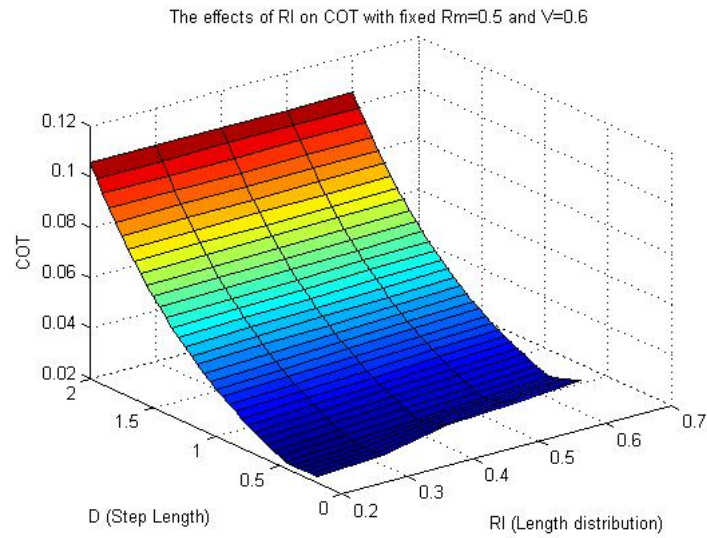


Figure 5.76: *The effects of RI on COT with fixed  $R_m=0.5$  and  $V=0.6$ .*

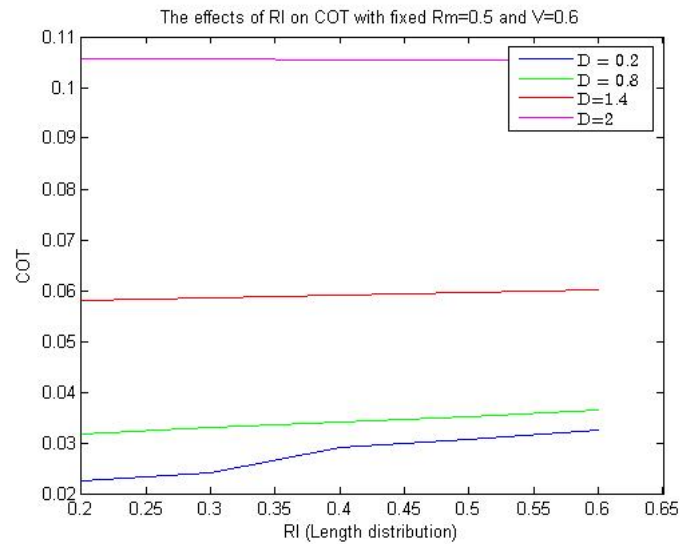


Figure 5.77: *The effects of  $R_m$  on COT with fixed  $R_m=0.5$  and  $V=0.6$  (Sectional Plot).*

As we can see, these Figures behave in a similar way with Figures 5.68-5.72, having only a greater influence of the  $R_l$  on the values of COT, thus larger values of COT.

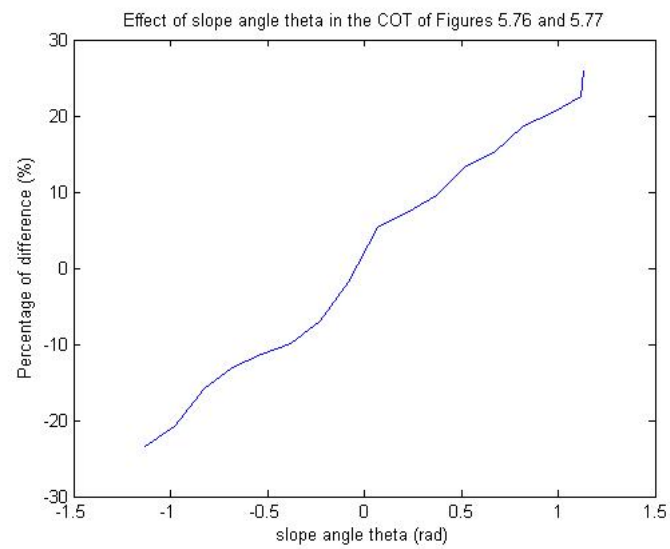


Figure 5.78: *Effect of slope angle theta in the COT of Figures 5.76 and 5.77.*

# Chapter 6

## Conclusion and Future Work

In the current thesis we proposed a novel approach for calculation of energy-optimal trajectories and effective trajectory tracking control for bipedal robot locomotion, called Decrease and Conquer Feedback Control. The proposed system consists of the Gait Generation and Trajectory Tracking Control Modules. We also developed two variants of the proposed system, based on two discretization methods: Direct Collocation and Discrete Mechanics.

The Decrease and Conquer Gait Generation Module (Direct Collocation/Discrete Mechanics) turns out to calculate the most energy efficient trajectories for the complete 4-DOF biped robot, in comparison with the related One Phase methods and the high performance commercial solver SNOPT. In particular, in the majority of the experiments, the Decrease and Conquer Approach requires less than half of the grid points to calculate energy-optimal trajectories. The other methods need at least twice as many grid points to calculate a suboptimal trajectory. The Direct Collocation method calculates always the most energy efficient trajectories.

The Trajectory Tracking Control Module turns out to apply a very effective tracking control scheme, under missing velocity signals and disturbances. As we have seen on Chapter 4, the small inaccuracies in the estimation of the velocities and disturbances (error of  $\approx 10^{-3} - 10^{-4}$ ) have minimal impact on the final energy consumption of the walking step ( $\leq 1.2\%$ ).

There are several directions in which we would like to extend our work. The main ones are

presented below:

1. The use and evaluation of a different robot model in the proposed system architecture, e.g. of a 5-link (7-DOF) biped robot model etc.
2. Implementation of a Decrease and Conquer approach utilizing other discretization methods (single/multiple shooting, adjoint methods etc.)
3. Utilization of code parallelism for the solution of the Gait Generation problems of the Second Phase.
4. Evaluation of the proposed system in more complex environments.
5. Real-time implementation of the proposed system.
6. Application of a Decrease and Conquer Approach for Gait Generation problems in other domains.

# Chapter 7

## Bibliography

- [1] M. Vukobratovic, B. Borovac, D. Surla, and D. Stokic, Biped Locomotion: Dynamics, Stability, Control and Application (Scientific Fundamentals of Robotics). Springer, 1990.
- [2] K. Hirai, M. Hirose, Y. Haikawa, and T. Takenaka, "The development of Honda humanoid robot," in Proceedings of the IEEE International Conference on Robotics and Automation, vol. 2, May 1998, pp. 1321-1326.
- [3] Q. Huang, K. Yokoi, S. Kajita, K. Kaneko, H. Arai, N. Koyachi, and K. Tanie, Planning walking patterns for a biped robot, IEEE Transactions on Robotics and Automation, vol. 17, no. 3, pp. 280-289, 2001.
- [4] S. Kajita and K. Tani, Experimental study of biped dynamic walking, IEEE Control System Magazine, vol. 16, no. 1, pp. 13 - 19, 1996
- [5] S. Kajita, F. Kanehiro, K. Kaneko, K. Fujiwara, K. Harada, K. Yokoi, and H. Hirukawa, Biped walking pattern generation by using preview control of zero-moment point, in Proceedings of the IEEE International Conference on Robotics and Automation, vol. 2, 2003, pp. 1620 - 1626.
- [6] S. Kajita, F. Kanehiro, K. Kaneko, K. Yokoi, and H. Hirukawa, The 3D linear inverted pendulum mode: a simple modeling for a biped walking pattern generation, in Proceedings of

---

the IEEE/RSJ International Conference on Intelligent Robots and Systems, vol. 1, 2001, pp. 239 - 246.

[7] S. Kajita, O. Matsumoto, and M. Saigo, Real-time 3D walking pattern generation for a biped robot with telescopic legs, in Proceedings of the IEEE International Conference on Robotics and Automation, vol. 3, 2001, pp. 2299 - 2306

[8] C. Chevallereau, D. Djoudi, and J. Grizzle, Stable bipedal walking with foot rotation through direct regulation of the zero moment point, IEEE Transactions on Robotics, vol. 24, no. 2, pp. 390 - 401, April 2008.

[9] K. Loffler, M. Gienger, F. Pfeiffer, and H. Ulbrich, Sensors and control concept of a biped robot, IEEE Transactions on Industrial Electronics, vol. 51, no. 5, pp. 972 - 980, 2004.

[10] T. Komura, H. Leung, S. Kudoh, and J. Kuffner, A feedback controller for biped humanoids that can counteract large perturbations during gait, in Proceedings of the IEEE International Conference on Robotics and Automation, April 2005, pp. 1989 - 1995.

[11] P. B. Wieber and C. Chevallereau, Online adaptation of reference trajectories for the control of walking systems, Robotics and Autonomous Systems, vol. 54, no. 7, pp. 559-566, 2006.

[12] C. Dembria, " Optimization of a point-mass walking model using Direct Collocation and Sequential Quadratic Programming", Project Report, Stanford University, 2005.

[13] D. Pekarek, A.D. Ames, J.E. Marsden, "Discrete Mechanics and Optimal Control applied to the Compass Gait Biped", In: 46th IEEE Conference on Decision and Control. Proceedings IEEE Conference on Decision and Control. IEEE, Piscataway, NJ, pp. 5376-5382, 2007.

[14] Z. Zhu, W. Zhang, Z. Geng, 'A feasible SQP method for nonlinear programming", Applied Mathematics and Computation, Elsevier, 2010.

[15] R. Silva, M. Ulbrich, S. Ulbrich, L.N. Vicente, "A Globally Convergent Primal-Dual Interior Point Filter Method For Nonlinear Programming: New Filter Optimality Measures and Computational Results", Mathematical Programming, Springer, 2004.

- [16] T. McGeer, Passive dynamic walking, *The International Journal of Robotics Research*, vol. 9, no. 2, pp. 6282, February 1990.
- [17] A. Goswami, B. Thuilot, and B. Espiau, A study of the passive gait of a compass-like biped robot: Symmetry and chaos, *International Journal of Robotics Research*, vol. 17, no. 12, pp. 12821301, December 1998.
- [18] S.H. Collins, A. Ruina, R. Tedrake, and M. Wisse, Efficient bipedal robots based on passive dynamic walkers, *Science*, vol. 307, pp. 10821085, 2005.
- [19] A. Goswami, B. Espiau, and A. Keramane, Limit cycles in a passive compass gait biped and passivity mimicking control laws, *Autonomous Robots*, vol. 4, pp. 273286, 1997.
- [20] M. Garcia, A. Chatterjee, A. Ruina, and M.J. Coleman, The simplest walking model: stability, complexity, and scaling, *ASME Journal of Biomech. Eng.*, vol. 120, no. 2, pp. 281288, February 1998.
- [21] J.W. Grizzle, G. Abba, and F. Plestan, Asymptotically stable walking for biped robots: Analysis via systems with impulse effects, *IEEE Trans. on Automatic Control*, vol. 46, no. 1, pp. 5164, January 2001.
- [21] J. Hass, J.M. Herrmann, and T. Geisel, Optimal mass distribution for passivity-based bipedal robots, *International Journal of Robotics Research*, vol. 25, no. 11, pp. 10871098, November 2006.
- [22] D.G.E. Hobbelen and M. Wisse, Swing-leg retraction for limit cycle walkers improves disturbance rejection, *IEEE Transactions on Robotics*, vol. 24, no. 2, pp. 377389, February 2008.
- [23] Q. Huang, K. Yokoi, S. Kajita, K. Kaneko, H. Arai, N. Koyachi, and K. Tanie, Planning walking patterns for a biped robot, *IEEE Transactions on Robotics and Automation*, vol. 17, no. 3, pp. 280289, March 2001.
- [24] P. Sardain and G. Bessonnet, Forces acting on a biped robot. center of pressure Zero moment point, *IEEE Transactions on Systems, Man, and Cybernetics, Part A: Systems and*

---

Humans, vol. 34, no. 5, pp. 630637, May 2004.

[25] Z.Sun, Y.Tian, H.Li, J.Wang, "A superlinear convergence feasible sequential quadratic programming algorithm for bipedal dynamic walking robot via discrete mechanics and optimal control", *Optimal Control Applications and Methods*, Wiley, 2015.

[26] K. Erbaturo and O. Kurt, Natural ZMP trajectories for biped robot reference generation, *IEEE Transactions on Industrial Electronics*, vol. 56, no. 3, pp. 835845, March 2009.

[27] G. Taga, Y. Yamaguchi, and H. Shimizu, Self-organized control of bipedal locomotion by neural oscillators in unpredictable environment, *Biological Cybernetics*, vol. 65, pp. 147159, 1991.

[28] W.T. Miller, Real-time neural network control of a biped walking robot, *IEEE Control Systems Magazine*, vol. 14, no. 1, pp. 4148, January 1994.

[29] J. Nakanishi, J. Morimoto, G. Endo, G. Cheng, S. Schaal, and M. Kawato, Learning from demonstration and adaptation of biped locomotion, *Robotics and Autonomous Systems*, vol. 47, pp. 7991, 2004.

[30] J. Morimoto and C.G. Atkeson, Learning biped locomotion: Application of poincare-map-based reinforcement learning, *IEEE Robotics & Automation Magazine*, vol. 14, no. 2, pp. 4151, June 2007.

[31] J.E. Marsden, G.W. Patrick, and S. Shkoller, Multisymplectic geometry, variational integrators and nonlinear PDEs, *Communications in Mathematical Physics*, vol. 199, pp. 351395, 1998.

[32] C. Kane, J.E. Marsden, M. Ortiz, and M. West, Variational integrators and the newmark algorithm for conservative and dissipative mechanical systems, *International Journal for Numerical Methods in Engineering*, vol. 49, pp. 12951325, 2000.

[33] J.E. Marsden and M. West, Discrete mechanics and variational integrators, *Acta Numerica*, vol. 10, pp. 35715145, 2001.

- [34] O. Junge, J.E. Marsden, and S. Ober-Blobaum, Discrete mechanics and optimal control, Proc. of 16th IFAC World Congress, Paper No. We-M14-TO/3, 2005.
- [35] A.M. Bloch, M. Leok, J.E. Marsden and D.V. Zenkov, Controlled lagrangians and stabilization of the discrete cart-pendulum system, Proc. of 44th IEEE CDC-ECC, pp. 65796584, 2005.
- [36] A.M. Bloch, M. Leok, J.E. Marsden, and D.V. Zenkov, Controlled lagrangians and potential shaping for stabilization of the discrete mechanical systems, Proc. of 45th IEEE CDC, pp. 33333338, 2006.
- [37] T. Kai and Y. Yamamoto, On analysis and control of the cart-pendulum system modeled by discrete mechanics, Proc. NOLTA07, pp. 485488, 2007.
- [38] T. Kai and K. Bito, Solvability analysis and stabilization of the cart-pendulum modeled by discrete mechanics with friction, Proc. NOLTA08, pp. 305308, 2008.
- [39] T. Kai and T. Shintani, Stabilization control and experiments of the cart-pendulum based on discrete mechanics, Proc. NOLTA09, pp. 8285, 2009.
- [40] C.B. Gurwitz, Sequential Quadratic Programming Methods Based on Approximating a Projected Hessian Matrix, General Books, 2001.
- [41] E.R. Westervelt, J.W. Grizzle, and C. Canudas de Wit, Switching and PI control of walking motions of planar biped walkers, IEEE Transactions on Automatic Control, vol. 48, no. 2, pp. 308312, February 2003.

# Chapter 8

## Appendix A: Modeling & Control of Lagrangian Mechanical Systems

### 8.1 Analytical Mechanics / Lagrangian mechanics

#### 8.1.1 Introduction

Lagrangian mechanics is a reformulation of classical mechanics. In Lagrangian mechanics, the trajectory of a system of particles is derived by solving the Lagrange equations in one of two forms, either the Lagrange equations of the first kind, which treat constraints explicitly as extra equations, often using Lagrange multipliers; or the Lagrange equations of the second kind, which incorporate the constraints directly by judicious choice of generalized coordinates. In each case, a mathematical function called the Lagrangian is a function of the generalized coordinates, their time derivatives, and time, and contains the information about the dynamics of the system.

In Newtonian Mechanics, Newton's laws can include non-conservative forces like friction, however they must include constraint forces explicitly and are best suited to Cartesian coordinates. Lagrangian mechanics is ideal for systems with conservative forces and for bypassing constraint forces in any coordinate system. Dissipative and driven forces can be accounted for by splitting

the external forces into a sum of potential and non-potential forces, leading to a set of modified Euler-Lagrange (EL) equations. Generalized coordinates can be chosen by convenience, to exploit symmetries in the system or the geometry of the constraints, which may simplify solving for the motion of the system. Lagrangian mechanics also reveals conserved quantities and their symmetries in a direct way, as a special case of Noether's theorem.

### 8.1.2 Holonomic constraints and degrees of freedom

Consider a system of  $N$  particles in two dimensional space, each with position vector  $r(t)$  for  $i = 1, \dots, N$ . Note that each  $r_i(t) \in \mathbb{R}^2$  is a 2-vector. We thus need  $2N$  coordinates to specify the system, this is the configuration space. Newton's second law tells us that the equation of motion for the  $i$ -th particle is:

$$\dot{p}_i = F_i^{\text{ext}} + F_i^{\text{con}} \quad (8.1)$$

for  $i = 1, \dots, N$ . Here  $p_i = m_i v_i$  is the linear momentum of the  $i$ th particle and  $v_i = \dot{r}_i$  is its velocity. We decompose the total force on the  $i$ th particle into an external force  $F_i^{\text{ext}}$  and a *constraint* force  $F_i^{\text{con}}$ . By external forces we imagine forces due to gravitational attraction or an electromagnetic field, and so forth.

By a constraint on a particles we imagine that the particle's motion is limited in some rigid way. For example the particle/bead may be constrained to move along a wire or its motion is constrained to a given surface. If the system of  $N$  particles constitute a rigid body, then the distances between all the particles are rigidly fixed and we have the constraint

$$|r_i(t) - r_j(t)| = c_{ij}, \quad (8.2)$$

for some constants  $c_{ij}$ , for all  $i, j = 1, \dots, N$ . All of these are examples of holonomic constraints.

**Definition 1 (Holonomic constraints).** For a system of particles with positions given by  $r(t)$  for  $i = 1, \dots, N$ , constraints that can be expressed in the form:

$$g(r_1, \dots, r_N, t) = 0 \quad (8.3)$$

are said to be holonomic. Note they only involve the configuration coordinates.

We will only consider systems for which the constraints are holonomic. Systems with constraints that are non-holonomic are: gas molecules in a container (the constraint is only expressible as an inequality); or a sphere rolling on a rough surface without slipping (the constraint condition is one of matched velocities).

Let us suppose that for the  $N$  particles there are  $m$  holonomic constraints given by:

$$g_k(r_1, \dots, r_N, t) = 0 \quad (8.4)$$

for  $k = 1, \dots, m$ . The positions  $r_i(t)$  of all  $N$  particles are determined by  $2N$  coordinates. However due to the constraints, the positions  $r_i(t)$  are not all independent. In principle, we can use the  $m$  holonomic constraints to eliminate  $m$  of the  $2N$  coordinates and we would be left with  $2N - m$  independent coordinates, i.e. the dimension of the configuration space is actually  $2N - m$ .

**Definition 2 (Degrees of freedom).** The dimension of the configuration space is called the number of degrees of freedom.

Thus we can transform from the previous coordinates  $r_1, \dots, r_N$  to new generalized coordinates  $q_1, \dots, q_n$  where  $n = 2N - m$ :

$$\begin{aligned} r_1 &= r_1(q_1, \dots, q_n, t), \\ &\cdot \\ &\cdot \\ &\cdot \\ r_N &= r_N(q_1, \dots, q_n, t). \end{aligned} \quad (8.5)$$

### 8.1.3 D'Alembert's principle

We will firstly restrict ourselves to systems for which the net work of the constraint forces is zero, i.e. we suppose:

$$\sum_{i=1}^N F_i^{\text{con}} \cdot dr_i = 0, \quad (8.6)$$

for every small change  $dr_i$  of the configuration of the system (for  $t$  fixed). Recall that the work done by a particle is given by the force acting on the particle times the distance travelled in the direction of the force. So here for the  $i$ th particle, the constraint force applied is  $F_i^{\text{con}}$  and suppose it undergoes a small displacement given by the vector  $dr_i$ . Since the dot product of two vectors gives the projection of one vector in the direction of the other, the dot product  $F_i^{\text{con}} \cdot dr_i$  gives the work done by  $F_i^{\text{con}}$  in the direction of the displacement  $dr_i$ .

If we combine the assumption that the net work of the constraint forces is zero with Newton's 2nd law :

$$\dot{p}_i = F_i^{\text{ext}} + F_i^{\text{con}} \quad (8.7)$$

from the last section we find:

$$\begin{aligned} \sum_{i=1}^N \dot{p}_i \cdot dr_i &= \sum_{i=1}^N (F_i^{\text{ext}} + F_i^{\text{con}}) \cdot dr_i \\ \Leftrightarrow \sum_{i=1}^N \dot{p}_i \cdot dr_i &= \sum_{i=1}^N F_i^{\text{ext}} \cdot dr_i + \sum_{i=1}^N F_i^{\text{con}} \cdot dr_i \\ \Leftrightarrow \sum_{i=1}^N \dot{p}_i \cdot dr_i &= \sum_{i=1}^N F_i^{\text{ext}} \cdot dr_i. \end{aligned} \quad (8.8)$$

In other words we have

$$\sum_{i=1}^N (\dot{p}_i - F_i^{\text{ext}}) \cdot dr_i = 0, \quad (8.9)$$

for every small change  $dr_i$ . This represents D'Alembert's principle. Note in particular that for now, no forces of constraint are present.

**Remark 1.** The assumption that the constraint force does no net work is quite general. It is true in particular for holonomic constraints. For example, for the case of a rigid body, the internal forces of constraint do no work as the distances  $|r_i - r_j|$  between particles is fixed, then  $d(r_i - r_j)$  is perpendicular to  $r_i - r_j$  and hence perpendicular to the force between them which

is parallel to  $r_i - r_j$ . Similarly for the case of the bead on a wire or particle constrained to move on a surface—the normal reaction forces are perpendicular to  $dr_i$ .

In his *Mécanique Analytique* [1788], Lagrange sought a coordinate invariant expression for mass times acceleration. This led to Lagrange's equations of motion. Consider the transformation to generalized coordinates

$$r_i = r_i(q_1, \dots, q_n, t) \quad (8.10)$$

for  $i = 1, \dots, N$ . If we consider a small increment in the displacements  $dr_i$  then the corresponding increment in the work done by the external forces is

$$\sum_{i=1}^N F_i^{\text{ext}} \cdot dr_i = \sum_{i,j=1}^{N,n} F_i^{\text{ext}} \cdot \frac{\partial r_i}{\partial q_j} dq_j = \sum_{j=1}^n Q_j dq_j \quad (8.11)$$

Here we have used the chain rule

$$dr_i = \sum_{j=1}^n \frac{\partial r_i}{\partial q_j} dq_j \quad (8.12)$$

and we set for  $j = 1, \dots, n$ ,

$$Q_j = \sum_{i=1}^N F_i^{\text{ext}} \cdot \frac{\partial r_i}{\partial q_j} \quad (8.13)$$

We think of the  $Q_j$  as generalized forces. We now assume the work done by these forces depends on the initial and final configurations only and not on the path between them. In other words we assume there exists a potential function  $V = V(q_1, \dots, q_n)$  such that

$$Q_j = -\frac{\partial V}{\partial q_j} \quad (8.14)$$

for  $j = 1, \dots, n$ . Such forces are said to be *conservative*. We define the total *kinetic energy* to be

$$T := \sum_{i=1}^N \frac{1}{2} m_i |v_i|^2 \quad (8.15)$$

and the Lagrange function or Lagrangian to be

$$L := T - V. \quad (8.16)$$

**Theorem 1 (Lagrange's equations).** *D'Alembert's principle is equivalent to the system of ordinary differential equations*

$$\frac{d}{dt}\left(\frac{\partial L}{\partial \dot{q}_j}\right) - \frac{\partial L}{\partial q_j} = 0 \quad (8.17)$$

for  $j = 1, \dots, n$ . These are known as Lagrange's equations of motion.

*Proof.* The change in kinetic energy mediated through the momentum—the first term in D'Alembert's principle—due to the increment in the displacements  $dr_i$  is given by

$$\sum_{i=1}^N \dot{p}_i \cdot dr_i = \sum_{i=1}^N m_i \dot{v}_i \cdot dr_i = \sum_{i,j=1}^{N,n} m_i \dot{v}_i \cdot \frac{\partial r_i}{\partial q_j} dq_j \quad (8.18)$$

From the product rule we know that

$$\frac{d}{dt}\left(v_i \cdot \frac{\partial r_i}{\partial q_j}\right) \equiv \dot{v}_i \cdot \frac{\partial r_i}{\partial q_j} + v_i \cdot \frac{d}{dt}\left(\frac{\partial r_i}{\partial q_j}\right) \equiv \dot{v}_i \cdot \frac{\partial r_i}{\partial q_j} + v_i \cdot \frac{\partial v_i}{\partial q_j} \quad (8.19)$$

Also, by differentiating the transformation to generalized coordinates we see:

$$\begin{aligned} v_i &\equiv \sum_{j=1}^n \frac{\partial r_i}{\partial q_j} \dot{q}_j \\ \frac{\partial v_i}{\partial \dot{q}_j} &\equiv \frac{\partial r_i}{\partial q_j} \end{aligned} \quad (8.20)$$

Using these last two identities we see that

$$\begin{aligned} \sum_{i=1}^N \dot{p}_i \cdot dr_i &= \sum_{j=1}^n \left(\sum_{i=1}^N m_i v_i \cdot \frac{\partial r_i}{\partial q_j}\right) dq_j \\ &= \sum_{j=1}^n \left(\sum_{i=1}^N \left(\frac{d}{dt}\left(m_i v_i \cdot \frac{\partial r_i}{\partial q_j}\right) - m_i v_i \cdot \frac{\partial v_i}{\partial q_j}\right)\right) dq_j \\ &= \sum_{j=1}^n \left(\sum_{i=1}^N \left(\frac{d}{dt}\left(m_i v_i \cdot \frac{\partial v_i}{\partial \dot{q}_j}\right) - m_i v_i \cdot \frac{\partial v_i}{\partial q_j}\right)\right) dq_j \\ &= \sum_{j=1}^n \left(\frac{d}{dt}\left(\frac{\partial}{\partial \dot{q}_j}\left(\sum_{i=1}^N \frac{1}{2} m_i |v_i|^2\right)\right) - \frac{\partial}{\partial q_j}\left(\sum_{i=1}^N \frac{1}{2} m_i |v_i|^2\right)\right) dq_j \end{aligned} \quad (8.21)$$

Hence we see that D'Alembert's principle is equivalent to

$$\sum_{j=1}^n \left(\frac{d}{dt}\left(\frac{\partial T}{\partial \dot{q}_j}\right) - \frac{\partial T}{\partial q_j} - Q_j\right) dq_j = 0 \quad (8.22)$$

Since the  $q_j$  for  $j = 1, \dots, n$ , where  $n = 2N - m$ , are all independent, we have

$$\frac{d}{dt} \left( \frac{\partial T}{\partial \dot{q}_j} \right) - \frac{\partial T}{\partial q_j} - Q_j = 0 \quad (8.23)$$

for  $j = 1, \dots, n$ . Using the definition for the generalized forces  $Q_j$  in terms of the potential function  $V$  gives the result.

**Remark 2** (*Configuration space*). As already noted, the  $n$ -dimensional subsurface of  $2N$ -dimensional space on which the solutions to Lagrange's equations lie is called the *configuration space*. It is parameterized by the  $n$  generalized coordinates  $q_1, \dots, q_n$ .

**Remark 3** (*Non-conservative forces*). If the system has forces that are not conservative it may still be possible to find a *generalized potential* function  $V$  such that

$$Q_j = -\frac{\partial V}{\partial q_j} + \frac{d}{dt} \left( \frac{\partial V}{\partial \dot{q}_j} \right) \quad (8.24)$$

for  $j = 1, \dots, n$ . From such potentials we can still deduce Lagrange's equations of motion. Examples of such generalized potentials are velocity dependent potentials due to electromagnetic fields, for example the Lorentz force on a charged particle.

### 8.1.4 Hamilton's Principle

We consider mechanical systems with holonomic constraints and all other forces conservative. Recall, we define the *Lagrange function* or *Lagrangian* to be

$$L = T - V \quad (8.25)$$

where

$$T = \sum_{i=1}^N \frac{1}{2} m_i |v_i|^2 \quad (8.26)$$

is the total kinetic energy for the system, and  $V$  is its potential energy.

**Definition 3** (**Action**). If the Lagrangian  $L$  is the difference of the kinetic and potential

energies for a system, i.e.  $L = T - V$ , we define the *action*  $A = A(q)$  from time  $t_1$  to  $t_2$ , where  $q = (q_1, \dots, q_n)^T$ , to be the functional

$$A(q) := \int_{t_1}^{t_2} L(q, \dot{q}, t) dt \quad (8.27)$$

Hamilton [1834] realized that Lagrange's equations of motion were equivalent to a variational principle.

**Theorem 2 (Hamilton's principle of least action).** *The correct path of motion of a mechanical system with holonomic constraints and conservative external forces, from time  $t_1$  to  $t_2$ , is a stationary solution of the action. Indeed, the correct path of motion  $q = q(t)$ , with  $q = (q_1, \dots, q_n)^T$ , necessarily and sufficiently satisfies Lagrange's equations of motion for  $j = 1, \dots, n$ :*

$$\frac{d}{dt} \left( \frac{\partial L}{\partial \dot{q}_j} \right) - \frac{\partial L}{\partial q_j} = 0 \quad (8.28)$$

The abovementioned relation is Hamilton's form of the principle of least action, because in many cases the action of  $q = q(t)$  is not only an extremal but also a minimum value of the action functional.

**Remark 4 (Non-uniqueness of the Lagrangian).** Two Lagrangian's  $L_1$  and  $L_2$  that differ by the total time derivative of any function of  $q = (q_1, \dots, q_n)^T$  and  $t$  generate the same equations of motion. In fact if

$$L_2(q, \dot{q}, t) = L_1(q, \dot{q}, t) + \frac{d}{dt}(f(q, t)) \quad (8.29)$$

then for  $j = 1, \dots, n$  direct calculation reveals that:

$$\frac{d}{dt} \left( \frac{\partial L_2}{\partial \dot{q}_j} \right) - \frac{\partial L_2}{\partial q_j} = \frac{d}{dt} \left( \frac{\partial L_1}{\partial \dot{q}_j} \right) - \frac{\partial L_1}{\partial q_j}. \quad (8.30)$$

### 8.1.5 Lagrangian Mechanical Systems with Forcing and Control

Our aim is to optimally control Lagrangian systems. For the description of their dynamics, we introduce a variational framework including external forcing resulting from dissipation, friction,

loading and in particular control forces.

Consider an  $n$ -dimensional configuration manifold  $Q$  with local coordinates  $q = (q^1, \dots, q^n)$ , the associated state space given by the tangent bundle  $TQ$  and a  $C^k$  Lagrangian  $L : TQ \rightarrow \mathbb{R}$ ,  $k \geq 2$ . Given a time interval  $[0, T]$ , we consider curves  $q$  in the *path space*  $C^{1,1}([0, T], Q)$  and the *action map*  $G : C^{1,1}([0, T], Q) \rightarrow \mathbb{R}$ ,

$$\mathcal{G}(q) = \int_0^T L(q(t), \dot{q}(t)) dt \quad (8.31)$$

To define control forces for Lagrangian systems, we introduce a *control manifold*  $U \subset \mathbb{R}^m$  and define the *control path space*  $L^\infty([0, T], U)$  with  $u(t) \in U$  also called the *control parameter*. With this notation we define a *Lagrangian control force* as a map  $f_L : TQ \times U \rightarrow T^*Q$ , which is given in coordinates as  $f_L : (q, \dot{q}, u) \mapsto (q, f_L(q, \dot{q}, u))$  where we assume that the control forces can also include configuration and velocity dependent forces resulting *e.g.* from dissipation and friction. We interpret a Lagrangian control force as a family of Lagrangian forces that are fiber-preserving maps  $f_L^u : TQ \rightarrow T^*Q$  over the identity  $id_Q$ , *i.e.* in coordinates  $f_L^u : (q, \dot{q}) \mapsto (q, f_L^u(q, \dot{q}))$ . Whenever we denote  $f_L(q, \dot{q}, u)$  as a one-form on  $TQ$ , we mean the family of horizontal one-forms  $f_L^u(q, \dot{q})$  on  $TQ$  induced by the family of fiber-preserving maps  $f_L^u$ . Given a control path  $u \in L^\infty([0, T], U)$ , the *Lagrange-d'Alembert principle* seeks curves  $q \in C^{1,1}([0, T], Q)$  satisfying

$$\delta \int_0^T L(q(t), \dot{q}(t)) dt + \int_0^T f_L(q(t), \dot{q}(t), u(t)) \cdot \delta q(t) dt = 0 \quad (8.32)$$

where  $\delta$  represents variations vanishing at the endpoints. The second integral in (2.32) is the *virtual work* acting on the mechanical system *via* the force  $f_L$ . Integration by parts shows that this is equivalent to the *forced Euler-Lagrange equations*

$$\frac{\partial L}{\partial q}(q, \dot{q}) - \frac{d}{dt} \left( \frac{\partial L}{\partial \dot{q}}(q, \dot{q}) \right) - f_L(q, \dot{q}, u) = 0 \quad (8.33)$$

These equations implicitly define a family of *forced Lagrangian vector fields*  $X_L^u : TQ \times [0, T] \rightarrow T(TQ)$  and associated *forced Lagrangian flows*  $F_L^u : TQ \times [0, T] \rightarrow TQ$  ( $u \in L^\infty([0, T], U)$ )

fixed) .

We distinguish between two notations: When we fix  $u \in U$  we always consider a family of Lagrangian control forces  $f_L^u$ . As soon as we consider evolutions given by differential equations or integrals, instead of fixing only one  $u \in U$ , we fix an entire curve  $u \in L^\infty([0, T], U)$ , such that for each time  $t$  we use the force  $f_L$  that corresponds to  $f_L(q(t), \dot{q}(t), u(t))$ . In particular, by fixing a control path  $u \in L^\infty([0, T], U)$  we obtain a non-autonomous system whose evolution is also dependent on the initial time  $t_0$ , such that the flow  $F_L^u$  would be defined on  $TQ \times [0, T]^2$  rather than on  $TQ \times [0, T]$ . In the following we will fix the initial time to be  $t_0 = 0$  so that we do not need to keep track on the initial time in the notation. This is no restriction since we consider all possible control paths  $u \in L^\infty([0, T], U)$ .

The one-form  $\Theta_L$  on  $TQ$  given in coordinates by  $\Theta_L = \frac{\partial L}{\partial \dot{q}^i} dq^i$  is called the *Lagrangian one-form*, and the *Lagrangian symplectic form*  $\Omega_L = d\Theta_L$  is given in coordinates by  $\Omega_L(q, \dot{q}) = \frac{\partial^2 L}{\partial q^i \partial \dot{q}^j} dq^i \wedge d\dot{q}^j + \frac{\partial^2 L}{\partial \dot{q}^i \partial \dot{q}^j} d\dot{q}^i \wedge d\dot{q}^j$ . Recall that in the absence of forces, the Lagrangian symplectic form is preserved under the Lagrangian flow.

**The Legendre Transform with Forces.** Given a Lagrangian  $L$ , we can take the standard *Legendre Transform*  $FL : TQ \rightarrow T^*Q$  defined by

$$FL(v_q) \cdot w_q = \left. \frac{d}{d\epsilon} \right|_{\epsilon=0} L(v_q + \epsilon w_q) \quad (8.34)$$

where  $v_q, w_q \in T_q Q$ , and which has coordinate form  $FL : (q, \dot{q}) \mapsto (q, p) = (q, \partial L / \partial \dot{q}(q, \dot{q}))$  and relate Hamiltonian and Lagrangian control forces by  $f_L^u = f_H^u \circ FL$ . If we also have a Hamiltonian  $H$  related to  $L$  by the Legendre transform as  $H(q, p) = FL(q, \dot{q}) \cdot q - L(q, \dot{q})$ , then the forced Euler-Lagrange equations and the forced Hamilton's equations are equivalent. That is, if  $X_L^u$  and  $X_H^u$  are the forced Lagrangian and Hamiltonian vector fields, respectively, then  $(FL)^*(X_H^u) = X_L^u$ , cf.

**Noether's theorem with forcing.** A key property of Lagrangian flows is their behavior with respect to group actions. Assume a Lie group  $G$  with Lie algebra  $\mathfrak{g}$  acts on  $Q$  by the (left or right) action  $\phi : G \times Q \rightarrow Q$ . Consider the tangent lift of this action to  $\phi^{TQ} : G \times TQ$

given by  $\phi_g^{TQ}(v_q) = T(\phi_g) \cdot v_q$ . For  $\xi \in \mathfrak{g}$  the *infinitesimal generators*  $\xi_Q : Q \rightarrow TQ$  and  $\xi_{TQ} : TQ \rightarrow T(TQ)$  are defined by  $\xi_Q(q) = \frac{d}{dg}(\phi_g(q)) \cdot \xi$  and  $\xi_{TQ}(v_q) = \frac{d}{dg}(\phi_g^{TQ}(v_q)) \cdot \xi$ , and the *Lagrangian momentum map*  $J_L : TQ \rightarrow \mathfrak{g}^*$  is defined to be  $J_L(v_q) \cdot \xi = \Theta_L \cdot \xi_{TQ}(v_q)$ . If the Lagrangian is *invariant* under the lift of the action, that is we have  $L \circ \phi_g^{TQ} = L$  for all  $g \in G$  (we also say, the group action is a *symmetry* of the Lagrangian), the Lagrangian momentum map is preserved of the Lagrangian flow in the absence of external forces. We now consider the effect of forcing on the evolution of momentum maps that arise from symmetries of the Lagrangian. In [64] it is shown that the evolution of the momentum map from time 0 to time T is given by the relation

$$[(J_L \circ (F_L^u)^T)(q(0), \dot{q}(0)) - J_L(q(0), \dot{q}(0))] \cdot \xi = \int_0^T f_L^u(q(t), \dot{q}(t)) \cdot \xi_Q(q(t)) dt \quad (8.35)$$

Equation (2.35) shows, that forcing will generally alter the momentum map. However, in the special case that the forcing is orthogonal to the group action, the above relation shows that Noether's theorem will still hold.

**Theorem(forced Noether's theorem).** *Consider a Lagrangian system  $L : TQ \rightarrow \mathbb{R}$  with control forcing  $f_L : TQ \times U \rightarrow T^*Q$  such that the Lagrangian is invariant under the lift of the (left or right) action  $\phi : G \times Q \rightarrow Q$  and  $\{f_L^u(q, \dot{q}), \xi_Q(q)\} = 0$  for all  $(q, \dot{q}) \in TQ, u \in U$  and all  $\xi \in \mathfrak{g}$ . Then the Lagrangian momentum map  $J_L : TQ \rightarrow \mathfrak{g}^*$  will be preserved by the flow, such that  $J_L \circ (F_L^u)^t = J_L$  for all  $t$ .*

### 8.1.6 Standard Form of the Euler-Lagrange Equations in a kinematic chain

In a kinematic chain, such as a biped robot, each link of the mechanical system can be approximated as a particle with mass  $m_i$  located at the center of mass of the link. Each particle is then connected using holonomic constraints on the form  $h_i(q_1, \dots, q_n) = 0$  where  $q_1, \dots, q_n$  are generalized coordinates measuring the orientation of each link. One possible choice of generalized coordinates is the absolute angle of each link measured from an axis defined in the

inertial frame.

Once the appropriate generalized coordinates have been assigned to the system, the holonomic constraints on the form (2.4) become trivial. The kinetic  $\mathcal{K}(q, \dot{q})$  and potential  $\mathcal{P}(q)$  energy of the robot can then easily be derived using the expressions for the generalized coordinates. The Lagrangian of the mechanical system is then formed as

$$\mathcal{L}(q, \dot{q}) = \mathcal{K}(q, \dot{q}) - \mathcal{P}(q) \quad (8.36)$$

where  $\mathcal{K}(q, \dot{q}) = \frac{1}{2} \dot{q}^T M(q) \dot{q}$ . Here  $q \in \mathbb{R}^n$  and  $\dot{q} \in \mathbb{R}^n$  are the vectors of generalized coordinates and velocities and  $M(q) \in \mathbb{R}^{n \times n}$  is the inertia matrix of the system. The Lagrangian can be used to obtain a set of differential equations that describe the time evolution of the system by substituting it into the expression

$$\frac{d}{dt} \left[ \frac{\partial \mathcal{L}(q, \dot{q})}{\partial \dot{q}} \right] - \frac{\partial \mathcal{L}(q, \dot{q})}{\partial q} = B(q)u \quad (8.37)$$

where  $B(q)$  is the applied forces selection matrix,  $u \in \mathbb{R}^m$  is a vector of independent control inputs. Assuming that the matrix  $M(q)$  is symmetric and positive definite for each  $q \in \mathbb{R}^n$  and that  $\mathcal{P} = \mathcal{P}(q)$  is independent of  $\dot{q}$ , relation (2.38) can be written in a compact matrix form known as the robot equations of motion

$$M(q)\ddot{q} + C(q, \dot{q})\dot{q} + G(q) = B(q)u \quad (8.38)$$

where  $C(q, \dot{q}) \in \mathbb{R}^{n \times n}$  is a matrix of centrifugal and Coriolis terms and  $G(q) \in \mathbb{R}^n$  is the gravity vector. Using the previously stated assumptions about the Lagrangian, the elements of the matrices on the left-hand side of (2.8) can be computed as

$$m_{kj}(q) = \frac{d}{dq_k} \left[ \frac{d}{dq_j} \mathcal{K}(q, \dot{q}) \right] \quad (8.39)$$

$$c_{kj}(q, \dot{q}) = \frac{1}{2} \sum_{i=1}^n \left( \frac{\partial m_{kj}}{\partial q_i} + \frac{\partial m_{ki}}{\partial q_j} + \frac{\partial m_{ij}}{\partial q_k} \right) \dot{q}_i \quad (8.40)$$

$$g_k(q) = \frac{\partial \mathcal{P}(q)}{\partial q_k} \quad (8.41)$$

where the subscript  $k$  is the row and  $j$  is the column of the appropriate matrix, and  $q_i, q_j$  and  $q_k$  are the appropriate elements of the generalized coordinate vector  $q$ . When (2.8) is used for simulating the dynamics of the mechanical system the equations of motion are usually reformulated as a state space model with the  $2n$ - dimensional state vector  $x = [q, \dot{q}]^T$ . The system can then be stated as system of  $2n$  first order differential equations

$$\begin{aligned} \dot{x} &= f(x) + g(x)u \\ y &= h(x) \end{aligned} \quad (8.42)$$

where  $y$  is the measured output.

## 8.2 Discrete Mechanics

**The discrete Lagrangian.** Again we consider a configuration manifold  $Q$ , and define the (discrete) state space to be  $Q \times Q$ . Rather than considering a configuration  $q$  and velocity  $\dot{q}$  (or momentum  $p$ ), we now consider two configurations  $q_0$  and  $q_1$ , which should be thought of as two points on a curve  $q$  which are a time step  $h > 0$  apart, *i.e.*  $q_0 \approx q(0)$  and  $q_1 \approx q(h)$  or generally the points  $q_k$  and  $q_{k+1}$ , where  $k \mapsto k \cdot h$  and  $k + 1 \mapsto k + (1 \cdot h)$ . It can be confirmed that:

$$q \approx (1 - \alpha)q_k + \alpha q_{k+1}, \quad \dot{q} \approx \frac{q_{k+1} - q_k}{h} \quad (8.43)$$

where  $\alpha$  is an internal division ratio ( $0 < \alpha < 1$ ) in discrete mechanics.

The manifold  $Q \times Q$  is locally isomorphic to  $TQ$  and thus contains the same amount of information. A *discrete Lagrangian* is a function  $L_d : Q \times Q \rightarrow \mathbb{R}$ , which we think of as approximating the action integral along the exact solution curve segment  $q$  between  $q_k$  and  $q_{k+1}$ :

$$L_d(q_k, q_{k+1}) \approx \int_0^h L(q(t), \dot{q}(t)) dt := hL\left((1 - \alpha)q_k + \alpha q_{k+1}, \frac{q_{k+1} - q_k}{h}\right) \quad (8.44)$$

We consider the grid  $\{t_k = kh | k = 0, \dots, N\}, Nh = T$ , and define the *discrete path space*  $\mathcal{P}_d(Q) = \{q_d : \{t_k\}_{k=0}^N \rightarrow Q\}$ . We will identify a discrete trajectory  $q_d \in \mathcal{P}_d(Q)$  with its image  $q_d = \{q_k\}_{k=0}^N$ , where  $q_k = q_d(t_k)$ . The *discrete action map*  $\mathcal{G}_d : \mathcal{P}_d(Q) \rightarrow \mathbb{R}$  along this sequence is calculated by summing the discrete Lagrangian on each adjacent pair and defined by  $G_d(q_d) = \sum_{k=0}^{N-1} L_d(q_k, q_{k+1})$ . As the discrete path space  $\mathcal{P}_d$  is isomorphic to  $Q \times \dots \times Q$  ( $N + 1$  copies), it can be given a smooth product manifold structure. The discrete action  $\mathcal{G}_d$  inherits the smoothness of the discrete Lagrangian  $L_d$ . The tangent space  $T_{q_d}\mathcal{P}_d(Q)$  to  $\mathcal{P}_d(Q)$  at  $q_d$  is the set of maps  $v_{q_d} : \{t_k\}_{k=0}^N \rightarrow TQ$  such that  $\tau_{q_d} \circ v_{q_d} = q_d$ , which we will denote by  $v_{q_d} = \{(q_k, v_k)\}_{k=0}^N$ . To complete the discrete setting for forced mechanical systems, we present a discrete formulation of the control forces introduced in the previous section. Since the control path  $u : [0, T] \rightarrow U$  has no geometric interpretation, we have to find an appropriate discrete formulation to identify a discrete structure for the Lagrangian control force.

**Discrete Lagrangian control forces.** Analogous to the replacement of the path space by a discrete path space, we replace the control path space by a discrete one. To this end we consider a refined grid  $\Delta\tilde{t}$ , generated *via* a set of control points  $0 \leq c_1 < \dots < c_s \leq 1$  as  $\Delta\tilde{t} = \{t_{k\ell} = t_k + c_\ell h | k = 0, \dots, N-1, \ell = 1, \dots, s\}$ . With this notation the *discrete control path space* is defined to be  $\mathcal{P}_d(U) = \{u_d : \Delta\tilde{t} \rightarrow U\}$ . We define the *intermediate control samples*  $u_k$  on  $[t_k, t_{k+1}]$  as  $u_k = (u_{k1}, \dots, u_{ks}) \in U^s$  to be the values of the control parameters guiding the system from  $q_k = q(t)$  to  $q_{k+1} = q_d(t_{k+1})$ , where  $u_{kl} = u(t_{kl})$  for  $l \in \{1, \dots, s\}$ . With this definition of the discrete control path space, we take two *discrete Lagrangian control forces*  $f_d^+, f_d^- : Q \times Q \times U^s \rightarrow T^*Q$ , given in coordinates as:

$$f_d^+(q_k, q_{k+1}, u_k) = (q_{k+1}, f_d^+(q_k, q_{k+1}, u_k)), \quad f_d^-(q_k, q_{k+1}, u_k) = (q_k, f_d^-(q_k, q_{k+1}, u_k)) \quad (8.45)$$

also called *left and right discrete forces*. It can be confirmed that:

$$\begin{aligned} f_d^+(q_k, q_{k+1}, v_k) &= f_d^+(\alpha, q_k, q_{k+1}, v_k) = (1 - \alpha)hf_L((1 - \alpha)q_k + \alpha q_{k+1}, \frac{q_{k+1} - q_k}{h}, u_k) \\ f_d^-(q_k, q_{k+1}, v_k) &= f_d^-(\alpha, q_k, q_{k+1}, v_k) = \alpha hf_L((1 - \alpha)q_k + \alpha q_{k+1}, \frac{q_{k+1} - q_k}{h}, u_k) \end{aligned} \quad (8.46)$$

where  $\alpha$  is an internal variable called internal division ratio.

Analogously to the continuous case, we interpret the two discrete Lagrangian control forces as two families of discrete fiber-preserving Lagrangian forces  $f_d^{u_k, \pm} : Q \times Q \rightarrow T^*Q$  in the sense that  $\pi_Q \circ f_d^{u_k, \pm} = \pi_Q^\pm$  with fixed  $u_k \in U^s$  and with the projection operators  $\pi_Q^\pm : Q \times Q \rightarrow Q, (q_k, q_{k+1}) \mapsto q_{k+1}$  and  $\pi_Q : Q \times Q \rightarrow Q, (q_k, q_{k+1}) \mapsto q_k$ . We combine the two discrete control forces to give a single one-form  $f_d^{u_k} : Q \times Q \rightarrow T^*(Q \times Q)$  defined by

$$f_d^{u_k}(q_k, q_{k+1}) \cdot (\delta q_k, \delta q_{k+1}) = f_d^{u_k, +}(q_k, q_{k+1}) \cdot \delta q_{k+1} + f_d^{u_k, -}(q_k, q_{k+1}) \cdot \delta q_k \quad (8.47)$$

where  $f_d(q_k, q_{k+1}, u_k)$  denotes the family of all one-forms  $f_d^{u_k}(q_k, q_{k+1})$  with fixed  $u_k \in U^s$ . To simplify the notation we denote the left and right discrete forces by  $f_k^\pm := f_d^\pm(q_k, q_{k+1}, u_k)$ , respectively, and the pair consisting of both by  $f_k := f_d(q_k, q_{k+1}, u_k)$ . We interpret the left discrete force  $f_{k-1}^+$  (and right discrete force  $f_k^-$ , respectively) as the force resulting from the continuous control force acting during the time span  $[t_{k-1}, t_k]$  (during the time span  $[t_k, t_{k+1}]$ , respectively) on the configuration node  $q_k$ .

**The discrete Lagrange-d'Alembert principle.** As with discrete Lagrangians, the discrete control forces also depend on the time step  $h$ , which is important when relating discrete and continuous mechanics. Given such forces, we modify the discrete Hamilton's principle, to the *discrete Lagrange-d'Alembert principle*, which seeks discrete curves  $\{q_k\}_{k=0}^N$  that satisfy

$$\delta \sum_{k=0}^{N-1} L_d(q_k, q_{k+1}) + \sum_{k=0}^{N-1} [f_d^-(q_k, q_{k+1}, u_k) \cdot \delta q_k + f_d^+(q_k, q_{k+1}, u_k) \cdot \delta q_{k+1}] = 0 \quad (8.48)$$

for all variations  $\{\delta q_k\}_{k=0}^N$  vanishing at the endpoints. This is equivalent to the *forced discrete Euler-Lagrange equations*

$$D_2 L_d(q_{k-1}, q_k) + D_1 L_d(q_k, q_{k+1}) - f_d^+(q_{k-1}, q_k, u_{k-1}) - f_d^-(q_k, q_{k+1}, u_k) = 0, k = 1, \dots, N-1 \quad (8.49)$$

These equations implicitly define the forced discrete Lagrangian map  $F_{L_d}^{u_{k-1}, u_k} : Q \times Q \rightarrow Q \times Q$  for fixed controls  $u_{k-1}, u_k \in U^s$ , mapping  $(q_{k-1}, q_k)$  to  $(q_k, q_{k+1})$ . The discrete Lagrangian one-forms  $\Theta_{L_d}^+$  and  $\Theta_{L_d}^-$  are in coordinates  $\Theta_{L_d}^+(q_0, q_1) = D_2 L_d(q_0, q_1) dq_1$  and  $\Theta_{L_d}^-(q_0, q_1) = -D_1 L_d(q_0, q_1) dq_0$ . In the absence of external forces, the discrete Lagrangian maps inherit

the properties of symplectic preservation from the continuous Lagrangian flows. That means the discrete Lagrangian symplectic form  $\Omega_{L_d} = d\Theta_{L_d}^+ = d\Theta_{L_d}^-$  is preserved under the discrete Lagrangian map as  $(F_{L_d})^*(\Omega_{L_d}) = \Omega_{L_d}$ , if no external forcing is present.

**The discrete Legendre transforms with forces.** Although in the continuous case we used the standard Legendre transform for systems with forcing, in the discrete case it is necessary to take the *forced discrete Legendre transforms*

$$\begin{aligned} F^{f+}L_d : (q_0, q_1, u_0) &\mapsto (q_1, p_1) = (q_1, D_2L_d(q_0, q_1) + f_d^+(q_0, q_1, u_0)) \\ F^{f-}L_d : (q_0, q_1, u_0) &\mapsto (q_0, p_0) = (q_0, -D_1L_d(q_0, q_1) - f_d^-(q_0, q_1, u_0)) \end{aligned} \quad (8.50)$$

Again, we denote with  $F^{f\pm}L_d^{u_0}$  the forced discrete Legendre transforms for fixed controls  $u_0 \in U^s$ . Using these definitions and the forced discrete Euler-Lagrange equations (2.46), we can see that the corresponding *forced discrete Hamiltonian map*  $\tilde{F}_{L_d}^{u_0} = F^{f\pm}L_d^{u_1} \circ F_{L_d}^{u_0, u_1} \circ (F^{f\pm}L_d^{u_0})^{-1}$  is given by the map  $\tilde{F}_{L_d}^{u_0} : (q_0, p_0) \mapsto (q_1, p_1)$ , where

$$p_0 = -D_1L_d(q_0, q_1) - f_d^{u_0, -}(q_0, q_1), \quad p_1 = D_2L_d(q_0, q_1) + f_d^{u_0, +}(q_0, q_1) \quad (8.51)$$

which is the same as the standard discrete Hamiltonian map with the discrete forces added.

One can show that the following two definitions of the forced discrete Hamiltonian map

$$\tilde{F}_{L_d}^{u_0} = F^{f\pm}L_d^{u_1} \circ F_{L_d}^{u_0, u_1} \circ (F^{f\pm}L_d^{u_0})^{-1}, \quad \tilde{F}_{L_d}^{u_0} = F^{f+}L_d^{u_0} \circ (F^{f-}L_d^{u_0})^{-1} \quad (8.52)$$

are equivalent with coordinate expression (2.48). Thus from the second expression in (2.49) it becomes clear, that the forced discrete Hamiltonian map that maps  $(q_0, p_0)$  to  $(q_1, p_1)$  depends on  $u_0$  only.

**The discrete Noether theorem with forcing.** As in the unforced case, we can formulate a discrete version of the forced Noether's theorem. To this end, the discrete momentum map in presence of forcing is defined as

$$J_{L_d}^{f+}(q_0, q_1) \cdot \xi = \{F^{f+}L_d^{u_0}(q_0, q_1), \xi_Q(q_1)\}, \quad J_{L_d}^{f-}(q_0, q_1) \cdot \xi = \{F^{f-}L_d^{u_0}(q_0, q_1), \xi_Q(q_0)\} \quad (8.53)$$

The evolution of the discrete momentum map is described by

$$[J_{L_d}^{f^+} \circ (F_{L_d}^{u_d})^{N-1} - J_{L_d}^{f^-}](q_0, q_1) \cdot \xi = \sum_{k=0}^{N-1} f_d^{u_k}(q_k, q_{k+1}) \cdot \xi_{Q \times Q}(q_k, q_{k+1}) \quad (8.54)$$

Again, in the case that the forcing is orthogonal to the group action we have the unique momentum map  $J_{L_d}^f : Q \times Q \rightarrow \mathfrak{g}^*$  and it holds:

**Forced discrete Noether's theorem.** *Consider a discrete Lagrangian system  $L_d: Q \times Q \rightarrow \mathbb{R}$  with discrete control forces  $f_d^+, f_d^- : Q \times Q \times U^s \rightarrow T^*Q$  such that the discrete Lagrangian is invariant under the lift of the (left or right) action  $\phi : G \times Q \rightarrow Q$  and  $\{f_d^{u_k}, \xi_{Q \times Q}\} = 0$  for all  $\xi \in \mathfrak{g}$  and  $u_k \in U^s, k \in \{0, \dots, N-1\}$ . Then the discrete Lagrangian momentum map  $J_{L_d}^f : Q \times Q \rightarrow \mathfrak{g}^*$  will be preserved by the discrete Lagrangian evolution map, such that  $J_{L_d}^f \circ F_{L_d}^{u_k, u_{k+1}} = J_{L_d}^f$ .*

## 8.3 Geometric Optimal Control of Lagrangian Mechanical Systems

### 8.3.1 The Continuous Case

On the configuration space  $Q$  we consider a mechanical system described by a regular Lagrangian  $L : TQ \rightarrow \mathbb{R}$ . Additionally, assume that a Lagrangian control force acts on the system and is defined by a map  $f_L : TQ \times U \rightarrow T^*Q$  with  $f_L : (q, \dot{q}, u) \mapsto (q, f_L(q, \dot{q}, u))$  and  $u : [0, T] \rightarrow U$ , the time-dependent control parameter. Note that the Lagrangian control force may include both dissipative forces within the mechanical system and external control forces resulting from actuators steering the system.

**The Lagrangian optimal control problem.** We now consider the following optimal control problem: During the time interval  $[0, T]$ , the mechanical system described by the Lagrangian  $L$  is to be moved on a curve  $q$  from an initial state  $(q(0), \dot{q}(0)) = (q^0, \dot{q}^0) \in TQ$  to a final state. The motion is influenced *via* a Lagrangian control force  $f_L$  with control parameter  $u$  such that

a given *objective functional*

$$J(q, u) = \int_0^T C(q(t), \dot{q}(t), u(t)) dt + \Phi(q(T), \dot{q}(T)) \quad (8.55)$$

is minimized. Here  $C : TQ \times U \rightarrow \mathbb{R}$  and  $\Phi : TQ \rightarrow \mathbb{R}$  (Mayer term) are continuously differentiable cost functions. The final state  $(q(T), \dot{q}(T))$  is required to fulfil a constraint  $r(q(T), \dot{q}(T), q^T, \dot{q}^T) = 0$  with  $r : TQ \times TQ \rightarrow \mathbb{R}^{n_r}$  and  $(q^T, \dot{q}^T) \in TQ$  given. The motion of the system is to satisfy the Lagrange-d'Alembert principle, which requires that:

$$\delta \int_0^T L(q(t), \dot{q}(t)) dt + \int_0^T f_L(q(t), \dot{q}(t), u(t)) \cdot \delta q(t) dt = 0 \quad (8.56)$$

for all variations  $\delta q$  with  $\delta q(0) = \delta q(T) = 0$ . In many cases, one encounters additional constraints on the states and controls given by  $h(q(t), \dot{q}(t), u(t)) \geq 0$  with  $h : TQ \times U \rightarrow \mathbb{R}^{n_h}$ , where  $V \geq 0$  for vectors  $V \in \mathbb{R}^n$  holds componentwise. To summarize, we are faced with the following Lagrangian Optimal Control Problem:

$$\begin{aligned} & \min_{q \in C^{1,1}([0, T], Q), u \in L^\infty([0, T], U)} J(q, u) \\ & \text{s.t.} \\ & \delta \int_0^T L(q(t), \dot{q}(t)) dt + \int_0^T f_L(q(t), \dot{q}(t), u(t)) \cdot \delta q(t) dt = 0 \\ & (q(0), \dot{q}(0)) = (q^0, \dot{q}^0) \\ & h(q(t), \dot{q}(t), u(t)) \geq 0, \quad t \in [0, T] \\ & r(q(T), \dot{q}(T), q^T, \dot{q}^T) = 0 \end{aligned} \quad (8.57)$$

The interval length  $T$  may either be fixed, or appear as degree of freedom in the optimization problem.

A curve  $(q, u) \in C^{1,1}([0, T], Q) \times L^\infty([0, T], U)$  is *feasible*, if it fulfills the constraints (2.54). The set of all feasible curves is the *feasible set* of (2.54). A feasible curve  $(q^*, u^*)$  is an *optimal solution* of (2.54), if  $J(q^*, u^*) \leq J(q, u)$  for all feasible curves  $(q, u)$ . A feasible curve  $(q^*, u^*)$  is a *local optimal solution*, if  $J(q^*, u^*) \leq J(q, u)$  in a neighborhood of  $(q^*, u^*)$ . The function  $q^*$  is called (*locally*) *optimal trajectory*, and  $u^*$  is the (*locally*) *optimal control*.

### 8.3.2 The discrete case

For the discrete solution we need a discretized version of (2.54). To this end we formulate an optimal control problem for the discrete mechanical system described by discrete variational mechanics introduced in subchapter 2.2. To obtain a discrete formulation, we replace each expression in (2.54) by its discrete counterpart in terms of discrete variational mechanics. As described in Section 1.2, we replace the state space  $TQ$  of the system by  $Q \times Q$  and a path  $q : [0, T] \rightarrow Q$  by a discrete path  $q_d : \{0, h, 2h, \dots, Nh = T\} \rightarrow Q$  with  $q_k = q_d(kh)$ . Analogously, the continuous control path  $u : [0, T] \rightarrow U$  is replaced by a discrete control path  $u_d : \Delta\tilde{t} \rightarrow U$  (writing  $u_k = (u_d(kh + c_\ell h))_{\ell=1}^s \in U^s$ ).

**The discrete Lagrange-d'Alembert principle.** Based on this discretization, the action integral in (2.2) is approximated on a time slice  $[kh, (k+1)h]$  by the *discrete Lagrangian*  $L_d : Q \times Q \rightarrow \mathbb{R}$ ,  $L_d(q_k, q_{k+1}) \approx \int_{kh}^{(k+1)h} L(q(t), \dot{q}(t)) dt$ , and likewise the virtual work by the left and right discrete forces,  $f_k^- \cdot \delta q_k + f_k^+ \cdot \delta q_{k+1} \approx \int_{kh}^{(k+1)h} f_L(q(t), \dot{q}(t), u(t)) \cdot \delta q(t) dt$ , where  $f_k^-, f_k^+ \in T^*Q$ . As introduced in equation (1.8), the discrete version of the Lagrange-d'Alembert principle (2.2) requires one to find discrete paths  $\{q_k\}_{k=0}^N$  such that for all variations  $\{\delta q_k\}_{k=0}^N$  with  $\delta q_0 = \delta q_N = 0$ , one has the discrete Lagrange-d'Alembert principle (1.8), or, equivalently, the forced discrete Euler-Lagrange equations (1.9).

**Boundary conditions.** In the next step, we need to incorporate the boundary conditions  $q(0) = q^0, \dot{q}(0) = \dot{q}^0$  and  $r(q(T), \dot{q}(T), q^T, \dot{q}^T) = 0$  into the discrete description. Those on the configuration level can be used as constraints in a straightforward way as  $q_0 = q^0$ . However, since in the present formulation velocities are approximated in a time interval  $[t_k, t_{k+1}]$  (as opposed to an approximation at the time nodes), the velocity conditions have to be transformed to conditions on the conjugate momenta. These are defined at each time node using the discrete Legendre transform. The presence of forces at the time nodes has to be incorporated into that transformation leading to the forced discrete Legendre transforms  $F^{f^-} L_d$  and  $F^{f^+} L_d$  defined in (1.10). Using the standard Legendre transform  $FL : TQ \rightarrow T^*Q, (q, \dot{q}) \mapsto (q, p) =$

$(q, D_2L(q, \dot{q}))$  leads to the discrete initial constraint on the conjugate momentum

$$D_2L(q^0, \dot{q}^0) + D_1L_d(q_0, q_1) - f_d^-(q_0, q_1, u_0) = 0 \quad (8.58)$$

As shown in the previous section, we can transform the boundary condition from a formulation with configuration and velocity to a formulation with configuration and conjugate momentum. Thus, instead of considering a discrete version of the final time constraint  $r$  on  $TQ$  we use a discrete version of the final time constraint  $r$  on  $T^*Q$ . We define the *discrete boundary condition* on the configuration level to be  $r_d: Q \times Q \times U^s \times TQ \rightarrow \mathbb{R}^{n_r}$ ,

$$r_d(q_{N-1}, q_N, u_{N-1}, q^T, \dot{q}^T) = r(F^{f^+}L_d(q_{N-1}, q_N, u_{N-1}), FL(q^T, \dot{q}^T)) \quad (8.59)$$

*i.e.* we used  $(q_N, p_N) = F^{f^+}L_d(q_{N-1}, q_N, u_{N-1})$  and  $(q^T, p^T) = FL(q^T, \dot{q}^T)$ , that is  $p_N = D_2L_d(q_{N-1}, q_N) + f_d^+(q_{N-1}, q_N, u_{N-1})$  and  $p^T = D_2L(q^T, \dot{q}^T)$ . Notice that for the simple final velocity constraint  $\dot{q}(T) - \dot{q}^T = 0$ , we obtain for the transformed condition on the momentum level  $r(q(T), p(T), q^T, p^T) = p(T) - p^T$  the discrete constraint:

$$-D_2L(q^T, \dot{q}^T) + D_2L_d(q_{N-1}, q_N) - f_d^+(q_{N-1}, q_N, u_{N-1}) = 0 \quad (8.60)$$

which together with equation (2.8) constitute the boundary constraints on momentum level.

**Discrete path constraints.** Opposed to the final time constraint we approximate the path constraint in (2.3d) on each time interval  $[t_k, t_{k+1}]$  rather than at each time node. Thus, we maintain the formulation on the velocity level and replace the continuous path constraint  $h(q(t), \dot{q}(t), u(t)) \geq 0$  by a *discrete path constraint*  $h_d: Q \times Q \times U^s \rightarrow \mathbb{R}^{s n_h}$  which suitably approximate the continuous constraint pointwise (see Sect. 2.4) with  $h_d(q_k, q_{k+1}, u_k) \geq 0, k = 0, \dots, N-1$ .

**Discrete objective function.** Similar to the Lagrangian we approximate the objective functional in (2.1) on the time slice  $[kh, (k+1)]$  by  $C_d(q_k, q_{k+1}, u_k) \approx \int_{kh}^{(k+1)h} C(q(t), \dot{q}(t), u(t)) dt$ . Analogously to the final time constraint, we approximate the final condition *via* a discrete ver-

sion  $\Phi_d : Q \times Q \times U^s \rightarrow \mathbb{R}$  yielding the *discrete objective function*

$$J_d(q_d, u_d) = \sum_{k=0}^{N-1} C_d(q_k, q_{k+1}, u_k) + \Phi_d(q_{N-1}, q_N, u_{N-1}) \quad (8.61)$$

**The discrete optimal control problem.** In summary, after performing the above discretization steps, one is faced with the following discrete optimal control problem.

$$\begin{aligned} & \min_{(q_d, u_d) \in \mathbb{P}_d(Q) \times \mathbb{T}_d(U)} J_d(q_d, u_d) \\ & \quad s.t. \\ & \quad q_0 = q^0 \\ & \quad D_2 L(q^0, \dot{q}^0) + D_1 L_d(q_0, q_1) - f_0^- = 0 \\ & \quad D_2 L_d(q_{k-1}, q_k) + D_1 L_d(q_k, q_{k+1}) - f_k^- - f_k^+ = 0, \quad k = 1, \dots, N-1 \\ & \quad h_d(q_k, q_{k+1}, u_k) \geq 0, \quad k = 0, \dots, N-1 \\ & \quad r_d(q_{N-1}, q_N, u_{N-1}, q^T, \dot{q}^T) = 0 \end{aligned} \quad (8.62)$$

### 8.3.3 Numerical Optimization Methods for Trajectory Generation

One of the most important issues of biped locomotion is the generation of trajectories (gaits) that ensure ultimate stability with specific constraints, e.g. extremely low energy consumption. Optimization based methods for Gait Generation utilize optimal control theory. In general, the optimal control can be classified as: dynamic programming, indirect methods and direct methods.

Although the dynamic programming is less sensitive to the initial guess of the design parameters, it suffers from the curse of dimensionality. The indirect approach represented by Pontryagin Maximum Principle demands necessary conditions for optimality, which results in nonlinear, two-boundary value problem. However, the computational solution may lead to highly nonlinear ODEs. Obtaining necessary conditions of optimality can be intricate for complex dynamic systems such as biped robot. In addition, the direct and indirect methods are very sensitive to the initial guess of the costate equations.

An important step in the above direction is to find more flexible methods for optimal control problems, represented by the direct methods, by transcribing the infinite dimension problem into finite-dimensional nonlinear programming (static or parameter optimization). This can be implemented by discretization of the controls or the states or both of them, depending on the selected discretization approach, and solving the problem using one of the nonlinear programming algorithms such as sequential quadratic programming (SQP), interior point methods, genetic algorithm (GA) etc. Although robustness, this method can only give suboptimal/approximate solution. The 2-Phases Gait Generation Module developed in the current thesis solves the abovementioned problem, giving stable, optimal, energy efficient gaits.

### 8.3.4 Forward-Dynamics Based Optimization

The formulation of the original optimal control problem can be described as follows:

Minimize:

$$J = c_0(x, t) + \int_{t_1}^{t_f} L(x(t), u(t), t) dt \quad (8.63)$$

Subject to:

$$\dot{x} = f(x(t), u(t), t) \quad (8.64)$$

$$a_1(x(t_0), u(t_0), t_0) \leq 0 \quad (8.65)$$

$$a_2(x(t_0), u(t_0), t_0) = 0$$

$$b_1(x(t_f), u(t_f), t_f) \leq 0 \quad (8.66)$$

$$b_2(x(t_f), u(t_f), t_f) = 0$$

$$c_1(x(t), u(t), t) \leq 0 \quad (8.67)$$

$$c_2(x(t), u(t), t) = 0$$

$$u_l \leq u(t) \leq u_u \quad (8.68)$$

$$x_l \leq x(t) \leq x_u$$

where  $u \in \mathbb{R}^n$  is the input control vector,  $c_0$  and  $L$  are scalar functions of the indicated arguments,  $J$  is a scalar performance index,  $x \in \mathbb{R}^n$  is the state vector,  $t$ ,  $t_1$  and  $t_f$  are the

time, initial and final time respectively,  $a_1$  and  $a_2$  are the initial constraints,  $b_1$  and  $b_2$  are the final constraints,  $c_1$  and  $c_2$  are the path constraints and (2.68) refer to the bound constraints of the input control and the states.

The formulation of discretized optimal control problem can be described as a nonlinear programming as follows:

Minimize:

$$J = c_0(x(t_N)) + \sum_{k=1}^N l_k(x(t_k), u(t_k), t_k) \Delta t \quad (8.69)$$

where  $N$  is the number of the time steps,  $N - 1$  is the number of time intervals and  $\Delta t = (t_f - t_1)/(N - 1)$ . Equation (2.69) can be solved by a numerical integration approach such as trapezoidal or composite Simpson's rule etc.

Subject to:

$$\begin{aligned} Z(Y) &= 0 \\ C_l &\leq C(Y) \leq C_u \\ Y_l &\leq Y \leq Y_u \end{aligned} \quad (8.70)$$

### Direct Collocation

A discretization of the time interval

$$t_1 < t_2 < \dots < t_N = t_f \quad (8.71)$$

is chosen. The parameters  $Y$  of the nonlinear program are the values of control and state variables at the grid points  $t_j, j = 1, \dots, N$ , and the final time  $t_f$

$$Y = (u(t_1), \dots, u(t_N), x(t_1), \dots, x(t_N), t_N) \in \mathbb{R}^{N(l+n)+1} \quad (8.72)$$

The controls are chosen as piecewise linear interpolating functions between  $u(t_k)$  and  $u(t_{k+1})$  for  $t_k \leq t < t_{k+1}$

$$u_{approx}(t) = u(t_k) + \frac{t - t_k}{t_{k+1} - t_k} (u(t_{k+1}) - u(t_k)) \quad (8.73)$$

The states are chosen as continuously differentiable functions and piecewise dened as cubic

polynomials between  $x(t_k)$  and  $x(t_{k+1})$  with  $\dot{x}_{approx}(s) := f(x(s), u(s), s)$  at  $s = t_k, t_{k+1}$ ,

$$x_{approx}(t) = \sum_{j=0}^3 c_j^k \left( \frac{t - t_k}{h_k} \right)^j, \quad t_k \leq t < t_{k+1}, \quad k = 1, \dots, N - 1 \quad (8.74)$$

$$c_0^k = x(t_k) \quad (8.75)$$

$$c_1^k = h_k f_k \quad (8.76)$$

$$c_2^k = -3x(t_k) - 2h_k f_k + 3x(t_{k+1}) - h_k f_{k+1} \quad (8.77)$$

$$c_3^k = 2x(t_k) + h_k f_k - 2x(t_{k+1}) + h_k f_{k+1} \quad (8.78)$$

where  $f_k := f(x(t_k), u(t_k), t_k)$ ,  $h_k := t_{k+1} - t_k$ .

The approximating functions of the states have to satisfy the state space model of the equations of motion at the grid points  $t_k, k = 1, \dots, N$ , and at the centers  $t_{c,k} := t_{k+1/2} := (t_k + t_{k+1})/2, k = 1, \dots, N - 1$ , of the discretization intervals. This scheme is also known as cubic collocation at Lobatto points. The chosen approximation (2.74)-(2.78) of  $x(t)$  already fulfills these constraints at  $t_k$ . Therefore, the only remaining constraints in the nonlinear programming problem are

- the collocation constraints at  $t_{c,k}$

$$f(x_{approx}(t_{c,k}), u_{approx}(t_{c,k}), t_{c,k}) - \dot{x}_{approx}(t_{c,k}) = 0, \quad k = 1, \dots, N - 1, \quad (8.79)$$

- the inequality constraints at the grid points  $t_j$

$$g(x_{approx}(t_k), u_{approx}(t_k), t_k) \geq 0, \quad k = 1, \dots, N, \quad (8.80)$$

- and the initial and end point constraints at  $t_1$  and  $t_N$

$$r(x_{approx}(t_1), x_{approx}(t_N), t_N) = 0 \quad (8.81)$$

In the equations above, the index *approx* for approximation is being used.

By this scheme the number of four free parameters for each cubic polynomial is reduced to two and the number of three collocation constraints per subinterval is reduced to one. Compared with other collocation schemes we have a reduced number of constraints to be fulfilled and a reduced number of free parameters to be determined by the numerical procedure. This results in a better performance of an implementation of this method in terms of convergence, reliability, and efficiency compared with other schemes.

Overall, the final discretized optimal control problem with direct collocation method is:

Minimize:

$$J = c_0(x(t_N)) + \sum_{k=1}^N l_k(x(t_k), u(t_k), t_k) \Delta t \quad (8.82)$$

Subject to:

$$f(x_{approx}(t_{c,k}), u_{approx}(t_{c,k}), t_{c,k}) - x_{approx}(t_{c,k}) = 0, k = 1, \dots, N - 1 \quad (8.83)$$

$$a_1(x_{approx}(t_0), u_{approx}(t_0), t_0) \leq 0 \quad (8.84)$$

$$a_2(x_{approx}(t_0), u_{approx}(t_0), t_0) = 0 \quad (8.85)$$

$$b_1(x_{approx}(t_N), u_{approx}(t_N), t_N) \leq 0 \quad (8.86)$$

$$b_2(x_{approx}(t_N), u_{approx}(t_N), t_N) = 0 \quad (8.87)$$

$$c_1(x_{approx}(t_k), u_{approx}(t_k), t_k) \leq 0, k = 1, \dots, N \quad (8.88)$$

$$c_2(x_{approx}(t_k), u_{approx}(t_k), t_k) = 0, k = 1, \dots, N \quad (8.89)$$

$$u_l \leq u(t_k) \leq u_u, k = 1, \dots, N \quad (8.90)$$

$$x_l \leq x(t_k) \leq x_u, k = 1, \dots, N \quad (8.91)$$

where

$$t_{c,k} = (t_k + t_{k+1})/2, k = 1, \dots, N - 1 \quad (8.92)$$

$$x_{approx}(t) = \sum_{j=0}^3 c_j^k \left( \frac{t - t_k}{h_k} \right)^j, t_k \leq t \leq t_{k+1}, k = 1, \dots, N - 1 \quad (8.93)$$

$$u_{approx}(t) = u(t_k) + \frac{t - t_k}{h_k}(u(t_{k+1}) - u(t_k)), t_k \leq t \leq t_{k+1}, k = 1, \dots, N - 1 \quad (8.94)$$

The advantages of the direct collocation method:

- The resulting solution is large scale system with sparse NLP.
- It can use the knowledge of the state vector in the initialization.
- It can cope with unstable system and different constraints reliably.

The disadvantages of the direct collocation method:

- It needs more computational time than single-shooting approach, due to large design parameters used.

When applying the forward-dynamics based optimization on the multi-body dynamics (robotic system), the following issues should be noticed:

- Equation (2.64) needs calculation of the inverse mass matrix of the robotic system which may result in computational difficulty.
- If the multibody dynamic systems move with constrained motion, the equality and inequality constraints may not have explicit expressions for the input control variables. Consequently, these constraints must be derived many times until the input control vector appears.
- To solve the NLP, it is necessary to choose feasible initial guess for the design variables. Consequently, it is not easy to get a good initial guess for the control variables at the forward-dynamics based methods.

### 8.3.5 Inverse-Dynamics Based Approach - The Discrete Mechanics Approach

The difference between the inverse-dynamics and forward-dynamics based optimization appears in the formulation of (2.64), such that the dynamics equation for the target system of the inverse-

dynamics approach is not written in the state space form. Therefore, the Discrete Mechanics based approach has three distinctive features:

- It does not need the inverse mass matrix.
- The ability to convert the original optimal control into algebraic equations which are easy to deal with.

For a multibody system (robotic system), the dynamics equation, as we have already seen in previous chapters, can be written in a standard Lagrangian equation as follows:

$$M\ddot{q} + C\dot{q} + G = Bu \quad (8.95)$$

where  $M \in \mathbb{R}^{n \times n}$  is the inertia matrix,  $n$  denotes the DOF of the target robot,  $q$ ,  $\dot{q}$  and  $\ddot{q} \in \mathbb{R}^n$ , are the absolute angular displacement, velocity and acceleration of the robot links,  $C \in \mathbb{R}^{n \times n}$  represents the Coriolis robot matrix,  $G \in \mathbb{R}^n$  is the gravity vector,  $B \in \mathbb{R}^{n \times n}$  is a mapping matrix derived by the principle of the virtual work and  $u \in \mathbb{R}^n$  is the control input vector. This equation is valid for open-chain robotic system. For closed-chain mechanism, the Lagrangian multipliers should appear to right side of (2.95).

In Discrete Mechanics, the velocity and acceleration of the dynamic system can be approximated directly using finite differences:

- For the first derivative:

Forward Difference:

$$\dot{q}(t_k) \approx \frac{(q(t_{k+1}) - q(t_k))}{h_k}, k = 0 \dots N - 1 \text{ (with truncation error } O(h_k)) \quad (8.96)$$

Backward Difference:

$$\dot{q}(t_k) \approx \frac{(q(t_k) - q(t_{k-1}))}{h_k}, k = 0 \dots N - 1 \text{ (with truncation error } O(h_k)) \quad (8.97)$$

and for the second derivative:

Central difference:

$$\ddot{q}(t_k) \approx \frac{q(t_{k+1}) - 2q(t_k) + q(t_{k-1}))}{h_k^2}, k = 0 \dots N - 1 \text{ (with truncation error } O(h_k^2)) \quad (8.98)$$

# Chapter 9

## Appendix B: First Phase of the Gait Generation Module

### 9.1 Analytical Expressions for the Swing Phase using Discrete Mechanics (Leg1=Stance, Leg2=Swing)

The analytical expression of (2.36) is:

$$\begin{aligned}
 & \frac{\left(2 q_{(1,k)}^{(i)} - 2 q_{(1,k-1)}^{(i)}\right) \left(\frac{I_1}{2} + \frac{m_1 a^2}{2} + \frac{M l^2}{2} + \frac{l^2 m_2}{2}\right)}{(h^{(i)})^2} + \frac{\left(2 q_{(1,k)}^{(i)} - 2 q_{(1,k+1)}^{(i)}\right) \left(\frac{I_1}{2} + \frac{m_1 a^2}{2} + \frac{M l^2}{2} + \frac{l^2 m_2}{2}\right)}{(h^{(i)})^2} \\
 & - \frac{b l m_2 \cos\left(\frac{q_{(1,k)}^{(i)}}{2} - \frac{q_{(2,k)}^{(i)}}{2} + \frac{q_{(1,k-1)}^{(i)}}{2} - \frac{q_{(2,k-1)}^{(i)}}{2}\right) \left(q_{(2,k)}^{(i)} - q_{(2,k-1)}^{(i)}\right)}{(h^{(i)})^2} \\
 & - \frac{b l m_2 \cos\left(\frac{q_{(1,k)}^{(i)}}{2} - \frac{q_{(2,k)}^{(i)}}{2} + \frac{q_{(1,k+1)}^{(i)}}{2} - \frac{q_{(2,k+1)}^{(i)}}{2}\right) \left(q_{(2,k)}^{(i)} - q_{(2,k+1)}^{(i)}\right)}{(h^{(i)})^2} \\
 & + \frac{b l m_2 \sin\left(\frac{q_{(1,k)}^{(i)}}{2} - \frac{q_{(2,k)}^{(i)}}{2} + \frac{q_{(1,k-1)}^{(i)}}{2} - \frac{q_{(2,k-1)}^{(i)}}{2}\right) \left(q_{(1,k)}^{(i)} - q_{(1,k-1)}^{(i)}\right) \left(q_{(2,k)}^{(i)} - q_{(2,k-1)}^{(i)}\right)}{2 (h^{(i)})^2} \\
 & + \frac{b l m_2 \sin\left(\frac{q_{(1,k)}^{(i)}}{2} - \frac{q_{(2,k)}^{(i)}}{2} + \frac{q_{(1,k+1)}^{(i)}}{2} - \frac{q_{(2,k+1)}^{(i)}}{2}\right) \left(q_{(1,k)}^{(i)} - q_{(1,k+1)}^{(i)}\right) \left(q_{(2,k)}^{(i)} - q_{(2,k+1)}^{(i)}\right)}{2 (h^{(i)})^2} \\
 & - \tau_{(1,k)}^{(i)} = 0, (k = 1, \dots, N) \quad (9.1)
 \end{aligned}$$

The analytical expression of (2.37) is:

$$\begin{aligned}
& \frac{g \sin\left(\frac{q_{(2,k)}^{(i)}}{2} + \frac{q_{(2,k-1)}^{(i)}}{2}\right) (m_1 a + M l + g m_2)}{2} + \frac{g \sin\left(\frac{q_{(2,k)}^{(i)}}{2} + \frac{q_{(2,k+1)}^{(i)}}{2}\right) (m_1 a + M l + g m_2)}{2} \\
& + \frac{\left(2 q_{(2,k)}^{(i)} - 2 q_{(2,k-1)}^{(i)}\right) \left(\frac{m_2 b^2}{2} + \frac{I_2}{2}\right)}{(h^{(i)})^2} + \frac{\left(2 q_{(2,k)}^{(i)} - 2 q_{(2,k+1)}^{(i)}\right) \left(\frac{m_2 b^2}{2} + \frac{I_2}{2}\right)}{(h^{(i)})^2} - \frac{b g m_2 \sin\left(\frac{q_{(2,k)}^{(i)}}{2} + \frac{q_{(2,k-1)}^{(i)}}{2}\right)}{2} \\
& - \frac{b g m_2 \sin\left(\frac{q_{(2,k)}^{(i)}}{2} + \frac{q_{(2,k+1)}^{(i)}}{2}\right)}{2} - \frac{b l m_2 \cos\left(\frac{q_{(1,k)}^{(i)}}{2} - \frac{q_{(2,k)}^{(i)}}{2} + \frac{q_{(1,k-1)}^{(i)}}{2} - \frac{q_{(2,k-1)}^{(i)}}{2}\right) \left(q_{(1,k)}^{(i)} - q_{(1,k-1)}^{(i)}\right)}{(h^{(i)})^2} \\
& - \frac{b l m_2 \cos\left(\frac{q_{(1,k)}^{(i)}}{2} - \frac{q_{(2,k)}^{(i)}}{2} + \frac{q_{(1,k+1)}^{(i)}}{2} - \frac{q_{(2,k+1)}^{(i)}}{2}\right) \left(q_{(1,k)}^{(i)} - q_{(1,k+1)}^{(i)}\right)}{(h^{(i)})^2} \\
& - \frac{b l m_2 \sin\left(\frac{q_{(1,k)}^{(i)}}{2} - \frac{q_{(2,k)}^{(i)}}{2} + \frac{q_{(1,k-1)}^{(i)}}{2} - \frac{q_{(2,k-1)}^{(i)}}{2}\right) \left(q_{(1,k)}^{(i)} - q_{(1,k-1)}^{(i)}\right) \left(q_{(2,k)}^{(i)} - q_{(2,k-1)}^{(i)}\right)}{2 (h^{(i)})^2} \\
& - \frac{b l m_2 \sin\left(\frac{q_{(1,k)}^{(i)}}{2} - \frac{q_{(2,k)}^{(i)}}{2} + \frac{q_{(1,k+1)}^{(i)}}{2} - \frac{q_{(2,k+1)}^{(i)}}{2}\right) \left(q_{(1,k)}^{(i)} - q_{(1,k+1)}^{(i)}\right) \left(q_{(2,k)}^{(i)} - q_{(2,k+1)}^{(i)}\right)}{2 (h^{(i)})^2} \\
& - \tau_{(2,k)}^{(i)} = 0, (k = 1, \dots, N) \quad (9.2)
\end{aligned}$$

The analytical expression of (2.38) is:

$$\begin{aligned}
& \frac{\left(2 q_{(1,1)}^{(i)} - 2 q_{(1,2)}^{(i)}\right) \left(\frac{I_1}{2} + \frac{m_1 a^2}{2} + \frac{M l^2}{2} + \frac{l^2 m_2}{2}\right)}{(h^{(i)})^2} + g \sin(q_{(1,1)}^{(i)}) (m_1 a + M l + g m_2) - b g m_2 \sin(q_{(1,1)}^{(i)}) \\
& - \frac{b l m_2 \cos\left(\frac{q_{(1,1)}^{(i)}}{2} + \frac{q_{(1,2)}^{(i)}}{2} - \frac{q_{(2,1)}^{(i)}}{2} - \frac{q_{(2,2)}^{(i)}}{2}\right) \left(q_{(2,1)}^{(i)} - q_{(2,2)}^{(i)}\right)}{(h^{(i)})^2} + b q_{(2,1)}^{(i)} l m_2 q_{(2,1)}^{(i)} \sin\left(q_{(1,1)}^{(i)} - q_{(1,1)}^{(i)}\right) \\
& + \frac{b l m_2 \sin\left(\frac{q_{(1,1)}^{(i)}}{2} + \frac{q_{(1,2)}^{(i)}}{2} - \frac{q_{(2,1)}^{(i)}}{2} - \frac{q_{(2,2)}^{(i)}}{2}\right) \left(q_{(1,1)}^{(i)} - q_{(1,2)}^{(i)}\right) \left(q_{(2,1)}^{(i)} - q_{(2,2)}^{(i)}\right)}{2 (h^{(i)})^2} \\
& - \tau_{(1,1)}^{(i)} = 0 \quad (9.3)
\end{aligned}$$

The analytical expression of (2.39) is:

$$2 q_{(2,1)}^{(i)} \left(\frac{m_2 b^2}{2} + \frac{I_2}{2}\right) + \frac{g \sin\left(\frac{q_{(2,1)}^{(i)}}{2} + \frac{q_{(2,2)}^{(i)}}{2}\right) (m_1 a + M l + g m_2)}{2} + \frac{\left(2 q_{(2,1)}^{(i)} - 2 q_{(2,2)}^{(i)}\right) \left(\frac{m_2 b^2}{2} + \frac{I_2}{2}\right)}{(h^{(i)})^2}$$

$$\begin{aligned}
 & - \frac{b g m_2 \sin\left(\frac{q_{(2,1)}^{(i)}}{2} + \frac{q_{(2,2)}^{(i)}}{2}\right)}{2} - b l m_2 q_{(2,1)}^{(i)} \cos\left(q_{(1,1)}^{(i)} - q_{(1,1)}^{(i)}\right) \\
 & - \frac{b l m_2 \cos\left(\frac{q_{(1,1)}^{(i)}}{2} + \frac{q_{(1,2)}^{(i)}}{2} - \frac{q_{(2,1)}^{(i)}}{2} - \frac{q_{(2,2)}^{(i)}}{2}\right) \left(q_{(1,1)}^{(i)} - q_{(1,2)}^{(i)}\right)}{(h^{(i)})^2} \\
 & - \frac{b l m_2 \sin\left(\frac{q_{(1,1)}^{(i)}}{2} + \frac{q_{(1,2)}^{(i)}}{2} - \frac{q_{(2,1)}^{(i)}}{2} - \frac{q_{(2,2)}^{(i)}}{2}\right) \left(q_{(1,1)}^{(i)} - q_{(1,2)}^{(i)}\right) \left(q_{(2,1)}^{(i)} - q_{(2,2)}^{(i)}\right)}{2 (h^{(i)})^2} \\
 & - \tau_{(2,1)}^{(i)} = 0 \quad (9.4)
 \end{aligned}$$

The analytical expression of (2.40) is:

$$\begin{aligned}
 & b g m_2 \sin(q_{(1,N)}^{(i)}) - g \sin(q_{(1,N)}^{(i)}) (m_1 a + M l + g m_2) \\
 & - \frac{\left(2 q_{(1,N)}^{(i)} - 2 q_{(1,N-1)}^{(i)}\right) \left(\frac{I_1}{2} + \frac{m_1 a^2}{2} + \frac{M l^2}{2} + \frac{l^2 m_2}{2}\right)}{(h^{(i)})^2} \\
 & + \frac{b l m_2 \cos\left(\frac{q_{(1,N)}^{(i)}}{2} - \frac{q_{(2,N)}^{(i)}}{2} + \frac{q_{(1,N-1)}^{(i)}}{2} - \frac{q_{(2,N-1)}^{(i)}}{2}\right) \left(q_{(2,N)}^{(i)} - q_{(2,N-1)}^{(i)}\right)}{(h^{(i)})^2} - b q_{(2,N)}^{(i)} l m_2 q_{(2,N)}^{(i)} \\
 & \sin\left(q_{(1,N)}^{(i)} - q_{(1,N)}^{(i)}\right) + \frac{b l m_2 \sin\left(\frac{q_{(1,N)}^{(i)}}{2} - \frac{q_{(2,N)}^{(i)}}{2} + \frac{q_{(1,N-1)}^{(i)}}{2} - \frac{q_{(2,N-1)}^{(i)}}{2}\right) \left(q_{(1,N)}^{(i)} - q_{(1,N-1)}^{(i)}\right) \left(q_{(2,N)}^{(i)} - q_{(2,N-1)}^{(i)}\right)}{2 (h^{(i)})^2} \\
 & - \tau_{(1,N)}^{(i)} = 0 \quad (9.5)
 \end{aligned}$$

The analytical expression of (2.41) is:

$$\begin{aligned}
 & \frac{g \sin\left(\frac{q_{(2,N)}^{(i)}}{2} + \frac{q_{(2,N-1)}^{(i)}}{2}\right) (m_1 a + M l + g m_2)}{2} \\
 & - 2 q_{(2,N)}^{(i)} \left(\frac{m_2 b^2}{2} + \frac{I_2}{2}\right) - \frac{\left(2 q_{(2,N)}^{(i)} - 2 q_{(2,N-1)}^{(i)}\right) \left(\frac{m_2 b^2}{2} + \frac{I_2}{2}\right)}{(h^{(i)})^2} \\
 & - \frac{b g m_2 \sin\left(\frac{q_{(2,N)}^{(i)}}{2} + \frac{q_{(2,N-1)}^{(i)}}{2}\right)}{2} + b l m_2 q_{(2,N)}^{(i)} \cos\left(q_{(1,N)}^{(i)} - q_{(1,N)}^{(i)}\right) \\
 & + \frac{b l m_2 \cos\left(\frac{q_{(1,N)}^{(i)}}{2} - \frac{q_{(2,N)}^{(i)}}{2} + \frac{q_{(1,N-1)}^{(i)}}{2} - \frac{q_{(2,N-1)}^{(i)}}{2}\right) \left(q_{(1,N)}^{(i)} - q_{(1,N-1)}^{(i)}\right)}{(h^{(i)})^2}
 \end{aligned}$$

$$\begin{aligned}
& \frac{bl m_2 \sin\left(\frac{q_{(1,N)}^{(i)}}{2} - \frac{q_{(2,N)}^{(i)} + \frac{q_{(1,N-1)}^{(i)}}{2} - \frac{q_{(2,N-1)}^{(i)}}{2}\right) \left(q_{(1,N)}^{(i)} - q_{(1,N-1)}^{(i)}\right) \left(q_{(2,N)}^{(i)} - q_{(2,N-1)}^{(i)}\right)}{2(h^{(i)})^2} \\
& - \tau_{(2,N)}^{(i)} = 0 \quad (9.6)
\end{aligned}$$

## 9.2 Swing Phase for the Direct Collocation Method (Leg1 = Swing, Leg2=Stance)

### 9.2.1 Derivation of the Euler-Lagrange Equations of Motion

The first step to deriving the Lagrangian of the biped is to define the homogeneous transfer matrices that describe the orientation and position of each link of the robot. One natural placement of local coordinate frames is indicated in Figure 9.1, where each frame is rigidly attached to the appropriate mass. The origins of each of these frames describe the following important points on the planar biped:

1.  $o_0$  - Global coordinate frame fixed to the ground.
2.  $o_1$  - Coordinate frame fixed to the center of mass for the swing leg(Leg 1).
3.  $o_M$  - Coordinate frame fixed to the center of mass of the hip joint.
4.  $o_2$  - Coordinate frame fixed to the center of mass for the stance leg(Leg 2).

These coordinate frames are used to form homogeneous transformation matrices on the form

$$H_j^i = \begin{bmatrix} R_j^i & p_j^i \\ 0_{1 \times 3} & 1 \end{bmatrix} \quad (9.7)$$

where  $R_j^i \in \mathbb{R}^{3 \times 3}$  is the rotation matrix from frame  $j$  to frame  $i$  and  $p_j^i \in \mathbb{R}^3$  is the distance between the origins of the respective frames expressed in frame  $i$ . Finding rotation matrices is complicated, requiring a parametrization of the total rotation of each frame in suitable coordinates. This process is greatly simplified by the fact that the planar biped only experiences

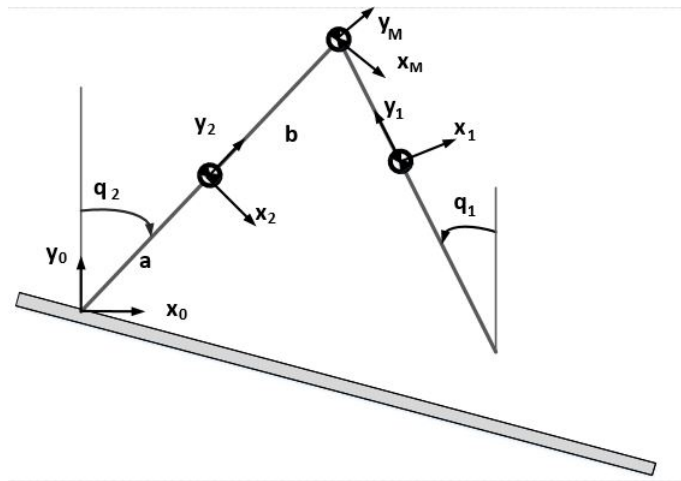


Figure 9.1: Assignment of origins for the coordinate frames of the biped.

motion in a 2-D plane. The transformation matrices can then be found by trigonometry and are stated for verification below:

$$\begin{aligned}
 H_2^0 &= \begin{bmatrix} \cos(q_2^{(i)}) & -\sin(q_2^{(i)}) & 0 & -a\sin(q_2^{(i)}) \\ -\sin(q_2^{(i)}) & \cos(q_2^{(i)}) & 0 & a\cos(q_2^{(i)}) \\ 0 & 0 & 1 & 0 \\ 0 & 0 & 0 & 1 \end{bmatrix} \\
 H_M^2 &= \begin{bmatrix} 1 & 0 & 0 & 0 \\ 0 & 1 & 0 & b \\ 0 & 0 & 1 & 0 \\ 0 & 0 & 0 & 1 \end{bmatrix} \\
 H_M^0 &= H_1^0 H_M^2 \\
 H_1^0 &= \begin{bmatrix} \cos(q_1^{(i)}) & -\sin(q_1^{(i)}) & 0 & l\sin(q_2^{(i)}) + b\sin(q_1^{(i)}) \\ \sin(q_1^{(i)}) & \cos(q_1^{(i)}) & 0 & l\cos(q_2^{(i)}) - b\cos(q_1^{(i)}) \\ 0 & 0 & 1 & 0 \\ 0 & 0 & 0 & 1 \end{bmatrix}
 \end{aligned} \tag{9.8}$$

The matrices (9.8) can now be employed to determine the position  $p^{(0)}$  and velocity  $v^{(0)}$  of the

center of mass of each mass in  $xy$  coordinates in the global frame  $o_0$  as

$$\begin{aligned} p_1^{(0)} &= [I_{2 \times 2} \ 0_{2 \times 2}] \cdot H_1^0 \cdot \begin{bmatrix} 0_{3 \times 1} \\ 1 \end{bmatrix}, v_1^{(0)} = \frac{d}{dt} p_1^{(0)} \\ p_M^{(0)} &= [I_{2 \times 2} \ 0_{2 \times 2}] \cdot H_M^0 \cdot \begin{bmatrix} 0_{3 \times 1} \\ 1 \end{bmatrix}, v_M^{(0)} = \frac{d}{dt} p_M^{(0)} \\ p_2^{(0)} &= [I_{2 \times 2} \ 0_{2 \times 2}] \cdot H_2^0 \cdot \begin{bmatrix} 0_{3 \times 1} \\ 1 \end{bmatrix}, v_2^{(0)} = \frac{d}{dt} p_2^{(0)} \end{aligned} \quad (9.9)$$

where  $I_{2 \times 2}$  is the identity matrix and  $p^{(0)}, v^{(0)} \in \mathbb{R}^2$ .

In order to form the Lagrangian of the system and compute the Euler-Lagrange equations, the kinetic and potential energy of the system must be determined. The potential energy is the sum of the potential energy at the center of mass for each mass and can be expressed as

$$\mathcal{P} = (m_1 h_1^{(0)} + M h_M^{(0)} + m_2 h_2^{(0)}) g \quad (9.10)$$

where  $g = (\sin(\theta_i) + \cos(\theta_i)) g_{const}$ , with  $g_{const} = 9.81 m/s^2$  and  $\theta_i$  defining the slope of the next walking step to be achieved, is the gravitational acceleration quantity in the horizontal and vertical axes and  $h^{(0)} = p^{(0)} \begin{bmatrix} 0 \\ 1 \end{bmatrix}$  is the height of the respective centers of mass expressed in the global frame  $o_0$ . The total kinetic energy is the sum of the body's centers-of-mass translational kinetic energy and the energy of rotation around the centers of mass (rotational energy), and can be expressed as

$$\mathcal{K} = \frac{1}{2} (m_1 v_1^T v_1 + M v_M^T v_M + m_2 v_2^T v_2) + \frac{1}{2} (I_1 (q_1^{(i)})^2 + I_2 (q_2^{(i)})^2) \quad (9.11)$$

Using the expressions (9.10) and (9.11) for the potential and kinetic energy, the Euler-Lagrange equations of motion can be calculated

$$\frac{d}{dt} \left( \frac{\partial \mathcal{L}}{\partial \dot{q}_{j^{(i)}}} \right) - \frac{\partial \mathcal{L}}{\partial q_{j^{(i)}}} = B_a \begin{bmatrix} \tau_1^{(i)} \\ \tau_2^{(i)} \end{bmatrix}, \quad j \in [1, 2] \quad (9.12)$$

where  $\mathcal{L}$  is the Lagrangian of the system derived from (9.10) and (9.11) as

$$\mathcal{L} = \mathcal{K} - \mathcal{P}$$

that extends to:

$$\begin{aligned} L(q_1^{(i)}, q_2^{(i)}, \dot{q}_1^{(i)}, \dot{q}_2^{(i)}) &= \frac{1}{2}(I_2 + m_1 a^2 + m_2 l^2 + M l^2) \dot{q}_2^{(i)2} + \frac{1}{2}(I_1 + m_2 b^2) \dot{q}_1^{(i)2} \\ &\quad - m_2 b l \cos(q_2^{(i)} - q_1^{(i)}) \dot{q}_1^{(i)} \dot{q}_2^{(i)} - (m_1 a + m_2 g + M l) g \cos(q_1^{(i)}) + m_2 g b \cos(q_1^{(i)}), \end{aligned} \quad (9.13)$$

$B_a$  is the applied forces selection matrix (it maps the applied forces and/or torques to the related generalized coordinates). Here,  $B_a = \begin{bmatrix} 1 & 0 \\ 0 & 1 \end{bmatrix}$  (thus, here  $B_a$  is a full row rank matrix)

assuming that, due to the use of the two hip actuators, the torques  $\tau_1^{(i)}$ ,  $\tau_2^{(i)}$  to the hip can be controlled. Using the expressions (8.39) – (8.41) for the elements of the respective matrices, the equations of motion for the biped can be formulated as

$$M(q^{(i)}) \ddot{q}^{(i)} + C(q^{(i)}, \dot{q}^{(i)}) \dot{q}^{(i)} + G(q^{(i)}, \theta_i) = B_a \begin{bmatrix} \tau_1^{(i)} \\ \tau_2^{(i)} \end{bmatrix} \quad (9.14)$$

$\Leftrightarrow$

$$M(q^{(i)}) \ddot{q}^{(i)} + C(q^{(i)}, \dot{q}^{(i)}) \dot{q}^{(i)} + G(q^{(i)}, \theta_i) = \begin{bmatrix} \tau_1^{(i)} \\ \tau_2^{(i)} \end{bmatrix}$$

where

$$M(q^{(i)}) = \begin{bmatrix} p_3 + I_1 & -p_2 \cos(q_2^{(i)} - q_1^{(i)}) \\ -p_2 \cos(q_2^{(i)} - q_1^{(i)}) & p_1 + I_2 \end{bmatrix} \quad (9.15)$$

$$C(q^{(i)}, \dot{q}^{(i)}) = \begin{bmatrix} p_2 \dot{q}_2^{(i)} \sin(q_2^{(i)} - q_1^{(i)}) & 0 \\ 0 & -p_2 \dot{q}_1^{(i)} \sin(q_2^{(i)} - q_1^{(i)}) \end{bmatrix} \quad (9.16)$$

$$G(q^{(i)}, \theta_i) = \begin{bmatrix} p_5 \sin(q_1^{(i)}) \\ -p_4 \sin(q_2^{(i)}) \end{bmatrix} \quad (9.17)$$

where  $I_1$ ,  $I_2$  are the moments of inertia of the Legs 1 and 2 about their centers of mass,

respectively, and with the constant parameters  $p_1 = Ml^2 + m_1a^2 + m_2l^2$ ,  $p_2 = m_2lb$ ,  $p_3 = m_2b^2$ ,  $p_4 = (m_1a + m_2l + Ml)g$ ,  $p_5 = m_2bg$ . The equations of motion (9.14) describe the continuous dynamics of the biped during the gait and is independent of the walking surface. In order to describe what happens to the robot during the impact phase, an impact map must be formulated to prevent trespassing of the surface during motion.

**•Initial discretization of the Swing Phase for the Direct Collocation Method (Leg1 = Swing, Leg2 = Stance)**

Now we will proceed with the initial discretization (without applying the Direct Collocation Conditions) of the Swing Phase of the 2-DOF Biped Robot for the case where the Leg 1 is the swing leg and the Leg 2 is the stance leg. Let  $k = 1, \dots, N$  the time steps of a walking step. In addition, let  $i = 1, \dots, H$  the number and the order of the total walking steps. So, when we refer to a generalized angle  $q_{(x,k)}^{(i)}$ , where  $x = 1, 2$ ,  $k = 1, \dots, N$  and  $i = 1, \dots, H$  we will actually mean the angle  $q_x$  of the  $k$ -th time step of the  $i$ -th walking step. A discretization of the time interval for a walking step

$$t_0 = t_1 < t_2 < \dots < t_N = t_f$$

is chosen. Without implementing the complete discretization process (it will be later explained in the current chapter), the Swing Phase becomes:

$$M(q_k^{(i)})\ddot{q}_k^{(i)} + C(q_k^{(i)}, \dot{q}_k^{(i)})\dot{q}_k^{(i)} + G(q_k^{(i)}, \theta_i) = B_a \begin{bmatrix} \tau_{(1,k)}^{(i)} \\ \tau_{(2,k)}^{(i)} \end{bmatrix}, k = 1, \dots, N \quad (9.18)$$

$\Leftrightarrow$

$$M(q_k^{(i)})\ddot{q}_k^{(i)} + C(q_k^{(i)}, \dot{q}_k^{(i)})\dot{q}_k^{(i)} + G(q_k^{(i)}, \theta_i) = \begin{bmatrix} \tau_{(1,k)}^{(i)} \\ \tau_{(2,k)}^{(i)} \end{bmatrix}, k = 1, \dots, N$$

where

$$M(q_k^{(i)}) = \begin{bmatrix} p_3 + I_1 & -p_2 \cos(q_{(2,k)}^{(i)} - q_{(1,k)}^{(i)}) \\ -p_2 \cos(q_{(2,k)}^{(i)} - q_{(1,k)}^{(i)}) & p_1 + I_2 \end{bmatrix}, k = 1, \dots, N \quad (9.19)$$

$$C(q_k^{(i)}, \dot{q}_k^{(i)}) = \begin{bmatrix} p_2 q_{(2,k)}^{(i)} \sin(q_{(2,k)}^{(i)} - q_{(1,k)}^{(i)}) & 0 \\ 0 & -p_2 \dot{q}_{(1,k)}^{(i)} \sin(q_{(2,k)}^{(i)} - q_{(1,k)}^{(i)}) \end{bmatrix}, k = 1, \dots, N \quad (9.20)$$

$$G(q_k^{(i)}, \theta_i) = \begin{bmatrix} p_5 \sin(q_{(1,k)}^{(i)}) \\ -p_4 \sin(q_{(2,k)}^{(i)}) \end{bmatrix}, k = 1, \dots, N \quad (9.21)$$

where  $I_1, I_2$  are the moments of inertia of the Legs 1 and 2 about their centers of mass, respectively, and with the constant parameters  $p_1 = Ml^2 + m_1 a^2 + m_2 l^2$ ,  $p_2 = m_2 l b$ ,  $p_3 = m_2 b^2$ ,  $p_4 = (m_1 a + m_2 l + Ml)g$ ,  $p_5 = m_2 b g$ .

### •State Space Equations of the Swing Phase for the Direct Collocation Method (Leg 1 = Swing, Leg 2 =Stance)

As we extensively developed the state space equations for the first case, we will now derive the state space equations for the case where Leg 1 is the Swing Leg and Leg 2 is the Stance Leg, and apply the Direct Collocation Conditions. The choice of state variables is the vector:

$$\begin{bmatrix} x_{(1,k)}^{(i)} \\ x_{(2,k)}^{(i)} \end{bmatrix} = \begin{bmatrix} q_k^{(i)} \\ \dot{q}_k^{(i)} \end{bmatrix}$$

$$\text{where } x_{(1,k)}^{(i)} = q_k^{(i)} = \begin{bmatrix} q_{(1,k)}^{(i)} \\ q_{(2,k)}^{(i)} \end{bmatrix} \text{ and } x_{(2,k)}^{(i)} = \dot{q}_k^{(i)} = \begin{bmatrix} \dot{q}_{(1,k)}^{(i)} \\ \dot{q}_{(2,k)}^{(i)} \end{bmatrix}$$

The state equations are:

$$\begin{bmatrix} \dot{x}_{(1,k)}^{(i)} \\ \dot{x}_{(2,k)}^{(i)} \end{bmatrix} = \begin{bmatrix} x_{(2,k)}^{(i)} \\ -M^{-1}(x_{(1,k)}^{(i)}) (C(x_{(1,k)}^{(i)}, x_{(2,k)}^{(i)}) x_{(2,k)}^{(i)} + G(x_{(1,k)}^{(i)}, \theta_i)) \end{bmatrix} + \begin{bmatrix} 0_{2 \times 2} \\ M^{-1}(x_{(1,k)}^{(i)}) B_a \end{bmatrix} u_k^{(i)}$$

$\Leftrightarrow$

$$\begin{bmatrix} \dot{x}_{(1,k)}^{(i)} \\ \dot{x}_{(2,k)}^{(i)} \end{bmatrix} =$$

$$\begin{aligned}
& \left[ \begin{array}{c} x_{(2,k)}^{(i)} \\ \frac{(I_1+p_3)(p_4 \sin(q_{(2,k)}^{(i)}) - q_{(1,k)}^{(i)})q_{(2,k)}^{(i)} p_2 \sin(q_{(1,k)}^{(i)} - q_{(2,k)}^{(i)}) - p_2 \cos(q_{(1,k)}^{(i)} - q_{(2,k)}^{(i)})(p_5 \sin(q_{(1,k)}^{(i)}) - q_{(1,k)}^{(i)})q_{(2,k)}^{(i)} p_2 \sin(q_{(1,k)}^{(i)} - q_{(2,k)}^{(i)})}{I_2 p_1 + I_1 p_3 + p_1 p_3 - p_2^2 \cos(q_{(1,k)}^{(i)} - q_{(2,k)}^{(i)})^2 + I_1^2} \\ \frac{p_2 \cos(q_{(1,k)}^{(i)} - q_{(2,k)}^{(i)})(p_4 \sin(q_{(2,k)}^{(i)}) - q_{(1,k)}^{(i)})q_{(2,k)}^{(i)} p_2 \sin(q_{(1,k)}^{(i)} - q_{(2,k)}^{(i)}) - (I_2 + p_1)(p_5 \sin(q_{(1,k)}^{(i)}) - q_{(1,k)}^{(i)})q_{(2,k)}^{(i)} p_2 \sin(q_{(1,k)}^{(i)} - q_{(2,k)}^{(i)})}{I_2 p_1 + I_1 p_3 + p_1 p_3 - p_2^2 \cos(q_{(1,k)}^{(i)} - q_{(2,k)}^{(i)})^2 + I_1^2} \end{array} \right] \\
& + \left[ \begin{array}{cc} 0 & 0 \\ 0 & 0 \\ \frac{p_2 \cos(q_{(1,k)}^{(i)} - q_{(2,k)}^{(i)})}{I_2 p_1 + I_1 p_3 + p_1 p_3 - p_2^2 \cos(q_{(1,k)}^{(i)} - q_{(2,k)}^{(i)})^2 + I_1^2} & \frac{(I_1 + p_3)}{I_2 p_1 + I_1 p_3 + p_1 p_3 - p_2^2 \cos(q_{(1,k)}^{(i)} - q_{(2,k)}^{(i)})^2 + I_1^2} \\ \frac{(I_2 + p_1)}{I_2 p_1 + I_1 p_3 + p_1 p_3 - p_2^2 \cos(q_{(1,k)}^{(i)} - q_{(2,k)}^{(i)})^2 + I_1^2} & \frac{p_2 \cos(q_{(1,k)}^{(i)} - q_{(2,k)}^{(i)})}{I_2 p_1 + I_1 p_3 + p_1 p_3 - p_2^2 \cos(q_{(1,k)}^{(i)} - q_{(2,k)}^{(i)})^2 + I_1^2} \end{array} \right] u_k^{(i)} \quad (9.22)
\end{aligned}$$

with the applied forces vector  $\tau_k^{(i)} = \begin{bmatrix} \tau_{(1,k)}^{(i)} \\ \tau_{(2,k)}^{(i)} \end{bmatrix}$  now denoted by  $u_k^{(i)} = \begin{bmatrix} u_{(1,k)}^{(i)} \\ u_{(2,k)}^{(i)} \end{bmatrix}$

The output function is:

$$y_k^{(i)} = x_{(1,k)}^{(i)}$$

For the Direct Collocation Method, based on subchapter 8.3.4, we proceed with the formulation

below. Let  $x_{approx}^{(i)}(t) = \begin{bmatrix} x_{(1,approx)}^{(i)}(t) \\ x_{(2,approx)}^{(i)}(t) \end{bmatrix}$ , where  $x_{(1,approx)}^{(i)}(t)$ ,  $x_{(2,approx)}^{(i)}(t)$  are the cubic approxi-

mations of the generalized coordinates  $q_1^{(i)}$ ,  $q_2^{(i)}$  as well as of their first and second derivatives, in the specified discretized time interval of the  $i$ -th walking step (relations 8.74-8.78). In addition,

let  $\tau_{approx}^{(i)}(t) = \begin{bmatrix} \tau_{(1,approx)}^{(i)}(t) \\ \tau_{(2,approx)}^{(i)}(t) \end{bmatrix}$ , where  $\tau_{(1,approx)}^{(i)}(t)$ ,  $\tau_{(2,approx)}^{(i)}(t)$  are the approximations

of the control inputs (torques)  $\tau_1^{(i)}$ ,  $\tau_2^{(i)}$  in the specified discretized time interval of the  $i$ -th walking step (relation 8.73). Thus, the state space equations of the Swing Phase for the case

where Leg 1 is the Stance Leg and Leg 2 is the Swing Leg are (relations 8.79, 8.92):

$$\begin{aligned}
& \begin{bmatrix} \dot{x}_{(1,approx)}^{(i)}(t_{ck}) \\ \dot{x}_{(2,approx)}^{(i)}(t_{ck}) \end{bmatrix} = \\
& \begin{bmatrix} x_{(2,approx)}^{(i)}(t_{ck}) \\ -M^{-1}(x_{(1,approx)}^{(i)}(t_{ck}))(C(x_{(1,approx)}^{(i)}(t_{ck}), x_{(2,approx)}^{(i)}(t_{ck}))x_{(2,approx)}^{(i)}(t_{ck}) + G(x_{(1,approx)}^{(i)}(t_{ck}), \theta_i)) \end{bmatrix}
\end{aligned}$$

$$+ \begin{bmatrix} 0_{2 \times 2} \\ M^{-1}(x_{(1,approx)}^{(i)}(t_{ck}))B_a \end{bmatrix} u_{(approx)}^{(i)}(t_{ck}) \quad (9.23)$$

which can be rewritten to the relation (9.22), having applied the collocation conditions. The output function is:

$$y_{approx}^{(i)}(t_{ck}) = x_{(1,approx)}^{(i)}(t_{ck})$$

### 9.2.2 Formulation of the Impact Map

When the swing foot impacts the surface of the ground, an update of the angular velocities  $\dot{q}_1^{(i)}, \dot{q}_2^{(i)}$  should occur to prevent the biped from falling through the floor. This update can be formulated as a mapping between the velocities just before and just after the collision with the ground on the form

$$\begin{bmatrix} \dot{q}_1^{(i,+)} \\ \dot{q}_2^{(i,+)} \end{bmatrix} = \Delta(q^{(i)}) \cdot \begin{bmatrix} \dot{q}_1^{(i,-)} \\ \dot{q}_2^{(i,-)} \end{bmatrix} \quad (9.24)$$

where  $-$ ,  $+$  denote the time instant right before and right after impact, respectively, so that specific time interval is considered extremely small. An important property of this impact mapping is the assumption that the configuration of the biped, the generalized coordinates  $q_1^{(i)}, q_2^{(i)}$ , remains unchanged during ground impact (which occurs in the abovementioned time interval). This is due to the fact that the impact forces  $F$  the biped experiences during impact are impulsive in nature. There are multiple ways of calculating the velocity updates of the biped. Presented below is a method that exploits properties of the impact to derive an impact map for the collision on the form (9.24).

### 9.2.3 Conservation of the angular momentum

Since the impact forces  $F$  are the only external forces affecting the biped (we assume that the torques applies to the biped during the impact are zero), the angular momentum about the impacting foot is conserved before and after the collision for the system. The angular

momentum  $L$  of a mass can be stated as

$$L = r \times mv + Iq_{COM}^{(i)} \quad (9.25)$$

where  $r$  is the position of the mass relative to a given reference point,  $m$  is the mass,  $v$  is the velocity of the mass,  $I$  is the moment of inertia around the particular center of mass and  $q_{COM}^{(i)}$  is the angular velocity of the particular leg where the center of mass is located. Given that the biped is a system of masses, the angular momentum of the robot about the impacting foot is given by:

$$L_{Biped}^{(0)} = \sum_i r_i^{(0)} \times m_i v_i^+ + I_1 q_1^{(i,+)} + I_2 q_2^{(i,+)} = \sum_i r_i^{(0)} \times m_i v_i^- + I_1 q_1^{(i,-)} + I_2 q_2^{(i,-)}, i \in \{1, 2, M\} \quad (9.26)$$

where the reference point is the origin  $o_0$ , and the position vectors  $r_i^{(0)}$  relative to this point is given by

$$\begin{aligned} r_1^{(0)} &= \begin{bmatrix} -a \sin(q_1^{(i,-)}) \\ a \cos(q_1^{(i,-)}) \\ 0 \end{bmatrix} \\ r_M^{(0)} &= \begin{bmatrix} -l \sin(q_1^{(i,-)}) \\ l \cos(q_1^{(i,-)}) \\ 0 \end{bmatrix} \\ r_2^{(0)} &= r_M^{(0)} + \begin{bmatrix} -b \sin(q_2^{(i,-)}) \\ -b \cos(q_2^{(i,-)}) \\ 0 \end{bmatrix} \end{aligned} \quad (9.27)$$

The translational velocities  $v_i^\pm$  are independent of the reference point and can be expressed using the angular velocities  $\dot{q}^\pm$  as

$$\begin{aligned}
v_M^- &= \begin{bmatrix} 0 \\ 0 \\ \dot{q}_2^{(i,-)} \end{bmatrix} \times \begin{bmatrix} l \sin(q_2^{(i,-)}) \\ l \cos(q_2^{(i,-)}) \\ 0 \end{bmatrix}, v_M^+ = \begin{bmatrix} 0 \\ 0 \\ \dot{q}_1^{(i,+)} \end{bmatrix} \times \begin{bmatrix} -l \sin(q_1^{(i,-)}) \\ l \cos(q_1^{(i,-)}) \\ 0 \end{bmatrix} \\
v_2^- &= \begin{bmatrix} 0 \\ 0 \\ \dot{q}_2^{(i,-)} \end{bmatrix} \times \begin{bmatrix} a \sin(q_2^{(i,-)}) \\ a \cos(q_2^{(i,-)}) \\ 0 \end{bmatrix}, v_2^+ = v_M^+ + \begin{bmatrix} 0 \\ 0 \\ \dot{q}_2^{(i,+)} \end{bmatrix} \times \begin{bmatrix} -b \sin(q_2^{(i,-)}) \\ -b \cos(q_2^{(i,-)}) \\ 0 \end{bmatrix} \\
v_1^- &= v_M^- + \begin{bmatrix} 0 \\ 0 \\ \dot{q}_1^{(i,-)} \end{bmatrix} \times \begin{bmatrix} b \sin(q_1^{(i,-)}) \\ -b \cos(q_1^{(i,-)}) \\ 0 \end{bmatrix}, v_1^+ = \begin{bmatrix} 0 \\ 0 \\ \dot{q}_1^{(i,+)} \end{bmatrix} \times \begin{bmatrix} -a \sin(q_1^{(i,-)}) \\ a \cos(q_1^{(i,-)}) \\ 0 \end{bmatrix}
\end{aligned} \tag{9.28}$$

Substituting (9.27) and (9.28) into (9.26) and computing the crossproducts, yields one equation for the two unknown velocities  $\dot{q}_1^{(i,+)}$ ,  $\dot{q}_2^{(i,+)}$ . This means that another equation is needed to solve the system.

The only forces that the pre-impact swing leg experiences during the collision is the constraint force acting on it from the hip joint. This means that the angular momentum of this leg about the hip is conserved through the impact, yielding another equation for the updated velocities on the form:

$$\begin{aligned}
L_{Swing}^{(M)} &= r_1^{(M)} \times m_1 v_1^+ + I_1 \dot{q}_1^{(i,+)} = r_1^{(M)} \times m_1 v_1^- + I_1 \dot{q}_1^{(i,-)} \\
r_1^{(M)} &= \begin{bmatrix} -b \sin(q_1^{(i,-)}) \\ -b \cos(q_1^{(i,-)}) \\ 0 \end{bmatrix}
\end{aligned} \tag{9.29}$$

where the reference point is the origin  $o_M$  and the velocities  $v_2^\pm$  is given in (9.28). Equations

(9.26) and (9.29) combined results in the linear system:

$$\begin{aligned} \begin{bmatrix} L_{Biped}^{(0)} \\ L_{Swing}^{(M)} \end{bmatrix} &= \mathcal{Q}_+ \dot{q}^{(i,+)} = \mathcal{Q}_- \dot{q}^{(i,-)} \\ \begin{bmatrix} L_{Biped}^{(0)} \\ L_{Swing}^{(M)} \end{bmatrix} &= \begin{bmatrix} p_8 + I_1 & -p_7 c_{21} \\ p_8 - p_7 c_{21} + I_1 & -p_7 c_{21} + p_6 + I_2 \end{bmatrix} \begin{bmatrix} \dot{q}_1^{(i,+)} \\ \dot{q}_2^{(i,+)} \end{bmatrix} = \begin{bmatrix} -p_9 + I_1 & 0 \\ p_{10} c_{21} + I_1 & -p_{11} + I_2 \end{bmatrix} \begin{bmatrix} \dot{q}_1^{(i,-)} \\ \dot{q}_2^{(i,-)} \end{bmatrix} \end{aligned} \quad (9.30)$$

where  $c_{21} = \cos(q_2^{(i,-)} - q_1^{(i,-)})$  and the parameters  $p_6 = m_1 l^2 + M l^2 + m_2 a^2$ ,  $p_7 = m_1 b l$ ,  $p_8 = m_1 b^2$ ,  $p_9 = m_1 a b$ ,  $p_{10} = m_2 l a + M l^2 + m_1 l a$ ,  $p_{11} = m_2 a b$ .

### •Discretization of the Impact Phase for both Methods (Leg1 = Swing, Leg2 = Stance)

Based on the extensive analysis of the impact phase above, we will now proceed with the discretization of the impact phase for the case where Leg1 is the swing leg and Leg2 is the stance leg. Let  $k = 1, \dots, N$  the time steps of a walking step. In addition, let  $i = 1, \dots, H$  the number and the order of the total walking steps. So, when we refer to a generalized angle  $q_{(x,k)}^{(i)}$ , where  $x = 1, 2$ ,  $k = 1, \dots, N$  and  $i = 1, \dots, H$  we will actually mean the angle  $q_x$  of the  $k$ -th time step of the  $i$ -th walking step. Each walking step has of course its own swing and impact phase.

We now define that the time instant before the impact of the swing leg at the ground (pre-impact phase) is the time step  $N$  of a walking step, and the time instant after the impact of the swing leg at the ground (post-impact phase) that also completes the current walking step is the time step 1 of the next walking step.

But at the time step  $N$  of a walking step the swing leg becomes the new stance leg and the stance leg becomes the new swing leg for the next walking step (both legs switch roles), so it is actually the first time step of the next walking step.

Hence:

- $\dot{q}_1^{(i,+)} = \dot{q}_{(1,1)}^{(i+1)}$ ,

- $\dot{q}_2^{(i,+)} = q_{(2,1)}^{(i+1)}$ ,
- $\dot{q}_1^{(i,-)} = q_{(1,N)}^{(i)}$ ,
- $\dot{q}_2^{(i,-)} = q_{(2,N)}^{(i)}$ .

Finally, (9.30) becomes:

$$\begin{bmatrix} p_8 + I_1 & -p_7 c_{21} \\ p_8 - p_7 c_{21} + I_1 & -p_7 c_{21} + p_6 + I_2 \end{bmatrix} \begin{bmatrix} q_{(1,1)}^{(i+1)} \\ q_{(2,1)}^{(i+1)} \end{bmatrix} = \begin{bmatrix} -p_9 + I_1 & 0 \\ p_{10} c_{21} + I_1 & -p_{11} + I_2 \end{bmatrix} \begin{bmatrix} q_{(1,N)}^{(i)} \\ q_{(2,N)}^{(i)} \end{bmatrix} \quad (9.31)$$

where  $c_{21} = \cos(q_{(2,N)}^{(i)} - q_{(1,N)}^{(i)})$  and the parameters  $p_6 = m_1 l^2 + M l^2 + m_2 a^2$ ,  $p_7 = m_1 b l$ ,  $p_8 = m_1 b^2$ ,  $p_9 = m_1 a b$ ,  $p_{10} = m_2 l a + M l^2 + m_1 l a$ ,  $p_{11} = m_2 a b$ .

Solving the system for  $\dot{q}^{(i,+)}$  by inverting the matrix  $\mathcal{Q}_+$  gives an impact map on the form (9.24)

$$\dot{q}^{(i+1)} = [\mathcal{Q}_+^{-1} \cdot \mathcal{Q}_-] \dot{q}^{(i)} \quad (9.32)$$

For the Direct Collocation Method, based on subchapter 8.3.4, we proceed with the formulation below. Let  $q_{approx}^{(i)}(t) = \begin{bmatrix} q_{(1,approx)}^{(i)}(t) \\ q_{(2,approx)}^{(i)}(t) \end{bmatrix}$ , where  $q_{(1,approx)}^{(i)}(t)$ ,  $q_{(2,approx)}^{(i)}(t)$  are the cubic approximations of the generalized coordinates  $q_1^{(i)}$ ,  $q_2^{(i)}$ , in the specified discretized time interval of the  $i$ -th walking step (relations 8.74-8.78). Thus, the Impact Phase for the case Leg 1 is the Stance Leg and Leg 2 is the Swing Leg are:

$$\begin{aligned} & \begin{bmatrix} p_8 + I_1 & -p_7 c_{21} \\ p_8 - p_7 c_{21} + I_1 & -p_7 c_{21} + p_6 + I_2 \end{bmatrix} \begin{bmatrix} \dot{q}_{(1,approx)}^{(i+1)}(t_1) \\ \dot{q}_{(2,approx)}^{(i+1)}(t_1) \end{bmatrix} \\ &= \begin{bmatrix} -p_9 + I_1 & 0 \\ p_{10} c_{21} + I_1 & -p_{11} + I_2 \end{bmatrix} \begin{bmatrix} \dot{q}_{(1,approx)}^{(i)}(t_N) \\ \dot{q}_{(2,approx)}^{(i)}(t_N) \end{bmatrix} \end{aligned} \quad (9.33)$$

where  $c_{21} = \cos(q_{(2,approx)}^{(i)}(t_N) - q_{(1,approx)}^{(i)}(t_N))$  and the parameters  $p_6 = m_1 l^2 + M l^2 + m_2 b^2$ ,  $p_7 = m_1 b l$ ,  $p_8 = m_1 b^2$ ,  $p_9 = m_1 a b$ ,  $p_{10} = m_2 l a + M l^2 + m_1 l a$ ,  $p_{11} = m_2 a b$ .

Solving the system for  $q_{approx}^{(i,+)}$  by inverting the matrix  $\mathcal{Q}_+$  gives an impact map on the

form (9.24)

$$\dot{q}_{approx}^{(i+1)} = [\mathcal{Q}_+^{-1} \cdot \mathcal{Q}_-] \dot{q}_{approx}^{(i)} \quad (9.34)$$

### 9.2.4 Definition of Impact Surface

The abovementioned impact map calculated the change in angular velocities that occur when the biped robot impacts with the ground. In order for this update to correctly be applied when the swing foot strikes the ground, the configurations of the robot that results in an impact must be determined. These configurations correspond to the hypersurface  $S$  known as the impact surface or switching surface. A configuration of the biped that leads to impact with the ground during the  $i$ -th walking step (it may be a downward or upward slope, a general rough terrain or just simply a flat ground) must satisfy the relation:

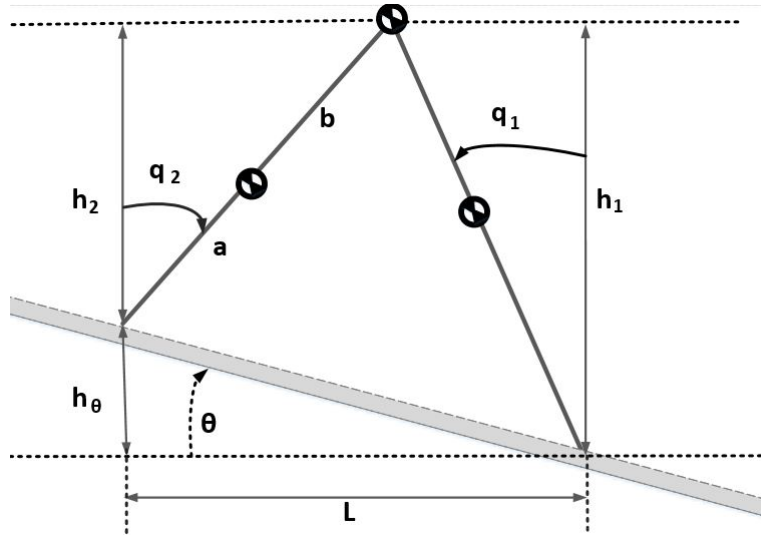


Figure 9.2: Different quantities used for the definition of the impact surface of the robot.

$$H(q_{(1,N)}^{(i)}, q_{(2,N)}^{(i)}, \theta_i) = h_2(q_{(2,N)}^{(i)}) + h_\theta(\theta_i) - h_1(q_{(1,N)}^{(i)}) = 0 \quad (9.35)$$

where

$$\begin{aligned} h_1(q_{(1,N)}^{(i)}) &= l \cos(q_{(1,N)}^{(i)}) \\ h_2(q_{(2,N)}^{(i)}) &= l \cos(q_{(2,N)}^{(i)}) \\ h_\theta(\theta_i) &= L \tan(\theta_i) \\ L &= l \sin(q_{(1,N)}^{(i)}) + l \sin(q_{(2,N)}^{(i)}) \end{aligned} \quad (9.36)$$

are found by trigonometry. Substituting these expressions and simplifying using trigonometric identities leads to the following derivation

$$\begin{aligned}
H(q_{(1,N)}^{(i)}, q_{(2,N)}^{(i)}, \theta_i) &= l \cos(q_{(2,N)}^{(i)}) + [l \sin(q_{(1,N)}^{(i)}) + l \sin(q_{(2,N)}^{(i)})] \frac{\sin(\theta_i)}{\cos(\theta_i)} - l \cos(q_{(1,N)}^{(i)}) = 0 \\
H(q_{(1,N)}^{(i)}, q_{(2,N)}^{(i)}, \theta_i) &= \cos(q_{(2,N)}^{(i)}) \cos(\theta_i) + \sin(q_{(1,N)}^{(i)}) \sin(\theta_i) - \cos(q_{(1,N)}^{(i)}) \cos(\theta_i) + \\
\sin(q_{(2,N)}^{(i)}) \sin(\theta_i) &= 0 \\
H(q_{(1,N)}^{(i)}, q_{(2,N)}^{(i)}, \theta_i) &= \cos(-q_{(2,N)}^{(i)}) \cos(\theta_i) - \sin(-q_{(1,N)}^{(i)}) \sin(\theta_i) - \cos(q_{(1,N)}^{(i)}) \cos(\theta_i) + \\
\sin(q_{(2,N)}^{(i)}) \sin(\theta_i) &= 0 \\
H(q_{(1,N)}^{(i)}, q_{(2,N)}^{(i)}, \theta_i) &= [\cos(-q_{(2,N)}^{(i)}) \cos(\theta_i) - \sin(-q_{(1,N)}^{(i)}) \sin(\theta_i)] - [\cos(q_{(1,N)}^{(i)}) \cos(\theta_i) - \\
\sin(q_{(2,N)}^{(i)}) \sin(\theta_i)] &= 0 \\
H(q_{(1,N)}^{(i)}, q_{(2,N)}^{(i)}, \theta_i) &= \cos(-q_{(2,N)}^{(i)} + \theta_i) - \cos(q_{(1,N)}^{(i)} + \theta_i) = 0
\end{aligned} \tag{9.37}$$

Furthermore, the configuration of the biped remains unchanged during ground impact, in the time interval between the  $N$ th time step of the  $i$ th walking step and the first time step of the  $i+1$ th walking step,  $[t_N^{(i)}, t_1^{(i+1)}]$ . Thus, the switching surface  $S$  is defined as all configurations  $q$  of the biped that satisfies the above relations and conditions and can be stated in set notation as:

$$\begin{aligned}
S = \{q_{(1,N)}^{(i)}, q_{(2,N)}^{(i)}, q_{(1,1)}^{(i+1)}, q_{(2,1)}^{(i+1)}, \theta_i \in \mathbb{R} : H(q_{(1,N)}^{(i)}, q_{(2,N)}^{(i)}, \theta_i) = \cos(-q_{(2,N)}^{(i)} + \theta_i) - \cos(q_{(1,N)}^{(i)} + \theta_i) = 0, \\
H(q_{(1,1)}^{(i+1)}, q_{(2,1)}^{(i+1)}, \theta_i) = \cos(-q_{(2,1)}^{(i+1)} + \theta_i) - \cos(q_{(1,1)}^{(i+1)} + \theta_i) = 0\} \tag{9.38}
\end{aligned}$$

For the Direct Collocation Method, based on subchapter 8.3.4, we proceed with the formulation below. Let  $q_{approx}^{(i)}(t) = \begin{bmatrix} q_{(1,approx)}^{(i)}(t) \\ q_{(2,approx)}^{(i)}(t) \end{bmatrix}$ , where  $q_{(1,approx)}^{(i)}(t)$ ,  $q_{(2,approx)}^{(i)}(t)$  are the cubic approximations of the generalized coordinates  $q_1^{(i)}$ ,  $q_2^{(i)}$ , in the specified discretized time interval of the  $i$ -th walking step (relations 8.74-8.78). Thus, with a similar proof as above (having applied the Direct Collocation Conditions), the switching surface  $S$  is defined as all configurations  $q_{approx}$  of the biped that satisfies the above relation and can be stated in set notation as:

$$S = \{q_{(1,approx)}^{(i)}(t_N), q_{(2,approx)}^{(i)}(t_N), q_{(1,approx)}^{(i+1)}(t_1), q_{(2,approx)}^{(i+1)}(t_1), \theta_i \in \mathbb{R} : H(q_{(1,approx)}^{(i)}(t_N), q_{(2,approx)}^{(i)}(t_N), \theta_i)$$

$$= \cos(-q_{(2,approx)}^{(i)}(t_N) + \theta_i) - \cos(q_{(1,approx)}^{(i)}(t_N) + \theta_i) = 0\} \quad (9.39)$$

### 9.3 Swing Phase using Discrete Mechanics (Leg1=Swing, Leg2=Stance)

We now develop the discretized Swing Phase of our 2-DOF biped robot via the use of the Discrete Mechanics Theory. We define some important notations. Let  $h^{(i)}$  be the sampling time for the  $i$ th walking step,  $r$  a division ratio quantity in discrete mechanics,  $k = 1, \dots, N$  the number of time steps,  $H$  the total number of walking steps,  $i = 1, 2, \dots, H$  the walking step index,  $q_{(1,k)}^{(i)}$ ,  $q_{(2,k)}^{(i)}$  the angles of Leg 1 and Leg 2 at the  $k$ -th time step in the  $i$ -th walking step respectively and  $\tau_{(1,k)}^{(i)}$ ,  $\tau_{(2,k)}^{(i)}$  the control inputs (torques) at the  $k$ -th time step in the  $i$ -th walking step for the swing and stance leg respectively.

We now derive the discretized swing phase and impact phase for the 2-DOF biped robot where Leg 1 is the swing leg and Leg 2 is the stance leg. We firstly calculate the Discrete Lagrangian  $L_r^d(q_{(1,k)}^{(i)}, q_{(1,k+1)}^{(i)}, q_{(2,k)}^{(i)}, q_{(2,k+1)}^{(i)})$  from (8.44), (9.13) as:

$$\begin{aligned} L_r^d(q_{(1,k)}^{(i)}, q_{(1,k+1)}^{(i)}, q_{(2,k)}^{(i)}, q_{(2,k+1)}^{(i)}) &= \frac{1}{2}(I_2 + m_1 a^2 + m_2 l^2 + Ml^2) \left( \frac{q_{(2,k+1)}^{(i)} - q_{(2,k)}^{(i)}}{h^{(i)}} \right)^2 + \\ &\frac{1}{2}(I_1 + m_2 b^2) \left( \frac{q_{(1,k+1)}^{(i)} - q_{(1,k)}^{(i)}}{h^{(i)}} \right)^2 - m_2 b l \cos((1-a)q_{(2,k)}^{(i)} + aq_{(2,k+1)}^{(i)} - (1-a)q_{(1,k)}^{(i)} - aq_{(1,k+1)}^{(i)}) \\ &\left( \frac{q_{(2,k+1)}^{(i)} - q_{(2,k)}^{(i)}}{h^{(i)}} \right) \left( \frac{q_{(1,k+1)}^{(i)} - q_{(1,k)}^{(i)}}{h^{(i)}} \right) - (m_1 a + m_2 g + Ml) g \cos((1-a)q_{(1,k)}^{(i)} + aq_{(1,k+1)}^{(i)}) + \\ &m_2 g b \cos((1-a)q_{(1,k)}^{(i)} + aq_{(1,k+1)}^{(i)}) \quad (9.40) \end{aligned}$$

Due to the fact that the left and right discrete forces (8.46) satisfy  $f_d^+(q_k, q_{k+1}, \tau_k) = f_d^-(q_k, q_{k+1}, \tau_k)$  for  $r = \frac{1}{2}$ , we set a type of control inputs (the torques for Leg1 and 2) that consists only of the left discrete external force  $f_d^-$  as:

$$\tau_k^{(i)} := f_d^-(q_k, q_{k+1}, \tau_k), k = 1, \dots, N \quad (9.41)$$

Substituting (9.40) into the discrete Euler-Lagrange Equations (8.49) while also deriving the boundary conditions (8.58, 8.60), and using the discrete control inputs (9.41), we develop the discretized Swing Phase of the biped:

$$D_2 L^d(q_{(1,k-1)}^{(i)}, q_{(1,k)}^{(i)}, q_{(2,k-1)}^{(i)}, q_{(2,k)}^{(i)}) + D_1 L^d(q_{(1,k)}^{(i)}, q_{(1,k+1)}^{(i)}, q_{(2,k)}^{(i)}, q_{(2,k+1)}^{(i)}) - \tau_{(1,k)}^{(i)} = 0, (k = 1, \dots, N) \quad (9.42)$$

$$D_4 L^d(q_{(1,k-1)}^{(i)}, q_{(1,k)}^{(i)}, q_{(2,k-1)}^{(i)}, q_{(2,k)}^{(i)}) + D_3 L^d(q_{(1,k)}^{(i)}, q_{(1,k+1)}^{(i)}, q_{(2,k)}^{(i)}, q_{(2,k+1)}^{(i)}) - \tau_{(2,k)}^{(i)} = 0, (k = 1, \dots, N) \quad (9.43)$$

The boundary conditions are given from the following equations:

$$D_2 L^c(q_{(1,1)}^{(i)}, q_{(1,1)}^{(i)}, q_{(2,1)}^{(i)}, q_{(2,1)}^{(i)}) + D_1 L^d(q_{(1,1)}^{(i)}, q_{(1,2)}^{(i)}, q_{(2,1)}^{(i)}, q_{(2,2)}^{(i)}) - \tau_{(1,1)}^{(i)} = 0 \quad (9.44)$$

$$D_4 L^c(q_{(1,1)}^{(i)}, q_{(1,1)}^{(i)}, q_{(2,1)}^{(i)}, q_{(2,1)}^{(i)}) + D_3 L^d(q_{(1,1)}^{(i)}, q_{(1,2)}^{(i)}, q_{(2,1)}^{(i)}, q_{(2,2)}^{(i)}) - \tau_{(2,1)}^{(i)} = 0 \quad (9.45)$$

$$-D_2 L^c(q_{(1,N)}^{(i)}, q_{(1,N)}^{(i)}, q_{(2,N)}^{(i)}, q_{(2,N)}^{(i)}) + D_1 L^d(q_{(1,N-1)}^{(i)}, q_{(1,N)}^{(i)}, q_{(2,N-1)}^{(i)}, q_{(2,N)}^{(i)}) - \tau_{(1,N)}^{(i)} = 0 \quad (9.46)$$

$$-D_4 L^c(q_{(1,N)}^{(i)}, q_{(1,N)}^{(i)}, q_{(2,N)}^{(i)}, q_{(2,N)}^{(i)}) + D_3 L^d(q_{(1,N-1)}^{(i)}, q_{(1,N)}^{(i)}, q_{(2,N-1)}^{(i)}, q_{(2,N)}^{(i)}) - \tau_{(2,N)}^{(i)} = 0 \quad (9.47)$$

Regarding some specific cases of values for the time step  $k$  for which the abovementioned equations are valid:

- For  $i = 1$  and  $k = 1$ ,  $q_{(1,k-1)}^{(i)} = q_{(1,0)}^{(1)} = 0$ ,  $q_{(2,k-1)}^{(i)} = q_{(2,0)}^{(1)} = 0$ ,  $\tau_{(1,k-1)}^{(i)} = \tau_{(1,0)}^{(1)} = 0$  and  $\tau_{(2,k-1)}^{(i)} = \tau_{(2,0)}^{(1)} = 0$  (due to the fact that  $k = [1, \dots, N]$ ),
- For  $i > 1$  and  $k = 1$ ,  $q_{(1,k-1)}^{(i)} = q_{(1,N)}^{(i-1)}$ ,  $q_{(2,k-1)}^{(i)} = q_{(2,N)}^{(i-1)}$ ,  $\tau_{(1,k-1)}^{(i)} = \tau_{(1,N)}^{(i-1)}$  and  $\tau_{(2,k-1)}^{(i)} = \tau_{(2,N)}^{(i-1)}$ ,
- For  $k = N$ ,  $q_{(1,k+1)}^{(i)} = q_{(1,1)}^{(i+1)}$  and  $q_{(2,k+1)}^{(i)} = q_{(2,1)}^{(i+1)}$ .

The analytical expression of (9.42) is:

$$\frac{g \sin\left(\frac{q_{(1,k)}^{(i)}}{2} + \frac{q_{(1,k-1)}^{(i)}}{2}\right) (m_1 a + M l + g m_2)}{2} + \frac{g \sin\left(\frac{q_{(1,k)}^{(i)}}{2} + \frac{q_{(1,k+1)}^{(i)}}{2}\right) (m_1 a + M l + g m_2)}{2} \\ + \frac{\left(2 q_{(1,k)}^{(i)} - 2 q_{(1,k-1)}^{(i)}\right) \left(\frac{m_2 b^2}{2} + \frac{I_1}{2}\right)}{(h^{(i)})^2} + \frac{\left(2 q_{(1,k)}^{(i)} - 2 q_{(1,k+1)}^{(i)}\right) \left(\frac{m_2 b^2}{2} + \frac{I_1}{2}\right)}{(h^{(i)})^2} - \frac{b g m_2 \sin\left(\frac{q_{(1,k)}^{(i)}}{2} + \frac{q_{(1,k-1)}^{(i)}}{2}\right)}{2}$$

$$\begin{aligned}
& \frac{b g m_2 \sin\left(\frac{q_{(1,k)}^{(i)}}{2} + \frac{q_{(1,k+1)}^{(i)}}{2}\right)}{2} - \frac{b l m_2 \cos\left(\frac{q_{(2,k)}^{(i)}}{2} - \frac{q_{(1,k)}^{(i)}}{2} + \frac{q_{(2,k-1)}^{(i)}}{2} - \frac{q_{(1,k-1)}^{(i)}}{2}\right) \left(q_{(2,k)}^{(i)} - q_{(2,k-1)}^{(i)}\right)}{(h^{(i)})^2} \\
& - \frac{b l m_2 \cos\left(\frac{q_{(2,k)}^{(i)}}{2} - \frac{q_{(1,k)}^{(i)}}{2} + \frac{q_{(2,k+1)}^{(i)}}{2} - \frac{q_{(1,k+1)}^{(i)}}{2}\right) \left(q_{(2,k)}^{(i)} - q_{(2,k+1)}^{(i)}\right)}{(h^{(i)})^2} \\
& - \frac{b l m_2 \sin\left(\frac{q_{(2,k)}^{(i)}}{2} - \frac{q_{(1,k)}^{(i)}}{2} + \frac{q_{(2,k-1)}^{(i)}}{2} - \frac{q_{(1,k-1)}^{(i)}}{2}\right) \left(q_{(2,k)}^{(i)} - q_{(2,k-1)}^{(i)}\right) \left(q_{(1,k)}^{(i)} - q_{(1,k-1)}^{(i)}\right)}{2 (h^{(i)})^2} \\
& - \frac{b l m_2 \sin\left(\frac{q_{(2,k)}^{(i)}}{2} - \frac{q_{(1,k)}^{(i)}}{2} + \frac{q_{(2,k+1)}^{(i)}}{2} - \frac{q_{(1,k+1)}^{(i)}}{2}\right) \left(q_{(2,k)}^{(i)} - q_{(2,k+1)}^{(i)}\right) \left(q_{(1,k)}^{(i)} - q_{(1,k+1)}^{(i)}\right)}{2 (h^{(i)})^2} \\
& - \tau_{(1,k)}^{(i)} = 0, (k = 1, \dots, N) \quad (9.48)
\end{aligned}$$

The analytical expression of (9.43) is:

$$\begin{aligned}
& \frac{\left(2 q_{(2,k)}^{(i)} - 2 q_{(2,k-1)}^{(i)}\right) \left(\frac{I_2}{2} + \frac{m_1 a^2}{2} + \frac{M l^2}{2} + \frac{l^2 m_2}{2}\right)}{(h^{(i)})^2} + \frac{\left(2 q_{(2,k)}^{(i)} - 2 q_{(2,k+1)}^{(i)}\right) \left(\frac{I_2}{2} + \frac{m_1 a^2}{2} + \frac{M l^2}{2} + \frac{l^2 m_2}{2}\right)}{(h^{(i)})^2} \\
& - \frac{b l m_2 \cos\left(\frac{q_{(2,k)}^{(i)}}{2} - \frac{q_{(1,k)}^{(i)}}{2} + \frac{q_{(2,k-1)}^{(i)}}{2} - \frac{q_{(1,k-1)}^{(i)}}{2}\right) \left(q_{(1,k)}^{(i)} - q_{(1,k-1)}^{(i)}\right)}{(h^{(i)})^2} \\
& - \frac{b l m_2 \cos\left(\frac{q_{(2,k)}^{(i)}}{2} - \frac{q_{(1,k)}^{(i)}}{2} + \frac{q_{(2,k+1)}^{(i)}}{2} - \frac{q_{(1,k+1)}^{(i)}}{2}\right) \left(q_{(1,k)}^{(i)} - q_{(1,k+1)}^{(i)}\right)}{(h^{(i)})^2} \\
& + \frac{b l m_2 \sin\left(\frac{q_{(2,k)}^{(i)}}{2} - \frac{q_{(1,k)}^{(i)}}{2} + \frac{q_{(2,k-1)}^{(i)}}{2} - \frac{q_{(1,k-1)}^{(i)}}{2}\right) \left(q_{(2,k)}^{(i)} - q_{(2,k-1)}^{(i)}\right) \left(q_{(1,k)}^{(i)} - q_{(1,k-1)}^{(i)}\right)}{2 (h^{(i)})^2} \\
& + \frac{b l m_2 \sin\left(\frac{q_{(2,k)}^{(i)}}{2} - \frac{q_{(1,k)}^{(i)}}{2} + \frac{q_{(2,k+1)}^{(i)}}{2} - \frac{q_{(1,k+1)}^{(i)}}{2}\right) \left(q_{(2,k)}^{(i)} - q_{(2,k+1)}^{(i)}\right) \left(q_{(1,k)}^{(i)} - q_{(1,k+1)}^{(i)}\right)}{2 (h^{(i)})^2} \\
& - \tau_{(2,k)}^{(i)} = 0, (k = 1, \dots, N) \quad (9.49)
\end{aligned}$$

The above set of equations, can be rewritten to a similar form of the model (9.14):

$$M(q_k^{(i)}) \cdot \left(\frac{q_{k+1}^{(i)} - 2q_k^{(i)} + q_{k-1}^{(i)}}{(h^{(i)})^2}\right) + C(q_k^{(i)}, \frac{q_{k+1}^{(i)} - q_k^{(i)}}{h^{(i)}}) \cdot \left(\frac{q_{k+1}^{(i)} - q_k^{(i)}}{h^{(i)}}\right) + G(q_k^{(i)}, \theta_i) = B_a \begin{bmatrix} \tau_{(1,k)}^{(i)} \\ \tau_{(2,k)}^{(i)} \end{bmatrix} \quad (9.50)$$

⇔

$$M(q_k^{(i)}) \cdot \left( \frac{q_{k+1}^{(i)} - 2q_k^{(i)} + q_{k-1}^{(i)}}{(h^{(i)})^2} \right) + C(q_k^{(i)}, \frac{q_{k+1}^{(i)} - q_k^{(i)}}{h^{(i)}}) \cdot \left( \frac{q_{k+1}^{(i)} - q_k^{(i)}}{h^{(i)}} \right) + G(q_k^{(i)}, \theta_i) = \begin{bmatrix} \tau_{(1,k)}^{(i)} \\ \tau_{(2,k)}^{(i)} \end{bmatrix}$$

⇔

$$\begin{bmatrix} p_3 + I_1 & -p_2 \cos(q_{(2,k)}^{(i)} - q_{(1,k)}^{(i)}) \\ -p_2 \cos(q_{(2,k)}^{(i)} - q_{(1,k)}^{(i)}) & p_1 + I_2 \end{bmatrix} \begin{bmatrix} \frac{q_{(1,k+1)}^{(i)} - 2q_{(1,k)}^{(i)} + q_{(1,k-1)}^{(i)}}{(h^{(i)})^2} \\ \frac{q_{(2,k+1)}^{(i)} - 2q_{(2,k)}^{(i)} + q_{(2,k-1)}^{(i)}}{(h^{(i)})^2} \end{bmatrix} + \begin{bmatrix} p_2 \left( \frac{q_{(2,k+1)}^{(i)} - q_{(2,k)}^{(i)}}{h^{(i)}} \right) \sin(q_{(2,k)}^{(i)} - q_{(1,k)}^{(i)}) & 0 \\ 0 & -p_2 \left( \frac{q_{(1,k+1)}^{(i)} - q_{(1,k)}^{(i)}}{h^{(i)}} \right) \sin(q_{(2,k)}^{(i)} - q_{(1,k)}^{(i)}) \end{bmatrix} \begin{bmatrix} \frac{q_{(1,k+1)}^{(i)} - q_{(1,k)}^{(i)}}{h^{(i)}} \\ \frac{q_{(2,k+1)}^{(i)} - q_{(2,k)}^{(i)}}{h^{(i)}} \end{bmatrix} + \begin{bmatrix} p_5 \sin(q_{(1,k)}^{(i)}) \\ -p_4 \sin(q_{(2,k)}^{(i)}) \end{bmatrix} = \begin{bmatrix} \tau_{(1,k)}^{(i)} \\ \tau_{(2,k)}^{(i)} \end{bmatrix} \quad (9.51)$$

where  $k = 1, \dots, N$ ,  $I_1, I_2$  are the moments of inertia of the Legs 1 and 2 about their centers of mass, respectively, and with the constant parameters  $p_1 = Ml^2 + m_1a^2 + m_2l^2$ ,  $p_2 = m_2lb$ ,  $p_3 = m_2b^2$ ,  $p_4 = (m_1a + m_2l + Ml)g$ ,  $p_5 = m_2bg$ .

The analytical expression of (9.44) is:

$$\begin{aligned} & 2 \dot{q}_{(1,1)}^{(i)} \left( \frac{m_2 b^2}{2} + \frac{I_1}{2} \right) + \frac{g \sin\left(\frac{q_{(1,1)}^{(i)}}{2} + \frac{q_{(1,2)}^{(i)}}{2}\right) (m_1 a + Ml + g m_2)}{2} + \frac{\left(2 \dot{q}_{(1,1)}^{(i)} - 2 \dot{q}_{(1,2)}^{(i)}\right) \left(\frac{m_2 b^2}{2} + \frac{I_1}{2}\right)}{(h^{(i)})^2} \\ & - \frac{b g m_2 \sin\left(\frac{q_{(1,1)}^{(i)}}{2} + \frac{q_{(1,2)}^{(i)}}{2}\right)}{2} - b l m_2 \dot{q}_{(1,1)}^{(i)} \cos\left(\dot{q}_{(2,1)}^{(i)} - \dot{q}_{(2,1)}^{(i)}\right) \\ & - \frac{b l m_2 \cos\left(\frac{q_{(2,1)}^{(i)}}{2} + \frac{q_{(2,2)}^{(i)}}{2} - \frac{q_{(1,1)}^{(i)}}{2} - \frac{q_{(1,2)}^{(i)}}{2}\right) \left(\dot{q}_{(2,1)}^{(i)} - \dot{q}_{(2,2)}^{(i)}\right)}{(h^{(i)})^2} \\ & - \frac{b l m_2 \sin\left(\frac{q_{(2,1)}^{(i)}}{2} + \frac{q_{(2,2)}^{(i)}}{2} - \frac{q_{(1,1)}^{(i)}}{2} - \frac{q_{(1,2)}^{(i)}}{2}\right) \left(\dot{q}_{(2,1)}^{(i)} - \dot{q}_{(2,2)}^{(i)}\right) \left(\dot{q}_{(1,1)}^{(i)} - \dot{q}_{(1,2)}^{(i)}\right)}{2 (h^{(i)})^2} \\ & - \tau_{(1,1)}^{(i)} = 0 \quad (9.52) \end{aligned}$$

The analytical expression of (9.45) is:

$$\begin{aligned}
& \frac{\left(2 q_{(2,1)}^{(i)} - 2 q_{(2,2)}^{(i)}\right) \left(\frac{I_2}{2} + \frac{m_1 a^2}{2} + \frac{M l^2}{2} + \frac{l^2 m_2}{2}\right)}{(h^{(i)})^2} + g \sin(q_{(2,1)}^{(i)}) (m_1 a + M l + g m_2) - b g m_2 \sin(q_{(2,1)}^{(i)}) \\
& - \frac{b l m_2 \cos\left(\frac{q_{(2,1)}^{(i)}}{2} + \frac{q_{(2,2)}^{(i)}}{2} - \frac{q_{(1,1)}^{(i)}}{2} - \frac{q_{(1,2)}^{(i)}}{2}\right) \left(q_{(1,1)}^{(i)} - q_{(1,2)}^{(i)}\right)}{(h^{(i)})^2} + b q_{(1,1)}^{(i)} l m_2 q_{(1,1)}^{(i)} \sin\left(q_{(2,1)}^{(i)} - q_{(2,1)}^{(i)}\right) \\
& + \frac{b l m_2 \sin\left(\frac{q_{(2,1)}^{(i)}}{2} + \frac{q_{(2,2)}^{(i)}}{2} - \frac{q_{(1,1)}^{(i)}}{2} - \frac{q_{(1,2)}^{(i)}}{2}\right) \left(q_{(2,1)}^{(i)} - q_{(2,2)}^{(i)}\right) \left(q_{(1,1)}^{(i)} - q_{(1,2)}^{(i)}\right)}{2 (h^{(i)})^2} \\
& - \tau_{(2,1)}^{(i)} = 0 \quad (9.53)
\end{aligned}$$

The analytical expression of (9.46) is:

$$\begin{aligned}
& \frac{g \sin\left(\frac{q_{(1,N)}^{(i)}}{2} + \frac{q_{(1,N-1)}^{(i)}}{2}\right) (m_1 a + M l + g m_2)}{2} - 2 q_{(1,N)}^{(i)} \left(\frac{m_2 b^2}{2} + \frac{I_1}{2}\right) \\
& - \frac{\left(2 q_{(1,N)}^{(i)} - 2 q_{(1,N-1)}^{(i)}\right) \left(\frac{m_2 b^2}{2} + \frac{I_1}{2}\right)}{(h^{(i)})^2} \\
& - \frac{b g m_2 \sin\left(\frac{q_{(1,N)}^{(i)}}{2} + \frac{q_{(1,N-1)}^{(i)}}{2}\right)}{2} + b l m_2 q_{(1,N)}^{(i)} \cos\left(q_{(2,N)}^{(i)} - q_{(2,N)}^{(i)}\right) \\
& + \frac{b l m_2 \cos\left(\frac{q_{(2,N)}^{(i)}}{2} - \frac{q_{(1,N)}^{(i)}}{2} + \frac{q_{(2,N-1)}^{(i)}}{2} - \frac{q_{(1,N-1)}^{(i)}}{2}\right) \left(q_{(2,N)}^{(i)} - q_{(2,N-1)}^{(i)}\right)}{(h^{(i)})^2} \\
& - \frac{b l m_2 \sin\left(\frac{q_{(2,N)}^{(i)}}{2} - \frac{q_{(1,N)}^{(i)}}{2} + \frac{q_{(2,N-1)}^{(i)}}{2} - \frac{q_{(1,N-1)}^{(i)}}{2}\right) \left(q_{(2,N)}^{(i)} - q_{(2,N-1)}^{(i)}\right) \left(q_{(1,N)}^{(i)} - q_{(1,N-1)}^{(i)}\right)}{2 (h^{(i)})^2} \\
& - \tau_{(1,N)}^{(i)} = 0 \quad (9.54)
\end{aligned}$$

The analytical expression of (9.47) is:

$$\begin{aligned}
& b g m_2 \sin(q_{(2,N)}^{(i)}) - g \sin(q_{(2,N)}^{(i)}) (m_1 a + M l + g m_2) \\
& - \frac{\left(2 q_{(2,N)}^{(i)} - 2 q_{(2,N-1)}^{(i)}\right) \left(\frac{I_2}{2} + \frac{m_1 a^2}{2} + \frac{M l^2}{2} + \frac{l^2 m_2}{2}\right)}{(h^{(i)})^2} \\
& + \frac{b l m_2 \cos\left(\frac{q_{(2,N)}^{(i)}}{2} - \frac{q_{(1,N)}^{(i)}}{2} + \frac{q_{(2,N-1)}^{(i)}}{2} - \frac{q_{(1,N-1)}^{(i)}}{2}\right) \left(q_{(1,N)}^{(i)} - q_{(1,N-1)}^{(i)}\right)}{(h^{(i)})^2} - b q_{(1,N)}^{(i)} l m_2 q_{(1,N)}^{(i)}
\end{aligned}$$

$$\sin\left(q_{(2,N)}^{(i)} - q_{(2,N)}^{(i)}\right) + \frac{bl m_2 \sin\left(\frac{q_{(2,N)}^{(i)}}{2} - \frac{q_{(1,N)}^{(i)}}{2} + \frac{q_{(2,N-1)}^{(i)}}{2} - \frac{q_{(1,N-1)}^{(i)}}{2}\right) \left(q_{(2,N)}^{(i)} - q_{(2,N-1)}^{(i)}\right) \left(q_{(1,N)}^{(i)} - q_{(1,N-1)}^{(i)}\right)}{2(h^{(i)})^2} - \tau_{(2,N)}^{(i)} = 0 \quad (9.55)$$

Hence, the discretized swing phase of the 2-DOF biped robot is described by the set of equations (9.42)-(9.47).

Now for the Impact Phase of the discretized biped robot, due to the fact that the impact phase is considered an instantaneous event, the Discrete Mechanics based model is the same as the one that was derived previously. So the Impact Phase of the biped robot using Discrete Mechanics is :

$$\begin{bmatrix} p_8 + I_1 & -p_7 c_{21} \\ p_8 - p_7 c_{21} + I_1 & -p_7 c_{21} + p_6 + I_2 \end{bmatrix} \begin{bmatrix} \frac{q_{(1,1)}^{(i+1)} - q_{(1,N)}^{(i)}}{h^{(i)}} \\ \frac{q_{(2,1)}^{(i+1)} - q_{(2,N)}^{(i)}}{h^{(i)}} \end{bmatrix} = \begin{bmatrix} -p_9 + I_1 & 0 \\ p_{10} c_{21} + I_1 & -p_{11} + I_2 \end{bmatrix} \begin{bmatrix} \frac{q_{(1,N)}^{(i)} - q_{(1,N-1)}^{(i)}}{h^{(i)}} \\ \frac{q_{(2,N)}^{(i)} - q_{(2,N-1)}^{(i)}}{h^{(i)}} \end{bmatrix} \quad (9.56)$$

where  $c_{21} = \cos(q_{(2,N)}^{(i)} - q_{(1,N)}^{(i)})$  and the parameters  $p_6 = m_1 l^2 + M l^2 + m_2 a^2$ ,  $p_7 = m_1 b l$ ,  $p_8 = m_1 b^2$ ,  $p_9 = m_1 a b$ ,  $p_{10} = m_2 l a + M l^2 + m_1 l a$ ,  $p_{11} = m_2 a b$ .

Solving the system for  $\dot{q}^{(i,+)}$  by inverting the matrix  $\mathcal{Q}_+$  gives and impact map on the form (3.62)

$$\dot{q}^{(i+1)} = [\mathcal{Q}_+^{-1} \cdot \mathcal{Q}_-] \dot{q}^{(i)} \quad (9.57)$$

# Chapter 10

## Appendix C: Second Phase of the Gait Generation Module

### 10.1 Swing Phase for the Direct Collocation Method (Leg1 = Swing, Leg2 = Stance)

Following the same methodology as for the case where Leg 1 is the Stance Leg and Leg 2 is the Swing Leg, we calculate the Lagrangian of the biped robot for the case where the Leg 1 is the Swing Leg and the Leg 2 is the Stance Leg:

$$\begin{aligned} L(q_1^{(i)}, q_2^{(i)}, q_3^{(i)}, q_4^{(i)}, \dot{q}_1^{(i)}, \dot{q}_2^{(i)}, \dot{q}_3^{(i)}, \dot{q}_4^{(i)}) &= \frac{m_2 \left( q_4^{(i)} + b q_1^{(i)} \sin(q_1^{(i)}) - q_2^{(i)} l \sin(q_2^{(i)}) \right)^2}{2} \\ &+ \frac{M \left( a q_2^{(i)} \cos(q_2^{(i)}) - q_3^{(i)} + b q_2^{(i)} \cos(q_2^{(i)}) \right)^2}{2} + \frac{M \left( a q_2^{(i)} \sin(q_2^{(i)}) - q_4^{(i)} + b q_2^{(i)} \sin(q_2^{(i)}) \right)^2}{2} \\ &+ \frac{m_1 \left( q_3^{(i)} - a q_2^{(i)} \cos(q_2^{(i)}) \right)^2}{2} + \frac{m_2 \left( q_3^{(i)} + q_1^{(i)} l \cos(q_1^{(i)}) + b q_1^{(i)} \cos(q_1^{(i)}) \right)^2}{2} + \frac{m_1 \left( q_4^{(i)} - a q_2^{(i)} \sin(q_2^{(i)}) \right)^2}{2} \\ &- g M \left( q_4^{(i)} + a \cos(q_2^{(i)}) + b \cos(q_2^{(i)}) \right) - g m_2 \left( q_4^{(i)} - b \cos(q_1^{(i)}) + l \cos(q_2^{(i)}) \right) \\ &- g m_1 \left( q_4^{(i)} + a \cos(q_2^{(i)}) \right) + \frac{1}{2} (I_2 (\dot{q}_2^{(i)})^2 + I_1 (\dot{q}_1^{(i)})^2) \quad (10.1) \end{aligned}$$

and the Swing Phase is described by the following equations of motion:

$$M(q^{(i)})\ddot{q}^{(i)} + C(q^{(i)}, \dot{q}^{(i)})\dot{q}^{(i)} + G(q^{(i)}, \theta_i) = B_a(q^{(i)}) \begin{bmatrix} \tau_1^{(i)} \\ \tau_2^{(i)} \\ F_{(PO,x)}^{(i)} \\ F_{(PO,y)}^{(i)} \end{bmatrix} + S_{con}^T \begin{bmatrix} f_{fr}^{(i)}(q^{(i)}, \dot{q}^{(i)}) \\ f_N^{(i)}(q^{(i)}, \dot{q}^{(i)}) \end{bmatrix} \quad (10.2)$$

$\Leftrightarrow$

$$M(q^{(i)})\ddot{q}^{(i)} + C(q^{(i)}, \dot{q}^{(i)})\dot{q}^{(i)} + G(q^{(i)}, \theta_i) = \begin{bmatrix} \tau_1^{(i)} \\ \tau_2^{(i)} \\ 0 \\ 0 \end{bmatrix} + \begin{bmatrix} 0 \\ 0 \\ f_{fr}^{(i)}(q^{(i)}, \dot{q}^{(i)}) \\ f_N^{(i)}(q^{(i)}, \dot{q}^{(i)}) \end{bmatrix}$$

where

$$M(q^{(i)}) = \begin{bmatrix} p_{14} + I_1 & -p_{13}\cos(q_2^{(i)}) & -p_{16}\cos(q_2^{(i)}) & -p_{16}\sin(q_2^{(i)}) \\ -p_{13}\cos(q_2^{(i)}) & p_{12} + I_2 & p_{15}\cos(q_1^{(i)}) & p_{15}\sin(q_1^{(i)}) \\ -p_{16}\cos(q_2^{(i)}) & p_{15}\cos(q_1^{(i)}) & p_{17} & 0 \\ -p_{16}\sin(q_2^{(i)}) & p_{15}\sin(q_1^{(i)}) & 0 & p_{17} \end{bmatrix} \quad (10.3)$$

$$C(q^{(i)}, \dot{q}^{(i)}) \Rightarrow C(:, 1) = \begin{bmatrix} p_{13}\sin(q_2^{(i)} - q_1^{(i)})(\dot{q}_2^{(i)} - \dot{q}_1^{(i)}) \\ p_{13}\sin(q_2^{(i)} - q_1^{(i)})\dot{q}_1^{(i)} + p_{16}(\sin(q_2^{(i)})\dot{q}_3^{(i)} - \cos(q_2^{(i)}))\dot{q}_4^{(i)} \\ p_{16}\sin(q_2^{(i)})\dot{q}_2^{(i)} \\ -p_{16}\cos(q_2^{(i)})\dot{q}_2^{(i)} \end{bmatrix}$$

$$C(:, 2) = \begin{bmatrix} p_{13}\sin(q_2^{(i)} - q_1^{(i)})\dot{q}_2^{(i)} - p_{15}\sin(q_1^{(i)})\dot{q}_3^{(i)} + p_{15}\cos(q_1^{(i)})\dot{q}_4^{(i)} \\ p_{13}\sin(q_2^{(i)} - q_1^{(i)})(\dot{q}_2^{(i)} - \dot{q}_1^{(i)}) \\ -p_{15}\sin(q_1^{(i)})\dot{q}_1^{(i)} \\ p_{15}\cos(q_1^{(i)})\dot{q}_1^{(i)} \end{bmatrix}$$

$$C(:, 3) = \begin{bmatrix} -p_{15}\sin(q_1^{(i)})\dot{q}_1^{(i)} \\ p_{16}\sin(q_2^{(i)})\dot{q}_2^{(i)} \\ 0 \\ 0 \end{bmatrix}$$

$$C(:, 4) = \begin{bmatrix} p_{15}\cos(q_1^{(i)})\dot{q}_1^{(i)} \\ -p_{16}\cos(q_2^{(i)})\dot{q}_2^{(i)} \\ 0 \\ 0 \end{bmatrix} \quad (10.4)$$

$$G(q^{(i)}, \theta_i) = \begin{bmatrix} bgm_2\sin(q_1^{(i)}) \\ -gM(asin(q_2^{(i)}) + bsin(q_2^{(i)})) - agm_1\sin(q_2^{(i)}) - glm_2\sin(q_2^{(i)}) \\ 0 \\ gm_1 + gm_2 + gM \end{bmatrix} \quad (10.5)$$

where  $I_1, I_2$  are the moments of inertia of the Legs 1 and 2 about their centers of mass, respectively,  $p_{12} = Ml^2 + m_1a^2 + m_2l^2, p_{13} = m_2bl, p_{14} = m_2b^2, p_{15} = m_2b, p_{16} = Ml + m_1a + m_2l, p_{17} = m_1 + m_2 + M$ .

**•Initial Discretization of the Swing Phase for the Direct Collocation Method (Leg1 = Swing, Leg2 = Stance)**

Using the same procedure as for the case where Leg 1 is the Stance Leg and Leg 2 is the Swing Leg, we proceed with the initial discretization (without applying the Direct Collocation Conditions) of the Swing Phase for the case where the Leg 1 is the Swing Leg and the Leg 2 is

the Stance Leg leads to the following equations of motion:

$$M(q_k^{(i)})\ddot{q}_k^{(i)} + C(q_k^{(i)}, \dot{q}_k^{(i)})\dot{q}_k^{(i)} + G(q_k^{(i)}, \theta_i) = B_a(q_k^{(i)}) \begin{bmatrix} \tau_{(1,k)}^{(i)} \\ \tau_{(2,k)}^{(i)} \\ F_{(PO,x)}^{(i)} \\ F_{(PO,y)}^{(i)} \end{bmatrix} + S_{con}^T f_{(con,k)}^{(i)}, \quad k = 1, \dots, N-2 \quad (10.6)$$

$\Leftrightarrow$

$$M(q_k^{(i)})\ddot{q}_k^{(i)} + C(q_k^{(i)}, \dot{q}_k^{(i)})\dot{q}_k^{(i)} + G(q_k^{(i)}, \theta_i) = \begin{bmatrix} \tau_{(1,k)}^{(i)} \\ \tau_{(2,k)}^{(i)} \\ 0 \\ 0 \end{bmatrix} + \begin{bmatrix} 0 \\ 0 \\ f_{(fr,k)}^{(i)} \\ f_{(N,k)}^{(i)} \end{bmatrix}, \quad k = 1, \dots, N-2$$

$$\text{where } f_{(con,k)}^{(i)} = \begin{bmatrix} f_{(fr,k)}^{(i)} \\ f_{(N,k)}^{(i)} \end{bmatrix} = \begin{bmatrix} f_{fr}^{(i)}(q_k^{(i)}, \dot{q}_k^{(i)}) \\ f_N^{(i)}(q_k^{(i)}, \dot{q}_k^{(i)}) \end{bmatrix}, \quad k = 1, \dots, N-2,$$

$$M(q_k^{(i)}) = \begin{bmatrix} p_{14} + I_1 & -p_{13}\cos(q_{(2,k)}^{(i)}) & -p_{16}\cos(q_{(2,k)}^{(i)}) & -p_{16}\sin(q_{(2,k)}^{(i)}) \\ -p_{13}\cos(q_{(2,k)}^{(i)}) & p_{12} + I_2 & p_{15}\cos(q_{(1,k)}^{(i)}) & p_{15}\sin(q_{(1,k)}^{(i)}) \\ -p_{16}\cos(q_{(2,k)}^{(i)}) & p_{15}\cos(q_{(1,k)}^{(i)}) & p_{17} & 0 \\ -p_{16}\sin(q_{(2,k)}^{(i)}) & p_{15}\sin(q_{(1,k)}^{(i)}) & 0 & p_{17} \end{bmatrix}, \quad k = 1, \dots, N-2 \quad (10.7)$$

$$C(q_k^{(i)}, \dot{q}_k^{(i)}) \Rightarrow C(:, 1) = \begin{bmatrix} p_{13}\sin(q_{(2,k)}^{(i)} - q_{(1,k)}^{(i)})(\dot{q}_{(2,k)}^{(i)} - \dot{q}_{(1,k)}^{(i)}) \\ p_{13}\sin(q_{(2,k)}^{(i)} - q_{(1,k)}^{(i)})\dot{q}_{(1,k)}^{(i)} + p_{16}(\sin(q_{(2,k)}^{(i)})\dot{q}_{(3,k)}^{(i)} - \cos(q_{(2,k)}^{(i)}))\dot{q}_{(4,k)}^{(i)} \\ p_{16}\sin(q_{(2,k)}^{(i)})\dot{q}_{(2,k)}^{(i)} \\ -p_{16}\cos(q_{(2,k)}^{(i)})\dot{q}_{(2,k)}^{(i)} \end{bmatrix}$$

$$C(:, 2) = \begin{bmatrix} p_{13}\sin(q_{(2,k)}^{(i)} - q_{(1,k)}^{(i)})\dot{q}_{(2,k)}^{(i)} - p_{15}\sin(q_{(1,k)}^{(i)})\dot{q}_{(3,k)}^{(i)} + p_{15}\cos(q_{(1,k)}^{(i)})\dot{q}_{(4,k)}^{(i)} \\ p_{13}\sin(q_{(2,k)}^{(i)} - q_{(1,k)}^{(i)})(\dot{q}_{(2,k)}^{(i)} - \dot{q}_{(1,k)}^{(i)}) \\ -p_{15}\sin(q_{(1,k)}^{(i)})\dot{q}_{(1,k)}^{(i)} \\ p_{15}\cos(q_{(1,k)}^{(i)})\dot{q}_{(1,k)}^{(i)} \end{bmatrix}$$

$$C(:, 3) = \begin{bmatrix} -p_{15}\sin(q_{(1,k)}^{(i)})\dot{q}_{(1,k)}^{(i)} \\ p_{16}\sin(q_{(2,k)}^{(i)})\dot{q}_{(2,k)}^{(i)} \\ 0 \\ 0 \end{bmatrix}, k = 1, \dots, N - 2$$

$$C(:, 4) = \begin{bmatrix} p_{15}\cos(q_{(1,k)}^{(i)})\dot{q}_{(1,k)}^{(i)} \\ -p_{16}\cos(q_{(2,k)}^{(i)})\dot{q}_{(2,k)}^{(i)} \\ 0 \\ 0 \end{bmatrix} \quad (10.8)$$

$$G(q^{(i)}, \theta_i) = \begin{bmatrix} bgm_2\sin(q_{(1,k)}^{(i)}) \\ -gM(asin(q_{(2,k)}^{(i)}) + bsin(q_{(2,k)}^{(i)})) - agm_1\sin(q_{(2,k)}^{(i)}) - glm_2\sin(q_{(2,k)}^{(i)}) \\ 0 \\ gm_1 + gm_2 + gM \end{bmatrix}, k = 1, \dots, N - 2 \quad (10.9)$$

where  $p_{12} = Ml^2 + m_1a^2 + m_2l^2$ ,  $p_{13} = m_2bl$ ,  $p_{14} = m_2b^2$ ,  $p_{15} = m_2b$ ,  $p_{16} = Ml + m_1a + m_2l$ ,  $p_{17} = m_1 + m_2 + M$ .

### •State Space Equations of the Swing Phase for the Direct Collocation Method (Leg1 = Swing, Leg2 = Stance)

For the case where the Leg 1 is the Swing Leg and the Leg 2 is the Stance Leg, we derive the state space equations similar to (3.16), where the matrices  $M$ ,  $C$ ,  $G$  are given from the

relations (10.7-10.9).

## 10.2 Analytical Expressions of Swing Phase using Discrete Mechanics(Leg 1= Stance, Leg 2 =Swing)

The discrete Lagrangian is given by the following relation:

$$\begin{aligned}
 & L_r^d(q_{(1,k)}^{(i)}, q_{(1,k+1)}^{(i)}, q_{(2,k)}^{(i)}, q_{(2,k+1)}^{(i)}, q_{(3,k)}^{(i)}, q_{(3,k+1)}^{(i)}, q_{(4,k)}^{(i)}, q_{(4,k+1)}^{(i)}) = \\
 & \frac{h^{(i)} M \left( \frac{a \cos\left(\frac{q_{(1,k)}^{(i)} + q_{(1,k+1)}^{(i)}}{2}\right) (q_{(1,k)}^{(i)} - q_{(1,k+1)}^{(i)})}{h^{(i)}} - \frac{q_{(3,k)}^{(i)} - q_{(3,k+1)}^{(i)}}{h^{(i)}} + \frac{b \cos\left(\frac{q_{(1,k)}^{(i)} + q_{(1,k+1)}^{(i)}}{2}\right) (q_{(1,k)}^{(i)} - q_{(1,k+1)}^{(i)})}{h^{(i)}} \right)^2}{2} \\
 & + \frac{h^{(i)} \left( \frac{I_1 (q_{(1,k)}^{(i)} - q_{(1,k+1)}^{(i)})^2}{(h^{(i)})^2} + \frac{I_2 (q_{(2,k)}^{(i)} - q_{(2,k+1)}^{(i)})^2}{(h^{(i)})^2} \right)}{2} + \\
 & \frac{h^{(i)} M \left( \frac{a \sin\left(\frac{q_{(1,k)}^{(i)} + q_{(1,k+1)}^{(i)}}{2}\right) (q_{(1,k)}^{(i)} - q_{(1,k+1)}^{(i)})}{h^{(i)}} - \frac{q_{(4,k)}^{(i)} - q_{(4,k+1)}^{(i)}}{h^{(i)}} + \frac{b \sin\left(\frac{q_{(1,k)}^{(i)} + q_{(1,k+1)}^{(i)}}{2}\right) (q_{(1,k)}^{(i)} - q_{(1,k+1)}^{(i)})}{h^{(i)}} \right)^2}{2} + \\
 & \frac{h m_2 \left( \frac{q_{(3,k)}^{(i)} - q_{(3,k+1)}^{(i)}}{h^{(i)}} + \frac{b \cos\left(\frac{q_{(2,k)}^{(i)} + q_{(2,k+1)}^{(i)}}{2}\right) (q_{(2,k)}^{(i)} - q_{(2,k+1)}^{(i)})}{h^{(i)}} + \frac{l \cos\left(\frac{q_{(2,k)}^{(i)} + q_{(2,k+1)}^{(i)}}{2}\right) (q_{(2,k)}^{(i)} - q_{(2,k+1)}^{(i)})}{h^{(i)}} \right)^2}{2} + \\
 & \frac{h^{(i)} m_2 \left( \frac{q_{(4,k)}^{(i)} - q_{(4,k+1)}^{(i)}}{h^{(i)}} + \frac{b \sin\left(\frac{q_{(2,k)}^{(i)} + q_{(2,k+1)}^{(i)}}{2}\right) (q_{(2,k)}^{(i)} - q_{(2,k+1)}^{(i)})}{h^{(i)}} - \frac{l \sin\left(\frac{q_{(1,k)}^{(i)} + q_{(1,k+1)}^{(i)}}{2}\right) (q_{(1,k)}^{(i)} - q_{(1,k+1)}^{(i)})}{h^{(i)}} \right)^2}{2} + \\
 & \frac{h^{(i)} m_1 \left( \frac{q_{(3,k)}^{(i)} - q_{(3,k+1)}^{(i)}}{h^{(i)}} - \frac{a \cos\left(\frac{q_{(1,k)}^{(i)} + q_{(1,k+1)}^{(i)}}{2}\right) (q_{(1,k)}^{(i)} - q_{(1,k+1)}^{(i)})}{h^{(i)}} \right)^2}{2} +
 \end{aligned}$$

$$\begin{aligned}
& \frac{h^{(i)} m_1 \left( \frac{q_{(4,k)}^{(i)} - q_{(4,k+1)}^{(i)}}{h^{(i)}} - \frac{a \sin\left(\frac{q_{(1,k)}^{(i)} + \frac{q_{(1,k+1)}^{(i)}}{2}\right) (q_{(1,k)}^{(i)} - q_{(1,k+1)}^{(i)})}{h^{(i)}} \right)^2}{2} \\
& \frac{h^{(i)} g m_1 \left( \frac{q_{(4,k)}^{(i)}}{2} + \frac{q_{(4,k+1)}^{(i)}}{2} + a \cos\left(\frac{q_{(1,k)}^{(i)}}{2} + \frac{q_{(1,k+1)}^{(i)}}{2}\right) \right) -}{2} \\
& h^{(i)} M g \left( \frac{q_{(4,k)}^{(i)}}{2} + \frac{q_{(4,k+1)}^{(i)}}{2} + a \cos\left(\frac{q_{(1,k)}^{(i)}}{2} + \frac{q_{(1,k+1)}^{(i)}}{2}\right) + b \cos\left(\frac{q_{(1,k)}^{(i)}}{2} + \frac{q_{(1,k+1)}^{(i)}}{2}\right) \right) - \\
& h^{(i)} g m_2 \left( \frac{q_{(4,k)}^{(i)}}{2} + \frac{q_{(4,k+1)}^{(i)}}{2} - b \cos\left(\frac{q_{(2,k)}^{(i)}}{2} + \frac{q_{(2,k+1)}^{(i)}}{2}\right) + l \cos\left(\frac{q_{(1,k)}^{(i)}}{2} + \frac{q_{(1,k+1)}^{(i)}}{2}\right) \right) \quad (10.10)
\end{aligned}$$

The analytical expression of (3.19) is:

$$\begin{aligned}
& h^{(i)} \left( \frac{a g m_1 \sin\left(\frac{q_{(1,k)}^{(i)}}{2} + \frac{q_{(1,k+1)}^{(i)}}{2}\right)}{2} + \frac{g l m_2 \sin\left(\frac{q_{(1,k)}^{(i)}}{2} + \frac{q_{(1,k+1)}^{(i)}}{2}\right)}{2} + M g \sin\left(\frac{q_{(1,k)}^{(i)}}{2} + \frac{q_{(1,k+1)}^{(i)}}{2}\right) \left(\frac{a}{2} + \frac{b}{2}\right) \right. \\
& \quad \left. - (2h^{(i)})^{-1} l m_2 \left( \frac{q_{(4,k)}^{(i)} - q_{(4,k+1)}^{(i)}}{h^{(i)}} + \frac{b \sin\left(\frac{q_{(2,k)}^{(i)}}{2} + \frac{q_{(2,k+1)}^{(i)}}{2}\right) (q_{(2,k)}^{(i)} - q_{(2,k+1)}^{(i)})}{h^{(i)}} \right) \right. \\
& \quad \left. \frac{l \sin\left(\frac{q_{(1,k)}^{(i)}}{2} + \frac{q_{(1,k+1)}^{(i)}}{2}\right) (q_{(1,k)}^{(i)} - q_{(1,k+1)}^{(i)})}{h^{(i)}} \right) \left( 2 \sin\left(\frac{q_{(1,k)}^{(i)}}{2} + \frac{q_{(1,k+1)}^{(i)}}{2}\right) + q_{(1,k)}^{(i)} \cos\left(\frac{q_{(1,k)}^{(i)}}{2} + \frac{q_{(1,k+1)}^{(i)}}{2}\right) - \right. \\
& \quad \left. q_{(1,k+1)}^{(i)} \cos\left(\frac{q_{(1,k)}^{(i)}}{2} + \frac{q_{(1,k+1)}^{(i)}}{2}\right) \right) - (((2h^{(i)})^2)^{-1}) \left( a m_1 \left( 2 \cos\left(\frac{q_{(1,k)}^{(i)}}{2} + \frac{q_{(1,k+1)}^{(i)}}{2}\right) - q_{(1,k)}^{(i)} \sin\left(\frac{q_{(1,k)}^{(i)}}{2} + \frac{q_{(1,k+1)}^{(i)}}{2}\right) + \right. \right. \\
& \quad \left. \left. q_{(1,k+1)}^{(i)} \sin\left(\frac{q_{(1,k)}^{(i)}}{2} + \frac{q_{(1,k+1)}^{(i)}}{2}\right) \right) (q_{(3,k)}^{(i)} - q_{(3,k+1)}^{(i)} - a q_{(1,k)}^{(i)} \cos\left(\frac{q_{(1,k)}^{(i)}}{2} + \frac{q_{(1,k+1)}^{(i)}}{2}\right) + a q_{(1,k+1)}^{(i)} \cos\left(\frac{q_{(1,k)}^{(i)}}{2} + \frac{q_{(1,k+1)}^{(i)}}{2}\right)) \right) - \\
& \quad \left( ((2h^{(i)})^2)^{-1} \left( a m_1 \left( 2 \sin\left(\frac{q_{(1,k)}^{(i)}}{2} + \frac{q_{(1,k+1)}^{(i)}}{2}\right) + q_{(1,k)}^{(i)} \cos\left(\frac{q_{(1,k)}^{(i)}}{2} + \frac{q_{(1,k+1)}^{(i)}}{2}\right) - q_{(1,k+1)}^{(i)} \cos\left(\frac{q_{(1,k)}^{(i)}}{2} + \frac{q_{(1,k+1)}^{(i)}}{2}\right) \right) \right. \right. \\
& \quad \left. \left. (q_{(4,k)}^{(i)} - q_{(4,k+1)}^{(i)} - a q_{(1,k)}^{(i)} \sin\left(\frac{q_{(1,k)}^{(i)}}{2} + \frac{q_{(1,k+1)}^{(i)}}{2}\right) + a q_{(1,k+1)}^{(i)} \sin\left(\frac{q_{(1,k)}^{(i)}}{2} + \frac{q_{(1,k+1)}^{(i)}}{2}\right)) \right) \right) + \\
& \quad \left( ((2h^{(i)})^2)^{-1} \left( M (a + b) \left( \frac{a \cos\left(\frac{q_{(1,k)}^{(i)}}{2} + \frac{q_{(1,k+1)}^{(i)}}{2}\right) (q_{(1,k)}^{(i)} - q_{(1,k+1)}^{(i)})}{h^{(i)}} - \frac{q_{(3,k)}^{(i)} - q_{(3,k+1)}^{(i)}}{h^{(i)}} + \right. \right. \right. \\
& \quad \left. \left. \frac{b \cos\left(\frac{q_{(1,k)}^{(i)}}{2} + \frac{q_{(1,k+1)}^{(i)}}{2}\right) (q_{(1,k)}^{(i)} - q_{(1,k+1)}^{(i)})}{h^{(i)}} \right) \left( 2 \cos\left(\frac{q_{(1,k)}^{(i)}}{2} + \frac{q_{(1,k+1)}^{(i)}}{2}\right) - q_{(1,k)}^{(i)} \sin\left(\frac{q_{(1,k)}^{(i)}}{2} + \frac{q_{(1,k+1)}^{(i)}}{2}\right) + \right. \right. \\
& \quad \left. \left. q_{(1,k+1)}^{(i)} \sin\left(\frac{q_{(1,k)}^{(i)}}{2} + \frac{q_{(1,k+1)}^{(i)}}{2}\right) \right) \right) \right) + (((2h^{(i)})^2)^{-1}) \left( M (a + b) \left( \frac{a \sin\left(\frac{q_{(1,k)}^{(i)}}{2} + \frac{q_{(1,k+1)}^{(i)}}{2}\right) (q_{(1,k)}^{(i)} - q_{(1,k+1)}^{(i)})}{h^{(i)}} - \frac{q_{(4,k)}^{(i)} - q_{(4,k+1)}^{(i)}}{h^{(i)}} \right. \right. \\
& \quad \left. \left. \frac{b \sin\left(\frac{q_{(1,k)}^{(i)}}{2} + \frac{q_{(1,k+1)}^{(i)}}{2}\right) (q_{(1,k)}^{(i)} - q_{(1,k+1)}^{(i)})}{h^{(i)}} \right) \left( 2 \sin\left(\frac{q_{(1,k)}^{(i)}}{2} + \frac{q_{(1,k+1)}^{(i)}}{2}\right) + q_{(1,k)}^{(i)} \cos\left(\frac{q_{(1,k)}^{(i)}}{2} + \frac{q_{(1,k+1)}^{(i)}}{2}\right) - \right. \right. \\
& \quad \left. \left. q_{(1,k+1)}^{(i)} \cos\left(\frac{q_{(1,k)}^{(i)}}{2} + \frac{q_{(1,k+1)}^{(i)}}{2}\right) \right) \right) \right) + h^{(i)} \left( \frac{a g m_1 \sin\left(\frac{q_{(1,k)}^{(i)}}{2} + \frac{q_{(1,k+1)}^{(i)}}{2}\right)}{2} + \frac{g l m_2 \sin\left(\frac{q_{(1,k)}^{(i)}}{2} + \frac{q_{(1,k+1)}^{(i)}}{2}\right)}{2} + \right.
\end{aligned}$$

$$\begin{aligned}
 & M g \sin\left(\frac{q_{(1,k)}^{(i)}}{2} + \frac{q_{(1,k-1)}^{(i)}}{2}\right) \left(\frac{a}{2} + \frac{b}{2}\right) - (((2h^{(i)}))^{-1})(l m_2 \left(\frac{q_{(4,k)}^{(i)} - q_{(4,k-1)}^{(i)}}{h^{(i)}} + \frac{b \sin\left(\frac{q_{(2,k)}^{(i)}}{2} + \frac{q_{(2,k-1)}^{(i)}}{2}\right) (q_{(2,k)}^{(i)} - q_{(2,k-1)}^{(i)})}{h^{(i)}}\right. \\
 & \left. - \frac{l \sin\left(\frac{q_{(1,k)}^{(i)}}{2} + \frac{q_{(1,k-1)}^{(i)}}{2}\right) (q_{(1,k)}^{(i)} - q_{(1,k-1)}^{(i)})}{h^{(i)}}\right) (2 \sin\left(\frac{q_{(1,k)}^{(i)}}{2} + \frac{q_{(1,k-1)}^{(i)}}{2}\right) + q_{(1,k)}^{(i)} \cos\left(\frac{q_{(1,k)}^{(i)}}{2} + \frac{q_{(1,k-1)}^{(i)}}{2}\right) - \\
 & q_{(1,k-1)}^{(i)} \cos\left(\frac{q_{(1,k)}^{(i)}}{2} + \frac{q_{(1,k-1)}^{(i)}}{2}\right)) - (((2h^{(i)})^2)^{-1})(a m_1 (2 \cos\left(\frac{q_{(1,k)}^{(i)}}{2} + \frac{q_{(1,k-1)}^{(i)}}{2}\right) - q_{(1,k)}^{(i)} \sin\left(\frac{q_{(1,k)}^{(i)}}{2} + \frac{q_{(1,k-1)}^{(i)}}{2}\right) + \\
 & q_{(1,k-1)}^{(i)} \sin\left(\frac{q_{(1,k)}^{(i)}}{2} + \frac{q_{(1,k-1)}^{(i)}}{2}\right)) (q_{(3,k)}^{(i)} - q_{(3,k-1)}^{(i)} - a q_{(1,k)}^{(i)} \cos\left(\frac{q_{(1,k)}^{(i)}}{2} + \frac{q_{(1,k-1)}^{(i)}}{2}\right) + a q_{(1,k-1)}^{(i)} \cos\left(\frac{q_{(1,k)}^{(i)}}{2} + \frac{q_{(1,k-1)}^{(i)}}{2}\right)) - \\
 & (((2h^{(i)})^2)^{-1})(a m_1 (2 \sin\left(\frac{q_{(1,k)}^{(i)}}{2} + \frac{q_{(1,k-1)}^{(i)}}{2}\right) + q_{(1,k)}^{(i)} \cos\left(\frac{q_{(1,k)}^{(i)}}{2} + \frac{q_{(1,k-1)}^{(i)}}{2}\right) - q_{(1,k-1)}^{(i)} \cos\left(\frac{q_{(1,k)}^{(i)}}{2} + \frac{q_{(1,k-1)}^{(i)}}{2}\right)) \\
 & (q_{(4,k)}^{(i)} - q_{(4,k-1)}^{(i)} - a q_{(1,k)}^{(i)} \sin\left(\frac{q_{(1,k)}^{(i)}}{2} + \frac{q_{(1,k-1)}^{(i)}}{2}\right) + a q_{(1,k-1)}^{(i)} \sin\left(\frac{q_{(1,k)}^{(i)}}{2} + \frac{q_{(1,k-1)}^{(i)}}{2}\right)) + (((2h^{(i)}))^{-1})(M (a+b) \\
 & \left(\frac{a \cos\left(\frac{q_{(1,k)}^{(i)}}{2} + \frac{q_{(1,k-1)}^{(i)}}{2}\right) (q_{(1,k)}^{(i)} - q_{(1,k-1)}^{(i)})}{h^{(i)}} - \frac{q_{(3,k)}^{(i)} - q_{(3,k-1)}^{(i)}}{h^{(i)}} + \frac{b \cos\left(\frac{q_{(2,k)}^{(i)}}{2} + \frac{q_{(2,k-1)}^{(i)}}{2}\right) (q_{(1,k)}^{(i)} - q_{(1,k-1)}^{(i)})}{h^{(i)}}\right) \\
 & \left. (2 \cos\left(\frac{q_{(1,k)}^{(i)}}{2} + \frac{q_{(1,k-1)}^{(i)}}{2}\right) - q_{(1,k)}^{(i)} \sin\left(\frac{q_{(1,k)}^{(i)}}{2} + \frac{q_{(1,k-1)}^{(i)}}{2}\right) + q_{(1,k-1)}^{(i)} \sin\left(\frac{q_{(1,k)}^{(i)}}{2} + \frac{q_{(1,k-1)}^{(i)}}{2}\right))\right) + \\
 & (((2h^{(i)}))^{-1})(M (a+b) \left(\frac{a \sin\left(\frac{q_{(1,k)}^{(i)}}{2} + \frac{q_{(1,k-1)}^{(i)}}{2}\right) (q_{(1,k)}^{(i)} - q_{(1,k-1)}^{(i)})}{h^{(i)}} - \frac{q_{(4,k)}^{(i)} - q_{(4,k-1)}^{(i)}}{h^{(i)}} + \right. \\
 & \left. \frac{b \sin\left(\frac{q_{(1,k)}^{(i)}}{2} + \frac{q_{(1,k-1)}^{(i)}}{2}\right) (q_{(1,k)}^{(i)} - q_{(1,k-1)}^{(i)})}{h^{(i)}}\right) (2 \sin\left(\frac{q_{(1,k)}^{(i)}}{2} + \frac{q_{(1,k-1)}^{(i)}}{2}\right) + q_{(1,k)}^{(i)} \cos\left(\frac{q_{(1,k)}^{(i)}}{2} + \frac{q_{(1,k-1)}^{(i)}}{2}\right) - \\
 & \left. q_{(1,k-1)}^{(i)} \cos\left(\frac{q_{(1,k)}^{(i)}}{2} + \frac{q_{(1,k-1)}^{(i)}}{2}\right))\right) - \tau_{(1,k)}^{(i)} = 0 \quad (10.11)
 \end{aligned}$$

The analytical expression of (3.20) is:

$$\begin{aligned}
 & h^{(i)} \left(m_2 \left(\frac{b \sin\left(\frac{q_{(2,k)}^{(i)}}{2} + \frac{q_{(2,k+1)}^{(i)}}{2}\right)}{h^{(i)}} + \frac{b \cos\left(\frac{q_{(2,k)}^{(i)}}{2} + \frac{q_{(2,k+1)}^{(i)}}{2}\right) (q_{(2,k)}^{(i)} - q_{(2,k+1)}^{(i)})}{2 h^{(i)}}\right) \left(\frac{q_{(4,k)}^{(i)} - q_{(4,k+1)}^{(i)}}{h^{(i)}} + \right. \\
 & \left. \frac{b \sin\left(\frac{q_{(2,k)}^{(i)}}{2} + \frac{q_{(2,k+1)}^{(i)}}{2}\right) (q_{(2,k)}^{(i)} - q_{(2,k+1)}^{(i)})}{h^{(i)}} - \frac{l \sin\left(\frac{q_{(1,k)}^{(i)}}{2} + \frac{q_{(1,k+1)}^{(i)}}{2}\right) (q_{(1,k)}^{(i)} - q_{(1,k+1)}^{(i)})}{h^{(i)}}\right) + m_2 \left(\frac{q_{(3,k)}^{(i)} - q_{(3,k+1)}^{(i)}}{h^{(i)}} + \right. \\
 & \left. \frac{b \cos\left(\frac{q_{(2,k)}^{(i)}}{2} + \frac{q_{(2,k+1)}^{(i)}}{2}\right) (q_{(2,k)}^{(i)} - q_{(2,k+1)}^{(i)})}{h^{(i)}} + \frac{l \cos\left(\frac{q_{(2,k)}^{(i)}}{2} + \frac{q_{(2,k+1)}^{(i)}}{2}\right) (q_{(2,k)}^{(i)} - q_{(2,k+1)}^{(i)})}{h^{(i)}}\right) \left(\frac{b \cos\left(\frac{q_{(2,k)}^{(i)}}{2} + \frac{q_{(2,k+1)}^{(i)}}{2}\right)}{h^{(i)}} + \right. \\
 & \left. \frac{l \cos\left(\frac{q_{(2,k)}^{(i)}}{2} + \frac{q_{(2,k+1)}^{(i)}}{2}\right)}{h^{(i)}} - \frac{b \sin\left(\frac{q_{(2,k)}^{(i)}}{2} + \frac{q_{(2,k+1)}^{(i)}}{2}\right) (q_{(2,k)}^{(i)} - q_{(2,k+1)}^{(i)})}{2 h^{(i)}} - \frac{l \sin\left(\frac{q_{(2,k)}^{(i)}}{2} + \frac{q_{(2,k+1)}^{(i)}}{2}\right) (q_{(2,k)}^{(i)} - q_{(2,k+1)}^{(i)})}{2 h^{(i)}}\right) - \\
 & \left.\frac{b g m_2 \sin\left(\frac{q_{(2,k)}^{(i)}}{2} + \frac{q_{(2,k+1)}^{(i)}}{2}\right)}{2}\right) + h^{(i)} \left(m_2 \left(\frac{b \sin\left(\frac{q_{(2,k)}^{(i)}}{2} + \frac{q_{(2,k-1)}^{(i)}}{2}\right)}{h^{(i)}} + \frac{b \cos\left(\frac{q_{(2,k)}^{(i)}}{2} + \frac{q_{(2,k-1)}^{(i)}}{2}\right) (q_{(2,k)}^{(i)} - q_{(2,k-1)}^{(i)})}{2 h^{(i)}}\right) \right. \\
 & \left. \left(\frac{q_{(4,k)}^{(i)} - q_{(4,k-1)}^{(i)}}{h^{(i)}} + \frac{b \sin\left(\frac{q_{(2,k)}^{(i)}}{2} + \frac{q_{(2,k-1)}^{(i)}}{2}\right) (q_{(2,k)}^{(i)} - q_{(2,k-1)}^{(i)})}{h^{(i)}} - \frac{l \sin\left(\frac{q_{(1,k)}^{(i)}}{2} + \frac{q_{(1,k-1)}^{(i)}}{2}\right) (q_{(1,k)}^{(i)} - q_{(1,k-1)}^{(i)})}{h^{(i)}}\right) + \right.
 \end{aligned}$$

$$\begin{aligned}
& m_2 \left( \frac{q_{(3,k)}^{(i)} - q_{(3,k-1)}^{(i)}}{h^{(i)}} + \frac{b \cos\left(\frac{q_{(2,k)}^{(i)} + \frac{q_{(2,k-1)}^{(i)}}{2}\right) (q_{(2,k)}^{(i)} - q_{(2,k-1)}^{(i)})}{h^{(i)}} + \frac{l \cos\left(\frac{q_{(2,k)}^{(i)} + \frac{q_{(2,k-1)}^{(i)}}{2}\right) (q_{(2,k)}^{(i)} - q_{(2,k-1)}^{(i)})}{h^{(i)}} \right) \\
& \left( \frac{b \cos\left(\frac{q_{(2,k)}^{(i)} + \frac{q_{(2,k-1)}^{(i)}}{2}\right)}{h^{(i)}} + \frac{l \cos\left(\frac{q_{(2,k)}^{(i)} + \frac{q_{(2,k-1)}^{(i)}}{2}\right)}{h^{(i)}} - \frac{b \sin\left(\frac{q_{(2,k)}^{(i)} + \frac{q_{(2,k-1)}^{(i)}}{2}\right) (q_{(2,k)}^{(i)} - q_{(2,k-1)}^{(i)})}{2 h^{(i)}} - \right. \\
& \left. \frac{l \sin\left(\frac{q_{(2,k)}^{(i)} + \frac{q_{(2,k-1)}^{(i)}}{2}\right) (q_{(2,k)}^{(i)} - q_{(2,k-1)}^{(i)})}{2 h^{(i)}} \right) - \frac{b g m_2 \sin\left(\frac{q_{(2,k)}^{(i)} + \frac{q_{(2,k-1)}^{(i)}}{2}\right)}{2} - \tau_{(2,k)}^{(i)} = 0 \quad (10.12)
\end{aligned}$$

The analytical expression of (3.21) is:

$$\begin{aligned}
& h^{(i)} \left( \frac{m_1 \left( \frac{q_{(3,k)}^{(i)} - q_{(3,k+1)}^{(i)}}{h^{(i)}} - \frac{a \cos\left(\frac{q_{(1,k)}^{(i)} + \frac{q_{(1,k+1)}^{(i)}}{2}\right) (q_{(1,k)}^{(i)} - q_{(1,k+1)}^{(i)})}{h^{(i)}} \right)}{h^{(i)}} + \frac{I_1 (2 q_{(1,k)}^{(i)} - 2 q_{(1,k+1)}^{(i)})}{2 (h^{(i)})^2} - \right. \\
& \left. \frac{M \left( \frac{a \cos\left(\frac{q_{(1,k)}^{(i)} + \frac{q_{(1,k+1)}^{(i)}}{2}\right) (q_{(1,k)}^{(i)} - q_{(1,k+1)}^{(i)})}{h^{(i)}} - \frac{q_{(3,k)}^{(i)} - q_{(3,k+1)}^{(i)}}{h^{(i)}} + \frac{b \cos\left(\frac{q_{(2,k)}^{(i)} + \frac{q_{(2,k+1)}^{(i)}}{2}\right) (q_{(1,k)}^{(i)} - q_{(1,k+1)}^{(i)})}{h^{(i)}} \right)}{h^{(i)}} + \right. \\
& \left. \frac{m_2 \left( \frac{q_{(3,k)}^{(i)} - q_{(3,k+1)}^{(i)}}{h^{(i)}} + \frac{b \cos\left(\frac{q_{(2,k)}^{(i)} + \frac{q_{(2,k+1)}^{(i)}}{2}\right) (q_{(2,k)}^{(i)} - q_{(2,k+1)}^{(i)})}{h^{(i)}} + \frac{l \cos\left(\frac{q_{(2,k)}^{(i)} + \frac{q_{(2,k+1)}^{(i)}}{2}\right) (q_{(2,k)}^{(i)} - q_{(2,k+1)}^{(i)})}{h^{(i)}} \right)}{h^{(i)}} \right) + \\
& h^{(i)} \left( \frac{m_1 \left( \frac{q_{(3,k)}^{(i)} - q_{(3,k-1)}^{(i)}}{h^{(i)}} - \frac{a \cos\left(\frac{q_{(1,k)}^{(i)} + \frac{q_{(1,k-1)}^{(i)}}{2}\right) (q_{(1,k)}^{(i)} - q_{(1,k-1)}^{(i)})}{h^{(i)}} \right)}{h^{(i)}} + \frac{I_1 (2 q_{(1,k)}^{(i)} - 2 q_{(1,k-1)}^{(i)})}{2 (h^{(i)})^2} - \right. \\
& \left. \frac{M \left( \frac{a \cos\left(\frac{q_{(1,k)}^{(i)} + \frac{q_{(1,k-1)}^{(i)}}{2}\right) (q_{(1,k)}^{(i)} - q_{(1,k-1)}^{(i)})}{h^{(i)}} - \frac{q_{(3,k)}^{(i)} - q_{(3,k-1)}^{(i)}}{h^{(i)}} + \frac{b \cos\left(\frac{q_{(2,k)}^{(i)} + \frac{q_{(2,k-1)}^{(i)}}{2}\right) (q_{(1,k)}^{(i)} - q_{(1,k-1)}^{(i)})}{h^{(i)}} \right)}{h^{(i)}} + \right. \\
& \left. \frac{m_2 \left( \frac{q_{(3,k)}^{(i)} - q_{(3,k-1)}^{(i)}}{h^{(i)}} + \frac{b \cos\left(\frac{q_{(2,k)}^{(i)} + \frac{q_{(2,k-1)}^{(i)}}{2}\right) (q_{(2,k)}^{(i)} - q_{(2,k-1)}^{(i)})}{h^{(i)}} + \frac{l \cos\left(\frac{q_{(2,k)}^{(i)} + \frac{q_{(2,k-1)}^{(i)}}{2}\right) (q_{(2,k)}^{(i)} - q_{(2,k-1)}^{(i)})}{h^{(i)}} \right)}{h^{(i)}} \right) - f_{(fr,k)}^{(i)} = 0 \quad (10.13)
\end{aligned}$$

The analytical expression of (3.22) is:

$$\begin{aligned}
& -h^{(i)} \left( \frac{M g}{2} + \frac{g m_1}{2} + \frac{g m_2}{2} - \frac{m_1 \left( \frac{q_{(4,k)}^{(i)} - q_{(4,k+1)}^{(i)}}{h^{(i)}} - \frac{a \sin\left(\frac{q_{(1,k)}^{(i)} + \frac{q_{(1,k+1)}^{(i)}}{2}\right) (q_{(1,k)}^{(i)} - q_{(1,k+1)}^{(i)})}{h^{(i)}} \right)}{h^{(i)}} - \frac{I_2 (2 q_{(2,k)}^{(i)} - 2 q_{(2,k+1)}^{(i)})}{2 (h^{(i)})^2} + \right. \\
& \left. \frac{M \left( \frac{a \sin\left(\frac{q_{(1,k)}^{(i)} + \frac{q_{(1,k+1)}^{(i)}}{2}\right) (q_{(1,k)}^{(i)} - q_{(1,k+1)}^{(i)})}{h^{(i)}} - \frac{q_{(4,k)}^{(i)} - q_{(4,k+1)}^{(i)}}{h^{(i)}} + \frac{b \sin\left(\frac{q_{(1,k)}^{(i)} + \frac{q_{(1,k+1)}^{(i)}}{2}\right) (q_{(1,k)}^{(i)} - q_{(1,k+1)}^{(i)})}{h^{(i)}} \right)}{h^{(i)}} - \right. \\
& \left. \frac{m_2 \left( \frac{q_{(4,k)}^{(i)} - q_{(4,k+1)}^{(i)}}{h^{(i)}} + \frac{b \sin\left(\frac{q_{(2,k)}^{(i)} + \frac{q_{(2,k+1)}^{(i)}}{2}\right) (q_{(2,k)}^{(i)} - q_{(2,k+1)}^{(i)})}{h^{(i)}} - \frac{l \sin\left(\frac{q_{(1,k)}^{(i)} + \frac{q_{(1,k+1)}^{(i)}}{2}\right) (q_{(1,k)}^{(i)} - q_{(1,k+1)}^{(i)})}{h^{(i)}} \right)}{h^{(i)}} \right) - h^{(i)} \left( \frac{M g}{2} + \frac{g m_1}{2} + \right.
\end{aligned}$$

$$\begin{aligned}
 & \frac{g m_2}{2} - \frac{m_1 \left( \frac{q_{(4,k)}^{(i)} - q_{(4,k-1)}^{(i)}}{h^{(i)}} - \frac{a \sin\left(\frac{q_{(1,k)}^{(i)} + \frac{q_{(1,k-1)}^{(i)}}{2}\right) (q_{(1,k)}^{(i)} - q_{(1,k-1)}^{(i)})}{h^{(i)}} \right)}{h^{(i)}} - \frac{I_2 (2 q_{(2,k)}^{(i)} - 2 q_{(2,k-1)}^{(i)})}{2 (h^{(i)})^2} + \\
 & \frac{M \left( \frac{a \sin\left(\frac{q_{(1,k)}^{(i)} + \frac{q_{(1,k-1)}^{(i)}}{2}\right) (q_{(1,k)}^{(i)} - q_{(1,k-1)}^{(i)})}{h^{(i)}} - \frac{q_{(4,k)}^{(i)} - q_{(4,k-1)}^{(i)}}{h^{(i)}} + \frac{b \sin\left(\frac{q_{(1,k)}^{(i)} + \frac{q_{(1,k-1)}^{(i)}}{2}\right) (q_{(1,k)}^{(i)} - q_{(1,k-1)}^{(i)})}{h^{(i)}} \right)}{h^{(i)}} - \\
 & \frac{m_2 \left( \frac{q_{(4,k)}^{(i)} - q_{(4,k-1)}^{(i)}}{h^{(i)}} + \frac{b \sin\left(\frac{q_{(2,k)}^{(i)} + \frac{q_{(2,k-1)}^{(i)}}{2}\right) (q_{(2,k)}^{(i)} - q_{(2,k-1)}^{(i)})}{h^{(i)}} - \frac{l \sin\left(\frac{q_{(1,k)}^{(i)} + \frac{q_{(1,k-1)}^{(i)}}{2}\right) (q_{(1,k)}^{(i)} - q_{(1,k-1)}^{(i)})}{h^{(i)}} \right)}{h^{(i)}} - f_{(N,k)}^{(i)} = 0
 \end{aligned} \tag{10.14}$$

The analytical expression of (3.23) is:

$$\begin{aligned}
 & h^{(i)} \left( M \left( \frac{a \cos\left(\frac{q_{(1,1)}^{(i)} + \frac{q_{(1,2)}^{(i)}}{2}\right) (q_{(1,1)}^{(i)} - q_{(1,2)}^{(i)})}{h^{(i)}} - \frac{q_{(3,1)}^{(i)} - q_{(3,2)}^{(i)}}{h^{(i)}} + \frac{b \cos\left(\frac{q_{(1,1)}^{(i)} + \frac{q_{(1,2)}^{(i)}}{2}\right) (q_{(1,1)}^{(i)} - q_{(1,2)}^{(i)})}{h^{(i)}} \right) \right. \\
 & \quad \left( \frac{a \cos\left(\frac{q_{(1,1)}^{(i)} + \frac{q_{(1,2)}^{(i)}}{2}\right)}{h^{(i)}} + \frac{b \cos\left(\frac{q_{(1,1)}^{(i)} + \frac{q_{(1,2)}^{(i)}}{2}\right)}{h^{(i)}} - \frac{a \sin\left(\frac{q_{(1,1)}^{(i)} + \frac{q_{(1,2)}^{(i)}}{2}\right) (q_{(1,1)}^{(i)} - q_{(1,2)}^{(i)})}{2 h^{(i)}} - \right. \\
 & \quad \left. \left. \frac{b \sin\left(\frac{q_{(1,1)}^{(i)} + \frac{q_{(1,2)}^{(i)}}{2}\right) (q_{(1,1)}^{(i)} - q_{(1,2)}^{(i)})}{2 h^{(i)}} \right) - m_2 \left( \frac{l \sin\left(\frac{q_{(1,1)}^{(i)} + \frac{q_{(1,2)}^{(i)}}{2}\right)}{h^{(i)}} + \frac{l \cos\left(\frac{q_{(1,1)}^{(i)} + \frac{q_{(1,2)}^{(i)}}{2}\right) (q_{(1,1)}^{(i)} - q_{(1,2)}^{(i)})}{2 h^{(i)}} \right) \right. \\
 & \quad \left. \left( \frac{q_{(4,1)}^{(i)} - q_{(4,2)}^{(i)}}{h^{(i)}} + \frac{b \sin\left(\frac{q_{(2,1)}^{(i)} + \frac{q_{(2,2)}^{(i)}}{2}\right) (q_{(2,1)}^{(i)} - q_{(2,2)}^{(i)})}{h^{(i)}} - \frac{l \sin\left(\frac{q_{(1,1)}^{(i)} + \frac{q_{(1,2)}^{(i)}}{2}\right) (q_{(1,1)}^{(i)} - q_{(1,2)}^{(i)})}{h^{(i)}} \right) - \right. \\
 & \quad \left. m_1 \left( \frac{q_{(3,1)}^{(i)} - q_{(3,2)}^{(i)}}{h^{(i)}} - \frac{a \cos\left(\frac{q_{(1,1)}^{(i)} + \frac{q_{(1,2)}^{(i)}}{2}\right) (q_{(1,1)}^{(i)} - q_{(1,2)}^{(i)})}{h^{(i)}} \right) \left( \frac{a \cos\left(\frac{q_{(1,1)}^{(i)} + \frac{q_{(1,2)}^{(i)}}{2}\right)}{h^{(i)}} - \right. \\
 & \quad \left. \frac{a \sin\left(\frac{q_{(1,1)}^{(i)} + \frac{q_{(1,2)}^{(i)}}{2}\right) (q_{(1,1)}^{(i)} - q_{(1,2)}^{(i)})}{2 h^{(i)}} \right) - m_1 \left( \frac{q_{(4,1)}^{(i)} - q_{(4,2)}^{(i)}}{h^{(i)}} - \frac{a \sin\left(\frac{q_{(1,1)}^{(i)} + \frac{q_{(1,2)}^{(i)}}{2}\right) (q_{(1,1)}^{(i)} - q_{(1,2)}^{(i)})}{h^{(i)}} \right) \\
 & \quad \left( \frac{a \sin\left(\frac{q_{(1,1)}^{(i)} + \frac{q_{(1,2)}^{(i)}}{2}\right)}{h^{(i)}} + \frac{a \cos\left(\frac{q_{(1,1)}^{(i)} + \frac{q_{(1,2)}^{(i)}}{2}\right) (q_{(1,1)}^{(i)} - q_{(1,2)}^{(i)})}{2 h^{(i)}} \right) + M \left( \frac{a \sin\left(\frac{q_{(1,1)}^{(i)} + \frac{q_{(1,2)}^{(i)}}{2}\right) (q_{(1,1)}^{(i)} - q_{(1,2)}^{(i)})}{h^{(i)}} - \right. \\
 & \quad \left. \frac{q_{(4,1)}^{(i)} - q_{(4,2)}^{(i)}}{h^{(i)}} + \frac{b \sin\left(\frac{q_{(1,1)}^{(i)} + \frac{q_{(1,2)}^{(i)}}{2}\right) (q_{(1,1)}^{(i)} - q_{(1,2)}^{(i)})}{h^{(i)}} \right) \left( \frac{a \sin\left(\frac{q_{(1,1)}^{(i)} + \frac{q_{(1,2)}^{(i)}}{2}\right)}{h^{(i)}} + \frac{b \sin\left(\frac{q_{(1,1)}^{(i)} + \frac{q_{(1,2)}^{(i)}}{2}\right)}{h^{(i)}} + \right. \\
 & \quad \left. \frac{a \cos\left(\frac{q_{(1,1)}^{(i)} + \frac{q_{(1,2)}^{(i)}}{2}\right) (q_{(1,1)}^{(i)} - q_{(1,2)}^{(i)})}{2 h^{(i)}} + \frac{b \cos\left(\frac{q_{(1,1)}^{(i)} + \frac{q_{(1,2)}^{(i)}}{2}\right) (q_{(1,1)}^{(i)} - q_{(1,2)}^{(i)})}{2 h^{(i)}} \right) + M g \left( \frac{a \sin\left(\frac{q_{(1,1)}^{(i)} + \frac{q_{(1,2)}^{(i)}}{2}\right)}{2} + \right. \\
 & \quad \left. \frac{b \sin\left(\frac{q_{(1,1)}^{(i)} + \frac{q_{(1,2)}^{(i)}}{2}\right)}{2} \right) + \frac{a g m_1 \sin\left(\frac{q_{(1,1)}^{(i)} + \frac{q_{(1,2)}^{(i)}}{2}\right)}{2} + \frac{g l m_2 \sin\left(\frac{q_{(1,1)}^{(i)} + \frac{q_{(1,2)}^{(i)}}{2}\right)}{2} \right) + M (a \cos(q_{(1,1)}^{(i)}) + b \cos(q_{(1,1)}^{(i)})) \\
 & \quad (a q_{(i,1)}^{(i)} \cos(q_{(1,1)}^{(i)}) - q_{(3,1)}^{(i)} + b q_{(i,1)}^{(i)} \cos(q_{(1,1)}^{(i)})) + M (a \sin(q_{(1,1)}^{(i)}) + b \sin(q_{(1,1)}^{(i)})) \\
 & \quad (a q_{(i,1)}^{(i)} \sin(q_{(1,1)}^{(i)}) - q_{(4,1)}^{(i)} + b q_{(i,1)}^{(i)} \sin(q_{(1,1)}^{(i)})) - a m_1 \cos(q_{(1,1)}^{(i)}) (q_{(3,1)}^{(i)} - a q_{(i,1)}^{(i)} \cos(q_{(1,1)}^{(i)})) - \\
 & \quad a m_1 \sin(q_{(1,1)}^{(i)}) (q_{(4,1)}^{(i)} - a q_{(i,1)}^{(i)} \sin(q_{(1,1)}^{(i)})) - l m_2 \sin(q_{(1,1)}^{(i)}) (q_{(4,1)}^{(i)} + b q_{(2,1)}^{(i)} \sin(q_{(2,1)}^{(i)})) -
 \end{aligned}$$

$$q_{(1,1)}^{(i)} l \sin(q_{(1,1)}^{(i)}) - \tau_{(1,1)}^{(i)} = 0 \quad (10.15)$$

The analytical expression of (3.24) is:

$$\begin{aligned} & h^{(i)} \left( m_2 \left( \frac{b \sin\left(\frac{q_{(2,1)}^{(i)}}{2} + \frac{q_{(2,2)}^{(i)}}{2}\right)}{h^{(i)}} + \frac{b \cos\left(\frac{q_{(2,1)}^{(i)}}{2} + \frac{q_{(2,2)}^{(i)}}{2}\right) (q_{(2,1)}^{(i)} - q_{(2,2)}^{(i)})}{2 h^{(i)}} \right) \left( \frac{q_{(4,1)}^{(i)} - q_{(4,2)}^{(i)}}{h^{(i)}} + \right. \right. \\ & \left. \frac{b \sin\left(\frac{q_{(2,1)}^{(i)}}{2} + \frac{q_{(2,2)}^{(i)}}{2}\right) (q_{(2,1)}^{(i)} - q_{(2,2)}^{(i)})}{h^{(i)}} - \frac{l \sin\left(\frac{q_{(1,1)}^{(i)}}{2} + \frac{q_{(1,2)}^{(i)}}{2}\right) (q_{(1,1)}^{(i)} - q_{(1,2)}^{(i)})}{h^{(i)}} \right) + m_2 \left( \frac{q_{(3,1)}^{(i)} - q_{(3,2)}^{(i)}}{h^{(i)}} + \right. \\ & \left. \frac{b \cos\left(\frac{q_{(2,1)}^{(i)}}{2} + \frac{q_{(2,2)}^{(i)}}{2}\right) (q_{(2,1)}^{(i)} - q_{(2,2)}^{(i)})}{h^{(i)}} + \frac{l \cos\left(\frac{q_{(2,1)}^{(i)}}{2} + \frac{q_{(2,2)}^{(i)}}{2}\right) (q_{(2,1)}^{(i)} - q_{(2,2)}^{(i)})}{h^{(i)}} \right) \left( \frac{b \cos\left(\frac{q_{(2,1)}^{(i)}}{2} + \frac{q_{(2,2)}^{(i)}}{2}\right)}{h^{(i)}} + \right. \\ & \left. \frac{l \cos\left(\frac{q_{(2,1)}^{(i)}}{2} + \frac{q_{(2,2)}^{(i)}}{2}\right)}{h^{(i)}} - \frac{b \sin\left(\frac{q_{(2,1)}^{(i)}}{2} + \frac{q_{(2,2)}^{(i)}}{2}\right) (q_{(2,1)}^{(i)} - q_{(2,2)}^{(i)})}{2 h^{(i)}} - \frac{l \sin\left(\frac{q_{(2,1)}^{(i)}}{2} + \frac{q_{(2,2)}^{(i)}}{2}\right) (q_{(2,1)}^{(i)} - q_{(2,2)}^{(i)})}{2 h^{(i)}} \right) - \\ & \left. \frac{b g m_2 \sin\left(\frac{q_{(2,1)}^{(i)}}{2} + \frac{q_{(2,2)}^{(i)}}{2}\right)}{2} \right) + m_2 (b \cos(q_{(2,1)}^{(i)}) + l \cos(q_{(2,1)}^{(i)})) (q_{(3,1)}^{(i)} + q_{(2,1)}^{(i)} l \cos(q_{(2,1)}^{(i)}) + b q_{(2,1)}^{(i)} \cos(q_{(2,1)}^{(i)})) + \\ & b m_2 \sin(q_{(2,1)}^{(i)}) (q_{(4,1)}^{(i)} + b q_{(2,1)}^{(i)} \sin(q_{(2,1)}^{(i)}) - q_{(1,1)}^{(i)} l \sin(q_{(1,1)}^{(i)})) - \tau_{(2,1)}^{(i)} = 0 \quad (10.16) \end{aligned}$$

The analytical expression of (3.25) is:

$$\begin{aligned} & I_1 q_{(1,1)}^{(i)} + h^{(i)} \left( \frac{m_1 \left( \frac{q_{(3,1)}^{(i)} - q_{(3,2)}^{(i)}}{h^{(i)}} - \frac{a \cos\left(\frac{q_{(1,1)}^{(i)}}{2} + \frac{q_{(1,2)}^{(i)}}{2}\right) (q_{(1,1)}^{(i)} - q_{(1,2)}^{(i)})}{h^{(i)}} \right)}{h^{(i)}} + \frac{I_1 (2 q_{(1,1)}^{(i)} - 2 q_{(1,2)}^{(i)})}{2 (h^{(i)})^2} - \right. \\ & \left. \frac{M \left( \frac{a \cos\left(\frac{q_{(1,1)}^{(i)}}{2} + \frac{q_{(1,2)}^{(i)}}{2}\right) (q_{(1,1)}^{(i)} - q_{(1,2)}^{(i)})}{h^{(i)}} - \frac{q_{(3,1)}^{(i)} - q_{(3,2)}^{(i)}}{h^{(i)}} + \frac{b \cos\left(\frac{q_{(1,1)}^{(i)}}{2} + \frac{q_{(1,2)}^{(i)}}{2}\right) (q_{(1,1)}^{(i)} - q_{(1,2)}^{(i)})}{h^{(i)}} \right)}{h^{(i)}} + \right. \\ & \left. \frac{m_2 \left( \frac{q_{(3,1)}^{(i)} - q_{(3,2)}^{(i)}}{h^{(i)}} + \frac{b \cos\left(\frac{q_{(2,1)}^{(i)}}{2} + \frac{q_{(2,2)}^{(i)}}{2}\right) (q_{(2,1)}^{(i)} - q_{(2,2)}^{(i)})}{h^{(i)}} + \frac{l \cos\left(\frac{q_{(2,1)}^{(i)}}{2} + \frac{q_{(2,2)}^{(i)}}{2}\right) (q_{(2,1)}^{(i)} - q_{(2,2)}^{(i)})}{h^{(i)}} \right)}{h^{(i)}} \right) - \\ & \frac{M (2 a q_{(1,1)}^{(i)} \cos(q_{(1,1)}^{(i)}) - 2 q_{(3,1)}^{(i)} + 2 b q_{(1,1)}^{(i)} \cos(q_{(1,1)}^{(i)}))}{2} + \frac{m_1 (2 q_{(3,1)}^{(i)} - 2 a q_{(1,1)}^{(i)} \cos(q_{(1,1)}^{(i)}))}{2} + \\ & \frac{m_2 (2 q_{(3,1)}^{(i)} + 2 q_{(2,1)}^{(i)} l \cos(q_{(2,1)}^{(i)}) + 2 b q_{(2,1)}^{(i)} \cos(q_{(2,1)}^{(i)}))}{2} - f_{(fr,1)}^{(i)} = 0 \quad (10.17) \end{aligned}$$

The analytical expression of (3.26) is:

$$I_2 q_{(2,1)}^{(i)} + \frac{m_2 (2 q_{(4,1)}^{(i)} + 2 b q_{(2,1)}^{(i)} \sin(q_{(2,1)}^{(i)}) - 2 q_{(1,1)}^{(i)} l \sin(q_{(1,1)}^{(i)}))}{2} - h^{(i)} \left( \frac{M g}{2} + \frac{g m_1}{2} + \frac{g m_2}{2} - \right.$$

$$\begin{aligned}
 & \frac{m_1 \left( \frac{q_{(4,1)}^{(i)} - q_{(4,2)}^{(i)}}{h^{(i)}} - \frac{a \sin\left(\frac{q_{(1,1)}^{(i)} + q_{(1,2)}^{(i)}}{2}\right) (q_{(1,1)}^{(i)} - q_{(1,2)}^{(i)})}{h^{(i)}} \right)}{h^{(i)}} - \frac{I_2 (2 q_{(2,1)}^{(i)} - 2 q_{(2,2)}^{(i)})}{2 (h^{(i)})^2} + \\
 & \frac{M \left( \frac{a \sin\left(\frac{q_{(1,1)}^{(i)} + q_{(1,2)}^{(i)}}{2}\right) (q_{(1,1)}^{(i)} - q_{(1,2)}^{(i)})}{h^{(i)}} - \frac{q_{(4,1)}^{(i)} - q_{(4,2)}^{(i)}}{h^{(i)}} + \frac{b \sin\left(\frac{q_{(1,1)}^{(i)} + q_{(1,2)}^{(i)}}{2}\right) (q_{(1,1)}^{(i)} - q_{(1,2)}^{(i)})}{h^{(i)}} \right)}{h^{(i)}} - \\
 & \frac{m_2 \left( \frac{q_{(4,1)}^{(i)} - q_{(4,2)}^{(i)}}{h^{(i)}} + \frac{b \sin\left(\frac{q_{(2,1)}^{(i)} + q_{(2,2)}^{(i)}}{2}\right) (q_{(2,1)}^{(i)} - q_{(2,2)}^{(i)})}{h^{(i)}} - \frac{l \sin\left(\frac{q_{(1,1)}^{(i)} + q_{(1,2)}^{(i)}}{2}\right) (q_{(1,1)}^{(i)} - q_{(1,2)}^{(i)})}{h^{(i)}} \right)}{h^{(i)}} - \\
 & \frac{M (2 a q_{(1,1)}^{(i)} \sin(q_{(1,1)}^{(i)}) - 2 q_{(4,1)}^{(i)} + 2 b q_{(1,1)}^{(i)} \sin(q_{(1,1)}^{(i)}))}{2} + \frac{m_1 (2 q_{(4,1)}^{(i)} - 2 a q_{(1,1)}^{(i)} \sin(q_{(1,1)}^{(i)}))}{2} - \\
 & f_{(N,1)}^{(i)} = 0 \quad (10.18)
 \end{aligned}$$

The analytical expression of (3.27) is:

$$\begin{aligned}
 & h^{(i)} \left( M \left( \frac{a \cos\left(\frac{q_{(1,N)}^{(i)} + q_{(1,N-1)}^{(i)}}{2}\right) (q_{(1,N)}^{(i)} - q_{(1,N-1)}^{(i)})}{h^{(i)}} - \frac{q_{(3,N)}^{(i)} - q_{(3,N-1)}^{(i)}}{h^{(i)}} + \frac{b \cos\left(\frac{q_{(1,N)}^{(i)} + q_{(1,N-1)}^{(i)}}{2}\right) (q_{(1,N)}^{(i)} - q_{(1,N-1)}^{(i)})}{h^{(i)}} \right. \right. \\
 & \left. \left. - \frac{a \sin\left(\frac{q_{(1,N)}^{(i)} + q_{(1,N-1)}^{(i)}}{2}\right) (q_{(1,N)}^{(i)} - q_{(1,N-1)}^{(i)})}{2 h^{(i)}} - \frac{b \sin\left(\frac{q_{(1,N)}^{(i)} + q_{(1,N-1)}^{(i)}}{2}\right) (q_{(1,N)}^{(i)} - q_{(1,N-1)}^{(i)})}{2 h^{(i)}} \right) - \right. \\
 & m_2 \left( \frac{l \sin\left(\frac{q_{(1,N)}^{(i)} + q_{(1,N-1)}^{(i)}}{2}\right)}{h^{(i)}} + \frac{l \cos\left(\frac{q_{(1,N)}^{(i)} + q_{(1,N-1)}^{(i)}}{2}\right) (q_{(1,N)}^{(i)} - q_{(1,N-1)}^{(i)})}{2 h^{(i)}} \right) \left( \frac{q_{(4,N)}^{(i)} - q_{(4,N-1)}^{(i)}}{h^{(i)}} + \right. \\
 & \left. \frac{b \sin\left(\frac{q_{(2,N)}^{(i)} + q_{(2,N-1)}^{(i)}}{2}\right) (q_{(2,N)}^{(i)} - q_{(2,N-1)}^{(i)})}{h^{(i)}} - \frac{l \sin\left(\frac{q_{(1,N)}^{(i)} + q_{(1,N-1)}^{(i)}}{2}\right) (q_{(1,N)}^{(i)} - q_{(1,N-1)}^{(i)})}{h^{(i)}} \right) - \\
 & m_1 \left( \frac{q_{(3,N)}^{(i)} - q_{(3,N-1)}^{(i)}}{h^{(i)}} - \frac{a \cos\left(\frac{q_{(1,N)}^{(i)} + q_{(1,N-1)}^{(i)}}{2}\right) (q_{(1,N)}^{(i)} - q_{(1,N-1)}^{(i)})}{h^{(i)}} \right) \\
 & \left( \frac{a \cos\left(\frac{q_{(1,N)}^{(i)} + q_{(1,N-1)}^{(i)}}{2}\right)}{h^{(i)}} - \frac{a \sin\left(\frac{q_{(1,N)}^{(i)} + q_{(1,N-1)}^{(i)}}{2}\right) (q_{(1,N)}^{(i)} - q_{(1,N-1)}^{(i)})}{2 h^{(i)}} \right) - m_1 \left( \frac{q_{(4,N)}^{(i)} - q_{(4,N-1)}^{(i)}}{h^{(i)}} - \right. \\
 & \left. \frac{a \sin\left(\frac{q_{(1,N)}^{(i)} + q_{(1,N-1)}^{(i)}}{2}\right) (q_{(1,N)}^{(i)} - q_{(1,N-1)}^{(i)})}{h^{(i)}} \right) \left( \frac{a \sin\left(\frac{q_{(1,N)}^{(i)} + q_{(1,N-1)}^{(i)}}{2}\right)}{h^{(i)}} + \frac{a \cos\left(\frac{q_{(1,N)}^{(i)} + q_{(1,N-1)}^{(i)}}{2}\right) (q_{(1,N)}^{(i)} - q_{(1,N-1)}^{(i)})}{2 h^{(i)}} \right) + \\
 & M \left( \frac{a \sin\left(\frac{q_{(1,N)}^{(i)} + q_{(1,N-1)}^{(i)}}{2}\right) (q_{(1,N)}^{(i)} - q_{(1,N-1)}^{(i)})}{h^{(i)}} - \frac{q_{(4,N)}^{(i)} - q_{(4,N-1)}^{(i)}}{h^{(i)}} + \frac{b \sin\left(\frac{q_{(1,N)}^{(i)} + q_{(1,N-1)}^{(i)}}{2}\right) (q_{(1,N)}^{(i)} - q_{(1,N-1)}^{(i)})}{h^{(i)}} \right) \\
 & \left( \frac{a \sin\left(\frac{q_{(1,N)}^{(i)} + q_{(1,N-1)}^{(i)}}{2}\right)}{h^{(i)}} + \frac{b \sin\left(\frac{q_{(1,N)}^{(i)} + q_{(1,N-1)}^{(i)}}{2}\right)}{h^{(i)}} + \frac{a \cos\left(\frac{q_{(1,N)}^{(i)} + q_{(1,N-1)}^{(i)}}{2}\right) (q_{(1,N)}^{(i)} - q_{(1,N-1)}^{(i)})}{2 h^{(i)}} + \right. \\
 & \left. \frac{b \cos\left(\frac{q_{(1,N)}^{(i)} + q_{(1,N-1)}^{(i)}}{2}\right) (q_{(1,N)}^{(i)} - q_{(1,N-1)}^{(i)})}{2 h^{(i)}} \right) + M g \left( \frac{a \sin\left(\frac{q_{(1,N)}^{(i)} + q_{(1,N-1)}^{(i)}}{2}\right)}{2} + \frac{b \sin\left(\frac{q_{(1,N)}^{(i)} + q_{(1,N-1)}^{(i)}}{2}\right)}{2} \right) + \\
 & \frac{a g m_1 \sin\left(\frac{q_{(1,N)}^{(i)} + q_{(1,N-1)}^{(i)}}{2}\right)}{2} + \frac{g l m_2 \sin\left(\frac{q_{(1,N)}^{(i)} + q_{(1,N-1)}^{(i)}}{2}\right)}{2} - M (a \cos(q_{(1,N)}^{(i)}) + b \cos(q_{(1,N)}^{(i)})) (a q_{(1,N)}^{(i)} \cos(q_{(1,N)}^{(i)}))
 \end{aligned}$$

$$\begin{aligned}
& -q_{(3,N)}^{(i)} + b q_{(1,N)}^{(i)} \cos(q_{(1,N)}^{(i)}) - M (a \sin(q_{(1,N)}^{(i)}) + b \sin(q_{(1,N)}^{(i)})) (a q_{(1,N)}^{(i)} \sin(q_{(1,N)}^{(i)}) - q_{(4,N)}^{(i)} + \\
& b q_{(1,N)}^{(i)} \sin(q_{(1,N)}^{(i)})) + a m_1 \cos(q_{(1,N)}^{(i)}) (q_{(3,N)}^{(i)} - a q_{(1,N)}^{(i)} \cos(q_{(1,N)}^{(i)})) + a m_1 \sin(q_{(1,N)}^{(i)}) (q_{(4,N)}^{(i)} - a q_{(1,N)}^{(i)} \\
& \sin(q_{(1,N)}^{(i)})) + l m_2 \sin(q_{(1,N)}^{(i)}) (q_{(4,N)}^{(i)} + b q_{(2,N)}^{(i)} \sin(q_{(2,N)}^{(i)}) - q_{(1,N)}^{(i)} l \sin(q_{(1,N)}^{(i)})) - \tau_{(1,N)}^{(i)} = 0
\end{aligned} \tag{10.19}$$

The analytical expression of (3.28) is:

$$\begin{aligned}
& h^{(i)} \left( m_2 \left( \frac{b \sin\left(\frac{q_{(2,N)}^{(i)}}{2} + \frac{q_{(2,N-1)}^{(i)}}{2}\right)}{h^{(i)}} + \frac{b \cos\left(\frac{q_{(2,N)}^{(i)}}{2} + \frac{q_{(2,N-1)}^{(i)}}{2}\right) (q_{(2,N)}^{(i)} - q_{(2,N-1)}^{(i)})}{2 h^{(i)}} \right) \left( \frac{q_{(4,N)}^{(i)} - q_{(4,N-1)}^{(i)}}{h^{(i)}} + \right. \\
& \left. \frac{b \sin\left(\frac{q_{(2,N)}^{(i)}}{2} + \frac{q_{(2,N-1)}^{(i)}}{2}\right) (q_{(2,N)}^{(i)} - q_{(2,N-1)}^{(i)})}{h^{(i)}} - \frac{l \sin\left(\frac{q_{(1,N)}^{(i)}}{2} + \frac{q_{(1,N-1)}^{(i)}}{2}\right) (q_{(1,N)}^{(i)} - q_{(1,N-1)}^{(i)})}{h^{(i)}} \right) + m_2 \left( \frac{q_{(3,N)}^{(i)} - q_{(3,N-1)}^{(i)}}{h^{(i)}} + \right. \\
& \left. \frac{b \cos\left(\frac{q_{(2,N)}^{(i)}}{2} + \frac{q_{(2,N-1)}^{(i)}}{2}\right) (q_{(2,N)}^{(i)} - q_{(2,N-1)}^{(i)})}{h^{(i)}} + \frac{l \cos\left(\frac{q_{(2,N)}^{(i)}}{2} + \frac{q_{(2,N-1)}^{(i)}}{2}\right) (q_{(2,N)}^{(i)} - q_{(2,N-1)}^{(i)})}{h^{(i)}} \right) \left( \frac{b \cos\left(\frac{q_{(2,N)}^{(i)}}{2} + \frac{q_{(2,N-1)}^{(i)}}{2}\right)}{h^{(i)}} + \right. \\
& \left. \frac{l \cos\left(\frac{q_{(2,N)}^{(i)}}{2} + \frac{q_{(2,N-1)}^{(i)}}{2}\right)}{h^{(i)}} - \frac{b \sin\left(\frac{q_{(2,N)}^{(i)}}{2} + \frac{q_{(2,N-1)}^{(i)}}{2}\right) (q_{(2,N)}^{(i)} - q_{(2,N-1)}^{(i)})}{2 h^{(i)}} - \frac{l \sin\left(\frac{q_{(2,N)}^{(i)}}{2} + \frac{q_{(2,N-1)}^{(i)}}{2}\right) (q_{(2,N)}^{(i)} - q_{(2,N-1)}^{(i)})}{2 h^{(i)}} \right) - \\
& \left. \frac{b g m_2 \sin\left(\frac{q_{(2,N)}^{(i)}}{2} + \frac{q_{(2,N-1)}^{(i)}}{2}\right)}{2} \right) - m_2 (b \cos(q_{(2,N)}^{(i)}) + l \cos(q_{(2,N)}^{(i)})) (q_{(3,N)}^{(i)} + q_{(2,N)}^{(i)} l \cos(q_{(2,N)}^{(i)}) + \\
& b q_{(2,N)}^{(i)} \cos(q_{(2,N)}^{(i)})) - b m_2 \sin(q_{(2,N)}^{(i)}) (q_{(4,N)}^{(i)} + b q_{(2,N)}^{(i)} \sin(q_{(2,N)}^{(i)}) - q_{(1,N)}^{(i)} l \sin(q_{(1,N)}^{(i)})) - \tau_{(2,N)}^{(i)} = 0
\end{aligned} \tag{10.20}$$

The analytical expression of (3.29) is:

$$\begin{aligned}
& h^{(i)} \left( \frac{m_1 \left( \frac{q_{(3,N)}^{(i)} - q_{(3,N-1)}^{(i)}}{h^{(i)}} - \frac{a \cos\left(\frac{q_{(1,N)}^{(i)}}{2} + \frac{q_{(1,N-1)}^{(i)}}{2}\right) (q_{(1,N)}^{(i)} - q_{(1,N-1)}^{(i)})}{h^{(i)}} \right)}{h^{(i)}} + \frac{I_1 (2 q_{(1,N)}^{(i)} - 2 q_{(1,N-1)}^{(i)})}{2 (h^{(i)})^2} - \right. \\
& \left. \frac{M \left( \frac{a \cos\left(\frac{q_{(1,N)}^{(i)}}{2} + \frac{q_{(1,N-1)}^{(i)}}{2}\right) (q_{(1,N)}^{(i)} - q_{(1,N-1)}^{(i)})}{h^{(i)}} - \frac{q_{(3,N)}^{(i)} - q_{(3,N-1)}^{(i)}}{h^{(i)}} + \frac{b \cos\left(\frac{q_{(1,N)}^{(i)}}{2} + \frac{q_{(1,N-1)}^{(i)}}{2}\right) (q_{(1,N)}^{(i)} - q_{(1,N-1)}^{(i)})}{h^{(i)}} \right)}{h^{(i)}} + \right. \\
& \left. \frac{m_2 \left( \frac{q_{(3,N)}^{(i)} - q_{(3,N-1)}^{(i)}}{h^{(i)}} + \frac{b \cos\left(\frac{q_{(2,N)}^{(i)}}{2} + \frac{q_{(2,N-1)}^{(i)}}{2}\right) (q_{(2,N)}^{(i)} - q_{(2,N-1)}^{(i)})}{h^{(i)}} + \frac{l \cos\left(\frac{q_{(2,N)}^{(i)}}{2} + \frac{q_{(2,N-1)}^{(i)}}{2}\right) (q_{(2,N)}^{(i)} - q_{(2,N-1)}^{(i)})}{h^{(i)}} \right)}{h^{(i)}} \right) - I_1 q_{(1,N)}^{(i)} + \\
& \frac{M (2 a q_{(1,N)}^{(i)} \cos(q_{(1,N)}^{(i)}) - 2 q_{(3,N)}^{(i)} + 2 b q_{(1,N)}^{(i)} \cos(q_{(1,N)}^{(i)}))}{2} - \frac{m_1 (2 q_{(3,N)}^{(i)} - 2 a q_{(1,N)}^{(i)} \cos(q_{(1,N)}^{(i)}))}{2} - \\
& \frac{m_2 (2 q_{(3,N)}^{(i)} + 2 q_{(2,N)}^{(i)} l \cos(q_{(2,N)}^{(i)}) + 2 b q_{(2,N)}^{(i)} \cos(q_{(2,N)}^{(i)}))}{2} - f_{HSx,N}^{(i)} = 0 \tag{10.21}
\end{aligned}$$

The analytical expression of (3.30) is:

$$\begin{aligned}
& \frac{M (2 a \dot{q}_{(1,N)}^{(i)} \sin(q_{(1,N)}^{(i)}) - 2 \dot{q}_{(4,N)}^{(i)} + 2 b \dot{q}_{(1,N)}^{(i)} \sin(q_{(1,N)}^{(i)}))}{2} \\
& \frac{m_2 (2 \dot{q}_{(4,N)}^{(i)} + 2 b \dot{q}_{(2,N)}^{(i)} \sin(q_{(2,N)}^{(i)}) - 2 \dot{q}_{(1,N)}^{(i)} l \sin(q_{(1,N)}^{(i)}))}{2} - h^{(i)} \left( \frac{M g}{2} + \frac{g m_1}{2} + \frac{g m_2}{2} - \right. \\
& \left. \frac{m_1 \left( \frac{q_{(4,N)}^{(i)} - q_{(4,N-1)}^{(i)}}{h^{(i)}} - \frac{a \sin\left(\frac{q_{(1,N)}^{(i)} + q_{(1,N-1)}^{(i)}}{2}\right) (q_{(1,N)}^{(i)} - q_{(1,N-1)}^{(i)})}{h^{(i)}} \right)}{h^{(i)}} - \frac{I_2 (2 \dot{q}_{(2,N)}^{(i)} - 2 \dot{q}_{(2,N-1)}^{(i)})}{2 (h^{(i)})^2} + \right. \\
& \left. \frac{M \left( \frac{a \sin\left(\frac{q_{(1,N)}^{(i)} + q_{(1,N-1)}^{(i)}}{2}\right) (q_{(1,N)}^{(i)} - q_{(1,N-1)}^{(i)})}{h^{(i)}} - \frac{q_{(4,N)}^{(i)} - q_{(4,N-1)}^{(i)}}{h^{(i)}} + \frac{b \sin\left(\frac{q_{(1,N)}^{(i)} + q_{(1,N-1)}^{(i)}}{2}\right) (q_{(1,N)}^{(i)} - q_{(1,N-1)}^{(i)})}{h^{(i)}} \right)}{h^{(i)}} \right) \\
& \frac{m_2 \left( \frac{q_{(4,N)}^{(i)} - q_{(4,N-1)}^{(i)}}{h^{(i)}} + \frac{b \sin\left(\frac{q_{(2,N)}^{(i)} + q_{(2,N-1)}^{(i)}}{2}\right) (q_{(2,N)}^{(i)} - q_{(2,N-1)}^{(i)})}{h^{(i)}} - \frac{l \sin\left(\frac{q_{(1,N)}^{(i)} + q_{(1,N-1)}^{(i)}}{2}\right) (q_{(1,N)}^{(i)} - q_{(1,N-1)}^{(i)})}{h^{(i)}} \right)}{h^{(i)}} - I_2 \dot{q}_{(2,N)}^{(i)} - \\
& \frac{m_1 (2 \dot{q}_{(4,N)}^{(i)} - 2 a \dot{q}_{(1,N)}^{(i)} \sin(q_{(1,N)}^{(i)}))}{2} - f_{HSy,N}^{(i)} = 0 \quad (10.22)
\end{aligned}$$

### 10.3 Swing Phase using Discrete Mechanics (Leg 1= Swing, Leg 2 =Stance)

Following the same methodology as for the first case where Leg 1 is the Stance Leg and Leg 2 is the Swing Leg, we calculate the Discrete Lagrangian of the biped robot for the case where the Leg 1 is the Swing Leg and the Leg 2 is the Stance Leg:

$$\begin{aligned}
& L_r^d(q_{(1,k)}^{(i)}, q_{(1,k+1)}^{(i)}, q_{(2,k)}^{(i)}, q_{(2,k+1)}^{(i)}, q_{(3,k)}^{(i)}, q_{(3,k+1)}^{(i)}, q_{(4,k)}^{(i)}, q_{(4,k+1)}^{(i)}) = \\
& \frac{h^{(i)} M \left( \frac{a \cos\left(\frac{q_{(2,k)}^{(i)} + q_{(2,k+1)}^{(i)}}{2}\right) (q_{(2,k)}^{(i)} - q_{(2,k+1)}^{(i)})}{h^{(i)}} - \frac{q_{(3,k)}^{(i)} - q_{(3,k+1)}^{(i)}}{h^{(i)}} + \frac{b \cos\left(\frac{q_{(2,k)}^{(i)} + q_{(2,k+1)}^{(i)}}{2}\right) (q_{(2,k)}^{(i)} - q_{(2,k+1)}^{(i)})}{h^{(i)}} \right)^2}{2} \\
& + \frac{h^{(i)} \left( \frac{I_1 (q_{(1,k)}^{(i)} - q_{(1,k+1)}^{(i)})^2}{(h^{(i)})^2} + \frac{I_2 (q_{(2,k)}^{(i)} - q_{(2,k+1)}^{(i)})^2}{(h^{(i)})^2} \right)}{2} +
\end{aligned}$$

$$\begin{aligned}
& \frac{h^{(i)} M \left( \frac{a \sin\left(\frac{q_{(2,k)}^{(i)} + \frac{q_{(2,k+1)}^{(i)}}{2}\right) (q_{(2,k)}^{(i)} - q_{(2,k+1)}^{(i)})}{h^{(i)}} - \frac{q_{(4,k)}^{(i)} - q_{(4,k+1)}^{(i)}}{h^{(i)}} + \frac{b \sin\left(\frac{q_{(2,k)}^{(i)} + \frac{q_{(2,k+1)}^{(i)}}{2}\right) (q_{(2,k)}^{(i)} - q_{(2,k+1)}^{(i)})}{h^{(i)}} \right)^2}{2} + \\
& \frac{h^{(i)} m_2 \left( \frac{q_{(3,k)}^{(i)} - q_{(3,k+1)}^{(i)}}{h^{(i)}} + \frac{b \cos\left(\frac{q_{(1,k)}^{(i)} + \frac{q_{(1,k+1)}^{(i)}}{2}\right) (q_{(1,k)}^{(i)} - q_{(1,k+1)}^{(i)})}{h^{(i)}} + \frac{l \cos\left(\frac{q_{(1,k)}^{(i)} + \frac{q_{(1,k+1)}^{(i)}}{2}\right) (q_{(1,k)}^{(i)} - q_{(1,k+1)}^{(i)})}{h^{(i)}} \right)^2}{2} + \\
& \frac{h^{(i)} m_2 \left( \frac{q_{(4,k)}^{(i)} - q_{(4,k+1)}^{(i)}}{h^{(i)}} + \frac{b \sin\left(\frac{q_{(1,k)}^{(i)} + \frac{q_{(1,k+1)}^{(i)}}{2}\right) (q_{(1,k)}^{(i)} - q_{(1,k+1)}^{(i)})}{h^{(i)}} - \frac{l \sin\left(\frac{q_{(2,k)}^{(i)} + \frac{q_{(2,k+1)}^{(i)}}{2}\right) (q_{(2,k)}^{(i)} - q_{(2,k+1)}^{(i)})}{h^{(i)}} \right)^2}{2} + \\
& \frac{h^{(i)} m_1 \left( \frac{q_{(3,k)}^{(i)} - q_{(3,k+1)}^{(i)}}{h^{(i)}} - \frac{a \cos\left(\frac{q_{(2,k)}^{(i)} + \frac{q_{(2,k+1)}^{(i)}}{2}\right) (q_{(2,k)}^{(i)} - q_{(2,k+1)}^{(i)})}{h^{(i)}} \right)^2}{2} + \\
& \frac{h^{(i)} m_1 \left( \frac{q_{(4,k)}^{(i)} - q_{(4,k+1)}^{(i)}}{h^{(i)}} - \frac{a \sin\left(\frac{q_{(2,k)}^{(i)} + \frac{q_{(2,k+1)}^{(i)}}{2}\right) (q_{(2,k)}^{(i)} - q_{(2,k+1)}^{(i)})}{h^{(i)}} \right)^2}{2} + \\
& h^{(i)} g m_1 \left( \frac{q_{(4,k)}^{(i)}}{2} + \frac{q_{(4,k+1)}^{(i)}}{2} + a \cos\left(\frac{q_{(2,k)}^{(i)}}{2} + \frac{q_{(2,k+1)}^{(i)}}{2}\right) \right) - \\
& h^{(i)} M g \left( \frac{q_{(4,k)}^{(i)}}{2} + \frac{q_{(4,k+1)}^{(i)}}{2} + a \cos\left(\frac{q_{(2,k)}^{(i)}}{2} + \frac{q_{(2,k+1)}^{(i)}}{2}\right) + b \cos\left(\frac{q_{(2,k)}^{(i)}}{2} + \frac{q_{(2,k+1)}^{(i)}}{2}\right) \right) - \\
& h^{(i)} g m_2 \left( \frac{q_{(4,k)}^{(i)}}{2} + \frac{q_{(4,k+1)}^{(i)}}{2} - b \cos\left(\frac{q_{(1,k)}^{(i)}}{2} + \frac{q_{(1,k+1)}^{(i)}}{2}\right) + l \cos\left(\frac{q_{(2,k)}^{(i)}}{2} + \frac{q_{(2,k+1)}^{(i)}}{2}\right) \right) \quad (10.23)
\end{aligned}$$

The discretized equations of the Swing Phase are:

$$M(q_k^{(i)}) \cdot \left( \frac{q_{k+1}^{(i)} - 2q_k^{(i)} + q_{k-1}^{(i)}}{(h^{(i)})^2} \right) + C(q_k^{(i)}, \frac{q_{k+1}^{(i)} - q_k^{(i)}}{h^{(i)}}) \cdot \left( \frac{q_{k+1}^{(i)} - q_k^{(i)}}{h^{(i)}} \right) + G(q_k^{(i)}, \theta_i) = B_a(q_k^{(i)}) \begin{bmatrix} \tau_{(1,k)}^{(i)} \\ \tau_{(2,k)}^{(i)} \\ F_{(PO,x)}^{(i)} \\ F_{(PO,y)}^{(i)} \end{bmatrix} + S_{con}^T f_{(con,k)}^{(i)}$$

⇔

$$M(q_k^{(i)}) \cdot \left( \frac{q_{k+1}^{(i)} - 2q_k^{(i)} + q_{k-1}^{(i)}}{(h^{(i)})^2} \right) + C(q_k^{(i)}, \frac{q_{k+1}^{(i)} - q_k^{(i)}}{h^{(i)}}) \cdot \left( \frac{q_{k+1}^{(i)} - q_k^{(i)}}{h^{(i)}} \right) + G(q_k^{(i)}, \theta_i) = \begin{bmatrix} \tau_{(1,k)}^{(i)} \\ \tau_{(2,k)}^{(i)} \\ 0 \\ 0 \end{bmatrix} + \begin{bmatrix} 0 \\ 0 \\ f_{(fr,k)}^{(i)} \\ f_{(N,k)}^{(i)} \end{bmatrix} \quad (10.24)$$

$$\text{where } f_{(con,k)}^{(i)} = \begin{bmatrix} f_{(fr,k)}^{(i)} \\ f_{(N,k)}^{(i)} \end{bmatrix} = \begin{bmatrix} f_{fr}^{(i)}(q_k^{(i)}, \dot{q}_k^{(i)}) \\ f_N^{(i)}(q_k^{(i)}, \dot{q}_k^{(i)}) \end{bmatrix}, \quad k = 1, \dots, N - 2,$$

$$M(q_k^{(i)}) = \begin{bmatrix} p_{14} + I_1 & -p_{13} \cos(q_{(2,k)}^{(i)}) & -p_{16} \cos(q_{(2,k)}^{(i)}) & -p_{16} \sin(q_{(2,k)}^{(i)}) \\ -p_{13} \cos(q_{(2,k)}^{(i)}) & p_{12} + I_2 & p_{15} \cos(q_{(1,k)}^{(i)}) & p_{15} \sin(q_{(1,k)}^{(i)}) \\ -p_{16} \cos(q_{(2,k)}^{(i)}) & p_{15} \cos(q_{(1,k)}^{(i)}) & p_{17} & 0 \\ -p_{16} \sin(q_{(2,k)}^{(i)}) & p_{15} \sin(q_{(1,k)}^{(i)}) & 0 & p_{17} \end{bmatrix}, \quad k = 1, \dots, N - 2 \quad (10.25)$$

$$C(:, 1) = \begin{bmatrix} p_{13} \sin(q_{(2,k)}^{(i)} - q_{(1,k)}^{(i)}) \left( \left( \frac{q_{(2,k+1)}^{(i)} - q_{(2,k)}^{(i)}}{h^{(i)}} \right) - \left( \frac{q_{(1,k+1)}^{(i)} - q_{(1,k)}^{(i)}}{h^{(i)}} \right) \right) \\ p_{13} \sin(q_{(2,k)}^{(i)} - q_{(1,k)}^{(i)}) \left( \frac{q_{(1,k+1)}^{(i)} - q_{(1,k)}^{(i)}}{h^{(i)}} \right) + p_{16} \left( \sin(q_{(2,k)}^{(i)}) \left( \frac{q_{(3,k+1)}^{(i)} - q_{(3,k)}^{(i)}}{h^{(i)}} \right) - \cos(q_{(2,k)}^{(i)}) \right) \left( \frac{q_{(4,k+1)}^{(i)} - q_{(4,k)}^{(i)}}{h^{(i)}} \right) \\ p_{16} \sin(q_{(2,k)}^{(i)}) \left( \frac{q_{(2,k+1)}^{(i)} - q_{(2,k)}^{(i)}}{h^{(i)}} \right) \\ -p_{16} \cos(q_{(2,k)}^{(i)}) \left( \frac{q_{(2,k+1)}^{(i)} - q_{(2,k)}^{(i)}}{h^{(i)}} \right) \end{bmatrix}$$

$$C(:, 2) = \begin{bmatrix} p_{13} \sin(q_{(2,k)}^{(i)} - q_{(1,k)}^{(i)}) \left( \frac{q_{(2,k+1)}^{(i)} - q_{(2,k)}^{(i)}}{h^{(i)}} \right) - p_{15} \sin(q_{(1,k)}^{(i)}) \left( \frac{q_{(3,k+1)}^{(i)} - q_{(3,k)}^{(i)}}{h^{(i)}} \right) + p_{15} \cos(q_{(1,k)}^{(i)}) \left( \frac{q_{(4,k+1)}^{(i)} - q_{(4,k)}^{(i)}}{h^{(i)}} \right) \\ p_{13} \sin(q_{(2,k)}^{(i)} - q_{(1,k)}^{(i)}) \left( \left( \frac{q_{(2,k+1)}^{(i)} - q_{(2,k)}^{(i)}}{h^{(i)}} \right) - \left( \frac{q_{(1,k+1)}^{(i)} - q_{(1,k)}^{(i)}}{h^{(i)}} \right) \right) \\ -p_{15} \sin(q_{(1,k)}^{(i)}) \left( \frac{q_{(1,k+1)}^{(i)} - q_{(1,k)}^{(i)}}{h^{(i)}} \right) \\ p_{15} \cos(q_{(1,k)}^{(i)}) \left( \frac{q_{(1,k+1)}^{(i)} - q_{(1,k)}^{(i)}}{h^{(i)}} \right) \end{bmatrix}$$

$$C(:, 3) = \begin{bmatrix} -p_{15} \sin(q_{(1,k)}^{(i)}) \left( \frac{q_{(1,k+1)}^{(i)} - q_{(1,k)}^{(i)}}{h^{(i)}} \right) \\ p_{16} \sin(q_{(2,k)}^{(i)}) \left( \frac{q_{(2,k+1)}^{(i)} - q_{(2,k)}^{(i)}}{h^{(i)}} \right) \\ 0 \\ 0 \end{bmatrix}, k = 1, \dots, N - 2$$

$$C(:, 4) = \begin{bmatrix} p_{15} \cos(q_{(1,k)}^{(i)}) \left( \frac{q_{(1,k+1)}^{(i)} - q_{(1,k)}^{(i)}}{h^{(i)}} \right) \\ -p_{16} \cos(q_{(2,k)}^{(i)}) \left( \frac{q_{(2,k+1)}^{(i)} - q_{(2,k)}^{(i)}}{h^{(i)}} \right) \\ 0 \\ 0 \end{bmatrix} \quad (10.26)$$

$$G(q^{(i)}, \theta_i) = \begin{bmatrix} b g m_2 \sin(q_{(1,k)}^{(i)}) \\ -g M (a \sin(q_{(2,k)}^{(i)}) + b \sin(q_{(2,k)}^{(i)})) - a g m_1 \sin(q_{(2,k)}^{(i)}) - g l m_2 \sin(q_{(2,k)}^{(i)}) \\ 0 \\ g m_1 + g m_2 + g M \end{bmatrix}, k = 1, \dots, N - 2 \quad (10.27)$$

where  $I_1, I_2$  are the moments of inertia of the Legs 1 and 2 about their centers of mass, respectively,  $p_{12} = Ml^2 + m_1 a^2 + m_2 l^2, p_{13} = m_2 b l, p_{14} = m_2 b^2, p_{15} = m_2 b, p_{16} = Ml + m_1 a + m_2 l, p_{17} = m_1 + m_2 + M$ .

The initial and terminal conditions for the second case are:

$$D_2 L^c(q_{(1,1)}^{(i)}, q_{(1,1)}^{(i)}, q_{(2,1)}^{(i)}, q_{(2,1)}^{(i)}, q_{(3,1)}^{(i)}, q_{(3,1)}^{(i)}, q_{(4,1)}^{(i)}, q_{(4,1)}^{(i)}) + D_1 L^d(q_{(1,1)}^{(i)}, q_{(1,2)}^{(i)}, q_{(2,1)}^{(i)}, q_{(2,2)}^{(i)}, q_{(3,1)}^{(i)}, q_{(3,2)}^{(i)}, q_{(4,1)}^{(i)}, q_{(4,2)}^{(i)}) - \tau_{(1,1)}^{(i)} = 0 \quad (10.28)$$

$$D_4 L^c(q_{(1,1)}^{(i)}, q_{(1,1)}^{(i)}, q_{(2,1)}^{(i)}, q_{(2,1)}^{(i)}, q_{(3,1)}^{(i)}, q_{(3,1)}^{(i)}, q_{(4,1)}^{(i)}, q_{(4,1)}^{(i)}) + D_3 L^d(q_{(1,1)}^{(i)}, q_{(1,2)}^{(i)}, q_{(2,1)}^{(i)}, q_{(2,2)}^{(i)}, q_{(3,1)}^{(i)}, q_{(3,2)}^{(i)}, q_{(4,1)}^{(i)}, q_{(4,2)}^{(i)}) - \tau_{(2,1)}^{(i)} = 0 \quad (10.29)$$

$$D_6 L^c(q_{(1,1)}^{(i)}, q_{(1,1)}^{(i)}, q_{(2,1)}^{(i)}, q_{(2,1)}^{(i)}, q_{(3,1)}^{(i)}, q_{(3,1)}^{(i)}, q_{(4,1)}^{(i)}, q_{(4,1)}^{(i)}) + \\ D_5 L^d(q_{(1,1)}^{(i)}, q_{(1,2)}^{(i)}, q_{(2,1)}^{(i)}, q_{(2,2)}^{(i)}, q_{(3,1)}^{(i)}, q_{(3,2)}^{(i)}, q_{(4,1)}^{(i)}, q_{(4,2)}^{(i)}) - f_{(fr,1)}^{(i)} = 0 \quad (10.30)$$

$$D_8 L^c(q_{(1,1)}^{(i)}, q_{(1,1)}^{(i)}, q_{(2,1)}^{(i)}, q_{(2,1)}^{(i)}, q_{(3,1)}^{(i)}, q_{(3,1)}^{(i)}, q_{(4,1)}^{(i)}, q_{(4,1)}^{(i)}) + \\ D_7 L^d(q_{(1,1)}^{(i)}, q_{(1,2)}^{(i)}, q_{(2,1)}^{(i)}, q_{(2,2)}^{(i)}, q_{(3,1)}^{(i)}, q_{(3,2)}^{(i)}, q_{(4,1)}^{(i)}, q_{(4,2)}^{(i)}) - f_{(N,1)}^{(i)} = 0 \quad (10.31)$$

The following terminal conditions, despite the fact that they are valid during the Heel Strike Phase, are given here for simplicity. Some undefined terms in the following equations (e.g.  $f_{HSx,N}^{(i)}$ ,  $f_{HSy,N}^{(i)}$ ) will be clarified in the Chapter 3.5.

$$- D_2 L^c(q_{(1,N)}^{(i)}, q_{(1,N)}^{(i)}, q_{(2,N)}^{(i)}, q_{(2,N)}^{(i)}, q_{(3,N)}^{(i)}, q_{(3,N)}^{(i)}, q_{(4,N)}^{(i)}, q_{(4,N)}^{(i)}) + \\ D_1 L^d(q_{(1,N-1)}^{(i)}, q_{(1,N)}^{(i)}, q_{(2,N-1)}^{(i)}, q_{(2,N)}^{(i)}, q_{(3,N-1)}^{(i)}, q_{(3,N)}^{(i)}, q_{(4,N-1)}^{(i)}, q_{(4,N)}^{(i)}) - \tau_{(1,N)}^{(i)} = 0 \quad (10.32)$$

$$- D_4 L^c(q_{(1,N)}^{(i)}, q_{(1,N)}^{(i)}, q_{(2,N)}^{(i)}, q_{(2,N)}^{(i)}, q_{(3,N)}^{(i)}, q_{(3,N)}^{(i)}, q_{(4,N)}^{(i)}, q_{(4,N)}^{(i)}) + \\ D_3 L^d(q_{(1,N-1)}^{(i)}, q_{(1,N)}^{(i)}, q_{(2,N-1)}^{(i)}, q_{(2,N)}^{(i)}, q_{(3,N-1)}^{(i)}, q_{(3,N)}^{(i)}, q_{(4,N-1)}^{(i)}, q_{(4,N)}^{(i)}) - \tau_{(2,N)}^{(i)} = 0 \quad (10.33)$$

$$- D_6 L^c(q_{(1,N)}^{(i)}, q_{(1,N)}^{(i)}, q_{(2,N)}^{(i)}, q_{(2,N)}^{(i)}, q_{(3,N)}^{(i)}, q_{(3,N)}^{(i)}, q_{(4,N)}^{(i)}, q_{(4,N)}^{(i)}) + \\ D_5 L^d(q_{(1,N-1)}^{(i)}, q_{(1,N)}^{(i)}, q_{(2,N-1)}^{(i)}, q_{(2,N)}^{(i)}, q_{(3,N-1)}^{(i)}, q_{(3,N)}^{(i)}, q_{(4,N-1)}^{(i)}, q_{(4,N)}^{(i)}) - f_{HSx,N}^{(i)} = 0 \quad (10.34)$$

$$- D_8 L^c(q_{(1,N)}^{(i)}, q_{(1,N)}^{(i)}, q_{(2,N)}^{(i)}, q_{(2,N)}^{(i)}, q_{(3,N)}^{(i)}, q_{(3,N)}^{(i)}, q_{(4,N)}^{(i)}, q_{(4,N)}^{(i)}) + \\ D_7 L^d(q_{(1,N-1)}^{(i)}, q_{(1,N)}^{(i)}, q_{(2,N-1)}^{(i)}, q_{(2,N)}^{(i)}, q_{(3,N-1)}^{(i)}, q_{(3,N)}^{(i)}, q_{(4,N-1)}^{(i)}, q_{(4,N)}^{(i)}) - f_{HSy,N}^{(i)} = 0 \quad (10.35)$$

The analytical expression of (10.28):

$$h^{(i)} (m_2 \left( \frac{b \sin\left(\frac{q_{(1,1)}^{(i)}}{2} + \frac{q_{(1,2)}^{(i)}}{2}\right)}{h^{(i)}} + \frac{b \cos\left(\frac{q_{(1,1)}^{(i)}}{2} + \frac{q_{(1,2)}^{(i)}}{2}\right) (q_{(1,1)}^{(i)} - q_{(1,2)}^{(i)})}{2 h^{(i)}} \right) \left( \frac{q_{(4,1)}^{(i)} - q_{(4,2)}^{(i)}}{h^{(i)}} + \right.$$

$$\begin{aligned}
& \frac{b \sin(\frac{q_{(1,1)}^{(i)}}{2} + \frac{q_{(1,2)}^{(i)}}{2}) (q_{(1,1)}^{(i)} - q_{(1,2)}^{(i)})}{h^{(i)}} - \frac{l \sin(\frac{q_{(2,1)}^{(i)}}{2} + \frac{q_{(2,2)}^{(i)}}{2}) (q_{(2,1)}^{(i)} - q_{(2,2)}^{(i)})}{h^{(i)}} + m_2 \left( \frac{q_{(3,1)}^{(i)} - q_{(3,2)}^{(i)}}{h^{(i)}} + \right. \\
& \left. \frac{b \cos(\frac{q_{(1,1)}^{(i)}}{2} + \frac{q_{(1,2)}^{(i)}}{2}) (q_{(1,1)}^{(i)} - q_{(1,2)}^{(i)})}{h^{(i)}} + \frac{l \cos(\frac{q_{(1,1)}^{(i)}}{2} + \frac{q_{(1,2)}^{(i)}}{2}) (q_{(1,1)}^{(i)} - q_{(1,2)}^{(i)})}{h^{(i)}} \right) \left( \frac{b \cos(\frac{q_{(1,1)}^{(i)}}{2} + \frac{q_{(1,2)}^{(i)}}{2})}{h^{(i)}} + \right. \\
& \left. \frac{l \cos(\frac{q_{(1,1)}^{(i)}}{2} + \frac{q_{(1,2)}^{(i)}}{2})}{h^{(i)}} - \frac{b \sin(\frac{q_{(1,1)}^{(i)}}{2} + \frac{q_{(1,2)}^{(i)}}{2}) (q_{(1,1)}^{(i)} - q_{(1,2)}^{(i)})}{2 h^{(i)}} - \frac{l \sin(\frac{q_{(1,1)}^{(i)}}{2} + \frac{q_{(1,2)}^{(i)}}{2}) (q_{(1,1)}^{(i)} - q_{(1,2)}^{(i)})}{2 h^{(i)}} \right) - \\
& \frac{b g m_2 \sin(\frac{q_{(1,1)}^{(i)}}{2} + \frac{q_{(1,2)}^{(i)}}{2})}{2} + m_2 (b \cos(q_{(1,1)}^{(i)}) + l \cos(q_{(1,1)}^{(i)})) (q_{(3,1)}^{(i)} + q_{(1,1)}^{(i)}) l \cos(q_{(1,1)}^{(i)}) + b q_{(1,1)}^{(i)} \cos(q_{(1,1)}^{(i)}) + \\
& b m_2 \sin(q_{(1,1)}^{(i)}) (q_{(4,1)}^{(i)} + b q_{(1,1)}^{(i)} \sin(q_{(1,1)}^{(i)}) - q_{(2,1)}^{(i)} l \sin(q_{(2,1)}^{(i)})) - \tau_{(1,1)}^{(i)} = 0 \quad (10.36)
\end{aligned}$$

The analytical expression of (10.29):

$$\begin{aligned}
& h^{(i)} \left( M \left( \frac{a \cos(\frac{q_{(2,1)}^{(i)}}{2} + \frac{q_{(2,2)}^{(i)}}{2}) (q_{(2,1)}^{(i)} - q_{(2,2)}^{(i)})}{h^{(i)}} - \frac{q_{(3,1)}^{(i)} - q_{(3,2)}^{(i)}}{h^{(i)}} + \frac{b \cos(\frac{q_{(2,1)}^{(i)}}{2} + \frac{q_{(2,2)}^{(i)}}{2}) (q_{(2,1)}^{(i)} - q_{(2,2)}^{(i)})}{h^{(i)}} \right) \right. \\
& \left. \left( \frac{a \cos(\frac{q_{(2,1)}^{(i)}}{2} + \frac{q_{(2,2)}^{(i)}}{2})}{h^{(i)}} + \frac{b \cos(\frac{q_{(2,1)}^{(i)}}{2} + \frac{q_{(2,2)}^{(i)}}{2})}{h^{(i)}} - \frac{a \sin(\frac{q_{(2,1)}^{(i)}}{2} + \frac{q_{(2,2)}^{(i)}}{2}) (q_{(2,1)}^{(i)} - q_{(2,2)}^{(i)})}{2 h^{(i)}} \right) \right. \\
& \left. \frac{b \sin(\frac{q_{(2,1)}^{(i)}}{2} + \frac{q_{(2,2)}^{(i)}}{2}) (q_{(2,1)}^{(i)} - q_{(2,2)}^{(i)})}{2 h^{(i)}} - m_2 \left( \frac{l \sin(\frac{q_{(2,1)}^{(i)}}{2} + \frac{q_{(2,2)}^{(i)}}{2})}{h^{(i)}} + \frac{l \cos(\frac{q_{(2,1)}^{(i)}}{2} + \frac{q_{(2,2)}^{(i)}}{2}) (q_{(2,1)}^{(i)} - q_{(2,2)}^{(i)})}{2 h^{(i)}} \right) \right. \\
& \left. \left( \frac{q_{(4,1)}^{(i)} - q_{(4,2)}^{(i)}}{h^{(i)}} + \frac{b \sin(\frac{q_{(1,1)}^{(i)}}{2} + \frac{q_{(1,2)}^{(i)}}{2}) (q_{(1,1)}^{(i)} - q_{(1,2)}^{(i)})}{h^{(i)}} - \frac{l \sin(\frac{q_{(2,1)}^{(i)}}{2} + \frac{q_{(2,2)}^{(i)}}{2}) (q_{(2,1)}^{(i)} - q_{(2,2)}^{(i)})}{h^{(i)}} \right) - \right. \\
& \left. m_1 \left( \frac{q_{(3,1)}^{(i)} - q_{(3,2)}^{(i)}}{h^{(i)}} - \frac{a \cos(\frac{q_{(2,1)}^{(i)}}{2} + \frac{q_{(2,2)}^{(i)}}{2}) (q_{(2,1)}^{(i)} - q_{(2,2)}^{(i)})}{h^{(i)}} \right) \left( \frac{a \cos(\frac{q_{(2,1)}^{(i)}}{2} + \frac{q_{(2,2)}^{(i)}}{2})}{h^{(i)}} - \right. \\
& \left. \frac{a \sin(\frac{q_{(2,1)}^{(i)}}{2} + \frac{q_{(2,2)}^{(i)}}{2}) (q_{(2,1)}^{(i)} - q_{(2,2)}^{(i)})}{2 h^{(i)}} \right) - m_1 \left( \frac{q_{(4,1)}^{(i)} - q_{(4,2)}^{(i)}}{h^{(i)}} - \frac{a \sin(\frac{q_{(2,1)}^{(i)}}{2} + \frac{q_{(2,2)}^{(i)}}{2}) (q_{(2,1)}^{(i)} - q_{(2,2)}^{(i)})}{h^{(i)}} \right) \\
& \left. \left( \frac{a \sin(\frac{q_{(2,1)}^{(i)}}{2} + \frac{q_{(2,2)}^{(i)}}{2})}{h^{(i)}} + \frac{a \cos(\frac{q_{(2,1)}^{(i)}}{2} + \frac{q_{(2,2)}^{(i)}}{2}) (q_{(2,1)}^{(i)} - q_{(2,2)}^{(i)})}{2 h^{(i)}} \right) + M \left( \frac{a \sin(\frac{q_{(2,1)}^{(i)}}{2} + \frac{q_{(2,2)}^{(i)}}{2}) (q_{(2,1)}^{(i)} - q_{(2,2)}^{(i)})}{h^{(i)}} \right. \\
& \left. \frac{q_{(4,1)}^{(i)} - q_{(4,2)}^{(i)}}{h^{(i)}} + \frac{b \sin(\frac{q_{(2,1)}^{(i)}}{2} + \frac{q_{(2,2)}^{(i)}}{2}) (q_{(2,1)}^{(i)} - q_{(2,2)}^{(i)})}{h^{(i)}} \right) \left( \frac{a \sin(\frac{q_{(2,1)}^{(i)}}{2} + \frac{q_{(2,2)}^{(i)}}{2})}{h^{(i)}} + \frac{b \sin(\frac{q_{(2,1)}^{(i)}}{2} + \frac{q_{(2,2)}^{(i)}}{2})}{h^{(i)}} + \right. \\
& \left. \frac{a \cos(\frac{q_{(2,1)}^{(i)}}{2} + \frac{q_{(2,2)}^{(i)}}{2}) (q_{(2,1)}^{(i)} - q_{(2,2)}^{(i)})}{2 h^{(i)}} + \frac{b \cos(\frac{q_{(2,1)}^{(i)}}{2} + \frac{q_{(2,2)}^{(i)}}{2}) (q_{(2,1)}^{(i)} - q_{(2,2)}^{(i)})}{2 h^{(i)}} \right) + M g \left( \frac{a \sin(\frac{q_{(2,1)}^{(i)}}{2} + \frac{q_{(2,2)}^{(i)}}{2})}{2} + \right. \\
& \left. \frac{b \sin(\frac{q_{(2,1)}^{(i)}}{2} + \frac{q_{(2,2)}^{(i)}}{2})}{2} \right) + \frac{a g m_1 \sin(\frac{q_{(2,1)}^{(i)}}{2} + \frac{q_{(2,2)}^{(i)}}{2})}{2} + \frac{g l m_2 \sin(\frac{q_{(2,1)}^{(i)}}{2} + \frac{q_{(2,2)}^{(i)}}{2})}{2} + M (a \cos(q_{(2,1)}^{(i)}) + b \cos(q_{(2,1)}^{(i)})) \\
& (a q_{(2,1)}^{(i)} \cos(q_{(2,1)}^{(i)}) - q_{(3,1)}^{(i)} + b q_{(2,1)}^{(i)} \cos(q_{(2,1)}^{(i)})) + M (a \sin(q_{(2,1)}^{(i)}) + b \sin(q_{(2,1)}^{(i)})) \\
& (a q_{(2,1)}^{(i)} \sin(q_{(2,1)}^{(i)}) - q_{(4,1)}^{(i)} + b q_{(2,1)}^{(i)} \sin(q_{(2,1)}^{(i)})) - a m_1 \cos(q_{(2,1)}^{(i)}) (q_{(3,1)}^{(i)} - a q_{(2,1)}^{(i)} \cos(q_{(2,1)}^{(i)})) -
\end{aligned}$$

$$a m_1 \sin(q_{(2,1)}^{(i)}) (\dot{q}_{(4,1)}^{(i)} - a \dot{q}_{(2,1)}^{(i)} \sin(q_{(2,1)}^{(i)})) - l m_2 \sin(q_{(2,1)}^{(i)}) (\dot{q}_{(4,1)}^{(i)} + b \dot{q}_{(1,1)}^{(i)} \sin(q_{(1,1)}^{(i)})) - \dot{q}_{(2,1)}^{(i)} l \sin(q_{(2,1)}^{(i)}) - \tau_{(2,1)}^{(i)} = 0 \quad (10.37)$$

The analytical expression of (10.30):

$$\begin{aligned} I_2 \dot{q}_{(2,1)}^{(i)} + \frac{m_2 (2 \dot{q}_{(4,1)}^{(i)} + 2 b \dot{q}_{(1,1)}^{(i)} \sin(q_{(1,1)}^{(i)}) - 2 \dot{q}_{(2,1)}^{(i)} l \sin(q_{(2,1)}^{(i)}))}{2} - h^{(i)} \left( \frac{M g}{2} + \frac{g m_1}{2} + \frac{g m_2}{2} - \right. \\ \left. \frac{m_1 \left( \frac{q_{(4,1)}^{(i)} - q_{(4,2)}^{(i)}}{h^{(i)}} - \frac{a \sin\left(\frac{q_{(2,1)}^{(i)} + \frac{q_{(2,2)}^{(i)}}{2}\right) (q_{(2,1)}^{(i)} - q_{(2,2)}^{(i)})}{h^{(i)}} \right)}{h^{(i)}} - \frac{I_2 (2 \dot{q}_{(2,1)}^{(i)} - 2 \dot{q}_{(2,2)}^{(i)})}{2 (h^{(i)})^2} + \right. \\ \left. \frac{M \left( \frac{a \sin\left(\frac{q_{(2,1)}^{(i)} + \frac{q_{(2,2)}^{(i)}}{2}\right) (q_{(2,1)}^{(i)} - q_{(2,2)}^{(i)})}{h^{(i)}} - \frac{q_{(4,1)}^{(i)} - q_{(4,2)}^{(i)}}{h^{(i)}} + \frac{b \sin\left(\frac{q_{(2,1)}^{(i)} + \frac{q_{(2,2)}^{(i)}}{2}\right) (q_{(2,1)}^{(i)} - q_{(2,2)}^{(i)})}{h^{(i)}} \right)}{h^{(i)}} - \right. \\ \left. \frac{m_2 \left( \frac{q_{(4,1)}^{(i)} - q_{(4,2)}^{(i)}}{h^{(i)}} + \frac{b \sin\left(\frac{q_{(1,1)}^{(i)} + \frac{q_{(1,2)}^{(i)}}{2}\right) (q_{(1,1)}^{(i)} - q_{(1,2)}^{(i)})}{h^{(i)}} - \frac{l \sin\left(\frac{q_{(2,1)}^{(i)} + \frac{q_{(2,2)}^{(i)}}{2}\right) (q_{(2,1)}^{(i)} - q_{(2,2)}^{(i)})}{h^{(i)}} \right)}{h^{(i)}} \right) - \\ \left. \frac{M (2 a \dot{q}_{(2,1)}^{(i)} \sin(q_{(2,1)}^{(i)}) - 2 \dot{q}_{(4,1)}^{(i)} + 2 b \dot{q}_{(2,1)}^{(i)} \sin(q_{(2,1)}^{(i)}))}{2} + \frac{m_1 (2 \dot{q}_{(4,1)}^{(i)} - 2 a \dot{q}_{(2,1)}^{(i)} \sin(q_{(2,1)}^{(i)}))}{2} \right. \\ \left. - f_{(fr,1)}^{(i)} = 0 \quad (10.38) \right. \end{aligned}$$

The analytical expression of (10.31):

$$\begin{aligned} I_1 \dot{q}_{(1,1)}^{(i)} + h^{(i)} \left( \frac{m_1 \left( \frac{q_{(3,1)}^{(i)} - q_{(3,2)}^{(i)}}{h^{(i)}} - \frac{a \cos\left(\frac{q_{(2,1)}^{(i)} + \frac{q_{(2,2)}^{(i)}}{2}\right) (q_{(2,1)}^{(i)} - q_{(2,2)}^{(i)})}{h^{(i)}} \right)}{h^{(i)}} + \frac{I_1 (2 \dot{q}_{(1,1)}^{(i)} - 2 \dot{q}_{(1,2)}^{(i)})}{2 (h^{(i)})^2} - \right. \\ \left. \frac{M \left( \frac{a \cos\left(\frac{q_{(2,1)}^{(i)} + \frac{q_{(2,2)}^{(i)}}{2}\right) (q_{(2,1)}^{(i)} - q_{(2,2)}^{(i)})}{h^{(i)}} - \frac{q_{(3,1)}^{(i)} - q_{(3,2)}^{(i)}}{h^{(i)}} + \frac{b \cos\left(\frac{q_{(2,1)}^{(i)} + \frac{q_{(2,2)}^{(i)}}{2}\right) (q_{(2,1)}^{(i)} - q_{(2,2)}^{(i)})}{h^{(i)}} \right)}{h^{(i)}} + \right. \\ \left. \frac{m_2 \left( \frac{q_{(3,1)}^{(i)} - q_{(3,2)}^{(i)}}{h^{(i)}} + \frac{b \cos\left(\frac{q_{(1,1)}^{(i)} + \frac{q_{(1,2)}^{(i)}}{2}\right) (q_{(1,1)}^{(i)} - q_{(1,2)}^{(i)})}{h^{(i)}} + \frac{l \cos\left(\frac{q_{(2,1)}^{(i)} + \frac{q_{(2,2)}^{(i)}}{2}\right) (q_{(2,1)}^{(i)} - q_{(2,2)}^{(i)})}{h^{(i)}} \right)}{h^{(i)}} \right) - \\ \left. \frac{M (2 a \dot{q}_{(2,1)}^{(i)} \cos(q_{(2,1)}^{(i)}) - 2 \dot{q}_{(3,1)}^{(i)} + 2 b \dot{q}_{(2,1)}^{(i)} \cos(q_{(2,1)}^{(i)}))}{2} + \frac{m_1 (2 \dot{q}_{(3,1)}^{(i)} - 2 a \dot{q}_{(2,1)}^{(i)} \cos(q_{(2,1)}^{(i)}))}{2} \right. \\ \left. + \frac{m_2 (2 \dot{q}_{(3,1)}^{(i)} + 2 \dot{q}_{(1,1)}^{(i)} l \cos(q_{(1,1)}^{(i)}) + 2 b \dot{q}_{(1,1)}^{(i)} \cos(q_{(1,1)}^{(i)}))}{2} - f_{(N,1)}^{(i)} = 0 \quad (10.39) \right. \end{aligned}$$

The analytical expression of (10.32):

$$\begin{aligned}
& h^{(i)} \left( m_2 \left( \frac{b \sin\left(\frac{q_{(1,N)}^{(i)}}{2} + \frac{q_{(1,N-1)}^{(i)}}{2}\right)}{h^{(i)}} + \frac{b \cos\left(\frac{q_{(1,N)}^{(i)}}{2} + \frac{q_{(1,N-1)}^{(i)}}{2}\right) (q_{(1,N)}^{(i)} - q_{(1,N-1)}^{(i)})}{2 h^{(i)}} \right) \left( \frac{q_{(4,N)}^{(i)} - q_{(4,N-1)}^{(i)}}{h^{(i)}} + \right. \right. \\
& \left. \left. \frac{b \sin\left(\frac{q_{(1,N)}^{(i)}}{2} + \frac{q_{(1,N-1)}^{(i)}}{2}\right) (q_{(1,N)}^{(i)} - q_{(1,N-1)}^{(i)})}{h^{(i)}} - \frac{l \sin\left(\frac{q_{(2,N)}^{(i)}}{2} + \frac{q_{(2,N-1)}^{(i)}}{2}\right) (q_{(2,N)}^{(i)} - q_{(2,N-1)}^{(i)})}{h^{(i)}} \right) + m_2 \left( \frac{q_{(3,N)}^{(i)} - q_{(3,N-1)}^{(i)}}{h^{(i)}} + \right. \right. \\
& \left. \left. \frac{b \cos\left(\frac{q_{(1,N)}^{(i)}}{2} + \frac{q_{(1,N-1)}^{(i)}}{2}\right) (q_{(1,N)}^{(i)} - q_{(1,N-1)}^{(i)})}{h^{(i)}} + \frac{l \cos\left(\frac{q_{(1,N)}^{(i)}}{2} + \frac{q_{(1,N-1)}^{(i)}}{2}\right) (q_{(1,N)}^{(i)} - q_{(1,N-1)}^{(i)})}{h^{(i)}} \right) \left( \frac{b \cos\left(\frac{q_{(1,N)}^{(i)}}{2} + \frac{q_{(1,N-1)}^{(i)}}{2}\right)}{h^{(i)}} + \right. \right. \\
& \left. \left. \frac{l \cos\left(\frac{q_{(1,N)}^{(i)}}{2} + \frac{q_{(1,N-1)}^{(i)}}{2}\right)}{h^{(i)}} - \frac{b \sin\left(\frac{q_{(1,N)}^{(i)}}{2} + \frac{q_{(1,N-1)}^{(i)}}{2}\right) (q_{(1,N)}^{(i)} - q_{(1,N-1)}^{(i)})}{2 h^{(i)}} - \frac{l \sin\left(\frac{q_{(1,N)}^{(i)}}{2} + \frac{q_{(1,N-1)}^{(i)}}{2}\right) (q_{(1,N)}^{(i)} - q_{(1,N-1)}^{(i)})}{2 h^{(i)}} \right) - \right. \\
& \left. \frac{b g m_2 \sin\left(\frac{q_{(1,N)}^{(i)}}{2} + \frac{q_{(1,N-1)}^{(i)}}{2}\right)}{2} \right) - m_2 (b \cos(q_{(1,N)}^{(i)}) + l \cos(q_{(1,N)}^{(i)})) (q_{(3,N)}^{(i)} + q_{(1,N)}^{(i)} l \cos(q_{(1,N)}^{(i)}) + \\
& b q_{(1,N)}^{(i)} \cos(q_{(1,N)}^{(i)})) - b m_2 \sin(q_{(1,N)}^{(i)}) (q_{(4,N)}^{(i)} + b q_{(1,N)}^{(i)} \sin(q_{(1,N)}^{(i)}) - q_{(2,N)}^{(i)} l \sin(q_{(2,N)}^{(i)})) - \tau_{(1,N)}^{(i)} = 0
\end{aligned} \tag{10.40}$$

The analytical expression of (10.33):

$$\begin{aligned}
& h^{(i)} \left( M \left( \frac{a \cos\left(\frac{q_{(2,N)}^{(i)}}{2} + \frac{q_{(2,N-1)}^{(i)}}{2}\right) (q_{(2,N)}^{(i)} - q_{(2,N-1)}^{(i)})}{h^{(i)}} - \frac{q_{(3,N)}^{(i)} - q_{(3,N-1)}^{(i)}}{h^{(i)}} \right. \right. \\
& \left. \left. + \frac{b \cos\left(\frac{q_{(2,N)}^{(i)}}{2} + \frac{q_{(2,N-1)}^{(i)}}{2}\right) (q_{(2,N)}^{(i)} - q_{(2,N-1)}^{(i)})}{h^{(i)}} \right) \left( \frac{a \cos\left(\frac{q_{(2,N)}^{(i)}}{2} + \frac{q_{(2,N-1)}^{(i)}}{2}\right)}{h^{(i)}} + \frac{b \cos\left(\frac{q_{(2,N)}^{(i)}}{2} + \frac{q_{(2,N-1)}^{(i)}}{2}\right)}{h^{(i)}} \right) \right. \\
& \left. - \frac{a \sin\left(\frac{q_{(2,N)}^{(i)}}{2} + \frac{q_{(2,N-1)}^{(i)}}{2}\right) (q_{(2,N)}^{(i)} - q_{(2,N-1)}^{(i)})}{2 h^{(i)}} - \frac{b \sin\left(\frac{q_{(2,N)}^{(i)}}{2} + \frac{q_{(2,N-1)}^{(i)}}{2}\right) (q_{(2,N)}^{(i)} - q_{(2,N-1)}^{(i)})}{2 h^{(i)}} \right) - \\
& m_2 \left( \frac{l \sin\left(\frac{q_{(2,N)}^{(i)}}{2} + \frac{q_{(2,N-1)}^{(i)}}{2}\right)}{h^{(i)}} + \frac{l \cos\left(\frac{q_{(2,N)}^{(i)}}{2} + \frac{q_{(2,N-1)}^{(i)}}{2}\right) (q_{(2,N)}^{(i)} - q_{(2,N-1)}^{(i)})}{2 h^{(i)}} \right) \left( \frac{q_{(4,N)}^{(i)} - q_{(4,N-1)}^{(i)}}{h^{(i)}} + \right. \\
& \left. \frac{b \sin\left(\frac{q_{(1,N)}^{(i)}}{2} + \frac{q_{(1,N-1)}^{(i)}}{2}\right) (q_{(1,N)}^{(i)} - q_{(1,N-1)}^{(i)})}{h^{(i)}} - \frac{l \sin\left(\frac{q_{(2,N)}^{(i)}}{2} + \frac{q_{(2,N-1)}^{(i)}}{2}\right) (q_{(2,N)}^{(i)} - q_{(2,N-1)}^{(i)})}{h^{(i)}} \right) - \\
& m_1 \left( \frac{q_{(3,N)}^{(i)} - q_{(3,N-1)}^{(i)}}{h^{(i)}} - \frac{a \cos\left(\frac{q_{(2,N)}^{(i)}}{2} + \frac{q_{(2,N-1)}^{(i)}}{2}\right) (q_{(2,N)}^{(i)} - q_{(2,N-1)}^{(i)})}{h^{(i)}} \right) \\
& \left( \frac{a \cos\left(\frac{q_{(2,N)}^{(i)}}{2} + \frac{q_{(2,N-1)}^{(i)}}{2}\right)}{h^{(i)}} - \frac{a \sin\left(\frac{q_{(2,N)}^{(i)}}{2} + \frac{q_{(2,N-1)}^{(i)}}{2}\right) (q_{(2,N)}^{(i)} - q_{(2,N-1)}^{(i)})}{2 h^{(i)}} \right) - m_1 \left( \frac{q_{(4,N)}^{(i)} - q_{(4,N-1)}^{(i)}}{h^{(i)}} - \right. \\
& \left. \frac{a \sin\left(\frac{q_{(2,N)}^{(i)}}{2} + \frac{q_{(2,N-1)}^{(i)}}{2}\right) (q_{(2,N)}^{(i)} - q_{(2,N-1)}^{(i)})}{h^{(i)}} \right) \left( \frac{a \sin\left(\frac{q_{(2,N)}^{(i)}}{2} + \frac{q_{(2,N-1)}^{(i)}}{2}\right)}{h^{(i)}} + \frac{a \cos\left(\frac{q_{(2,N)}^{(i)}}{2} + \frac{q_{(2,N-1)}^{(i)}}{2}\right) (q_{(2,N)}^{(i)} - q_{(2,N-1)}^{(i)})}{2 h^{(i)}} \right) + \\
& M \left( \frac{a \sin\left(\frac{q_{(2,N)}^{(i)}}{2} + \frac{q_{(2,N-1)}^{(i)}}{2}\right) (q_{(2,N)}^{(i)} - q_{(2,N-1)}^{(i)})}{h^{(i)}} - \frac{q_{(4,N)}^{(i)} - q_{(4,N-1)}^{(i)}}{h^{(i)}} + \frac{b \sin\left(\frac{q_{(2,N)}^{(i)}}{2} + \frac{q_{(2,N-1)}^{(i)}}{2}\right) (q_{(2,N)}^{(i)} - q_{(2,N-1)}^{(i)})}{h^{(i)}} \right) \\
& \left( \frac{a \sin\left(\frac{q_{(2,N)}^{(i)}}{2} + \frac{q_{(2,N-1)}^{(i)}}{2}\right)}{h^{(i)}} + \frac{b \sin\left(\frac{q_{(2,N)}^{(i)}}{2} + \frac{q_{(2,N-1)}^{(i)}}{2}\right)}{h^{(i)}} + \frac{a \cos\left(\frac{q_{(2,N)}^{(i)}}{2} + \frac{q_{(2,N-1)}^{(i)}}{2}\right) (q_{(2,N)}^{(i)} - q_{(2,N-1)}^{(i)})}{2 h^{(i)}} \right) +
\end{aligned}$$

$$\begin{aligned}
& \frac{b \cos\left(\frac{q_{(2,N)}^{(i)}}{2} + \frac{q_{(2,N-1)}^{(i)}}{2}\right) (q_{(2,N)}^{(i)} - q_{(2,N-1)}^{(i)})}{2 h^{(i)}} + M g \left( \frac{a \sin\left(\frac{q_{(2,N)}^{(i)}}{2} + \frac{q_{(2,N-1)}^{(i)}}{2}\right)}{2} + \frac{b \sin\left(\frac{q_{(2,N)}^{(i)}}{2} + \frac{q_{(2,N-1)}^{(i)}}{2}\right)}{2} \right) + \\
& \frac{a g m_1 \sin\left(\frac{q_{(2,N)}^{(i)}}{2} + \frac{q_{(2,N-1)}^{(i)}}{2}\right)}{2} + \frac{g l m_2 \sin\left(\frac{q_{(2,N)}^{(i)}}{2} + \frac{q_{(2,N-1)}^{(i)}}{2}\right)}{2} - M (a \cos(q_{(2,N)}^{(i)}) + b \cos(q_{(2,N)}^{(i)})) (a \dot{q}_{(2,N)}^{(i)} \cos(q_{(2,N)}^{(i)}) \\
& - \dot{q}_{(3,N)}^{(i)} + b \dot{q}_{(2,N)}^{(i)} \cos(q_{(2,N)}^{(i)})) - M (a \sin(q_{(2,N)}^{(i)}) + b \sin(q_{(2,N)}^{(i)})) (a \dot{q}_{(2,N)}^{(i)} \sin(q_{(2,N)}^{(i)}) - \dot{q}_{(4,N)}^{(i)} + \\
& b \dot{q}_{(2,N)}^{(i)} \sin(q_{(2,N)}^{(i)})) + a m_1 \cos(q_{(2,N)}^{(i)}) (\dot{q}_{(3,N)}^{(i)} - a \dot{q}_{(2,N)}^{(i)} \cos(q_{(2,N)}^{(i)})) + a m_1 \sin(q_{(2,N)}^{(i)}) (\dot{q}_{(4,N)}^{(i)} - a \dot{q}_{(2,N)}^{(i)} \\
& \sin(q_{(2,N)}^{(i)})) + l m_2 \sin(q_{(2,N)}^{(i)}) (\dot{q}_{(4,N)}^{(i)} + b \dot{q}_{(1,N)}^{(i)} \sin(q_{(1,N)}^{(i)}) - \dot{q}_{(2,N)}^{(i)} l \sin(q_{(2,N)}^{(i)})) - \tau_{(2,N)}^{(i)} = 0
\end{aligned} \tag{10.41}$$

The analytical expression of (10.34):

$$\begin{aligned}
& \frac{M (2 a \dot{q}_{(2,N)}^{(i)} \sin(q_{(2,N)}^{(i)}) - 2 \dot{q}_{(4,N)}^{(i)} + 2 b \dot{q}_{(2,N)}^{(i)} \sin(q_{(2,N)}^{(i)}))}{2} - \\
& \frac{m_2 (2 \dot{q}_{(4,N)}^{(i)} + 2 b \dot{q}_{(1,N)}^{(i)} \sin(q_{(1,N)}^{(i)}) - 2 \dot{q}_{(2,N)}^{(i)} l \sin(q_{(2,N)}^{(i)}))}{2} - h^{(i)} \left( \frac{M g}{2} + \frac{g m_1}{2} + \frac{g m_2}{2} - \right. \\
& \left. \frac{m_1 \left( \frac{q_{(4,N)}^{(i)} - q_{(4,N-1)}^{(i)}}{h^{(i)}} - \frac{a \sin\left(\frac{q_{(2,N)}^{(i)}}{2} + \frac{q_{(2,N-1)}^{(i)}}{2}\right) (q_{(2,N)}^{(i)} - q_{(2,N-1)}^{(i)})}{h^{(i)}} \right)}{h^{(i)}} - \frac{I_2 (2 \dot{q}_{(2,N)}^{(i)} - 2 \dot{q}_{(2,N-1)}^{(i)})}{2 (h^{(i)})^2} + \right. \\
& \left. \frac{M \left( \frac{a \sin\left(\frac{q_{(2,N)}^{(i)}}{2} + \frac{q_{(2,N-1)}^{(i)}}{2}\right) (q_{(2,N)}^{(i)} - q_{(2,N-1)}^{(i)})}{h^{(i)}} - \frac{q_{(4,N)}^{(i)} - q_{(4,N-1)}^{(i)}}{h^{(i)}} + \frac{b \sin\left(\frac{q_{(2,N)}^{(i)}}{2} + \frac{q_{(2,N-1)}^{(i)}}{2}\right) (q_{(2,N)}^{(i)} - q_{(2,N-1)}^{(i)})}{h^{(i)}} \right)}{h^{(i)}} \right. \\
& \left. \frac{m_2 \left( \frac{q_{(4,N)}^{(i)} - q_{(4,N-1)}^{(i)}}{h^{(i)}} + \frac{b \sin\left(\frac{q_{(1,N)}^{(i)}}{2} + \frac{q_{(1,N-1)}^{(i)}}{2}\right) (q_{(1,N)}^{(i)} - q_{(1,N-1)}^{(i)})}{h^{(i)}} - \frac{l \sin\left(\frac{q_{(2,N)}^{(i)}}{2} + \frac{q_{(2,N-1)}^{(i)}}{2}\right) (q_{(2,N)}^{(i)} - q_{(2,N-1)}^{(i)})}{h^{(i)}} \right)}{h^{(i)}} \right) - I_2 \dot{q}_{(2,N)}^{(i)} - \\
& \frac{m_1 (2 \dot{q}_{(4,N)}^{(i)} - 2 a \dot{q}_{(2,N)}^{(i)} \sin(q_{(2,N)}^{(i)}))}{2} - f_{HSx,N}^{(i)} = 0 \tag{10.42}
\end{aligned}$$

The analytical expression of (10.35):

$$\begin{aligned}
& h^{(i)} \left( \frac{m_1 \left( \frac{q_{(3,N)}^{(i)} - q_{(3,N-1)}^{(i)}}{h^{(i)}} - \frac{a \cos\left(\frac{q_{(2,N)}^{(i)}}{2} + \frac{q_{(2,N-1)}^{(i)}}{2}\right) (q_{(2,N)}^{(i)} - q_{(2,N-1)}^{(i)})}{h^{(i)}} \right)}{h^{(i)}} + \frac{I_1 (2 \dot{q}_{(1,N)}^{(i)} - 2 \dot{q}_{(1,N-1)}^{(i)})}{2 (h^{(i)})^2} - \right. \\
& \left. \frac{M \left( \frac{a \cos\left(\frac{q_{(2,N)}^{(i)}}{2} + \frac{q_{(2,N-1)}^{(i)}}{2}\right) (q_{(2,N)}^{(i)} - q_{(2,N-1)}^{(i)})}{h^{(i)}} - \frac{q_{(3,N)}^{(i)} - q_{(3,N-1)}^{(i)}}{h^{(i)}} + \frac{b \cos\left(\frac{q_{(2,N)}^{(i)}}{2} + \frac{q_{(2,N-1)}^{(i)}}{2}\right) (q_{(2,N)}^{(i)} - q_{(2,N-1)}^{(i)})}{h^{(i)}} \right)}{h^{(i)}} + \right. \\
& \left. \frac{m_2 \left( \frac{q_{(3,N)}^{(i)} - q_{(3,N-1)}^{(i)}}{h^{(i)}} + \frac{b \cos\left(\frac{q_{(1,N)}^{(i)}}{2} + \frac{q_{(1,N-1)}^{(i)}}{2}\right) (q_{(1,N)}^{(i)} - q_{(1,N-1)}^{(i)})}{h^{(i)}} + \frac{l \cos\left(\frac{q_{(2,N)}^{(i)}}{2} + \frac{q_{(2,N-1)}^{(i)}}{2}\right) (q_{(1,N)}^{(i)} - q_{(1,N-1)}^{(i)})}{h^{(i)}} \right)}{h^{(i)}} \right) - I_1 \dot{q}_{(1,N)}^{(i)} +
\end{aligned}$$

$$\frac{M (2 a q_{(2,N)}^{(i)} \cos(q_{(2,N)}^{(i)}) - 2 \dot{q}_{(3,N)}^{(i)} + 2 b q_{(2,N)}^{(i)} \cos(q_{(2,N)}^{(i)}))}{2} - \frac{m_1 (2 \dot{q}_{(3,N)}^{(i)} - 2 a q_{(2,N)}^{(i)} \cos(q_{(2,N)}^{(i)}))}{2} - \frac{m_2 (2 \dot{q}_{(3,N)}^{(i)} + 2 \dot{q}_{(1,N)}^{(i)} l \cos(q_{(1,N)}^{(i)}) + 2 b q_{(1,N)}^{(i)} \cos(q_{(1,N)}^{(i)}))}{2} - f_{HSy,N}^{(i)} = 0 \quad (10.43)$$

Hence, the discretized Swing Phase of the 4-DOF biped robot is described by the set of equations (10.24, 10.28-10.31).

## 10.4 Modeling of Constraint Forces at Stance Foot

### 10.4.1 Constraint Forces at Stance Foot during the Swing Phase (Leg1 = Swing, Leg2 = Stance)

For the case where the Leg 1 is the Swing Leg and the Leg 2 is the Stance Leg, using the related equations of motion for the Swing Phase and equation (3.35), the constraint force at stance foot becomes:

$$f_{con}^{(i)}(q^{(i)}, \dot{q}^{(i)}) = \begin{bmatrix} \dot{q}_1^{(i)} \dot{q}_2^{(i)} (p_{16} \sin(q_2^{(i)}) - p_{15} \sin(q_1^{(i)})) \\ -\dot{q}_1^{(i)} \dot{q}_2^{(i)} (p_{16} \cos(q_2^{(i)}) + p_{15} \cos(q_1^{(i)})) + p_{17}g \end{bmatrix} \quad (10.44)$$

By proceeding with the initial discretization and applying the Direct Collocation Conditions, the relation above becomes:

$$f_{(con,appr)}^{(i)}(t_{ck}) = \begin{bmatrix} q_{(1,appr)}^{(i)}(t_{ck}) \dot{q}_{(2,appr)}^{(i)}(t_{ck}) (p_{16} \sin(q_{(2,appr)}^{(i)}(t_{ck})) - p_{15} \sin(q_{(1,appr)}^{(i)}(t_{ck}))) \\ -q_{(1,appr)}^{(i)}(t_{ck}) \dot{q}_{(2,appr)}^{(i)}(t_{ck}) (p_{16} \cos(q_{(2,appr)}^{(i)}(t_{ck})) + p_{15} \cos(q_{(1,appr)}^{(i)}(t_{ck}))) + p_{17}g \end{bmatrix} \quad (10.45)$$

and using the Discrete Mechanics Approach, it becomes:

$$f_{(con,k)}^{(i)} = \begin{bmatrix} \left( \frac{q_{(1,k+1)}^{(i)} - q_{(1,k)}^{(i)}}{h} \right) \left( \frac{q_{(2,k+1)}^{(i)} - q_{(2,k)}^{(i)}}{h} \right) (p_{16} \sin(q_{(2,k)}^{(i)}) - p_{15} \sin(q_{(1,k)}^{(i)})) \\ - \left( \frac{q_{(1,k+1)}^{(i)} - q_{(1,k)}^{(i)}}{h} \right) \left( \frac{q_{(2,k+1)}^{(i)} - q_{(2,k)}^{(i)}}{h} \right) (p_{16} \cos(q_{(2,k)}^{(i)}) + p_{15} \cos(q_{(1,k)}^{(i)})) + p_{17}g \end{bmatrix} \quad (10.46)$$

### 10.4.2 Constraint Forces at Stance Foot during the Push-Off Phase (Leg1 = Swing, Leg2 = Stance)

For the case where the Leg 1 is the Swing Leg and the Leg 2 is the Stance Leg, using the related equations of motion for the Push-Off Phase and equation (3.35), the constraint force at stance foot becomes:

$$f_{con}^{(i,PO-)}(q^{(i,PO-)}, \dot{q}^{(i,PO-)}) = \begin{bmatrix} q_1^{(i,\dot{P}O-)} q_2^{(i,\dot{P}O-)} (p_{16} \sin(q_2^{(i,PO-)}) - p_{15} \sin(q_1^{(i,PO-)})) - F_{(PO,x)}^{(i,PO-)} \\ -q_1^{(i,\dot{P}O-)} q_2^{(i,\dot{P}O-)} (p_{16} \cos(q_2^{(i,PO-)}) + p_{15} \cos(q_1^{(i,PO-)})) + p_{17}g - F_{(PO,y)}^{(i,PO-)} \end{bmatrix} \quad (10.47)$$

By proceeding with the initial discretization and applying the Direct Collocation Conditions, the relation above becomes:

$$f_{(con,appr)}^{(i)}(t_{N-1}) = \begin{bmatrix} q_{(1,appr)}^{(i)}(t_{N-1}) q_{(2,appr)}^{(i)}(t_{N-1}) (p_{16} \sin(q_{(2,appr)}^{(i)}(t_{N-1})) - p_{15} \sin(q_{(1,appr)}^{(i)}(t_{N-1}))) - \\ F_{(PO,x,appr)}^{(i)}(t_{N-1}) \\ -q_{(1,appr)}^{(i)}(t_{N-1}) q_{(2,appr)}^{(i)}(t_{N-1}) (p_{16} \cos(q_{(2,appr)}^{(i)}(t_{N-1})) + p_{15} \cos(q_{(1,appr)}^{(i)}(t_{N-1}))) + p_{17}g - \\ F_{(PO,y,appr)}^{(i)}(t_{N-1}) \end{bmatrix} \quad (10.48)$$

and using the Discrete Mechanics Approach, it becomes:

$$f_{(con,k)}^{(i)} = \begin{bmatrix} \left( \frac{q_{(1,k+1)}^{(i)} - q_{(1,k)}^{(i)}}{h} \right) \left( \frac{q_{(2,k+1)}^{(i)} - q_{(2,k)}^{(i)}}{h} \right) (p_{16} \sin(q_{(2,k)}^{(i)}) - p_{15} \sin(q_{(1,k)}^{(i)})) - F_{PO,x,N-1}^{(i)} \\ - \left( \frac{q_{(1,k+1)}^{(i)} - q_{(1,k)}^{(i)}}{h} \right) \left( \frac{q_{(2,k+1)}^{(i)} - q_{(2,k)}^{(i)}}{h} \right) (p_{16} \cos(q_{(2,k)}^{(i)}) + p_{15} \cos(q_{(1,k)}^{(i)})) + p_{17}g - F_{PO,y,N-1}^{(i)} \end{bmatrix} \quad (10.49)$$

## 10.5 The Impact Phase Redefined: Derivation of the Heel Strike and Push-Off Phases of Walking

### 10.5.1 The Heel Strike Phase of Walking (Leg1 = Swing, Leg2 = Stance)

Based on the same methodology as for the case where Leg1 is the Stance Leg and Leg2 is the Swing Leg, we derive similar equations for the Heel Strike Phase of the biped (3.48-3.63) for the case where Leg 1 is the Swing Leg and Leg 2 is the Stance Leg. We must take into account that the matrices  $M$ ,  $C$ ,  $G$  are taken from the relations (10.3-10.5). In addition, the contact point of the swing leg with the ground surface has the Cartesian Coordinates:

For the Direct Collocation Method:

$$Y = \begin{bmatrix} q_{(3,appr)}^{(i)}(t_N) + l\sin(q_{(2,appr)}^{(i)}(t_N)) + l\sin(q_{(1,appr)}^{(i)}(t_N)) \\ q_{(4,appr)}^{(i)}(t_N) + l\cos(q_{(2,appr)}^{(i)}(t_N)) - l\cos(q_{(1,appr)}^{(i)}(t_N)) \end{bmatrix} \quad (10.50)$$

For Discrete Mechanics:

$$Y = \begin{bmatrix} q_{(3,N)}^{(i)} + l\sin(q_{(2,N)}^{(i)}) + l\sin(q_{(1,N)}^{(i)}) \\ q_{(4,N)}^{(i)} + l\cos(q_{(2,N)}^{(i)}) - l\cos(q_{(1,N)}^{(i)}) \end{bmatrix} \quad (10.51)$$

In addition the following relation is valid:

For the Direct Collocation Method:

$$E = \frac{\partial Y}{\partial q_{(x,appr)}^{(i)}(t_N)} = \begin{bmatrix} l\cos(q_{(1,appr)}^{(i)}(t_N)) & l\cos(q_{(2,appr)}^{(i)}(t_N)) & 1 & 0 \\ l\sin(q_{(1,appr)}^{(i)}(t_N)) & -l\sin(q_{(1,appr)}^{(i)}(t_N)) & 0 & 1 \end{bmatrix}. \quad (10.52)$$

For Discrete Mechanics:

$$E = \frac{\partial Y}{\partial q_{(x,N)}^{(i)}} = \begin{bmatrix} l\cos(q_{(1,N)}^{(i)}) & l\cos(q_{(2,N)}^{(i)}) & 1 & 0 \\ l\sin(q_{(1,N)}^{(i)}) & -l\sin(q_{(1,N)}^{(i)}) & 0 & 1 \end{bmatrix} \quad (10.53)$$

With these modifications, we derive relations similar to (3.61, 3.63).

### 10.5.2 The Push-Off Phase of Walking (Leg 1 = Swing, Leg 2 = Stance)

Based on the same methodology as for the case where Leg1 is the Stance Leg and Leg2 is the Swing Leg, we derive similar equations for the Push-Off Phase of the biped (3.64 -3.72) for the case where Leg 1 is the Swing Leg and Leg 2 is the Stance Leg. We must take into account that the matrices  $M$ ,  $C$ ,  $G$  are taken from the relations (10.3-10.5). In addition,  $J_{PO} = \begin{bmatrix} 0 & 0 & -\sin(q_{(2,N)}^{(i)}) & \cos(q_{(2,N)}^{(i)}) \end{bmatrix}$  (due to the fact that now the stance leg is the Leg 2). With these modifications, we derive relations similar to (3.71, 3.72).

# Chapter 11

## Appendix D: Implemented Optimization Algorithms for the Gait Generation Problems

### 11.1 Introduction

In this section we will mention the optimization algorithms that we used and implemented for solving the gait generation problems utilizing Discrete Mechanics and Direct Collocation based discretization. More specifically, for the Discrete Mechanics based optimization problems we are going to implement a Feasible sequential quadratic programming algorithm (FSQP) to solve them [14]. In addition, for the related Direct Collocation based optimization problems, we are going to implement Nonlinear Interior Point Methods [15].

## 11.2 A FSQP Algorithm for the Discrete Mechanics based Gait Generation Problems

Feasible sequential quadratic programming algorithms (FSQP) are methods for solving nonlinearly constrained optimization problems or nonlinear programming problems. As the name suggests, feasible SQP methods constrain all of the iterates to be feasible. As a result, they are more expensive than standard SQP algorithms, but they are useful when the objective function  $f$  is difficult or impossible to calculate outside the feasible set or when termination of the algorithm at an infeasible point is undesirable.

These algorithms seem to fit best for our proposed system, since that, at any case (e.g. providing a random initial vector of values instead of guessing "good" initial values for the algorithms), those algorithms will not lead to undesiring termination and as a result, to "corrupted" trajectories.

FSQP algorithms solve problems of the form:

$$\begin{aligned}
 & \text{minimize } f(x) \\
 & \text{s.t. } g_j(x) \leq 0, \quad j = 1, 2, \dots, m, \\
 & \quad g_j(x) \leq 0, \quad j = m + 1, \dots, m + l,
 \end{aligned} \tag{11.1}$$

where  $f, g_j (j = 1, 2, \dots, m + l) : R^n \rightarrow R$  are smooth functions.

In these algorithms, the step is defined as a combination of the SQP direction, a strictly feasible direction (which points into the interior of the feasible set) and, possibly, a second-order correction direction. This mix of directions is adjusted to ensure feasibility while retaining fast local convergence properties. Feasible algorithms have the additional advantage that the objective function  $f$  can be used as a merit function, since, by definition, the constraints are always satisfied. FSQP also solves problems in which  $f$  is not itself smooth but instead is the maximum of a finite set of smooth functions:

$$f_i : R^n \rightarrow R \tag{11.2}$$

SQP algorithms generate iteratively the main search direction  $d_0$  of the problem above by solving a QP subproblem:

$$\begin{aligned}
 & \text{minimize } \nabla f(x)^T d + \frac{1}{2} d^T H d \\
 & \text{s.t. } g_j(x) + \nabla g_j(x)^T d \leq 0, \quad j = 1, \dots, m \\
 & \quad g_j(x) + \nabla g_j(x)^T d = 0, \quad j = m + 1, \dots, m + l,
 \end{aligned} \tag{11.3}$$

where  $H \in R^{n \times n}$  is a symmetric positive definite matrix.

However, there is a serious drawback that SQP methods require a solution of the QP above at each iteration.

We denote:

$$X = \{x \in R^n \mid g_j(x) \leq 0, \quad j = 1, \dots, m, \quad g_j(x) = 0, \quad j = m + 1, \dots, m + l\}, \quad I = \{1, 2, \dots, m\},$$

$$E = \{m + 1, \dots, m + l\}, \quad L = I \cup E, \quad I(x) = \{j \in I \mid g_j(x) = 0\}, \quad L(x) = I(x) \cup E$$

Given a parameter  $c > 0$ , construct the corresponding auxiliary programming with (3.93):

$$\begin{aligned}
 & \text{minimize } F_c(x) \\
 & \text{s.t. } g_j(x) \leq 0, \quad j \in L = I \cup E.
 \end{aligned} \tag{11.4}$$

where

$$F_c(x) = f(x) - c \sum_{j \in E} g_j(x). \tag{11.5}$$

Denote the feasible set of the problem (3.96) as follows:

$$X_+ = \{x \in R^n \mid g_j(x) \leq 0, \quad j \in L = I \cup E\}$$

The following general assumptions are true for the use of the specific algorithm:

- Feasible sets of (3.93) and (3.96) are nonempty, i.e.,  $X \neq \emptyset$ ,  $X_+ \neq \emptyset$ .

- The functions  $f(x)$ ,  $g_j(x)$  ( $j \in L$ ) are two-times continuously differentiable.
- For all  $x \in X_+$ , the vectors  $\{\nabla g_j(x), j \in L(x)\}$  are linearly independent.

Given a point  $x \in X$ , the following matrices are defined:

$$D(x) = \text{diag}(D_j(x), j \in L), \quad D_j(x) = \begin{cases} g_j^2(x), & j \in I, \\ 0, & j \in E, \end{cases} \quad (11.6)$$

$$N(x) = (\nabla g_j(x), j \in L), \quad Q(x) = (N(x)^T N(x) + D(x))^{-1} N(x)^T.$$

### •Algorithm

Parameters:  $\alpha \in (0, \frac{1}{2})$ ,  $v > 2$ ,  $\delta \in (2, v)$ ,  $\tau \in (2, 3)$ ,  $\epsilon_0 > 0$ ,  $\epsilon > 0$ ,  $\rho > 0$ ,  $\theta, \beta \in (0, 1)$ .

Data:  $x^0 \in X_+$ ,  $H_0 \in R^{n \times n}$ ,  $c_0 = \rho$ .

**Step 0.** Initialization, and set  $k = 0$ .

**Step 1.** Computation of the approximate active set  $J_k$ :

(1.1). Set  $i = 0$ ,  $\epsilon_{k,i} = \epsilon_0$ .

(1.2). Compute:

$$\tilde{J}_{k,i} = \{j \in I \mid -\epsilon_{k,i} \leq g_j(x^k) \leq 0\}, \quad J_{k,i} = \tilde{J}_{k,i} \cup E, \quad A_{k,i} = (\nabla g_k(x^k), j \in J_{k,i}). \quad (11.7)$$

If  $A_{k,i}$  is of full rank, let:

$$\tilde{J}_k = \tilde{J}_{k,i}, \quad J_k = J_{k,i}, \quad A_k = A_{k,i}, \quad i_k = i,$$

and go to step 2.

(1.3). Set  $i = i + 1$ ,  $\epsilon_{k,i} = \frac{1}{2}\epsilon_{k,i-1}$ , and go to 1.2.

**Step 2.** Updating of parameter  $c_k$ :

According to (3.98) and the equation:

$$\pi(x) = -(N(x)^T N(x) + D(x))^{-1} N(x)^T \nabla f(x) = -Q(x) \nabla f(x) \quad (11.8)$$

compute  $Q_k = Q(x^k)$ ,  $\pi^k = \pi(x^k)$ , and set

$$s_k = \max\{|\pi_j^k|, j \in E\}, \quad c_k = \begin{cases} \max\{s_k + c_0, c_{k-1} + \epsilon\}, & c_{k-1} < s_k + c_0, \\ c_{k-1}, & c_{k-1} \geq s_k + c_0. \end{cases} \quad (11.9)$$

**Step 3.** Computation of the search direction:

**(3.1).** Computation of the descent  $d_0^k$ :

Solve the following equality constrained QP subproblem at  $x^k$ :

$$\begin{aligned} & \text{minimize } \nabla F_{c_k}(x^k)^T d + \frac{1}{2} d^T H_k d \\ & \text{s.t. } \alpha_j^k + \nabla g_j(x^k)^T d = 0, \quad j \in J_k \setminus E, \\ & \quad g_j(x^k) + \nabla g_j(x^k)^T d^k = 0, \quad j \in E. \end{aligned} \quad (11.10)$$

where

$$\alpha_j^k = \begin{cases} g_j(x^k), & j \in J_k \setminus E, \quad \pi_j^k \geq 0, \\ -\pi_j^k, & j \in J_k \setminus E, \quad \pi_j^k < 0. \end{cases} \quad (11.11)$$

Let  $(d_0^k, \tilde{u}^k)$  be the KKT point pair. If  $d_0^k = 0$ , STOP.

**(3.2)** Computation of the feasible descent direction  $d^k$ :

**(3.2.1).** Solve the second equality constraint QP as follows:

$$\begin{aligned} & \text{minimize } \nabla F_{c_k}(x^k)^T d + \frac{1}{2} d^T H_k d \\ & \text{s.t. } g_j(x^k) + \nabla g_j(x^k)^T d = -\|d_0^k\|^v, \quad j \in J_k \end{aligned} \quad (11.12)$$

Let  $(d_1^k, \lambda^k)$  be the KKT point pair. If

$$\nabla F_{c_k}(x^k)^T d_1^k \leq \xi \|d_1^k\|^\delta, \quad (11.13)$$

let  $d^k = d_1^k$ , go to step 3.3.

(3.2.2). Solve the following system of linear equations:

$$\begin{bmatrix} H_k & A_k \\ A_k^T & G_k \end{bmatrix} \begin{bmatrix} d \\ \lambda \end{bmatrix} = - \begin{bmatrix} \nabla F_{c_k}(x^k) \\ 0 \end{bmatrix}, \quad (11.14)$$

where

$$G_k = \text{diag}(g_j(x^k), j \in J_k).$$

Let  $(d_2^k, \tilde{\pi}^k)$  be the solution.

(3.2.3). Solve the following system of linear equations:

$$\begin{bmatrix} H_k & A_k \\ A_k^T & G_k \end{bmatrix} \begin{bmatrix} d \\ \lambda \end{bmatrix} = - \begin{bmatrix} \nabla F_{c_k}(x^k) \\ V^k \end{bmatrix}, \quad (11.15)$$

where

$$V_k^j = \begin{cases} -\tilde{\pi}_j^k, & \tilde{\pi}_j^k \leq 0, j \in J_k, \\ 0, & \tilde{\pi}_j^k > 0, j \in J_k. \end{cases} \quad (11.16)$$

Let  $(d_3^k, \tilde{v}^k)$  be the solution.

(3.2.4). Denote  $\tau_k = -\nabla F_{c_k}(x^k)^T d_3^k$ . Establish a convex combination of  $d_1^k$  and  $d_3^k$  as follows:

$$d^k = \tau_k((1 - \rho_k)d_3^k + \rho_k d_1^k), \quad \rho_k = \begin{cases} 1, & \nabla F_{c_k}(x^k)^T d_1^k \leq \theta \nabla F_{c_k}(x^k)^T d_3^k \\ \frac{(1-\theta)\nabla F_{c_k}(x^k)^T d_3^k}{\nabla F_{c_k}(x^k)^T (d_3^k - d_1^k)}, & \nabla F_{c_k}(x^k)^T d_1^k > \theta \nabla F_{c_k}(x^k)^T d_3^k \end{cases} \quad (11.17)$$

(3.3). Computation of the high-order corrected direction  $\tilde{d}^k$ :

Solve the third equality constrained QP as follows:

$$\begin{aligned} & \mathbf{minimize} \quad \nabla F_{c_k}(x^k)^T d + \frac{1}{2}(d^k + d)^T H_k(d^k + d) \\ & \mathbf{s.t.} \quad g_j(x^k + d^k) + \nabla g_j(x^k)^T d = -\|d^k\|^\tau, \quad j \in J_k. \end{aligned} \quad (11.18)$$

Let  $(\tilde{d}^k, \tilde{\lambda}^k)$  be the KKT point pair. If  $\|\tilde{\delta}^k\| > \|\delta^k\|$ , set  $\tilde{\delta}^k = 0$ .

**Step 4.** The line search: Compute  $t_k$ , the first number  $t$  in the sequence  $\{1, \beta, \beta^2, \beta^3, \dots\}$

satisfying:

$$F_{c_k}(x^k + td^k + t\tilde{d}^k) \leq F_{c_k}(x^k) + \alpha t \nabla F_{c_k}(x^k)^T d^k, \quad (11.19)$$

$$g_j(x^k + td^k + t^2\tilde{d}^k) \leq 0, \quad j \in L. \quad (11.20)$$

**Step 5.** Update:

Obtain  $H_{k+1}$  by updating the positive definite matrix  $H_k$  using the Broyden-Fletcher-Goldfarb-Shanno formulas, namely:

$$H_{k+1} = H_k + \frac{y^k y^{kT}}{y^{kT} s^k} - \frac{H_k s^k s^{kT} H_k}{s^{kT} H_k s^k}, \quad (11.21)$$

where  $y^k = \nabla F_{c_k}(x^{k+1}) - \nabla F_{c_k}(x^k)$  and  $s^k = x^{k+1} - x^k$ . Set  $x^{k+1} = x^k + t_k d^k + t_k^2 \tilde{d}^k$ .

Go to step 1.

### • Global Convergence of the FSQP Algorithm

In this section, it is shown that the abovementioned algorithm is correctly stated. Some assumptions are made and let them hold for the algorithm.

- The sequence  $\{x^k\}$ , which is generated by the algorithm, is bounded.
- There exist two constants  $b \geq a > 0$ , such that

$$\alpha \|y\|^2 \leq y^T H_k y \leq b \|y\|^2, \quad \text{for all } k \text{ and for all } y \in R^n.$$

**(Lemma 1).** For any iteration  $k$ , there is no infinite cycle in step 1. Moreover, if  $\{x^k\}_{k \in K} \rightarrow x^*$ , then there is a constant  $\tilde{\epsilon} > 0$ , such that  $\epsilon_{k,i_k} \geq \tilde{\epsilon}$ , for  $k \in K$ ,  $k$  large enough.

**(Lemma 2).** Let  $(d_0^k, \tilde{u})$  be the solution of (3.102). If  $d_0^k = 0$ , then  $x^k$  is a KKT point of (3.93), otherwise, the direction  $d^k$  computed in step 3.2 is a feasible descent direction of (3.96) at  $x^k$ .

**(Lemma 3).** The line search in step 4 yields a stepsize  $t_k = \beta^j$  for some finite  $j = j(k)$ .

**(Lemma 4).** There exists a positive integer  $k_0$ , such that

$$c_k \equiv c_{k_0} = c, \quad \text{for all } k \geq k_0.$$

**(Lemma 5).** Under above assumptions,  $d_0^k \rightarrow 0$ ,  $k \in K$ .

**(Theorem 1).** The algorithm either stops at the KKT point  $x^k$  of the problem (3.93) in finite iteration, or generates an infinite sequence  $\{x^k\}$  whose any accumulation point  $x^*$  is a KKT point of (3.93).

• **Rate of Convergence of the FSQP Algorithm**

Some further lemmas and theorems follow, regarding the rate of convergence of the implemented algorithm. For that reason, some stronger regularity assumptions are added:

- $H_k \rightarrow H_*$ ,  $k \rightarrow \infty$ .
- The second-order sufficiency conditions with strict complementary slackness are satisfied at the KKT point  $x^*$  and the corresponding multiplier vector  $u^*$ .

**(Lemma 6).** Under above conditions, the entire sequence  $\{x^k\}$  converges to  $x^*$ , i.e.,  $x^k \rightarrow x^*$ ,  $k \rightarrow \infty$ .

**(Lemma 7).** For  $k$  large enough, it holds that  $J_k \equiv L(x^*) = I(x^*) \cup E$ , and

$$d_0^k \rightarrow 0, \quad \pi^k \rightarrow u^*, \quad \tilde{u}_j^k \rightarrow u_j^*, \quad j \in I(x^*), \quad \tilde{u}_j^k \rightarrow u_j^* + c > 0, \quad j \in E, \quad k \rightarrow \infty.$$

**(Lemma 8).** For  $k$  large enough,  $(d^k, \lambda^k)$  obtained in step 3.2 and  $\tilde{d}^k$  obtained by (3.110) satisfy that

$$d^k = d_1^k, \quad \|d^k\| \sim \|d_0^k\|, \quad \|\tilde{d}^k\| = O(\|d^k\|^2), \quad \lambda^k \rightarrow u^*, \quad j \in I(x^*), \quad \lambda^k \rightarrow u^* + c, \quad j \in E, \quad k \rightarrow \infty,$$

and it holds that

$$\begin{aligned} \nabla F_c(x^k) + H_k d^k + A_k \lambda^k &= 0, \\ g_j(x^k) + \nabla g_j(x^k)^T d^k &= o(\|d^k\|^2), \quad j \in L(x^*). \end{aligned} \tag{11.22}$$

**(Lemma 9).** Denote:

$$G(x^k) = (g_j(x^k), \quad j \in I(x^*) \cup E), \quad P_k = E_n - A_k(A_k^T A_k)^{-1} A_k^T, \quad d^k = P_k d^k + \bar{d}^k,$$

then, we have:

$$\|\tilde{d}^k\| = O(\|d^k\|) = O(\|G(x^k)\|) + o(\|d^k\|^2).$$

**(Lemma 10).** For  $k$  large enough, the full step of one is always accepted, i.e.,

$$t_k \equiv 1, \quad x^{k+1} = x^k + d^k + \tilde{d}^k.$$

**(Theorem 2).** Under all stated assumptions, the algorithm is superlinearly convergent, i.e., the sequence  $\{x^k\}$  generated by the algorithm satisfies  $\|x^{k+1} - x^*\| = o(\|x^k - x^*\|)$ .

### 11.3 A Nonlinear Interior-Point Algorithm for the Direct Collocation based Gait Generation Problems

Interior-point methods for nonlinear programming, also called barrier methods, rose from the need for effective solving of large-scale optimization problems. In particular, for NLP problems with large numbers of inequality constraints, these methods offer a serious alternative to active-set strategies. Within the last fifteen years researchers has led to a better understanding of the convergence of interior-point methods and has also developed effective computational algorithms with desirable global and local convergence properties. The term interior-point method was used for the first time by Fiacco and McCormick in 1968 in the book (Fiacco and McCormick, 1968), for any algorithm that was designed for the calculation of a local minimum of an NLP problem by the solution of a determined sequence of unconstrained minimization problems. Such a definition evolved to the form, in which as of the IP method we think of any algorithm for solving a set of optimization problems associated with a decreasing value of the  $\mu$  multiplier, to find local solutions lying in the interior of the feasibility set determined by nonlinear constraints of the NLP problem.

To allow convergence from "bad" starting points for interior-point methods in both trust region and line-search versions, researchers developed exact penalty merit functions that ensure progress toward the solution (Byrd *et al.*, 2000; Tits *et al.*, 2002). On the other hand, Fletcher

and Leyffer (Fletcher and Leyffer, 2002; Fletcher *et al.*, 2006) proposed recently filter methods, as an alternative to merit functions which guarantee the global convergence for nonlinear programming algorithms. They are based on the idea of the approval of trial points generated by the optimization algorithm in the case when they improve the value of the objective function or improve the value of a constraint violation, instead of a combination of those two measures defined by a merit function.

More recently, this filter technique has been adapted to barrier methods. In (Ulbrich *et al.*, 2004), the authors consider a trust-region filter method, in which the consequent iterations of the solution are accepted on the basis of the norm of optimality conditions. Also, in (Benson *et al.*, 2001), the authors proposed several heuristics based on the concept of filter methods, for which the efficiency improvement was obtained as compared with their previous experience with merit functions. Finally, in (Wachter and Biegler, 2005), global convergence analysis of an interior-point algorithm with a filter line-search was provided.

### • Algorithm

In this section we describe a primal-dual interior-point algorithm with line-search minimization based on the filter method. The authors of the algorithm assumed the following formulation of the original NLP problem:

$$(P) \min_{y \in \mathbb{R}^{m_y}} \{J(y) \mid h(y) = 0, y \geq 0\}, \quad (11.23)$$

where the objective function  $J : \mathbb{R}^{m_y} \rightarrow \mathbb{R}$  and the equality constraints  $h : \mathbb{R}^{m_y} \rightarrow \mathbb{R}^{m_h}$  with  $m_h < m_y$  are assumed to be twice continuously differentiable. NLP problems with general inequality constraints  $g(y) \geq 0$  can be reformulated to the above form by introducing slack variables, i.e.,  $s$ , where  $g(y) - s = 0, s \geq 0$ .

The barrier algorithm is based on the replacement of the sign constraints on decision variables,  $y \geq 0$ , with an additional component in the objective function—the logarithmic barrier:

$$(P) \min_{y \in \mathbb{R}^{m_y}} J_\mu(y) = J(y) - \mu \sum_{j=1}^{m_y} \ln(y^j) \mid h(y) = 0, \quad (11.24)$$

where  $\mu > 0$  is the barrier parameter and  $y^j$  is the  $j$ -th element of the vector  $y$ . Since the objective function for Problem (P) may attain arbitrarily large values when  $y^j$  reaches one of its bounds, the local solution  $y_*(\mu)$  to that problem is located in the interior of the set determined by the constraints  $y_*(\mu) > 0$ . The scale of the barrier influence is determined by the size of the  $\mu$  parameter and on certain assumptions, as  $\mu \rightarrow 0$ , the solution  $y_*(\mu)$  converges to a local solution  $y_*$  of the original problem (P). As a result, the algorithm to determine a solution to the original problem (P) is based on solving a sequence of barrier problems ( $P_\mu$ ) with decreasing values of the parameter  $\mu_l, \{\mu_l\} \rightarrow 0$ .

The interior-point algorithm finds a solution for primal-dual stationarity conditions for the problem ( $P_\mu$ ), formulated as the following nonlinear system of equations:

$$\begin{aligned} \nabla_y J(y) + \nabla_y h(y)\lambda - z &= 0 \\ h(y) &= 0, \\ YZ - \mu e_y &= 0, \end{aligned} \tag{11.25}$$

where  $Y$  and  $Z$  are diagonal matrices with elements  $y$  and  $z$ , respectively,  $e_y$  is the vector of ones of dimension  $m_y$ ,  $\lambda \in \mathbb{R}^{m_h}$  is the vector of Lagrange multipliers for equality constraints of the problem (P), and  $z \in \mathbb{R}^{m_y}$  corresponds to the vector of Lagrange multipliers for the sign constraints of the problem (P), in the limit, as  $\mu \rightarrow 0$ . Note that the system of equalities (3.117) for  $\mu = 0$ , together with the additional condition  $y, z \geq 0$ , is equivalent to KKT optimality conditions for the original problem (P). For the solution of the system of equalities (3.117) for a fixed value of the parameter  $\mu$ , the iterative Newton method is being applied, based on the solution of the following system of linear equations:

$$\begin{bmatrix} W_k & \nabla_y h(y_k) & -I \\ \nabla_y h(y_k)^T & 0 & 0 \\ Z_k & 0 & Y_k \end{bmatrix} \begin{bmatrix} d_k^y \\ d_k^\lambda \\ d_k^z \end{bmatrix} = - \begin{bmatrix} \nabla_y J(y_k) + \nabla_y h(y_k)\lambda_k - z_k \\ h(y_k) \\ Y_k Z_k - \mu e_y \end{bmatrix} \tag{11.26}$$

where  $W_k$  denotes the exact Hessian matrix for the Lagrange function of the original problem

(P):

$$W_k = \nabla_{yy}J(y_k) + \sum_{i=1}^{m_h} \lambda_k^i \nabla_{yy}h^i(y_k), \quad (11.27)$$

or some approximation of it. The Lagrange function has the form

$$\mathcal{L}(y, \lambda, z) := J(y) + h(y)^T \lambda - z. \quad (11.28)$$

Here, the index  $k$  denotes the counter of inner iterations of Newton's method, the vector  $(y_k, \lambda_k, z_k)$  is the current iterate, and  $(d_k^y, d_k^\lambda, d_k^z)$  is the obtained new search direction.

Instead of solving the nonsymmetric system of linear equalities (3.118) directly, the the equivalent solution is obtained by first solving the symmetric linear system of a smaller dimension:

$$\begin{bmatrix} W_k + \Sigma_k & \nabla_y h(y_k) \\ \nabla_y h(y_k)^T & 0 \end{bmatrix} \begin{bmatrix} d_k^y \\ \lambda_k^+ \end{bmatrix} = - \begin{bmatrix} J_\mu(y_k) \nabla_y \\ h(y_k) \end{bmatrix} \quad (11.29)$$

where  $\Sigma_k := Y_k^{-1} Z_k$ . The equations for the system D34 are derived from those of the system (3.118) by eliminating the last block row. And then, the direction  $d_k^\lambda$  is computed from

$$d_k^\lambda = \lambda_k^+ - \lambda_k \quad (11.30)$$

and the direction  $d_k^z$  from

$$d_k^z = \mu Y_k^{-1} e_y - z_k - \Sigma_k d_k^y \quad (11.31)$$

After computing new search directions from (3.126-3.128) we calculate the next iterate as follows:

$$(y_{k+1}, \lambda_{k+1}, z_{k+1}) := (y_k, \lambda_k, z_k) + (\alpha_k d_k^y, \alpha_k d_k^\lambda, \alpha_k^z d_k^z), \quad (11.32)$$

where  $\alpha, \alpha_k^z \in (0, 1]$  are the stepsizes. Note that for  $z$  variables it is allowed to take a different stepsize than for the other variables.

Since we know that the variables  $y$  and  $z$  are positive at an optimal solution of the barrier problem  $(P_\mu)$ , the interior-point algorithm maintains this property for all iterates. As a result,

the following rule of the step length selection is applied:

$$\begin{aligned}\bar{\alpha}_k &:= \max\{\alpha \in (0, 1] : y_k + \alpha d_k^y \geq (1 - \tau)y_k\}, \\ \bar{\alpha}_k^z &:= \max\{\alpha \in (0, 1] : z_k + \alpha d_k^z \geq (1 - \tau)z_k\},\end{aligned}\tag{11.33}$$

for the parameter  $\tau \in (0, 1)$ , usually close to 1 (e.g.,  $\tau = 0.995$ ). For the  $z$  variables the step length is chosen as  $\alpha_k^z := \bar{\alpha}_k^z$ , while the step length  $\alpha_k \in (0, \bar{\alpha}_k]$  for the remaining variables is determined by a backtracking line-search procedure using a decreasing sequence of trial stepsizes,  $\alpha_{k,l} = 2^{-l}\bar{\alpha}_k$ , with  $l = 0, 1, 2, \dots$  -here a variant of Fletcher and Leyffer's filter method (Fletcher and Leyffer, 2002) is used, which guarantees global convergence of the interior-point algorithm to the solution of the problem  $(P_\mu)$ .

Filter minimization methods are based on the idea of two-criteria optimization in which, apart from minimizing the barrier objective function  $J_\mu(y)$ , we want to minimize the constraint violation  $\theta(y) := \|h(y)\|$  in order to assure the convergence to a feasible point. In the interior-point algorithm, the following safeguards have been added by the authors to this simple procedure of next iterate acceptance:

- In the case when the current iterate is (almost) feasible but not sufficiently optimal, the above condition of a sufficient decrease in one of two measures for  $y_k$  is replaced by the condition of a sufficient decrease in the barrier function value  $J_\mu$ .
- In order to prevent cycling, the  $(\theta, J_\mu)$  pairs corresponding to previous iterate that create a certain envelope (in our example these are  $y_{l_1}$  and  $y_{l_2}$  iterates) are added to a filter; a trial point is only accepted if it guarantees a sufficient decrease in one of two measures relative to all those points.
- It may happen that there is no trial stepsize  $\alpha_{k,l}$  that generates an acceptable point. After detecting such a situation, the algorithm switches to a *feasibility restoration phase* in which the minimization of infeasibility is carried out (ignoring the objective function) until either a new acceptable iterate is found or it is no longer possible to reduce the infeasibility, e.g., if the problem  $P$  is (locally) infeasible.

In comparison with traditional line-search algorithms, such as a single merit function technique, the filter method is usually less conservative and makes it possible to take larger stepsizes. Moreover, the protection in the form of a restoration phase makes the filter algorithm resistant to unnecessary errors, such as those presented in (Wachter and Biegler, 2000). The computationally most expensive part of the optimization algorithm implemented in the nonlinear interior point algorithm (not including computations of the objective function, constraints and their derivatives) is the solution of the linear system of equations (3.121), which is most often of high order and has a sparse structure, e.g., for dynamic optimization problems it is very sparse. For its factorization and solution, the nonlinear interior-point algorithm uses external sparse direct linear solvers.